ENZYME-ASSISTED SUPERCRITICAL CARBON DIOXIDE EXTRACTION OF ACTIVE PRINCIPLES OF BLACK PEPPER AND SMALL CARDAMOM AND APPLICATIONS OF THE EXTRACTS FOR DESIGN OF NUTRACEUTICAL FOODS AND SUPPLEMENTS

THESIS SUBMITTED BY

SAYANTANI DUTTA

DOCTOR OF PHILOSOPHY (ENGINEERING)

DEPARTMENT OF FOOD TECHNOLOGY AND BIOCHEMICAL ENGINEERING
FACULTY COUNCIL OF ENGINEERING & TECHNOLOGY
JADAVPUR UNIVERSITY
KOLKATA, INDIA

2017

DEDICATED

TO

MY

GRANDFATHER

JADAVPUR UNIVERSITY
KOLKATA 700 032, INDIA

INDEX NO. 198/13/E

1. Title of the thesis:

Enzyme-assisted supercritical carbon dioxide extraction of active principles of black pepper and small cardamom and applications of the extracts for design of nutraceutical foods and supplements

2. Name, Designation & Institution of the Supervisor:

Dr. Paramita Bhattacharjee
Reader
Department of Food Technology and Biochemical Engineering
Jadavpur University, Kolkata

3. List of Publications:

Research Articles

Accepted/Published:

1. Sayantani Dutta and Paramita Bhattacharjee. Enzyme-assisted supercritical carbon dioxide extraction of black pepper oleoresin for enhanced yield of piperine-rich extract. **Journal of Bioscience and Bioengineering**, *120*, 17-23, **2015**.
2. Sayantani Dutta and Paramita Bhattacharjee. Microencapsulation of enzyme-assisted supercritical carbon dioxide extract of small cardamom by spray drying. **Food Measurement and Characterization**, **2016**. http://dx.doi.org/10.1007/s11694-016-9398-9.
3. Sayantani Dutta and Paramita Bhattacharjee. Microencapsulated supercritical carbon dioxide extract of small cardamom enriches the nutraceutical value of custard. **Nutrafoods**, *16*, 1-6, **2017**.
4. Sayantani Dutta and Paramita Bhattacharjee. Nanoliposomal encapsulates of piperine-rich black pepper extract obtained by enzyme-assisted supercritical carbon dioxide extraction. **Journal of Food Engineering**, *201*, 49-56, **2017**.
5. Sayantani Dutta, Paramita Bhattacharjee and Nabarun Bhattacharyya. Assessment of shelf-lives of black pepper and small cardamom cookies by metal oxide based electronic nose using spoilage index. **Food and Bioprocess Technology**, *10*, 2023-2033, **2017**.

Publication as Co-author:

1. Sudip Ghosh, Sayantani Dutta, Probir Kumar Ghosh, Paramita Bhattacharjee and Satadal Das. Design of a polyherbal mix by supercritical carbon dioxide extraction and

its encapsulation by spray drying: Phytochemical properties and shelf-life study of the encapsulate. **Journal of Food Process Engineering, 2016**. DOI: 10.1111/jfpe.12505

2. Kaninika Paul, Sayantani Dutta and Paramita Bhattacharjee. FT-Raman spectroscopic analysis of enhanced activity of supercritical carbon dioxide treated bacterial α-amylase. **Enzyme and Microbial Technology**, *104*, 44-46, **2017**.

Full Papers in Proceedings of Conferences/Seminars:

1. Sayantani Dutta and Paramita Bhattacharjee. Modeling of supercritical carbon dioxide extraction of piperine from Malabar black pepper. **Materials Today: Proceedings**, 3, 3238-3252, **2016**. Proceedings of International Conference on Advances in Bioprocess Engineering and Technology 2016 (ICABET 2016), organized by Heritage Institute of Technology, Kolkata.

4. List of Patents:

Nil

5. List of Presentations in National/International Conferences and Seminars:

Oral:

1. Sayantani Dutta and Paramita Bhattacharjee. Spray drying of small cardamom extract obtained by enzyme-assisted supercritical carbon dioxide extraction**. 23rd West Bengal State Science & Technology Congress, Section: Engineering Science and Technology**, Kolkata, February 28-29, **2016.**
2. Sayantani Dutta and Paramita Bhattacharjee. Modeling of supercritical carbon dioxide extraction of piperine from Malabar black pepper. **International Conference on Advances in Bioprocess Engineering and Technology 2016 (ICABET 2016)**, Kolkata, January 20-22, **2016.**
3. Sayantani Dutta and Paramita Bhattacharjee. Enzyme assisted supercritical carbon dioxide extraction for enhanced yield of piperine-rich fraction from black pepper**. 102nd Indian Science Congress: Section on Engineering Sciences**, Mumbai, January 3-7, **2015.**
4. Sayantani Dutta and Paramita Bhattacharjee. Design and characterization of nanoliposomal encapsulates of piperine-rich black pepper extract obtained by enzyme-assisted supercritical carbon dioxide extraction. **7th European Food Safety & Standards Conference**, Athens, Greece, November 13-14, **2017**.

Poster:

1. Kaninika Paul, Sayantani Dutta and Paramita Bhattacharjee, Mitigation of oxidative stress related disorders using 1,8-cineole-rich supercritical carbon dioxide extract of small cardamom seeds, Poster presentation in ***National Symposium on Recent Advances in Medical and Allied Sciences,*** organized by Central Calcutta Society for Advancement of Human Development and Research, July 21, **2016**.

2. Dipan Chatterjee, Sudip Ghosh, Probir Kumar Ghosh, Sayantani Dutta, Sayani Pal, Soumi Chakrabarty, Kaninika Paul and Paramita Bhattacharjee, Recent advances in biotechnology: Non-thermal technologies for development of green products as preventive medicines, Poster presentation in ***National Seminar on Recent Advances in Biotechnology,*** organized by IICB-JU Kolkata Chapter of The Biotech Research Society [BRS(I)], CSIR-Indian Institute of Chemical Biology, Kolkata, April 17, **2015**.
3. Sayantani Dutta, Probir Kumar Ghosh, Sayani Pal, Soumi Chakraborty, Dipan Chatterjee, Sudip Ghosh and Paramita Bhattacharjee, Non-thermal technologies for development of green products as preventive medicine, Poster presentation in ***One-day Symposium on 'Preventive Medicne: Current Prospectives'***, organized by Central Calcutta Society for Advancement of Human Development and Research, July 21, **2014**.

Abstracts in Proceedings/Souvenirs of Conferences/Seminars:

1. Dipan Chatterjee, Sayantani Dutta, Probir Kumar Ghosh and Paramita Bhattacharjee, Supercritical carbon dioxide extraction of anthocyanin from eggplant, piperine from black pepper (enzyme-assisted) and fractionation of coconut copra into lauric acid-rich oil and lauric acid-lean copra meal, in **15th European Meeting on Supercritical Fluids**, Essen, Germany, May 9-11, **2016.**
2. Sayantani Dutta and Paramita Bhattacharjee. Spray drying of small cardamom extract obtained by enzyme-assisted supercritical carbon dioxide extraction**. 23rd West Bengal State Science & Technology Congress, Section: Engineering Science and Technology,** February 28**, 2016.**
3. Dipan Chatterjee, Sudip Ghosh, Probir Kumar Ghosh, Sayantani Dutta, Sayani Pal, Soumi Chakrabarty, Kaninika Paul and Paramita Bhattacharjee, Recent Advances in Biotechnology: Non-thermal Technologies for Development of Green Products as Preventive Medicines, Abstract no. 11, p. 19-20, in Souvenir of **National Seminar on Recent Advances in Biotechnology**, Organized by IICB-JU Kolkata Chapter of The Biotech Research Society [BRS(I)], CSIR-Indian Institute of Chemical Biology, Kolkata, April 17, **2015**.
4. Sayantani Dutta and Paramita Bhattacharjee. Enzyme assisted supercritical carbon dioxide extraction for enhanced yield of piperine-rich fraction from black pepper. **102nd Indian Science Congress: Section on Engineering Sciences,** Mumbai, January 3-7**, 2015.**
5. Sayantani Dutta and Paramita Bhattacharjee. Design and characterization of nanoliposomal encapsulates of piperine-rich black pepper extract obtained by enzyme-assisted supercritical carbon dioxide extraction. Journal of Food: Microbiology, Safety & Hygiene, DOI: 10.4172/2476-2059-C1-005. **7th European Food Safety & Standards Conference**, Athens, Greece, November 13-14, **2017**.

CERTIFICATE FROM THE SUPERVISOR

This is to certify that the thesis entitled "Enzyme-assisted Supercritical Carbon Dioxide Extraction of Active Principles of Black Pepper and Small Cardamom and Applications of the Extracts for Design of Nutraceutical Foods and Supplements" submitted by Smt. Sayantani Dutta, who got her name registered on August 06, 2013, for the award of Ph. D (Engg.) degree of Jadavpur University is absolutely based upon her own work under the supervision of Dr. Paramita Bhattacharjee and that neither her thesis nor any part of the thesis has been submitted for any degree/diploma or any other academic award anywhere before.

P. Bhattacharjee 15.3.2017

Signature of the Supervisor and date with Office Seal

Dr. Paramita Bhattacharjee
Reader
Department of Food Technology & Biochemical Engineering
Jadavpur University, Kolkata-700 032 (India)

ACKNOWLEDGEMENTS

This thesis work would remain incomplete without acknowledging the contribution of those who helped me in the research work.

First of all, I would like to express my sincere gratitude to my Research Guide, Dr. Paramita Bhattacharjee, Reader, Department of Food Technology and Biochemical Engineering (FTBE), Jadavpur University (JU), who constantly guided me and provided valuable suggestions for my work. I am indebted to her for her constant support and encouragement.

I would also express my thankfulness to Prof. Uma Ghosh (Head, Dept. of FTBE) for the Departmental laboratory facilities and her co-operation. I would also like to thank all the faculty members of the Department for their support.

I would like to thank the non-teaching staff of the Department and the University workshop personnel for their help. I am also thankful to the Departmental and Central libraries of the University for books and journals.

I am also thankful to:

Department of Science and Technology, Government of West Bengal (WBDST), India for providing R&D project fellowship.

Late Dr. Chhanda Mandal, Dr. Alok Kumar Hazra and Mr. Soumya Mandal of Ramakrishna Mission Ashrama, Narendrapur, for their assistance in conducting HPTLC analyses.

Late Prof. Tuhinadri Sen and his team, Department of Pharmaceutical Sciences, Jadavpur University, for providing analytical facilities.

Dr. K. K. Chattopadhyay and his team, Director, School of Materials Science and Nanotechnology, Jadavpur University for providing TEM facility.

Mr. Smriti Ranjan Maji, Technical Officer, Central Instrument Facility (P. D. Lab), Bose Institute, Kolkata, for support in GC-MS analyses.

Dr. Satadal Das and his team, Peerless Hospital & B. K. Roy Research Centre, Kolkata, for their support in conducting microbiological analyses.

Dr. Nabarun Bhattacharyya and his team, Centre for Development of Advanced Computing (C-DAC), Kolkata, for providing electronic nose facility.

Dr. Surajit Sinha, Associate Professor and Head, Department of Organic Chemistry, Indian Association for the Cultivation of Science, Jadavpur, for providing NMR facility.

Prof. Rina Ghosh, Department of Organic Chemistry, Jadavpur University, Kolkata for extending her support on NMR and FTIR analyses.

I would also like to thank Dr. O. Yesil-Celiktas for her support in conducting SC-CO_2 treatment of enzyme.

I am also thankful to my labmates Sayani, Soumi, Kaninika and Anupama for their co-operation. I would like to thank my seniors Dr. Dipan Chatterjee, Dr. Sudip Ghosh and Dr. Probir Kumar Ghosh for their help. Past labmates Subhankar, Renuka, Sabyasachi and Kona are also fondly remembered.

I am grateful to my parents and younger sister for their constant inspiration and untiring support. I would also express my gratitude to my late grandparents for their blessings from the Heaven!

Last but not the least, I am ever grateful to God for His love and affection.

I sincerely apologize for any omissions and thank all concerned.

Sayantani Dutta

TABLE OF CONTENTS

Chapter 1

Introduction

Introduction

Spices constitute an important class of nutraceuticals since ancient times. Besides improving the flavor of foods, spices also act as preservatives and have been known to possess medicinal value. In the time of chemical drugs for curing diseases, spices are used extensively in *Ayurveda, Sidha* and *Unani* medicines for alleviating ailments, with success (Peter, 2012). Although spices and condiments are two broad categories of natural nutraceuticals; according to the International Organization for Standardization (ISO), there is no division between spices and condiments and have been described as "*such natural plant or vegetable products or mixtures thereof, in whole or ground form, as are used for imparting flavor, aroma and piquancy to and for seasoning of foods*" (Pruthi, 2014).

India is known as the 'land of spices', which produces more than 65 varieties of spices among total 109 varieties listed by ISO (IBEF, 2016). In 2013, India was the largest producer and exporter of spices in the world (FAOstat, 2016). During 2015-16, a total of 8,43,255 tons of spices and spice products valued at Rs. 16238.23 crore (USD 2482.83 Million) have been exported from India (Spices Board India, 2016). In India, the major spices produced are black pepper, capsicum/chillies, ginger, turmeric and cardamom (small and large) (Pruthi, 2014). Among these spices, the present study envisaged employing black pepper, the 'King of spices' and small cardamom, the 'Queen of spices' for development of novel functional food and dietary supplements.

Black pepper, the 'King of spices'

Black pepper is the dried, fully mature, unripe berry of *Piper nigrum* L., a perennial climber belonging to the family Piperaceae, native to the evergreen forests in the Western Ghats of South India (Ravindran and Kallupurackal, 2001). It is the most important commercial spice consumed globally and occupies 60% of the total volume of the spice trade. The value of the spice trade is known primarily to depend on price of black pepper. India was the third largest producer of black pepper in the world in 2015-16 (Agriwatch, 2016). According to Export Import Data Bank, Department of Commerce, India, 9136.42 tons of black pepper worth USD 7,61,02,755.51 has been exported from India in 2015-16 (Department of Commerce, India, 2016a). Domestic consumption of black pepper is highest in India, compared to other countries (Nedspice, 2015).

Small cardamom, the 'Queen of spices'

Small cardamom, known as the 'Queen of spices', is the third most expensive spice in the world and is extensively employed in food processing globally. It is the dried fruit of a perennial herbaceous plant, *Elettaria cardamomum* (L.) Maton., which belongs to the family Zingiberaceae (Parthasarathy and Prasath, 2012). It is also used widely in *Ayurveda*. India is the second largest producer of small cardamom at present. In 2015, production of small cardamom in India was around 11318.37 tons and domestic consumption alone was about 90% of the produce (Food and Beverage News, 2015). According to Export Import Data Bank, Department of Commerce, India, 822.32 tons of small cardamom seeds worth USD 89,49,745.88 has been exported from India in 2015-16 (Department of Commerce, India, 2016b).

Extraction of *spiceuticals* from spices using green technology

Spiceuticals (bioactive principles or components of spices) are extracted from spices conventionally by hydrodistillation, steam distillation and solvent extractions (Allwyn Sundar Raj et al., 2014). However, these methods are cumbersome, time consuming and the high process temperatures involved in these techniques have detrimental effects on the 'ceutic' properties of the spice extracts. The extracts typically contain residual toxic solvents and undesirable components co-extracted with the target compounds. Hence spice extracts obtained from these conventional extractions are not safe for food applications (Mukhopadhyay, 2000). Therefore, in the present study, green technologies of extraction have been employed to obtain bioactive-rich 'green' extracts of black pepper and small cardamom, appropriate for use in formulation of nutraceutical foods and supplements. The details of the processes developed in the present work for extraction and protection of *spiceuticals* of these spices and formulation of nutraceutical/functional food employing the same have been presented as a graphical abstract in Fig. 1.1.

Extraction of bioactive components from spices employing green technology in compliance with regulatory guidelines, has gained importance in recent times. Among various green techniques of extraction, supercritical fluid extraction (SFE) has gained substantial importance. This extraction technique has many advantages over other green technologies such as selective extraction of bioactive compounds (nutraceutical/*spiceutical*) from the sample matrices; no adverse effect of process temperature on potencies of nutraceutical/*spiceutical* and elimination of cumbersome downstream processing for recovery of the same (Ghosh, 2016). The properties of supercritical fluids (SCF), such as high (liquid-like) density, low (gas-like) viscosity and high diffusivity

provide high penetrating power to SCF into the sample matrix (Chatterjee, 2013). Therefore, extraction of bioactive compounds from spices by SFE is now recommended globally to obtain low volume-high value extracts, safe for food applications.

Supercritical carbon dioxide (SC-CO_2) extraction of spiceuticals from black pepper and small cardamom

Carbon dioxide (CO_2) is the most preferred SCF for extraction since it is natural, clean, generally regarded as safe (GRAS), non-inflammable, non-toxic, non-polluting, inexpensive solvent, most commonly used for natural products (Mukhopadhyay, 2000; Ghosh, 2016). Extractions of *spiceuticals* by SC-CO_2 have been reported by several researchers (Oliveira et al., 2016; Ashraf et al., 2016; Haiyee et al., 2016; Silva and Martínez, 2014; Salea et al., 2013; Chatterjee and Bhattacharjee, 2013).

Piperine, the principal bioactive of black pepper

The characteristic pungent flavor of black pepper is contributed principally by its bioactive component piperine, which is priced at USD 242.84 per kg (Zauba, 2016). India exported piperine worth USD 155,905 in June 2016 (Zauba, 2016). Piperine is known to have therapeutic value and has antioxidant and anti-inflammatory potencies (Naidu and Thippeswamy, 2002; Mittal and Gupta, 2000); enhances bioavailability of several drugs and bioactives (Majeed et al., 1998; Shoba et al., 1998); stimulates the digestive enzymes and has antimutagenic and tumor inhibitory properties (Platel and Srinivasan, 2000; Sunila and Kuttan, 2004).

SC-CO_2 extraction of piperine from black pepper has been previously carried out by some researchers (Dang and Phan, 2014; Lin et al., 2013; Kumoro et al., 2009; Perakis et al., 2005;

Tipsrisukond et al., 1998 and Sovová et al., 1995). One of the objectives of this investigation was to improve the yield of piperine from black pepper by SC-CO_2 extraction, using specific treatment, compared to the yield obtained without the treatment.

1,8-cineole, the principal bioactive of small cardamom

The *spiceutical* of small cardamom is 1,8-cineole which is also known for its therapeutic properties such as antioxidant, anti-inflammatory and antimicrobial potencies (Ghosh, 2014; Kaushik et al., 2010) along with analgesic, antispasmodic and gastroprotective properties (Jamal et al., 2006; Al-Zuhair et al., 1996). Few researchers have worked on SC-CO_2 extraction of 1,8-cineole from small cardamom seeds (Ghosh et al., 2015; Marongiu et al., 2004; Gopalakrishnan and Narayanan, 1991). In this investigation, similar to piperine, the objective was to improve the yield of 1,8-cineole-rich SC-CO_2 extract from small cardamom, using specific treatment. The details of SC-CO_2 extractions of piperine from black pepper and 1,8-cineole from small cardamom have been provided in subsequent chapters of this thesis.

For both black pepper and small cardamom, without any treatment of the feed (spice matrix) during SC-CO_2 extraction, the yields of the *spiceuticals* are low. This renders the extraction process costly and time consuming (for obtaining a specific quantity of the extract) for development of food and therapeutic supplements using these extracts. To investigate the reason, proximate analyses of the spices were conducted and the results revealed that carbohydrate was the major constituent in both the spices. This finding was in agreement with the proximate values for these spices reported by Pruthi (2014). It was opined that starch being the predominant source of carbohydrate in these spices (Figs. 1.2, 1.3), could possibly have impeded the extractions of *spiceuticals* from these spices. Therefore, the primary objective of this study was to explore the

enhancement of yield of *spiceuticals* from black pepper and small cardamom by *in situ* enzymatic hydrolysis of seed starch in the spice matrices (which is the feed in the extraction vessel) concurrently with SC-CO_2 extractions of *spiceuticals*.

SC-CO_2 extraction procedure employed in this study

SC-CO_2 extraction unit employed in this investigation was a laboratory scale 'SCF Green Technology SPE-ED SFE 2' model of Applied Separations, PA, USA (Fig. 1.4). The equipment consists of a precision high pressure pump that maintains the pressure of CO_2 inside the extraction vessels, a refrigerated cooling bath (RCB) to chill the pump head to -2 to -5 °C for liquefaction of gaseous CO_2 and an oven module that holds the extraction vessels [SS316; length (L) = 304.8 mm, internal diameter (i.d.) = 13.9 mm] and maintains the required temperature inside the vessels. The working procedure and limitations of the equipment have been previously described by Ghosh (2016) and Chatterjee (2013) in their Ph.D. theses.

The total time of SC-CO_2 extraction is the summation of static and dynamic time for all extractions. The static time of extraction is the equilibration time, in which inlet valve is kept open and SC-CO_2 passes through the sample matrix within the extraction vessel, while the outlet valve is kept closed. In this time, SC-CO_2 equilibrates with the analyte (*spiceuticals*) (i.e., SC-CO_2 gets saturated with *spiceuticals*) present in the sample matrix inside the extraction vessel. During dynamic time, the outlet valve is kept open and the extract loaded SC-CO_2 passes through a throttle valve and precipitates the extract in the collection vial at reduced atmospheric pressure and temperature, while CO_2 in gaseous form is vented out into the atmosphere through a bubble flow meter. The desired flow rate of gaseous CO_2 is achieved using a micrometering valve attached at the collection end of the extraction module.

In this investigation, SC-CO_2 extraction equipment was operated in two modes: batch mode and continuous mode. In the batch mode of extraction, both static and dynamic time of extraction were employed; while in continuous mode, the dynamic time of extraction alone has been considered. In batch mode, CO_2 was allowed to flush through the extraction vessel for a certain period of time (i.e., static time), during which the outlet valve was kept closed (Fig. 1.5a). After the required static time, the outlet valve was opened and the extract was recovered through the outlet and the micro-metering valves provided at the collection end (Fig. 1.5b). The inlet valve remained open throughout the batch mode of extraction, while the outlet valve was kept open only during the dynamic time of extraction (Fig. 1.5). On the other hand, in the continuous mode, the CO_2 entering through the inlet valve into the sample matrix in the vessel was discharged through the outlet valve along with the extract at a constant flow rate of 1 L/min. Unlike the batch mode, in this mode of extraction, there was no static time and both the inlet and outlet valves were kept open throughout the total extraction time (Fig. 1.6).

Enzyme-assisted treatment of spice matrices in SC-CO_2

SC-CO_2 has been utilized as favorable medium for several enzyme-catalyzed reactions. SC-CO_2 system has been investigated for production of biodiesel, by trans-esterification of lipids extracted from *Scenedesmus sp*. employing lipase (Taher et al., 2015); by lipase-catalyzed methanolysis of canola oil with methanol (Lee et al., 2014) and alcoholysis of corn oil using immobilized lipase as catalyst (Ciftci and Temelli, 2013). Lipase-assisted hydrolysis in SC-CO_2 has also been investigated to obtain free fatty acids (FFA) from Sacha inchi (*Plukenetia volubilis*) oil (Prado and Saldaña, 2013). Application of immobilized lipase has been investigated for determination of vitamin A and E contents in dairy and meat products (Turner et al., 2001).

In another investigation, fibrous cellulose was enzymatically acylated with vinyl laurate in SC-CO_2 to obtain cellulose laurate, employing immobilized lipase, and immobilized esterase and immobilized cutinase (Gremos et al., 2012).

In the current study, α-amylase (E.C.3.2.1.1) has been employed *in situ* in SC-CO_2 individually with black pepper and small cardamom, for hydrolysis of the seed starch for improved yield of *spiceuticals*. Researches on α-amylase-assisted SC-CO_2 treatments/extractions for enhanced yields and/or quality of products are scarce. On the day this thesis was compiled, 24 published research articles were cited on Scopus web engine on use of α-amylase in SC-CO_2 system. Among them, three reports reported in this thesis, are three research papers of my work which were not reported previously by other researchers. Lee et al. (1993) investigated hydrolysis of corn starch powder in SC-CO_2 by α-amylase and glucoamylase to enhance the production of glucose. To the best of my knowledge, there is no other report on α-amylase-assisted SC-CO_2 extraction till date.

Encapsulation of extracts for enhanced shelf-lives of *spiceuticals*

The bioactive-rich extracts obtained in this investigation were found to be unstable in the presence of oxygen, heat, light and moisture. Therefore, encapsulation technology was employed in this study to improve the shelf-lives of the extracts, by protecting the *spiceuticals* from degradation.

Spray drying technology

Among the different encapsulation technologies, spray drying is most commonly employed for microencapsulation in food industries (Chatterjee, 2013). Spray drying has reportedly been

conducted by few researchers for encapsulation of *spiceuticals* employing different wall materials, such as, encapsulation of Turkish oregano extract using maltodextrin and gum arabic (Baranauskaite et al., 2016), saffron extract employing mixture of maltodextrin, gum arabic and gelatin (Rajabi et al., 2015), SC-CO_2 extract of clove buds using maltodextrin and gum arabic for encapsulation of eugenol (Chatterjee and Bhattacharjee, 2013) and encapsulation of curcumin in casein nanoparticles (Pan et al., 2013).

In this investigation, 1,8-cineole-rich small cardamom extract obtained by enzyme-assisted SC-CO_2 extraction was microencapsulated by spray drying using maltodextrin and gum arabic as wall materials. The spray drying process was conducted employing Mini Spray Dryer B-290 model of Buchi, Switzerland. The working principle of spray dryer has been elaborated by Chatterjee (2013). The spray drying process parameters employed in this investigation are detailed in the respective chapters of this thesis. On the day this thesis was compiled, two published research articles were cited on Scopus web engine on encapsulation of small cardamom extract by spray drying. These two reports include one of my research papers on the work reported in this thesis which has not been reported by other workers.

Nanoliposomal encapsulation of spiceuticals

Liposomes are closed, continuous, vesicular structures composed mainly of phospholipid bilayers that incorporate hydrophilic molecules inside the aqueous core and lipophilic molecules in their bilayer (Mozafari and Mortazavi, 2005; Riaz, 1996). Liposome-mediated drug delivery is one of the advanced methods for targeted delivery of bioactives, which can improve the therapeutic activity and safety of bioactives along with sustained release of the same for prolonged periods (Hasan et al., 2014).

Liposomes have promising applications in the food industries for encapsulation and controlled release of food constituents besides enhancing the bioavailability, stability and shelf-life of its sensitive ingredients (Mozafari et al., 2008). Liposomal encapsulation of *spiceuticals* has reportedly been conducted, such as, nanoliposomes formulated with nisin co-encapsulated with garlic extract (Pinilla and Brandelli, 2016), curcumin (Chen et al., 2015), safranal (Malaekeh-Nikouei et al., 2013) and crocin (Rastgoo et al., 2013). In this investigation, piperine in SC-CO_2 extract of black pepper was encapsulated by formulation of nanoliposomes which can work as vehicles for *spiceuticals* in food engineering. On the day this thesis was compiled, five published research articles were cited on Scopus web engine on nanoliposomal encapsulation of piperine. These five reports include one research article of my work reported in this thesis which has not been previously reported by other researchers.

Product development employing SC-CO_2 extracts of black pepper and small cardamom

Black pepper and small cardamom extracts obtained by enzyme-assisted SC-CO_2 extractions could be termed as 'herbal preparations' and their respective encapsulates 'finished herbal products', in accordance with WHO guidelines (2000). The extracts were employed as natural antioxidants in formulation of novel functional foods. It was envisaged that these extracts would enhance the nutraceutical properties along with shelf-lives of the designed food products. Besides the extracts *per se*, the sample matrices, post-extraction, have also been utilized in formulation of functional or nutraceutical foods, to allow complete utilization of the phytochemical properties retained in the residual spice matrices. The products to be developed in this work have been shown in Fig. 1.7.

The present study focuses on:

Part I: Black pepper

- Extraction of major bioactive compound piperine from black pepper by SC-CO_2 technology; optimization and packed bed characterization of the process for futuristic scale up to pilot plant and/or industrial extractions and estimation of extraction kinetics of piperine from black pepper.
- α-amylase-assisted SC-CO_2 extraction for enhanced yield of piperine-rich extract from black pepper.
- Formulation of black pepper cookies as nutraceutical food and assessment of their shelf-lives using electronic nose technology.

Part II: Small cardamom

- α-amylase-assisted SC-CO_2 extraction for enhanced yield of 1,8-cineole-rich extract from small cardamom.
- Formulation of small cardamom cookies as functional food and assessment of their shelf-lives using electronic nose technology.

Part III: Encapsulation of black pepper and small cardamom extracts

- Microencapsulation of 1,8-cineole rich-small cardamom extract using spray drying and design of nutraceutical custard with the encapsulate.
- Nanoliposomal encapsulation of piperine-rich black pepper extract.

The thesis has been divided into the following sections:

Supercritical carbon dioxide extraction of piperine from black pepper

Black pepper, the 'King of Spices' is globally known for its pungency contributed by its major bioactive compound, piperine. The first section of this thesis reports on the SC-CO_2 extraction of piperine from Malabar black pepper. A 3^3 full factorial design of experiment has been employed for optimization of the extraction process parameters to obtain an extract having maximum yield of piperine along with the best combination of phytochemical properties. Solubilities of piperine in SC-CO_2 in different temperature-pressure regimes were determined and a correlated equation was generated for prediction of solubility of piperine in SC-CO_2 under different extraction conditions. Estimation of hydrodynamic parameters of the packed bed (of black pepper) and generation of mathematical relationship among the dimensionless numbers of mass transfer were conducted for scaling up this laboratory scale extraction to pilot plant and futuristic commercial scales. The results obtained in this work have been presented in **section 2.1 of Chapter 2**.

It was opined that starch being one of the major constituents of the black pepper coat, possibly impedes extraction of piperine from black pepper. Therefore, to enhance the yield of piperine-rich extract, α-amylase was employed *in situ* in SC-CO_2 extraction for single step hydrolysis of black pepper starch and concomitant extraction of piperine from the hydrolyzed pepper matrix. The SC-CO_2 extraction equipment was operated in two modes in this study. All extracts were characterized for their phytochemical and antimicrobial potencies. Gas chromatography-mass spectrometry (GC-MS) analyses were performed for identification of major compounds present in the extracts. Enhancement of specific activity of α-amylase in SC-CO_2 conditions was also investigated. ^{1}H NMR analysis was performed to study the structural and/or conformational

changes of the recovered enzyme. This work has been elaborately presented in **section 2.2 of Chapter 2**.

The piperine-rich extract of black pepper obtained from enzyme-assisted SC-CO_2 extraction was successively employed for design of nutraceutical/functional cookies with envisaged high shelf stability. Apart from the extract, the sample matrix of black pepper, post-extraction, was also employed in formulation of cookies. Evaluation of nutraceutical properties of black pepper cookies was conducted and shelf-lives of the cookies were assessed by e-nose technology using 'spoilage index'. The work has been elaborated in **section 2.3 of Chapter 2**.

Supercritical carbon dioxide extraction of 1,8-cineole from small cardamom

Small cardamom, the 'Queen of Spices' is extensively used in food processing for its pleasant flavour and in *Ayurveda* for its therapeutic properties. Similar to black pepper, one of the major constituents of small cardamom seeds is starch. This section describes α-amylase-assisted SC-CO_2 extraction to hydrolyze the seed starch to achieve enhanced yield of 1,8-cineole-rich extract from Alleppey green small cardamom. The extracts were characterized for their pungency and phytochemical and antimicrobial potencies. GC-MS analyses revealed the major compounds of these extracts. The details of this work have been presented in **section 3.1 of Chapter 3**.

In the subsequent section, small cardamom extract obtained by α-amylase-assisted SC-CO_2 extraction was employed in designing nutraceutical cookies to enhance the nutraceutical properties along with shelf-lives of the same. The post-extraction sample matrix was also employed in formulation of functional cookies. E-nose technology was employed to estimate

shelf-lives of cookies. The detailed methodologies and findings of this section have been described in **section 3.2 of Chapter 3**.

Encapsulation of black pepper and small cardamom extracts

The 1,8-cineole-rich small cardamom extract obtained from enzyme-assisted SC-CO_2 extraction was microencapsulated to enhance the shelf stability of 1,8-cineole in the encapsulate. The microencapsulation was carried out by spray drying using maltodextrin and gum arabic as wall materials. Optimization of microencapsulation parameters was conducted on the basis of microencapsulation efficiencies of the encapsulates. The encapsulate obtained at the optimized condition was characterized and subjected to FE-SEM, EDX, DSC analyses. *In vitr*o release of 1,8-cineole from the encapsulate and evaluation of shelf stability of the same were also carried out. This work has been elaborated in detail in **section 4.1 of Chapter 4**.

The encapsulate of small cardamom extract was further employed in designing a new antioxidant-fortified custard to minimize the loss of the phytochemical properties of the extract during thermal processing (necessary for custard preparation). The newly formulated custard was characterized for sensory, physicochemical and nutraceutical properties. This work has been critically assessed in **section 4.2 of Chapter 4**.

Piperine, the major bioactive compound of black pepper extract obtained from enzyme-assisted SC-CO_2 extraction (described in section 2.2 of Chapter 2), is highly photosensitive. Therefore, the piperine-rich extract needs to be protected from light, heat, oxygen and other environmental hazards for long term storage-stability. Nanoliposomal encapsulation of this extract was conducted to ensure sustained release of piperine and concomitantly minimize its degradation

during storage. Optimization of encapsulation parameters was carried out to obtain stable nanoliposomes with highest encapsulation of piperine. *In vitro* release of piperine and storage stability of nanoliposome of black pepper extract was carried out. The data obtained from this study has been elaborated in **section 4.3 of Chapter 4**.

The specific research objectives have been mentioned in the respective sections in the chapters along with a line on novelty of each investigation. The highlights of the important findings have been presented in the 'Summary'; and 'Suggestions for Future Work' has been provided at the end of the thesis.

References

Agriwatch (2016). Spices-monthly-research-report, July 06, 2016. Indian Agribusiness Systems Pvt. Ltd. (IASL), India.

AllwynSundarRaj A., I S. A., Seihenbalg S. S., Tiroutchelvamae D. and Ranganathan T. V. (2014). Review on- Recent trends in isolation of antioxidants from spices and its biological effects of essential oils. *International Journal of Engineering Research and Applications*, **4**, 75-84.

Al-Zuhair H., El-Sayeh B., Ameen H. A., and Al-Shoora H. (1996). Pharmacological studies of cardamom oil in animals. *Pharmacological Research*, **34**, 79-82.

Ashraf H., Butt M. S., Asghar A., and Shahid M. (2016). Comparative study of conventional solvent and supercritical fluid extracts of turmeric using high performance liquid chromatography. *Pakistan Journal of Agricultural Sciences*, **53**, 941- 946.

Baranauskaite J., Ivanauskas L., Masteikova R., Kopustinskiene D., Baranauskas A., and Bernatoniene J. (2016). Formulation and characterization of Turkish oregano microcapsules prepared by spray-drying technology. *Pharmaceutical Development and Technology*, http://dx.doi.org/10.1080/10837450.2016.1189934.

Chatterjee D. (2013). Studies in supercritical carbon dioxide extraction technology for development of novel supplements. *Ph.D. Thesis, Jadavpur University*, India.

Chatterjee D. and Bhattacharjee P. (2013). Supercritical carbon dioxide extraction of eugenol from clove buds. *Food and Bioprocess Technology*, **6**, 2587–2599.

Chen X., Zou L., Niu J., Liu W., Peng S., and Liu C. (2015). The stability, sustained release and cellular antioxidant activity of curcumin nanoliposomes. *Molecules*, **20**, 14293-14311.

Ciftci O. N., and Temelli F. (2013). Enzymatic conversion of corn oil into biodiesel in a batch supercritical carbon dioxide reactor and kinetic modeling. *The Journal of Supercritical Fluids*, **75**, 172–180.

Dang, Q. T., and Phan, N. N. (2014). Optimization of supercritical CO_2 extraction of oleoresin from black pepper (*Piper nigrum* L.) and antioxidant capacity of the oleoresin. *International Food Research Journal*, **21**, 1489-1493.

Department of Commerce (2016a). Export:: Commodity-wise all countries, Commodity: 09041130, July 25, 2016. Department of Commerce, India.

Department of Commerce (2016b). Export:: Commodity-wise all countries, Commodity: 09083220, July 25, 2016. Department of Commerce, India.

FAOSTAT (2016). Value of agricultural production, Food and Agriculture Organization of the United Nations. Accessed from: http://www.fao.org/faostat/en/#data, on November 15, 2016.

Food and Beverage News (2015). Cardamom - The third most expensive spice in the world, FNB News, India. Accessed from: www.fnbnews.com/Spices/Cardamom---The-third-most-expensive-spice-in-the-world, on November 16, 2016.

Ghosh P. K. (2016). Studies on supercritical carbon dioxide extraction, encapsulation and gamma irradiation technologies for development of novel supplements from food and horticulture products. *Ph.D. Thesis, Jadavpur University*, India.

Ghosh S. (2014). Studies on novel herbal formulations as food and therapeutic supplements using solvent-less extraction technologies. *Ph.D. Thesis, Jadavpur University*, India.

Ghosh S., Bhattacharjee P., and Das S. (2015). 1,8-cineol-rich cardamom seed (*Elettaria cardamomum*) extracts using green technologies and conventional extractions: Process analysis, phytochemical characterization, and food application. *Separation Science and Technology*, **50**, 1974-1985.

Gopalakrishnan N., and Narayanan C. S. (1991). Supercritical carbon dioxide extraction of cardamom, *Journal of Agricultural and Food Chemistry*, 39, 1976-1970.

Govindarajan V. S., and Stahl W. H. (1977). Pepper- chemistry, technology, and quality evaluation. *C R C Critical Reviews in Food Science and Nutrition*, **9**, 115-225.

Gremos S., Kekos D., and Kolisis F. (2012). Supercritical carbon dioxide biocatalysis as a novel and green methodology for the enzymatic acylation of fibrous cellulose in one step. *Bioresource Technology*, **115**, 96-101.

Haiyee Z. A., Shah S. H. M., Ismail K., Hashim N., and Ismail W. I. W. (2016). Quality parameters of *Curcuma longa* L. extracts by supercritical fluid extraction (SFE) and ultrasonic assisted extraction (UAE). *Malaysian Journal of Analytical Sciences*, **3**, 626-632.

Hasan, M., Belhaj, N., Benachour, H., Barberi-Heyob, M., Kahn, C.J.F., Jabbari, E., Linder, M., Arab-Tehrany, E., 2014. Liposome encapsulation of curcumin: physico-chemical

characterizations and effects on MCF7 cancer cell proliferation. *International Journal of Pharmaceutics*, **461**, 519-528.

IBEF (India Brand Equity Foundation) (2016). Spices statistics. Accessed from: http://www.teacoffeespiceofindia.com/spice/spice-statistics, on November 15, 2016.

Jamal A., Javed K., Aslam M., and Jafri M. A. (2006). Gastroprotective effect of cardamom, *Elettaria cardamomum* Maton. fruits in rats. *Journal of Ethnopharmacology*, **103**, 149-153.

Kaushik P., Goyal P., Chauhan A., and Chauhan G. (2010). *In vitro* evaluation of antibacterial potential of dry fruit extracts of *Elettaria cardamomum* Maton (chhoti elaichi). *Iranian Journal of Pharmaceutical Research*, **9**, 287-292.

Kumoro A. C., Singh H., and Hasan M. (2009). Solubility of piperine in supercritical and near critical carbon dioxide. *Chinese Journal of Chemical Engineering*, **17**, 1014-1020.

Lee D., Jho Y., and Lee C.S. (2014). Effects of soybean and canola oil-based biodiesel blends on spray, combustion, and emission characteristics in a diesel engine. *Journal of Energy Engineering*. DOI: http://dx.doi.org/10.1061/(ASCE)EY.1943-7897.0000160

Lee H. S., Lee W. G., Park S., Lee H., and Chang H. N. (1993). Starch hydrolysis using enzyme in supercritical carbon dioxide. *Biotechnology Techniques*, **7**, 267-270.

Lin T. M., Ping T. S., Saptoro A., and Freddie P. (2013). Mass transfer coefficients and correlation of supercritical carbon dioxide extraction of Sarawak black pepper. *International Journal of Food Engineering*. DOI 10.1515/ijfe-2012-0219.

Majeed M., Badmaev V., Rajendran R. (1998). Use of piperine as a bioavailability enhancer. *US Patent* 5744161 A.

Malaekeh-Nikouei B., Mousavi S. H., Shahsavand S., Mehri S., Nassirli H., and Moallem S. A. (2013). Assessment of cytotoxic properties of safranal and nanoliposomal safranal in various cancer cell lines. *Phytotherapy Research*, **27**, 1868-1873.

Marongiu B., Piras A., and Porcedda S. (2004). Comparative analysis of the oil and supercritical CO_2 extract of *Elettaria cardamomum* (L.) Maton. *Journal of Agricultural and Food Chemistry*, **52**, 6278-6282.

Mittal, R., and Gupta, R. L. (2000). In vitro antioxidant activity of piperine. *Methods and Findings in Experimental and Clinical Pharmacology*, **22**, 271.

Mozafari, M.R., Johnson, C., Hatziantoniou, S., Demetzos, C., 2008. Nanoliposomes and their applications in food nanotechnology. *Journal of Liposome Research*, **18**, 309-327.

Mozafari, M.R., Mortazavi, S.M., 2005. *Nanoliposomes: from Fundamentals to Recent Developments*. Trafford Pub. Ltd., Oxford, UK.

Mukhopadhyay M. (2000). Spice Extracts. In: *Natural Extracts using Supercritical Carbon dioxide*, CRC Press, Boca Raton, pp. 177-200.

Naidu K. A., and Thippeswamy N. B. (2002). Inhibition of human low density lipoprotein oxidation by active principles from spices. *Molecular and Cellular Biochemistry*, **229**, 19-23.

Nedspice (2015). Pepper crop report 2015. Nedspice, Netherlands. Accessed from: www.nedspice.com/upload/docs/Nedspice_Pepper_Crop_report_2015.pdf, on November 15, 2016.

Oliveira M. S. de, Costa W. A. da, Pereira D. S., Botelho J. R. S., Menezes T. O. de A., Andrade E. H. de A., Silva S. H. M. da, Filho A. P. da S. S., and Carvalho R. N. de (2016). Chemical composition and phytotoxic activity of clove (*Syzygium aromaticum*) essential oil obtained with supercritical CO_2. *The Journal of Supercritical Fluids*. http://dx.doi.org/10.1016/j.supflu.2016.08.010

Pan K., Zhong Q., and Baek S. J. (2013). Enhanced dispersibility and bioactivity of curcumin by encapsulation in casein nanocapsules. *Journal of Agricultural and Food Chemistry*, **61**, 6036-6043.

Parthasarathy V. A., and Prasath D. (2012). Cardamom. In: *Handbook of Herbs and Spices*, vol. 1, Peter K.V. (Ed.), CRC Press, Boca Raton, pp. 131-170.

Perakis C., Louli V., and Magoulas K. (2005). Supercritical fluid extraction of black pepper oil. *Journal of Food Engineering*, **71**, 386–393.

Peter K. V. (2012). Introduction to herbs and spices: definitions, trade and applications. In: *Handbook of Herbs and Spices*, vol. 1, Peter K.V. (Ed.), CRC Press, Boca Raton, pp. 1-24.

Pinilla C. M. B., and Brandelli A. (2016). Antimicrobial activity of nanoliposomes co-encapsulating nisin and garlic extract against Gram-positive and Gram-negative bacteria in milk. *Innovative Food Science and Emerging Technologies*, **36**, 287-293.

Platel K., and Srinivasan K. (2000). Influence of dietary spices and their active principles on pancreatic digestive enzymes in albino rats. *Nahrung*, **44**, 158-163.

Prado G. H. C., and Saldaña M. D. A. (2013). Optimization of enzymatic hydrolysis of sacha inchi oil using conventional and supercritical carbon dioxide processes. *Journal of the American Oil Chemists' Society*, **90**, 731-742.

Pruthi J. S. (2014). *Spices and Condiments*, National Book Trust, India.

Rajabi H., Ghorbani M., Jafari S. M., Mahoonak A. S., and Rajabzadeh G. (2015). Retention of saffron bioactive components by spray drying encapsulation using maltodextrin, gum Arabic and gelatin as wall materials. *Food Hydrocolloids*, **51**, 327-337.

Rastgoo M., Hosseinzadeh H., Alavizadeh H., Abbasi A., Ayati Z., Jaafari M. R. (2013). Antitumor activity of PEGylated nanoliposomes containing crocin in mice bearing C26 colon carcinoma. *Planta Medica*, **79**, 447-451.

Ravindran P. N., and Kallupurackal J. A. (2001). Black pepper. In: *Handbook of Herbs and Spices*, vol. 1, Peter K. V. (Ed.), CRC Press, Boca Raton, pp. 62-110.

Riaz, M., 1996. Liposomes preparation methods. *Pakistan Journal of Pharmaceutical Sciences*, **19**, 65-77.

Salea R., Widjojokusumo E., Hartanti A. W., Veriansyah B., and Tjandrawinata R. R. (2013). Supercritical fluid carbon dioxide extraction of Nigella sativa (black cumin) seeds using taguchi method and full factorial design. *Biochemical Compounds*. DOI: 10.7243/2052-9341-1-1.

Shoba G., Joy D., Joseph T., Majeed M., Rajendran R., and Srinivas P. S. S. R. (1998). Influence of piperine on the pharmacokinetics of curcumin in animals and human volunteers. *Planta Medica*, **64**, 353-356.

Silva L. P. S., and Martínez J. (2014). Mathematical modeling of mass transfer in supercritical fluid extraction of oleoresin from red pepper. *Journal of Food Engineering*, **133**, 30–39.

Sovová H., Jez J., Bártlová M., and St'astová J. (1995). Supercritical carbon dioxide extraction of black pepper, *The Journal of Supercritical Fluids*, **8**, 295-301.

Spices Board India (2016). Major itemwise export, Spices Board India. Accessed from: http://www.indianspices.com/export/major-itemwise-export, on November 15, 2016.

Sunila E. S., and Kuttan G. (2004). Immunomodulatory and antitumor activity of *Piper longum* Linn. and piperine. *Journal of Ethnopharmacology*, **90**, 339-46.

Taher H., Al-Zuhair S., Al-Marzouqi A., Haik Y., and Farid M. (2015). Growth of microalgae using CO_2 enriched air for biodiesel production in supercritical CO_2. *Renewable Energy*, **82**, 61-70.

Tipsrisukond N., Fernando L. N., and Clarke A. D. (1998). Antioxidant effects of essential oil and oleoresin of black pepper from supercritical carbon dioxide extractions in ground pork. *Journal of Agricultural and Food Chemistry*, **46**, 4329-4333.

Turner C., King J. W., and Mathiasson L. (2001). On-line supercritical fluid extraction/enzymatic hydrolysis of vitamin A esters: A new simplified approach for the determination of vitamins A and E in food. *Journal of Agricultural and Food Chemistry*, **49**, 553-558.

WHO (World Health Organization). (2000). General guidelines for methodologies on research and evaluation of traditional medicine, Available at: http://apps.who.int/medicinedocs/en/d/Jwhozip42e/4.1.html, Accessed on November 3, 2015.

YourArticleLibrary (2016). Cardamom: Sources, preparation and uses (with diagram). Accessed from: http://www.yourarticlelibrary.com/biology/plants/cardamom-sources-preparation-and-uses-with-diagram/49816/, on November 17, 2016.

Zauba (2016). Export analysis and trends of piperine. Legumex Impex Pvt. Ltd., India. Accessed from: https://www.zauba.com/exportanalysis-PIPERINE, on November 15, 2016.

Figures

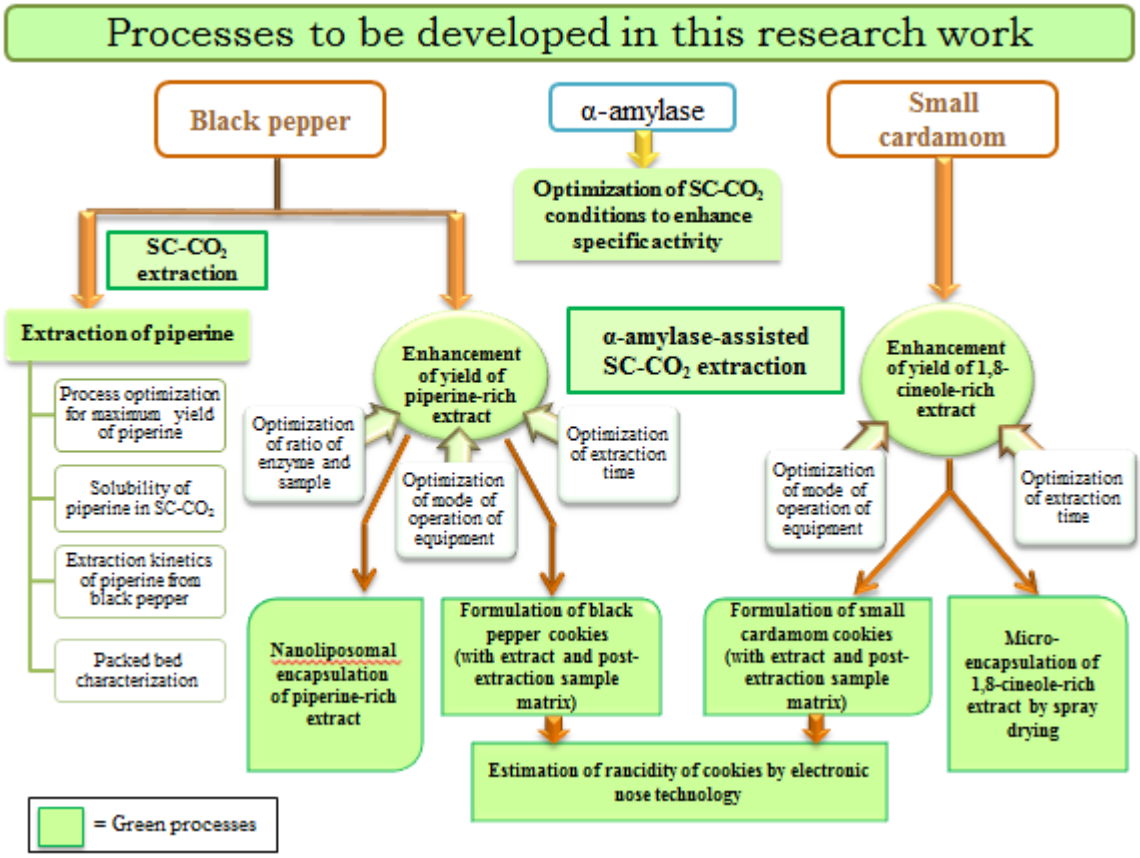

Fig. 1.1. Processes to be developed in this study using green technology.

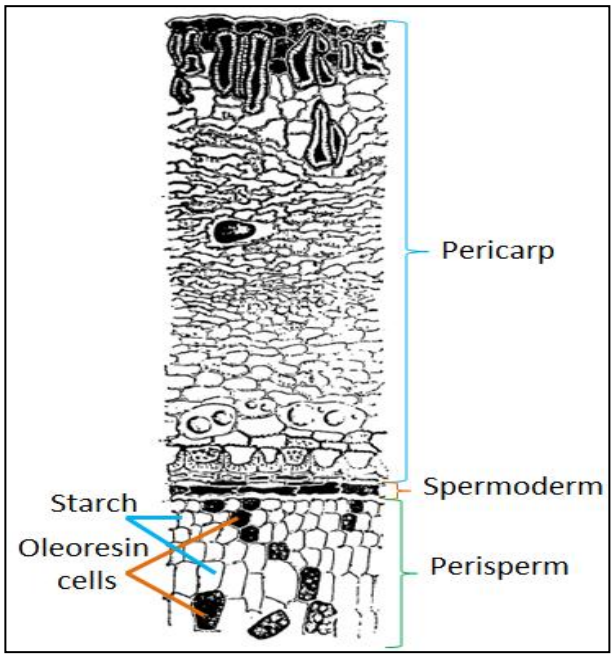

Fig. 1.2. Structural details in cross section of black pepper berry, displaying oleoresin cells surrounded by starch granules (adapted from Govindarajan and Stahl, 1977).

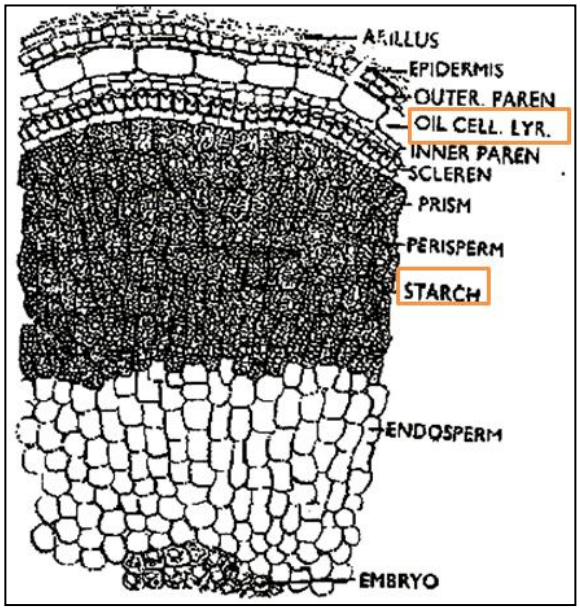

Fig. 1.3. Structural details in cross section of small cardamom seed, displaying positions of oil cells and starch granules (adapted from YourArticleLibrary, 2016).

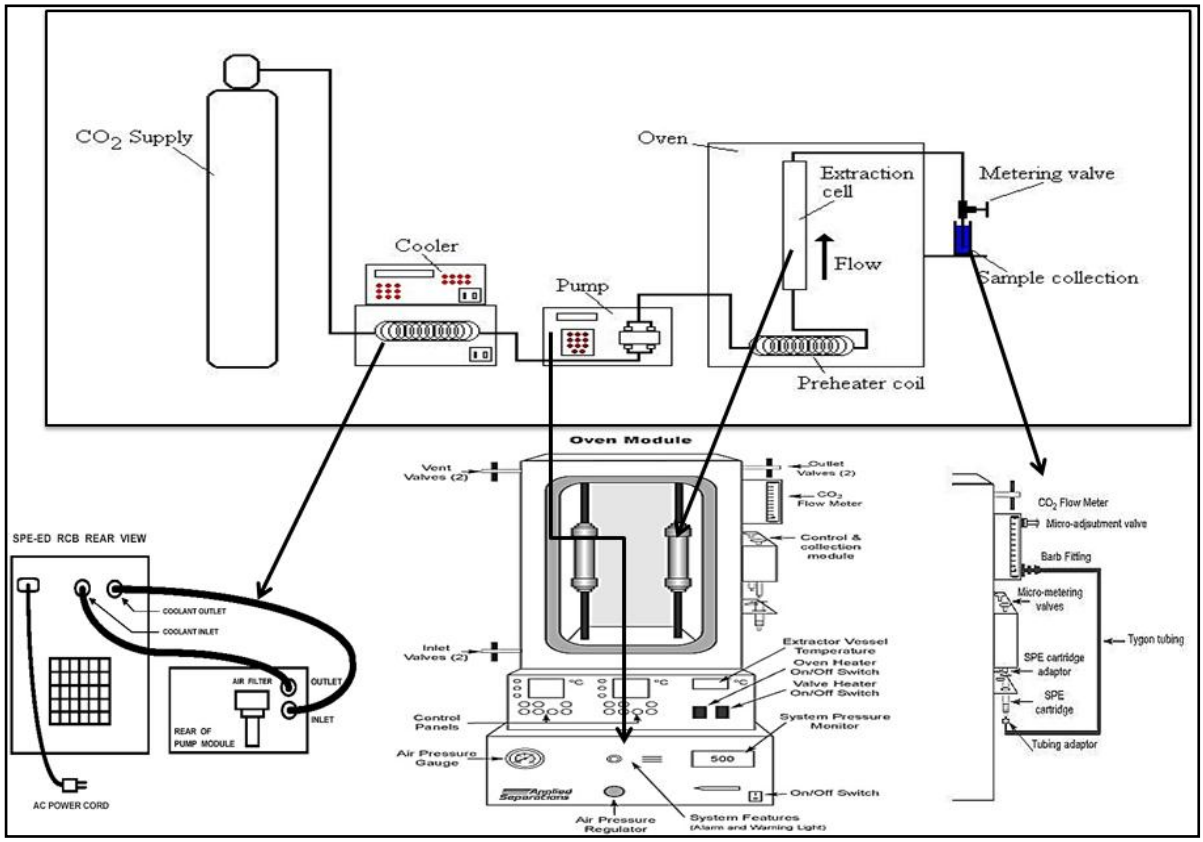

Fig. 1.4. Schematic diagram of SC-CO_2 extraction unit.

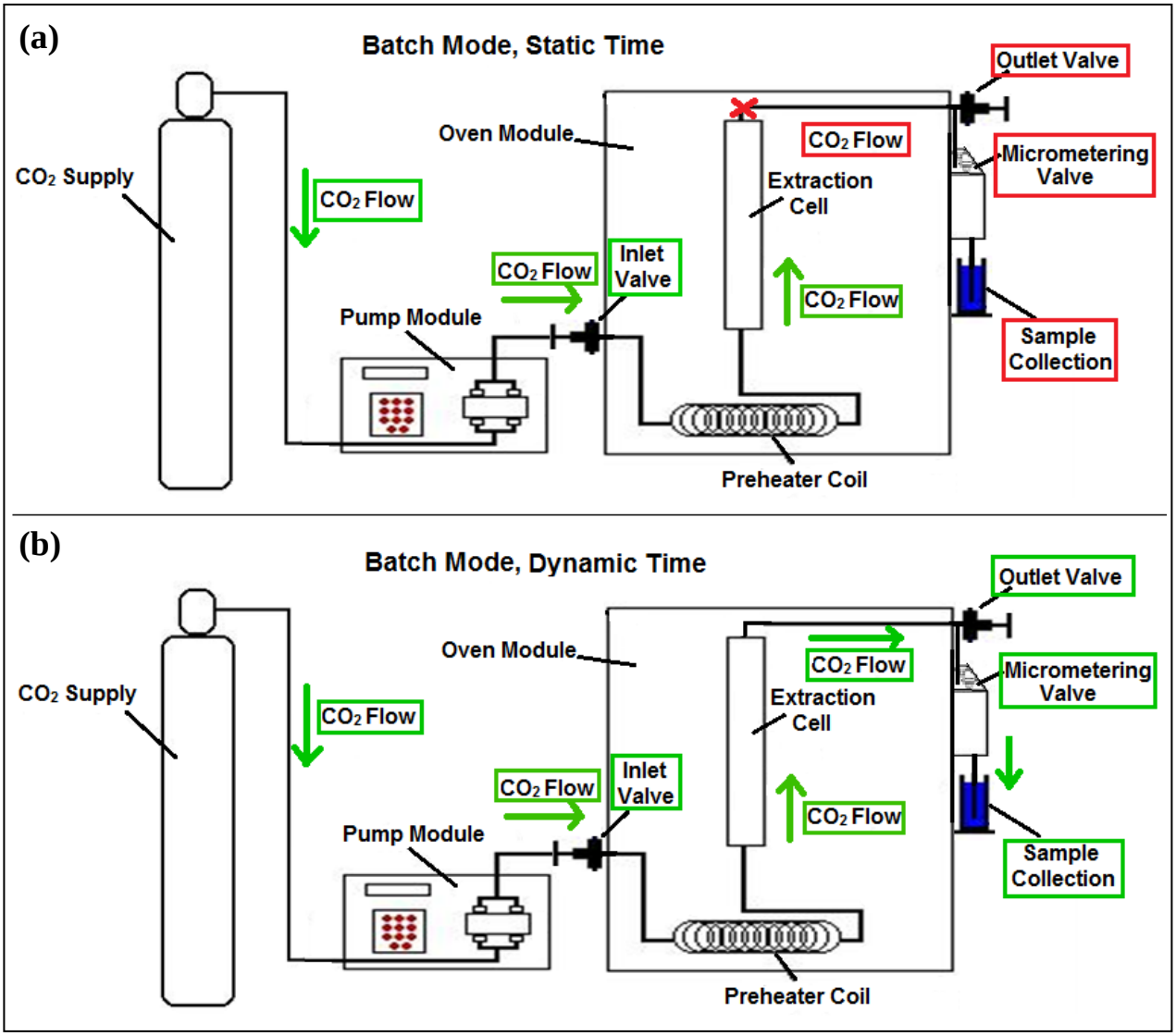

Fig. 1.5. Schematic diagram of batch mode of SC-CO_2 extraction. a) Static time of extraction, b) Dynamic time of extraction.

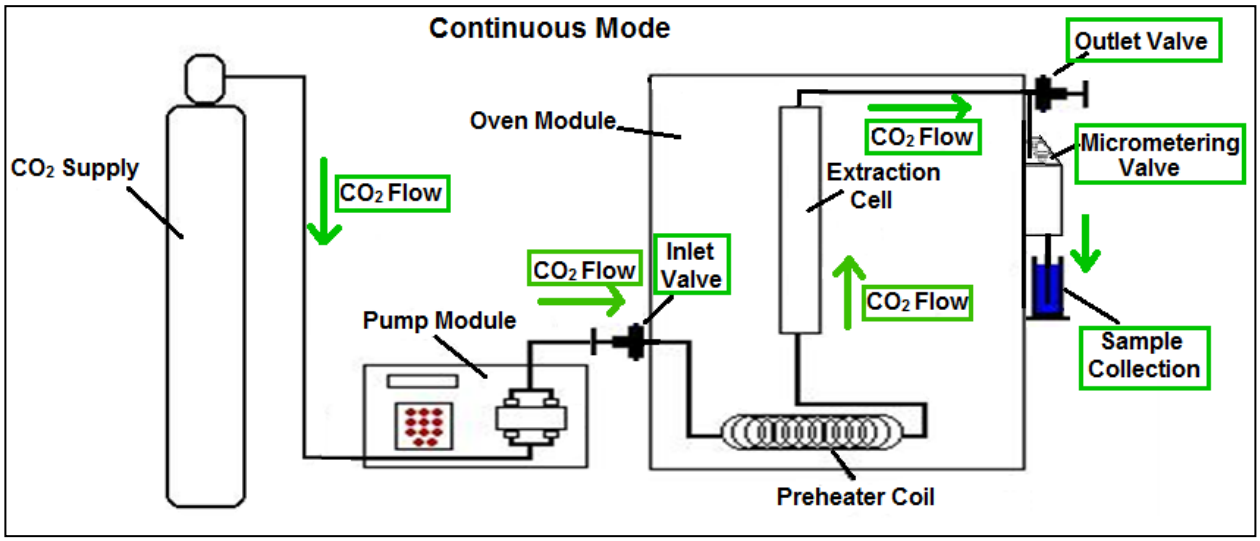

Fig. 1.6. Schematic diagram of continuous mode of SC-CO_2 extraction.

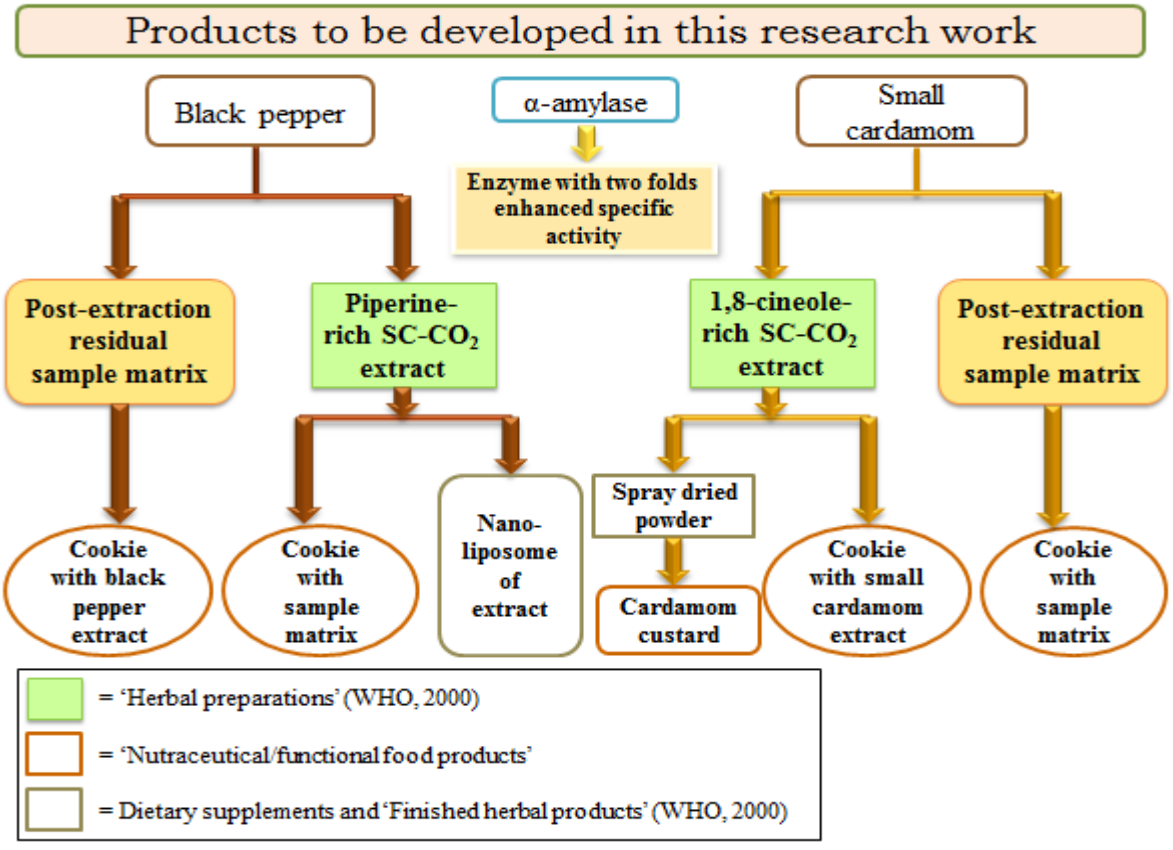

Fig. 1.7. Products to be developed in this study using green technology.

Chapter 2

Supercritical carbon dioxide extraction of piperine from black pepper

Section 2.1

Supercritical carbon dioxide extraction of piperine from black pepper: Process optimization, packed bed characterization and extraction kinetics

Introduction

Extraction of piperine from black pepper is reportedly carried out using organic solvents in a Soxhlet assembly (Kapoor et al., 2009; Singh et al., 2004) or by using standard shake flasks (Sunila and Kuttan, 2004). However, these solvent extraction techniques are not recommended at present (detailed in Chapter 1), which necessitates employing SC-CO_2 extraction, for obtaining piperine-rich, safe natural extracts for food and therapeutic applications.

The best Indian black pepper known worldwide for its excellent aroma, flavor and pungency is the Malabar pepper (Ismadji and Bhatia, 2003). The present investigation is focused on optimization of SC-CO_2 extraction parameters of pressure, temperature and time to obtain maximum yield of piperine from black pepper. The solubility of piperine in SC-CO_2 in different temperature-pressure regimes has also been investigated. The investigation also encompasses kinetics of extraction and characterization of the packed bed by empirical equations using dimensionless numbers of mass transfer.

Sovová et al. (1995) have worked on SC-CO_2 extraction of black pepper (cultivar not reported) and obtained extracts containing both piperine and essential oil. They simulated the experimental results by extended Lack's model using mass transfer coefficients in the solvent and solid phase with grinding efficiency as parameters. However, their approach, experimental parameters studied (280±0.1 bar pressure, 24-60 °C temperature, 6-61 g batch size with mean particle size of 0.05 mm), and most importantly, the variety of black pepper investigated are not similar to those

reported in the current investigation. Kumoro et al. (2009) have studied solubility of pure piperine (97%) at near critical and supercritical conditions of CO_2 (pressures ranging from 100 to 200 bar and temperatures at 20, 27, 40, 50 and 60 °C) in a dynamic extraction apparatus and found increase in solubility with increasing pressure at all temperatures. The authors have used 'Chrastil model' and 'dilute solution model' to correlate the solubility data with density of CO_2. However, a pure chemical standard of piperine has been used in their study.

In the current investigation, optimization of the process parameters of SC-CO_2 extraction has been performed using a three-level full factorial design to selectively extract maximum amount of piperine from black pepper matrix. Thereafter, solubility of piperine in SC-CO_2 in different temperature-pressure regimes have been determined to explain the differences in yields of piperine at different extraction conditions and to obtain a correlated equation for prediction of solubility of piperine in SC-CO_2 under different extraction conditions. Modeling the process in terms of hydrodynamic parameters of the packed bed (of black pepper) using dimensionless numbers of mass transfer was carried out to aid in futuristic pilot plant and commercial scale extraction of piperine using the mathematical relationship among the dimensionless numbers. This approach of complete characterization of laboratory scale SC-CO_2 extraction of piperine from black pepper is essential for scale up process operations of the *spiceutical*. To the best of my knowledge, this work reports for the first time on these aspects of modeling the SC-CO_2 extraction of piperine from Malabar black pepper matrix.

Materials and Methods

Materials

Malabar Garbled black pepper was procured from Spices Board, Cochin, India. Standard piperine (97% pure) was procured from Sigma, India; methanol, ethanol and *n*-hexane were procured from E-Merck, India. All chemicals were of AR grade. CO_2 (food grade) was procured from BOC India Ltd., Kolkata, India.

Characterization of black pepper powder

Black pepper berries were ground using an electric mixer grinder (HL 1618, Philips, India) and particle diameters were determined using the sieve analysis method by screening the black pepper powder through a set of standard sieves in a sieve shaker in accordance with the method reported by Bhattacharjee et al. (2012).

From preliminary SC-CO_2 extractions, it was observed that black pepper powder with mean particle diameter (d_p) higher than 0.42 mm, resulted in lower extract yield (2.01 g extract/100 g dry black pepper) owing to decreased surface to volume ratio of the powder in the packed bed; while a lower d_p resulted in tight packing of sample matrix in the extraction vessel, restricting free channeling of SC-CO_2 through the sample bed. This lowered the mass transfer rate resulting in decreased yield of extract. Therefore, d_p of black pepper was maintained at 0.42±0.02 mm for successive experiments.

Black pepper powder was subjected to proximate analyses by standard methods. Moisture (Dean and Stark method, AOAC official method 986.21, 2006); protein (Kjeldahl method, AOAC official method 984.13, 2006); fat (AOAC official method 920.39A, 2006); crude fibre (AOAC

official method 978.10, 2006); ash (AOAC official method 942.05, 2006); carbohydrates (by difference) and total starch (Direct acid hydrolysis, ASTA method 8.0, 1997) were determined.

Solvent extraction of piperine from black pepper by Soxhlet assembly

For Soxhlet extraction, 5 g ground black pepper was extracted with *n*-hexane for 8 h (AOAC method 920.39, 920.39A, 2006). Post extraction the extract was concentrated by rotary vacuum evaporator (Eyela Corp., Japan) at 40-45 °C and 0.05 bar and stored in amber colored screw capped glass vials in an inert atmosphere of nitrogen at 4±1 °C in the dark, until further analyses.

Extraction of piperine from black pepper by green technology

Extraction of piperine using ethanol by reflux method

In the reflux method, 10 g ground black pepper and 50 mL ethanol were set for reflux heating for 1 h at 50±2 °C in accordance with the method reported by Musenga et al. (2007). The solvent was filtered by Whatman no. 1 filter paper and the residue was re-extracted by the same process. The extract was concentrated according to the method discussed above and stored at 4±1 °C in the dark, until further analyses.

Extraction of piperine in shake flask

Shake flask method has also been investigated in which 10 g ground black pepper was subjected to extraction using 50 mL ethanol at 60±2 °C in an incubator shaker (110 rpm) (model IS 02, Incon, India) for 1 h and for 3 h in separate batches. The extracts collected were concentrated and stored at 4±1 °C in the dark, until further analyses.

Optimization of SC-CO_2 extraction of piperine from black pepper powder

Optimization of extraction parameters (pressure, temperature and extraction time) for piperine was carried out using a 3^3 full factorial design in laboratory scale 'SCF Green Technology SPE-ED SFE 2' model of Applied Separations, PA, USA. 20 g of ground black pepper (d_p=0.42±0.02 mm) was charged into a 50 mL extraction vessel (SS 316). The batch size of 20 g was optimized from preliminary trials and employed for all extractions. Varying extraction pressure (200, 250 and 300 bar), temperature (40, 50 and 60 °C) and time (30, 45 and 75 min) were investigated for maximum yield of piperine. The flow rate of CO_2 above 2 L/min resulted in sputtering of the extract in the wall of the collection vial and carryover and entrainment of the same in the outlet tubing leading to loss in extract yield; therefore it was maintained at 2 L/min.

From preliminary extractions, it was observed that increase in static time (equilibration time) increased the yield of piperine, therefore static time of extraction was varied at three levels of 15, 30 and 45 min to optimize the same. The dynamic time was kept constant for 15 min, beyond which no extract was obtained in the collection vial (ascertained from preliminary extractions). The extracts were collected in amber colored screw capped glass vials in an ice bath. Post extraction, the extracts were weighed gravimetrically, dissolved in methanol and stored in the dark at 4±1 °C, until further analyses.

Densitometric analyses of black pepper extracts for determination of piperine

To estimate the total piperine contents of the extracts, densitometric analyses of the extracts were conducted by high performance thin layer chromatography (HPTLC). Test samples (20 mL) were spotted as bands of 8 mm length on pre-coated silica gel 60 F_{254} Al plates (200 mm × 100 mm) using Camag Linomat 5 (Camag, Switzerland). Distance between two consecutive bands

was kept 10 mm. The chromatogram was developed in the solvent system; toluene: ethyl acetate:: 7:3 at 25±2 °C in a Twin Trough Chamber (200 mm×100 mm). The plates were scanned with Camag TLC Scanner 3 at 337 nm using a Deuterium lamp at a scanning speed of 20 mm/s. Piperine contents of the extracts were determined from the standard curve prepared using standard piperine.

Gas chromatography-mass spectrometry (GC-MS) analysis of black pepper extract

Black pepper extract obtained from the optimized conditions of extraction was analyzed by GC-MS for identification of its chemical constituents. A Polaris Q Mass Spectrometer coupled with Trace GC Ultra Gas Chromatography and DB-5 MS fused silica capillary column (30 m×0.25 mm i.d.; 0.25 µm film thickness) (Thermo Scientific, USA) was employed. The GC injector and MS transfer line temperatures were set at 230 °C and 270 °C, respectively and split less mode was selected. The oven temperature was programmed as follows: initial hold at 85 °C for 3 min, 85 to 200 °C at 2 °C/min, hold at 200 °C for 1 min, 200 to 250 °C at 10 °C/min and a final hold at 250 °C for 10 min. The carrier gas was He at a flow rate of 1 mL/min. The injected volume of extract was 1 µL. The ionization of the sample was performed in the EI mode (70 eV) and the acquisition mass range was set at 40-600 amu. Identification of components of the extract was based on its computer matching with the NIST (2007) library and Adams (2007).

Statistical analysis of yield of piperine under different extraction conditions

One-way analysis of variance (ANOVA) was performed to study the effects of pressure, temperature and total time of extraction on the yield of piperine, using P value of 0.05 to verify the significance of the tests. Response surface methodology (RSM) and second-order regression modeling have been carried out to correlate the yield of piperine with the extraction parameters

(pressure, temperature and time). All experiments were conducted in triplicate and the data was expressed as mean±SD of three independent experimental runs. Statistical analysis was conducted using STATISTICA 8.0 software (StatSoft, Oklahoma, USA).

Determination of solubility of piperine in SC-CO_2

The solubility of piperine in SC-CO_2 was determined by the method described by Chatterjee and Bhattacharjee (2013). Black pepper powder was packed in SC-CO_2 extraction vessel and extracted at pressures 200, 250 and 300 bar, temperatures 40, 50 and 60 ºC and 45 min (time optimized using full factorial design). The solubility of piperine was calculated as the ratio of the total mass of extracted piperine to the mass of CO_2 consumed in the extraction process as:

$$Y = \text{mass of piperine}/\text{mass of } CO_2 = M_0/\rho V \quad (1)$$

where, Y is the yield (mass fraction) of piperine in SC-CO_2 extracts, M_o is the total mass of piperine extracted (mg), V is the volume of CO_2 (mL) used for extraction and ρ is the density of SC-CO_2 (kg/m^3) under different operational conditions. The densities of SC-CO_2 under different conditions of temperature and pressure were calculated using empirical Peng-Robinson cubic equation of state (Peng and Robinson, 1976) in accordance with the method reported by Bhattacharjee et al. (2012).

Determination of the Hildebrand solubility parameter of piperine

The Hildebrand solubility parameter, developed by Hildebrand and Scott (Hildebrand and Scott, 1950) has been adopted to study the changes of solubility of piperine in SC-CO_2 with varying extraction conditions. For determination of Hildebrand solubility parameter (δ), the most popular method employed is the Fedors group contribution method (Fedors, 1974) which is applied when

the solute molecular structure is known (Sajilata et al., 2010), which is true in this investigation. Hildebrand solubility parameter of a given solute can be estimated by:

$$\delta(\text{bar})^{1/2} = [\Sigma_i(\Delta E_v)_i / \Sigma_i(\Delta V)_i]^{1/2} \quad (2)$$

where $\Sigma_i(\Delta E_v)$ is the summation of cohesive energies (cal/mol) of functional groups in the molecular structure and $\Sigma_i(\Delta V_i)$ is the summation of molar volumes (cm^3/mol) (King, 1995).

The values of cohesive energies of piperine were calculated using Fedors group contribution method (Reid et al., 1987). The molar volume of SC-CO_2 has been determined using Peng-Robinson cubic equation of state as has been reported by Bhattacharjee et al. (2012).

Evaluation of solubility of piperine in SC-CO_2 using Chrastil equation

Many semi-empirical models have been developed to correlate solubility of solute in SC-CO_2 (such as, models reported by Chrastil; Kumar and Johnston; del Valle and Aguilera; Méndez-Santiago and Teja; Jouyban; and Sparks), among them Chrastil equation has been reportedly most used to estimate solubility of solute in SC-CO_2 (Martinez-Correa et al., 2010; Ismadji and Bhatia, 2003; Medina and Bueno, 2000; Fat'hi et al., 1998). In other research, well-correlated Chrastil equations have been derived for estimation of solubilities of squalene from *Amaranthus paniculatus* (Bhattacharjee et al., 2012) and eugenol from *Syzygium aromaticum* Linn in SC-CO_2 (Chatterjee and Bhattacharjee, 2013). The Chrastil equation gives a linear relationship between the logarithm of solubility of a solute and the logarithm of SC-CO_2 density and is represented as (Catchpole and Kamp, 1997):

$$\ln S = k \ln \rho + F + G/T \quad (3)$$

where, S is the solubility of solute in the gas phase (g/kg), k is the association constant related to the total number of molecules in the complex (Westerman et al., 2006), ρ is the density of CO_2 (kg/m^3), F and G are empirical constants in density correlation and T is the temperature (K).

The values of k, F and G of Eq. (3) were determined and a linear equation was developed which allows the prediction of solubility of piperine in SC-CO_2 under varying extraction conditions (Chatterjee and Bhattacharjee, 2013).

Assessment of SC-CO_2 extraction of piperine with time and analysis of kinetics of extraction

The effect of extraction time on yield of piperine has been studied under the extraction condition (temperature, pressure) that yielded maximum piperine from black pepper. This allowed us to empirically model the release of piperine from black pepper into the extraction fluid, i.e., SC-CO_2.

Release kinetics of piperine was studied by different kinetic equations, namely, zero order (cumulative percentage piperine released vs. time), first order (log cumulative piperine retained vs. time), sub-types of first order such as Higuchi model (cumulative percentage piperine released vs. √time), Peppas (log cumulative piperine released vs. log time) and Hixson-Crowell's cube root model [(percentage piperine retained)$^{1/3}$ vs. time] equations. The kinetic model that best fitted the extraction data was determined by comparing the correlation coefficient (r) values obtained from these models.

Characterization of the SC-CO_2 process of extraction of piperine from black pepper

Among the different approaches of characterization of SC-CO_2 process, the one considering the process to have overall fixed bed behaviour for solutes and mass transfer coefficients in

supercritical phases has been mostly adopted when solubility equilibria or external diffusion is the limiting factor. This approach has been employed for characterizing the fractionation of liquids by SC-CO_2 (Martin and Cocero, 2007) and for SC-CO_2 extraction of essential oil from fennel seeds (Reverchon et al., 1999).

In this investigation, a two-phase model comprising the solid and supercritical fluid (SCF) phases was used. The extraction vessel was a cylinder (L = 304.8 mm, i.d. = 13.9 mm) and the particles of the black pepper matrix were considered to be spherical and of the same size (d_p= 0.42±0.02 mm).

The steps of extraction are:

(1) CO_2 penetration and diffusion into the black pepper powder.

(2) Solubilization of compound (piperine) in SC-CO_2 bulk phase.

(3) Product diffusion through the solid particle.

(4) Product diffusion through the SCF film.

In steps 1 and 3, equimolar counter diffusion has been presumed. Moreover, since information on the kinetics of the above-mentioned individual steps is limited, the same stages have been considered together (lumped form) using the definition of overall solid phase diffusivity. Similarly, stage 4 has been represented as an overall solid phase-supercritical fluid diffusivity (Bhattacharjee et al., 2012; Chatterjee and Bhattacharjee, 2013). The assumptions of the model have been discussed by Bhattacharjee et al. (2012).

To obtain the mass transfer rate (K_{sl}) of the process of SC-CO_2 extraction of piperine from black pepper, the following assumptions were considered (Tan et al., 1988):

(a) Steady state exists.

(b) An overall mass transfer coefficient can be used since the black pepper particles are small and a mean piperine concentration may be assigned to them.

(c) The overall mass transfer coefficient is independent of the concentration of piperine present in the black pepper powder.

The material flux of piperine in these conditions, i.e., the net mass out must fit the transport equation at the external surface of the black pepper particles in a packed bed extractor as given by (Chatterjee and Bhattacharjee, 2013)

$$dc/dt = N_s = K_{sl}a(C^* - C) \quad (4)$$

where N_s is the material flux of piperine (g/s cm^2), K_{sl} is the overall particle to fluid-phase mass transfer coefficient (cm/s), a is the specific interfacial area for mass transfer (cm^2/cm^3) of a particle, 'C*' is the equilibrium concentration of piperine (expressed as % of total piperine) in the fluid film in equilibrium with the piperine inside the black pepper particle and 'C' is the concentration of piperine (expressed as % of total piperine) in the supercritical phase at time t. Integrating between the boundary conditions from time t=0 to t=t, the equation obtained

$$\ln(C^* - C) = K_{sl}a \times t \quad (5)$$

Extraction curves were plotted under different conditions of pressure (200, 250 and 300 bar), temperature (40, 50 and 60 °C). Mass transfer $K_{sl}a$ was determined (Bhattacharjee et al., 2012; Chatterjee and Bhattacharjee, 2013). Considering the black pepper particles to be spherical in shape, the specific interfacial area (a) of black pepper particle was estimated using the following equation (Tan et al., 1988)

$$a = 6 \times (1 - \varepsilon)/(d_p) \quad (6)$$

where ε is the void fraction of the extractor and d_p is the grain diameter (mm).

Fractional voids were determined by the method reported by Chatterjee and Bhattacharjee (2013). The operating mass transfer coefficients (K_{sl}) calculated under different extraction conditions were used to establish the relation between mass transfer to the other process parameters using dimensionless numbers.

To evaluate the dimensionless numbers, the physical properties of SC-CO_2 such as density, viscosity and diffusivity of piperine were calculated. Using the K_{sl} values, Sherwood number ($Sh=K_{sl}d_p/D$) was calculated. Other process parameter values such as Reynolds number ($Re=d_p\rho u/\mu$) and Schmidt number ($Sc=\mu/\rho D$) were also determined and fitted into a model equation for single spheres.

Results and Discussion

Characterization of black pepper powder

Proximate analysis of Malabar black pepper powder revealed a composition of 5.9±0.1% moisture, 13.6±0.1% protein, 1.5±0.1% fat, 8.9±0.1% crude fiber, 5.4±0.1% ash and 58.4±0.1% carbohydrates on a dry weight basis (d.w.b). Starch constituted the major portion of carbohydrates, amounting to 30.4±0.1% of dry black pepper.

Solvent extraction of piperine from black pepper by Soxhlet assembly

Yield of black pepper extract obtained from Soxhlet extraction was 5.4 ± 0.1 g/100 g dry sample and piperine content of the extract was 374.1±3 mg/100 g dry black pepper.

Extraction of piperine from black pepper by green technology

Extraction of piperine using ethanol

Yield of black pepper extract obtained from reflux method was the highest (9.1 ± 0.1 g/100 g dry sample) among the extractions conducted with ethanol, followed by that obtained by shake flask extraction for 3 h (5.53±0.10 g/100 g dry sample) and shake flask extraction for 1 h (5.50±0.11 g/100 g dry sample). Piperine content of the extract obtained from reflux method was the highest (Fig. 2.1.1).

SC-CO_2 extraction of piperine from black pepper

Optimization of SC-CO_2 conditions for maximum yield of piperine from black pepper

Piperine contents of SC-CO_2 extracts at different pressures and temperatures are shown in Table 2.1.1. Maximum yield of piperine (131.7±6 mg/100 g dry black pepper) was obtained at 300 bar, 60 °C and 45 min. Although yield of piperine in black pepper extract was higher (2.7 times) by conventional Soxhlet extraction compared to that obtained by SC-CO_2 extraction, cost estimation of the processes revealed a favorable cost (15.5 times lower) for the former product. This was owing to high price of *n*-hexane vis-à-vis inexpensive CO_2.

From the ANOVA study (Table 2.1.2), it was found that yield of piperine increases significantly (P=0.0000) with increasing extraction pressure from 200 to 300 bar; however, there was no significant effect of extraction temperature from 40 to 60 °C (P=0.3857) and time from 30 to 75 min (P=0.2329), on the yield of piperine from black pepper. Similar trends have been reported by Lin et al. (2013) for SC-CO_2 extraction of oil from Sarawak black pepper at 207-344 bar, 45-55 °C with 0.4-1 mm particle size distribution. They observed that the yield was mainly influenced by pressure, particle size and coupled-interactions between these two variables.

Generation of response surface curves

Optimization of the yield of piperine in relation to the extraction pressure, extraction temperature and extraction time is shown in Fig. 2.1.2. The extraction pressure, extraction temperature and time of extraction were fixed at their middle values of 250 bar, 50 °C and 45 min in Fig. 2.1.2 a-c, respectively. The response surfaces were characterized by regression modeling.

Regression modeling

The second-order polynomial equation that describes the extraction yield is given below:

$$Y = B_0 + \sum B_i X_i + \sum B_{ii} X_i^2 + \sum B_{ij} X_i X_j \quad (7)$$

where, Y represents the experimental response (yield of piperine), B_0, B_i, B_{ii}, and B_{ij} are constants and regression coefficients of the model and X_i and X_j are independent variables in coded forms. The expanded model includes linear, quadratic and cross-product terms as shown below (with intercept):

$$Y = 112.311 + 9.509X_1 - 0.614X_2 + 0.838X_3 + 2.218X_1^2 - 2.219X_2^2 + 0.999X_3^2 + 7.848X_1X_2 + 0.896X_1X_3 + 1.423X_2X_3 \quad (8)$$

where X_1, X_2 and X_3 are the extraction pressure, temperature and time respectively. This equation explains the effect of the variables on the response Y.

It was observed that there was a significant dependence of yield of piperine on extraction pressure (P=0.0000). Among all the second-order terms (X_1^2, X_2^2 and X_3^2) of the three processing parameters, extraction pressure (X_1^2) and extraction temperature (X_2^2) has significant effect on piperine extraction (P=0.0004 for both the parameters). Among the two-level interaction factors (X_1X_2, X_1X_3 and X_2X_3), X_1X_2 has significant effect (P=0.0000) on the yield of

piperine, other two interaction factors containing the time of extraction (X_1X_3 and X_2X_3) did not have significant effects. ANOVA of the model showed a high F value (Fisher's variance ratio) ranging from 13 to 182, indicating interaction among the variables to be highly significant (Table 2.1.2).

The adequacy of the above regression model and violations of the basic assumptions were validated by a residual analysis of the experimental data in accordance with Chatterjee and Bhattacharjee (2013). It was found that the residuals were 'structure less', i.e., having no obvious pattern, which proved the adequacy of the model. Thus, a statistically significant multiple regression relationship between the yield of piperine and the extraction parameters was obtained. The quadratic model had a reasonably good fit (r=0.89). Furthermore, the plot of the predicted vs. observed yield of piperine showed a close fit (r=0.947) (Fig. 2.1.3), further establishing the adequacy of the model.

Characterization of the Response Surface

Stationary point of this experimental design was determined from the first partial derivatives of the regression equation conducted with respect to X_1, X_2 and X_3 and set to zero. This was done by putting the second order regression equation in matrix form as described by Montgomery (2001b) and Ge et al. (2002). The point thus obtained is known as the stationary point, X_{1S}, X_{2S}, X_{3S} (X_{1S} = 281.61 bar, X_{2S} = 44.86 °C and X_{3S} = 55.87 min). The predicted amount of piperine extracted in this stationary point (X_S) was found to be 117.12 mg/100 g dry black pepper. The experimentally obtained highest yield of piperine (131.7±6 mg/100 g dry black pepper) was significantly higher (P=0.000) than the predicted value.

Characterization of the response curves has been conducted by transforming the regression equation to the canonical form and the eigenvalues were determined to find whether the stationary point is a point of maxima, minima or a saddle point (Chatterjee and Bhattacharjee, 2013). The eigenvalues obtained were 0.9844, -0.1577 and -0.0776. The different signs of eigenvalues show that the stationary point is a saddle point.

Optimization of SC-CO_2 conditions for maximum yield of piperine

The predicted yield of piperine (117.12 mg/100 g dry black pepper) at the conditions of the saddle point obtained from statistical analyses cannot be considered as optimum and also because the yield was much lower than the experimentally obtained highest yield of piperine (131.7±6 mg /100 g dry black pepper). ANOVA studies revealed that extraction pressure had a significant effect on the yield of piperine (Table 2.1.2). Therefore, additional runs were conducted at 350, 400 and 500 bar, to investigate the effect of high pressure on the yield of piperine (maintaining the temperature and time of extraction at 60 °C and 45 min, respectively). HPTLC results revealed that the yield of piperine decreased with increasing pressure (Fig. 2.1.4). For prediction of pressure where maximum yield of piperine could be obtained, the extraction curve was plotted and the equation was subjected to first and second order partial derivatization. The first partial derivative was set to zero and the point of maximum obtained from the second partial derivative was 389.09 bar. The yield of piperine at this pressure was predicted to be 150.14 mg/100 g dry black pepper, which is higher than the actual yield.

This indicated possible co-extraction of other compounds along with piperine at high pressure regime as revealed by the GC-MS analysis of the black pepper extract obtained at 300 bar, 60 °C (Fig. 2.1.5). This was also evident visibly in appreciable stickiness of the extracts. This stickiness was conferred to co-extraction of starch as was validated by proximate analysis of ground black

pepper which revealed high starch content (30.4±0.1%, on d.w.b) [in agreement with Pruthi (2014) who reported starch content of black pepper to be 34.8%]. Also, cells of oleoresin (containing piperine) in black pepper are located among starch molecules (Fig. 1.1) (Govindarajan and Stahl, 1977). Therefore, it could be inferred that cellular starch of black pepper impeded the release of piperine from the oleoresin containing cells, decreasing its yield (lower than the predicted value). In this investigation, the optimized SC-CO_2 conditions for maximum extraction of piperine from black pepper were therefore 300 bar extraction pressure, 60 °C extraction temperature and 45 min of total extraction time.

Solubility of piperine in SC-CO_2

The experimentally determined solubility of piperine in SC-CO_2 was found to vary significantly with the extraction conditions (Table 2.1.3). At lower pressure regime (<250 bar), solubility of piperine decreases with increasing temperature (40 to 60 °C) and at higher pressure regime (>250 bar), it increases with increasing temperature, in accordance with the retrograde phenomenon reported for SC-CO_2 (Mukhopadhyay, 2000). Maximum solubility of piperine (0.99 mg/kg CO_2) in SC-CO_2 was obtained at 300 bar, 60 °C where highest yield of piperine was also obtained (Table 2.1.1). Kumoro et al. (2009) observed higher solubility of piperine (933.8 mg/kg CO_2) in SC-CO_2 since they investigated the solubility of pure piperine. In this study, the solubility of piperine in SC-CO_2 is relatively poor since the piperine is extracted into the solvent from the black pepper matrix with several constituents, principally starch, impeding its diffusion.

Hildebrand solubility parameter of piperine

Cohesive energy of various functional groups in piperine and molar volumes of SC-CO_2 were used for evaluation of the modified Hildebrand equation at different conditions of SC-CO_2

extractions. Table 2.1.4 represents the cohesive energy values of functional groups of piperine by Fedors group contribution method and molar volume of SC-CO_2 by Peng Robinson Cubic Equation of State, used to calculate Hildebrand parameter at SC-CO_2 conditions. From the analysis of Hildebrand parameter (δ) with respect to extraction pressure (Fig. 2.1.6a), it was found that δ of piperine decreases significantly (P=0.0334) with increasing temperature (from 40 °C to 60 °C). From the SCF-phase equilibrium behaviour, it is known that at higher pressure zones, isobaric increase in extraction temperature resulted in increase of yield and solubility of solutes in SC-CO_2. Since the δ values did not follow the SCF phase equilibrium principle at higher pressure regimes (250-300 bar), Hildebrand solubility parameter cannot be considered for estimation of solubility of piperine in SC-CO_2. A similar trend on solubility of SC-CO_2 extracted eugenol from clove buds has been reported by Chatterjee and Bhattacharjee (2013). In the present work, solubility of piperine in SC-CO_2 has been determined by Charstil equation method, discussed below.

Solubility of piperine using Chrastil equation

The two most important factors that affect the solubility of a solute in supercritical state are solvent density and temperature of extraction (Chatterjee and Bhattacharjee, 2013) and data of this investigation were in agreement to these. It has been observed that the solubility of piperine in SC-CO_2 increases significantly (P=0.0001) with increase of temperature from 40 ºC to 60 ºC in high pressure regime (250-300 bar). From the values of the solubility of piperine, a linear regression equation was developed according to the Chrastil equation.

$$\ln S = 0.301 \ln \rho - 952.927/T + 0.776 \quad (9)$$

The regression coefficient (r) obtained using this equation was 0.80, and the standard error of the equation was 0.06. The validity of the fitted model was indicated by the insignificant lack of fit (P=0.070) for this equation.

From this Chrastil equation, logarithm of calculated solubility was plotted against logarithm of SC-CO_2 density (Chatterjee and Bhattacharjee, 2013). It was found that the plots were linear and the isotherms at 40, 50 and 60 °C were parallel to each other (Fig. 2.1.6b) which affirmed the suitability of Chrastil equation in this work. The solubility values of piperine calculated at different extraction conditions were in good agreement with the solubility values predicted by Chrastil equation; therefore, Eq. (9) can certainly be used to predict the solubility of piperine in SC-CO_2. Kumoro et al. (2009) have also developed a Chrastil model; however it has been observed that their model does not well correlate the solubility of piperine with the density of SC-CO_2 under varying experimental conditions.

Study of effect of time on SC-CO_2 extraction of piperine

The mass transfer phenomenon that explains the SC-CO_2 extraction of piperine from black pepper has been explained by plotting the yields at 60 °C, 300 bar (where highest yield was obtained) against varying extraction time (Fig. 2.1.7). The investigation revealed that maximum release of piperine was achieved within 45 min of extraction time (30 min static time + 15 min dynamic time). It was observed that the first part of the extraction curve followed first-order kinetics; while the second part showed an asymptotic behaviour owing to decrease in the extraction rate due to depletion of the continuous layer of piperine from black pepper particles inside the packed bed. The entire extraction curve indicated ‘plug flow’ validating the assumption of Sovová et al. (1995) for SC-CO_2 extraction of oleoresin from black pepper.

The first phase of extraction showed linear increase in yield with time, and then plateaued after 35 min. This phenomenon has been explained by Sovovà et al. (1994) for SFE of essential oil from caraway seeds; and Özkal et al. (2005) for SC-CO_2 extraction of apricot kernel oil. According to these authors, the packed bed of sample consists of cells broken up during communition and cells which are intact, which was also true for this investigation. The cells of oleoresin (containing piperine) are known to be located in the perisperm of pepper berries (Govindarajan and Stahl, 1977). These cells rupture under SC-CO_2 temperature-pressure regimes, releasing piperine to the surface of the ground particles forming a film around the same. During static time, equilibration of concentration of piperine occurs between the film of piperine at the surface of black pepper particles and the bulk SC-CO_2 phase; while during dynamic time, piperine solubilized in SC-CO_2 is swept into the collector. During the first phase of extraction (considering both static and dynamic time), release of piperine occurs from the broken cells which is easily accessible to SC-CO_2 (up to 35 min in this investigation). In the second phase of extraction, piperine content in the broken cells is exhausted and extraction occurs from the undestroyed cells resulting in decrease in the rate of extraction of piperine from packed bed into bulk SC-CO_2, i.e., after 35 min of extraction.

Study of kinetics of SC-CO_2 extraction of piperine from black pepper

The release profile of piperine (Fig. 2.1.7) was fitted into different kinetic equations and their corresponding regression coefficient (r) was determined. For the different release kinetics models studied, the 'r' values were: Higuchi (0.979) > Peppas (0.960) > Zero order (0.955) > First order (0.905) > Hixson Crowell's (0.694). Therefore, the release of piperine from black pepper packed bed was explained by the Higuchi model (highest 'r' value). This release mechanism is given by the Higuchi equation (Aucoin et al., 2013).

$$M_t = k_H \times t^{1/2} \quad (10)$$

where, M_t is the concentration of piperine released at time t and k_H is the Higuchi dissolution constant. The k_H of this release profile was calculated to be 1.233.

The Higuchi model considers the concentration of the compound in the matrix to be initially higher than its solubility, with constant diffusivity and unidirectional diffusion (Aucoin et al., 2013). In the findings of this study also, the initial concentration of piperine in black pepper was much higher than the solubility of piperine in SC-CO_2; with increase in extraction time, there was an increase in release of piperine from the matrix until 35 min and thereafter plateaued. Diffusion of piperine was unidirectional, from the packed bed into bulk SC-CO_2; also the diffusion was constant at a particular temperature and pressure of extraction.

Packed bed characterization of SC-CO_2 extraction of piperine from black pepper

The orders of magnitude (10^{-4} P) for the viscosity of SC-CO_2 under the experimental conditions (Table 2.1.3) were in agreement with that reported for supercritical fluids (Chatterjee and Bhattacharjee, 2013). The values of molecular diffusivities of piperine estimated by the Wilke-Chang equation were in the order of 10^{-4} cm^2/s (Table 2.1.3) which was lower than those reported for SCFs in general [10^{-3} cm^2/s, (Perry et al., 1977)] and higher than those for essential oils [1.5 to 2.8 x 10^{-5} cm^2/s (Bartle et al., 1990)]. Similar observations have been reported by Bhattacharjee et al. (2012) for calculation of diffusivities of squalene (1.1 to 87.7 x 10^{-5} cm^2/s) employing Wilke-Chang equation. The Schmidt number (Sc) were in the range of 7-10, which was in agreement with Tan et al. (1988) and Paulitis et al. (1983), who have reported the value to be around 10 for SCFs.

The mass transfer coefficient of piperine from black pepper particles in the packed bed was evaluated by plotting graphs of ln (C*-C) vs. time for each extraction condition. The values of overall mass transfer coefficient, K_{sl}, were in the order of 10^{-3} (cm/s) (Table 2.1.3) which is in accordance with the report for fluid-solid systems (10^{-4} to 10^{-3}cm/s) (1988). In the pressure and temperature range where most supercritical extractions are operated, there are no generally accepted correlations for mass transfer coefficients (Bhattacharjee et al., 2012; Chatterjee and Bhattacharjee, 2013). In this investigation, Re values are in the range of 1119.14 to 1212.23, which reflects the zone of turbulent forced convection (Re>150) (Stuber et al., 1996).

The general correlation for relating these dimensionless numbers- Sh, Sc and Re is given by (Norhuda and Mohd. Omar, 2009):

$$\mathrm{Sh} = \mathrm{A}(\mathrm{Re})^{\mathrm{a}}(\mathrm{Sc})^{1/3} \quad (11)$$

Upon substitution of the calculated Sh, Re and Sc numbers in Eq. (11) and application of regression analysis the equation obtained is:

$$\ln\left(\mathrm{Sh}/\mathrm{Sc}^{1/3}\right) = -7.598 + 0.96\ln(\mathrm{Re}) \quad (12)$$

The correlation coefficient 'r' of this equation was 0.96 and the standard error was 0.01. Therefore, the mass transfer equation correlating the dimensionless numbers was found to be:

$$\mathrm{Sh} = 5.015 \times 10^{-4}\mathrm{Re}^{0.96}\mathrm{Sc}^{1/3} \quad (13)$$

Fig. 2.1.8 shows the dependence of Sherwood number on Reynolds number with linear relation between $(Sh)/(Sc)^{1/3}$ and (Re) (r=0.96). High correlation of the empirical equation suggests that the extraction process was satisfactorily modeled and could be used in development of futuristic

pilot plant and commercial scale extraction of piperine from similar matrices by the food and bioprocess industries.

Conclusions

In the present investigation, piperine was extracted from ground Malabar black pepper using SC-CO_2 extraction. The optimum yield of piperine (131.7±6 mg/100 g dry black pepper) was obtained employing 20 g dry black pepper powder (d_p= 0.42±0.02 mm) at the extraction conditions of 300 bar, 60 °C with 45 min extraction time and a constant flow rate of 2 L/min of gaseous CO_2. Statistical analyses revealed that pressure (in quadratic and linear form), temperature (in quadratic form) and interdependence between pressure and temperature of extraction showed significant effects on yield of piperine. High starch content of black pepper (30.4±0.1% on d.w.b) impeded the extraction of piperine which resulted in lower yield of the bioactive than that predicted by statistical analysis.

Solubility of piperine in SC-CO_2 at different extraction conditions was successfully determined by Chrastil equation and a correlated equation was generated to predict the solubility of piperine in SC-CO_2 under different extraction conditions. The extraction of piperine followed 'plug flow' model and its release was explained best by Higuchi model.

The hydrodynamic parameters of the packed bed matrix of black pepper were characterized using an empirical correlation, deduced from Reynolds, Schmidt and Sherwood numbers. High correlation coefficient (r=0.96) of the empirical equation suggest that the extraction process was satisfactorily modeled and could be used in development of future pilot plant and commercial scale extractions of piperine from similar matrices. This work on modeling would benefit the food and bioprocess industries for extraction of piperine from Malabar black pepper.

Novelty

The novelty of the work is that it has reported for the first time on optimization of the SC-CO_2 extraction procedure for obtaining piperine from Malabar black pepper; on development of a correlated Chrastil equation which could predict the solubility of piperine in SC-CO_2 under different extraction conditions and on characterization of hydrodynamic parameters of the packed bed matrix using dimensionless numbers, useful for scale up production of piperine.

References

Adams R. P. (2007). *Identification of Essential Oil Components by Gas Chromatography/mass Spectroscopy*, 4th ed., Allured Publishing Corporation, IL, USA.

AOAC International (2006). AOAC methods 986.21, 984.13, 920.39, 920.39A, 978.10, 942.05, In: *Official methods of analysis of AOAC International*, 18th ed., Horwitz, W. (Ed.), AOAC International, Gaithersburg, MD, USA.

ASTA (American Spice Trade Association) (1997). ASTA method 8.0, Starch (direct acid hydrolysis). In: *Official Analytical Methods of the American Spice Trade Association*, 4th ed. American Spice Trade Association Inc., Washington, DC, pp. 39-42.

Aucoin H. R., Wilson A. N., Wilson A. M., Ishihara K., and Guiseppi-Elie A. (2013). Release of potassium ion and calcium ion from phosphorylcholine group bearing hydrogels. *Polymers*, **5**, 1241-1257.

Bartle K. D., Clifford A. A., Hawthorne S. B., Langenfeld J. J., Miller D. J., and Robinson R. (1990). A model for dynamic extraction using a supercritical fluid. *The Journal of Supercritical Fluids*, **3**, 143-149.

Bhattacharjee P., Chatterjee D., and Singhal R. S. (2012). Supercritical carbon dioxide extraction of squalene from *Amaranthus paniculatus*: Experiments and process characterization. *Food and Bioprocess Technology*, **5**, 2506-2521.

Catchpole O. J., and Kamp J. C. Von (1997). Phase equilibrium for the extraction of squalene from shark liver oil using supercritical carbon dioxide. *Industrial and Engineering Chemistry Research*, **36**, 3762-3768.

Chatterjee D., and Bhattacharjee P. (2013). Supercritical carbon dioxide extraction of eugenol from clove buds. *Food and Bioprocess Technology*, **6**, 2587-2599.

Fat'hi M. R., Yamini Y., Sharghi H., and Shamsipur M. (1998). Solubilities of some 1,4-dihydroxy-9,10-anthraquinone derivatives in supercritical carbon dioxide. *Journal of Chemical and Engineering Data*, **43**, 400-402.

Fedors R. F. (1974). A method for estimating both the solubility parameters and the molar volumes of liquids. *Polymer Engineering and Science*, **14**, 147–154.

Ge Y., Ni Y., Yan H., Chen Y., and Cai T. (2002). Optimization of the supercritical fluid extraction of natural vitamin E from wheat germ using response surface methodology. *Journal of Food Science*, **67**, 239-243.

Govindarajan V. S., and Stahl W. H. (1977). Pepper- chemistry, technology, and quality evaluation. *C R C Critical Reviews in Food Science and Nutrition*, **9**, 115-225.

Hildebrand J. H., and Scott R. L. (1950). *The Solubility of Nonelectrolytes*, 3rd ed., Dover Publications Inc., New York.

Ismadji S., and Bhatia S. K. (2003). Solubility of selected esters in supercritical carbon dioxide. *The Journal of Supercritical Fluids*, **27**, 1-11.

Kapoor I. P. S., Singh B., Singh G., Heluani C. S. De, Lampasona M. P. De, and Catalan C. A. N. (2009) Chemistry and *in vitro* antioxidant activity of volatile oil and oleoresins of black pepper (*Piper nigrum*). *Journal of Agricultural and Food Chemistry*, **57**, 5358-5364.

King J. W. (1995). Determination of the solubility parameter of soybean oil by inverse gas chromatography. *LWT-Food Science and Technology*, **28**, 190–195.

Kumoro A. C., Singh H., and Hasan M. (2009). Solubility of piperine in supercritical and near critical carbon dioxide. *Chinese Journal of Chemical Engineering*, **17**, 1014-1020.

Lin T. M., Ping T. S., Saptoro A., and Freddie P. (2013). Mass transfer coefficients and correlation of supercritical carbon dioxide extraction of Sarawak black pepper. *International Journal of Food Engineering*. DOI 10.1515/ijfe-2012-0219.

Martin A., and Cocero M. J. (2007). Mathematical modeling of the fractionation of liquids with supercritical CO_2 in a countercurrent packed column. *The Journal of Supercritical Fluids*, **39**, 304-314.

Martinez-Correa H. A., Gomes D. C. A., Kanehisa S. L., and Cabral F. A. (2010). Measurements and thermodynamic modeling of the solubility of squalene in supercritical carbon dioxide. *Journal of Food Engineering*, **96**, 43-50.

Medina I., and Bueno J. L. (2000). Solubilities of 2-nitroanisole and 3-phenyl-1-propanol in supercritical carbon dioxide. *Journal of Chemical and Engineering Data*, **45**, 298-300.

Montgomery D.C. (2001). Response surface methods and other approaches to process optimization. In: *Design and Analysis of Experiments*, John Wiley & Sons, New York. pp. 427-510.

Mukhopadhyay M. (2000). *Natural Extracts using Supercritical Carbon dioxide*, CRC Press, Boca Raton.

Musenga A., Mandrioli R., Ferranti A., D'Orazio G., Fanali S., and Raggi M. A. (2007). Analysis of aromatic and terpenic constituents of pepper extracts by capillary electrochromatography. *Journal of Separation Science*, **30**, 612-619.

NIST Mass Spec Data Center (2007). Stein S.E., director, mass spectra. Mallard Gaithersburg NIST chemistry WebBook. In: *NIST Standard Reference Database Number 69*, Linstrom, P., Mallard, W.G. (Eds.). National Institute of Standards and Technology, Gaithersburg, MD, USA. http://webbbok.nist.gov (Accessed 20 November, 2015).

Norhuda I., and Mohd. Omar A. K. (2009). Mass transfer modeling in a packed bed of palm kernels under supercritical conditions. *International Journal of Chemical and Biological Engineering*, **2**, 10-13.

Özkal S. G., Yener M. E., and Bayındırlı L. (2005). Mass transfer modeling of apricot kernel oil extraction with supercritical carbon dioxide. *The Journal of Supercritical Fluids*, **35**, 119-127.

Paulaitis M. E., Krukonis V. J., Kurnik Y., and Reid R. C. (1983). Supercritical fluid extraction. *Reviews in Chemical Engineering*, **1**, 179-250.

Peng D. Y., and Robinson D. B. (1976). A new two-constant equation of state. *Industrial and Engineering Chemistry Fundamentals*, **15**, 59–64.

Perry R. H., Green D. W., and Maloney J. O. (1997). *Perry's Chemical Engineer's Handbook*, 7th ed., McGraw-Hill, New York, pp. 15-22.

Pruthi J. S. (2014). Pepper, black, white, green. In: *Spices and Condiments*, National Book Trust, India, pp. 198-209.

Reid R. C., Prausnitz J. M., and Poling B. E. (1987). *The Properties of Gases and Liquids*, 4th ed., Mc-Graw-Hill, New York.

Reverchon E., Daghero J., Marrone C., Mattea M., and Poletto M. (1999). Supercritical fractional extraction of fennel seed oil and essential oil: experiments and mathematical modeling. *Industrial and Engineering Chemistry Research*, **38**, 3069-3075.

Sajilata M. G., Bule M. V., Chavan P., Singhal R. S., and Kamat M. Y. (2010). Development of efficient supercritical carbon dioxide extraction methodology for zeaxanthin from dried biomass of *Paracoccus zeaxanthinifaciens*. *Separation and Purification Technology*, **71**, 173-177.

Singh G., Marimuthu P., Catalan C., and deLampasona M. P. (2004). Chemical, antioxidant and antifungal activities of volatile oil of black pepper and its acetone extract. *Journal of the Science of Food and Agriculture*. DOI: 10.1002/jsfa.1863.

Sovová H., Jez J., Bártlová M., and St'astová J. (1995). Supercritical carbon dioxide extraction of black pepper, *The Journal of Supercritical Fluids*, **8**, 295-301.

Sovová H., Komers R., Kucera J., and Jez J. (1994). Supercritical carbon dioxide extraction of caraway seed oil. *Chemical Engineering Science*, **49**, 2499-2505.

Stuber F., Ma A., Ma V., Larrayoz A., and Recasens F. (1996). Supercritical fluid extraction of packed beds: External mass transfer in upflow and downflow operation. *Industrial and Engineering Chemistry Research*, **35**, 3618-3628.

Sunila E. S., and Kuttan G. (2004). Immunomodulatory and antitumor activity of *Piper longum* Linn. and piperine. *Journal of Ethnopharmacology*, **90**, 339-46.

Tan C. S., Liang S. K., and Liou D.C. (1988). Fluid-solid mass transfer in a supercritical fluid extractor. *Chemical Engineering Journal*, **38**, 17-22.

Westerman D., Santos R. C. D., Bosley J. A., Rogers J. S., and Al-Duri B. (2006). Extraction of amaranth seed oil by supercritical carbon dioxide. *The Journal of Supercritical Fluids*, **37**, 38-52.

Tables:

Table 2.1.1. Yield of piperine at different conditions of SC-CO_2 extraction.

Pressure (bar)	Temperature (°C)	Total extraction time (min)	Yield of piperine (mg/100 g dry black pepper)[a]
200	40	30	111.1±4
200	40	45	112.5±7
200	40	75	107.3±4
200	50	30	99.8±5
200	50	45	101.7±8
200	50	75	102.1±5
200	60	30	90.9±3
200	60	45	93.7±6
200	60	75	93.7±4
250	40	30	118.9±4
250	40	45	119.1±4
250	40	75	114.7±5
250	50	30	108.8±5
250	50	45	112.7±5
250	50	75	112.2±4
250	60	30	115.5±4
250	60	45	117.3±5
250	60	75	117.3±4
300	40	30	114.0±5
300	40	45	116.2±8
300	40	75	116.8±5
300	50	30	113.7±4
300	50	45	116.6±9
300	50	75	115.9±5
300	60	30	124.6±5
300	60	45	131.7±6
300	60	75	131.2±5

[a] Yields of piperine are mean±SD of three experimental runs.

Table 2.1.2. ANOVA study to detect the effect of extraction parameters on the yield of piperine.

Effect	Degree of freedom	Yield of piperine (mg/100 g dry black pepper) SS	Yield of piperine (mg/100 g dry black pepper) MS	Yield of piperine (mg/100 g dry black pepper) F	Yield of piperine (mg/100 g dry black pepper) P
X_1^*	1	4797.0	4797.0	182.95	0.000
X_1^2	1	354.3	354.3	13.51	0.001
X_2^*	1	19.9	19.9	0.76	0.386
X_2^2	1	354.4	354.4	13.52	0.001
X_3^*	1	37.9	37.9	1.45	0.233
X_3^2	1	69.2	69.2	2.64	0.109
X_1X_2	1	2217.4	2217.4	84.57	0.000
X_1X_3	1	29.9	29.9	1.14	0.289
X_2X_3	1	75.6	75.6	2.88	0.094
Error	71	1861.6	26.2		
Total SS	80	9797.5			

* X_1, X_2 and X_3 are the extraction pressure, temperature and time respectively.

Table 2.1.3. Physical properties of carbon dioxide, diffusivity and solubility of piperine in SC-CO_2 and dimensionless numbers for packed bed characterization of SC-CO_2 extraction estimated under different extraction conditions.

Pressure (bar)	Temperature (°C)	Density of CO_2[a] (kg/m^3)	Viscosity of CO_2[b] x 10^{-4} (P)	Solubility of piperine[c] (mg/kg CO_2)	Diffusivity of piperine in SC-CO_2[d] $x10^{-4}$ (cm^2/s)	Mass transfer coefficient $x10^{-3}$ (cm^2/s)	Reynolds number (Re)	Schmidt number (Sc)	Sherwood number (Sh)
200	40	830.9	6.6	0.85±0.02	0.94	2.09	1212.2	8.4	0.94
200	50	764.3	6.3	0.83±0.02	1.02	2.18	1162.4	8.1	0.90
200	60	695.7	5.7	0.84±0.01	1.17	2.39	1164.4	7.0	0.86
250	40	886.4	7.2	0.81±0.02	0.86	1.95	1182.5	9.5	0.96
250	50	831.5	6.9	0.83±0.02	0.93	2.05	1154.7	8.9	0.92
250	60	775.2	6.6	0.99±0.02	1.02	2.16	1133.7	8.3	0.89
300	40	929.1	7.7	0.78±0.02	0.79	1.83	1150.3	10.5	0.97
300	50	881.1	7.4	0.83±0.01	0.87	1.91	1137.0	9.7	0.92
300	60	832.4	7.1	0.99±0.02	0.94	1.99	1119.1	9.1	0.89

[a]Calculated from Peng–Robinson cubical equation of state,
[b] Calculated from Reichenberg equation,
[c]The solubility of piperine is the mean±SD of three experimental runs,
[d]Calculated from Wilke-Chang equation.

Table 2.1.4. Cohesive energy values of functional groups of piperine by Fedors group contribution method and molar volume of SC-CO_2 by Peng Robinson Cubic Equation of State.

Functional groups in piperine	Units of groups	Cohesive energy of each group (cal/mole)[a]	Pressure (MPa)	Tempe -rature (°C)	Molar volume of SC-CO_2 (cm^3/mole)[b]
CH_2	6	1180	20	40	52.97
CH=	7	1030	20	50	57.58
C=	3	1030	20	60	63.26
C=O	1	4150	25	40	49.65
O	2	800	25	50	52.93
N	1	1000	25	60	56.77
6-membered ring	2	250	30	40	47.37
5-membered ring	1	250	30	50	49.95
Conjugated double bond	5	400	30	60	52.87

[a] Energy values of functional groups obtained from Fedors group contribution method
[b] Calculated from Peng Robinson Cubic Equation of State

Figures:

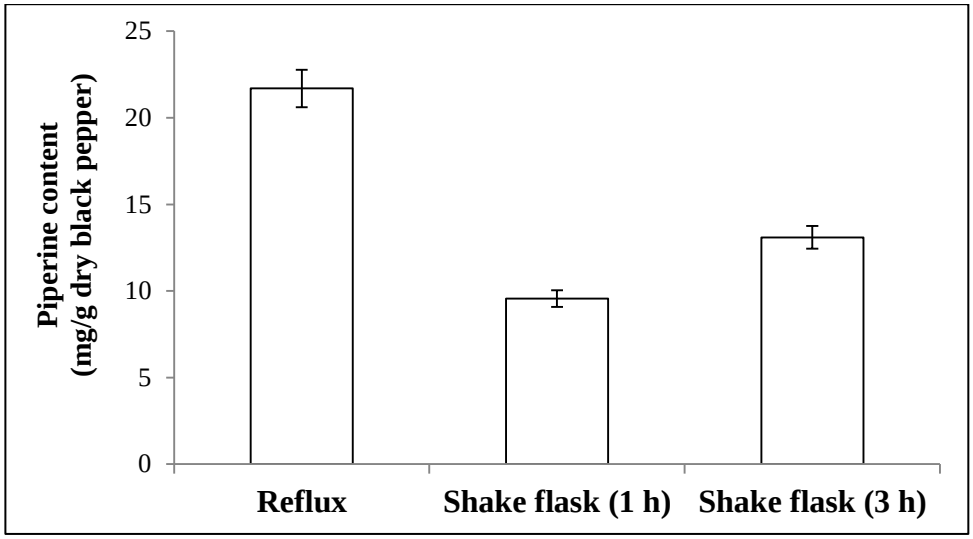

Fig. 2.1.1. Piperine contents of solvent extracts.

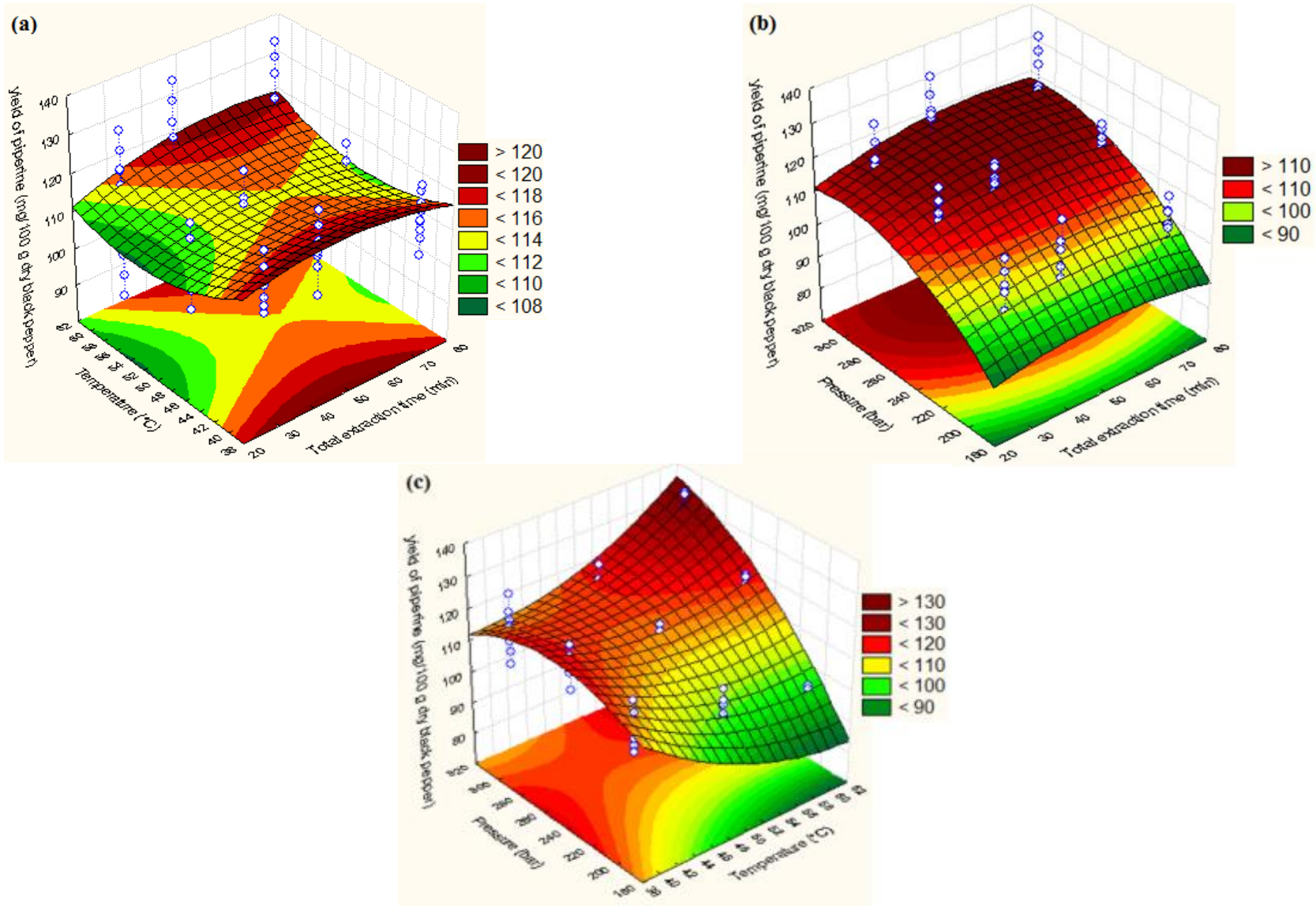

Fig. 2.1.2. Response surface indicating yield of piperine (a) As a function of temperature and time at 250 bar (b) As a function of pressure and time at 50 °C and (c) As a function of pressure and temperature at 45 min.

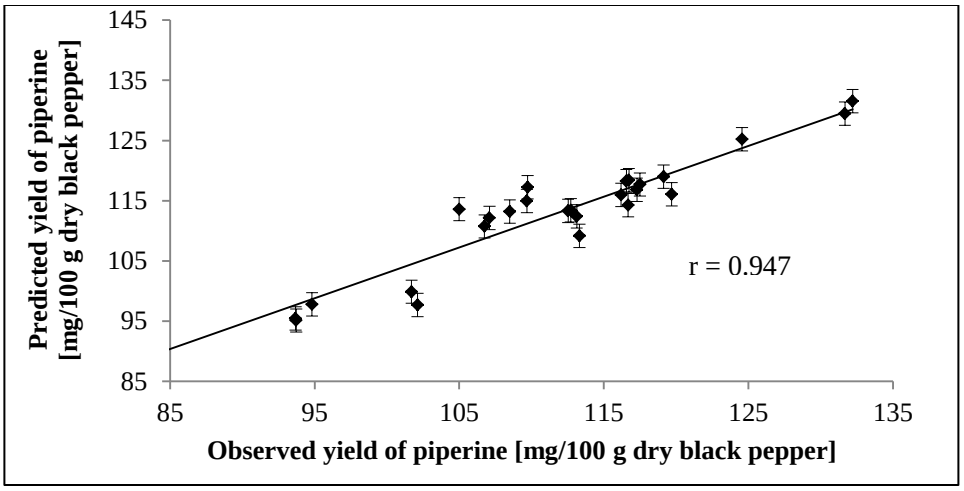

Fig. 2.1.3. Plot of predicted vs. observed values of yield of piperine.

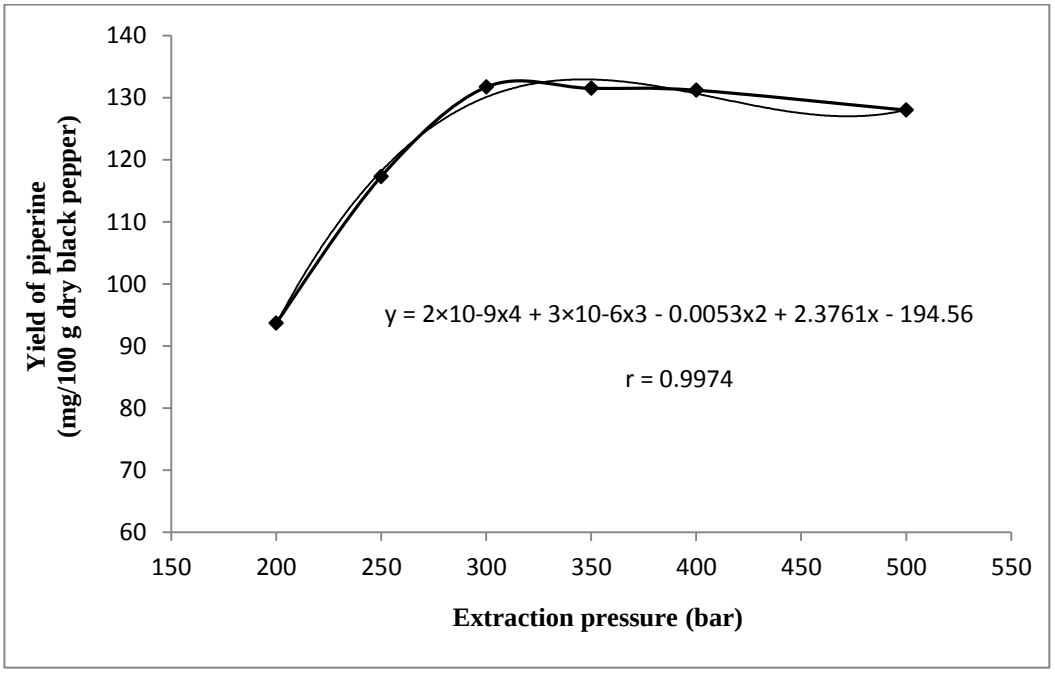

Fig. 2.1.4. Yield of piperine at different extraction pressures.

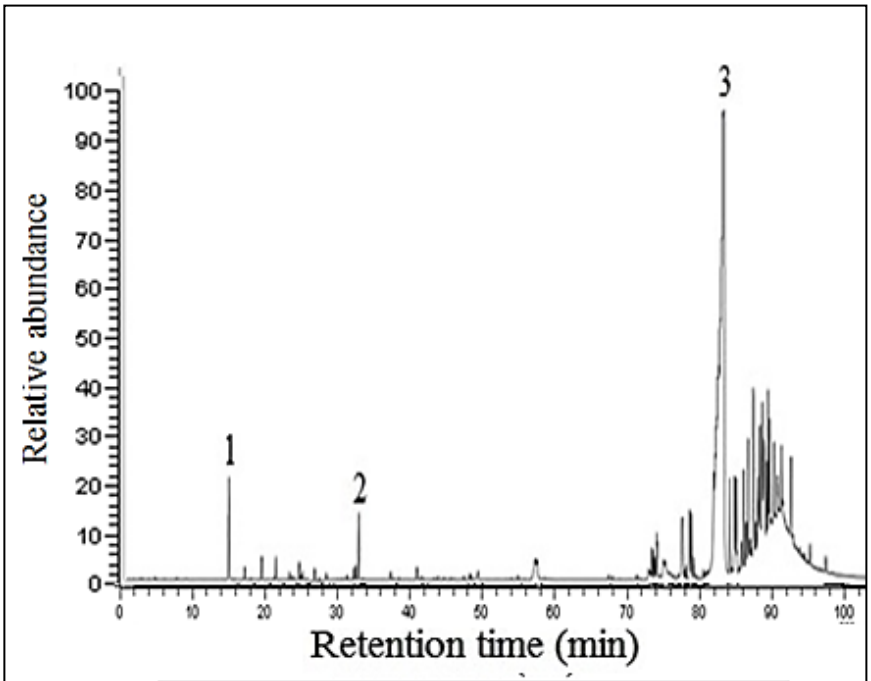

Peak no.	R.T. (min)	% Peak area	Identified compounds
1	16.34	15.33	Piperonal
2	34.57	10.98	β-caryophyllene
3	83.36	73.68	Piperine

R.T.: Retention time

Fig. 2.1.5. Total ion chromatogram and list of identified compounds in black pepper extracts obtained at 300 bar, 60 °C and 45 min of extraction.

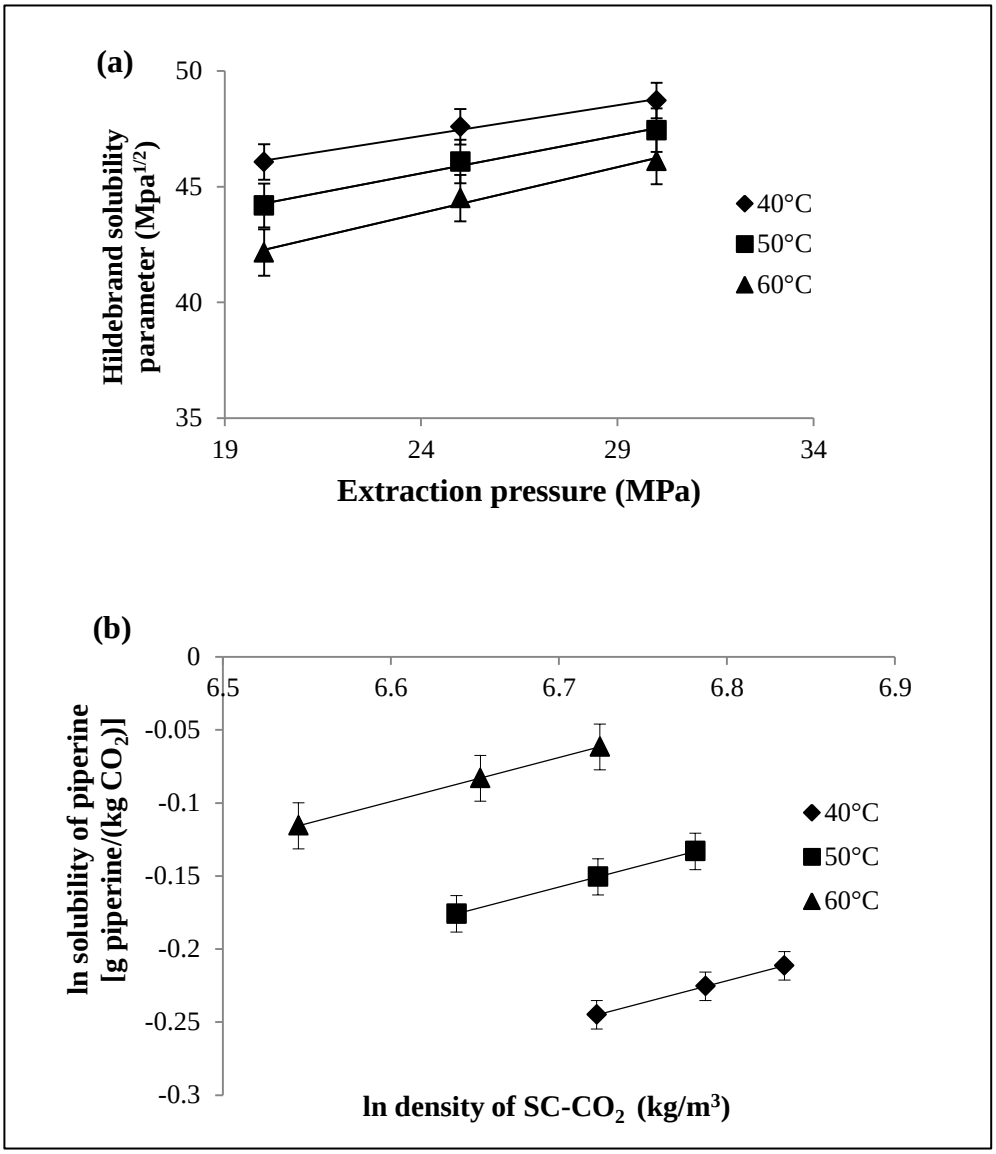

Fig. 2.1.6. Study of solubility of piperine in SC-CO_2. (a) Dependence of Hildebrand solubility parameter of piperine in SC-CO_2 on extraction pressure, (b) Solubility of piperine in SC-CO_2 predicted by Chrastil equation as a function of solvent density.

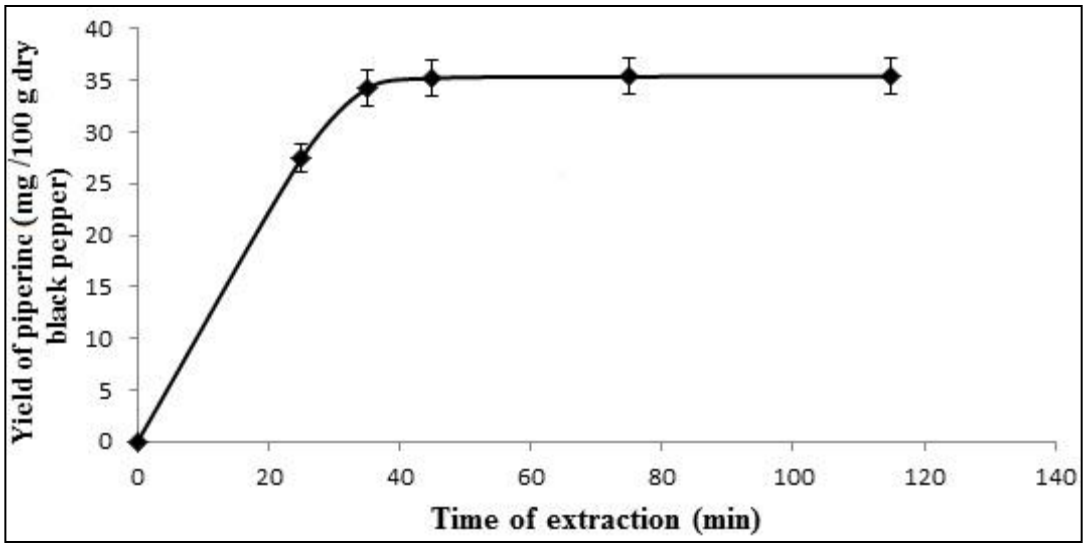

Fig. 2.1.7. Yield of piperine from black pepper by SC-CO_2 extraction at 300 bar, 60 °C as a function of total extraction time (i.e. static time + dynamic time).

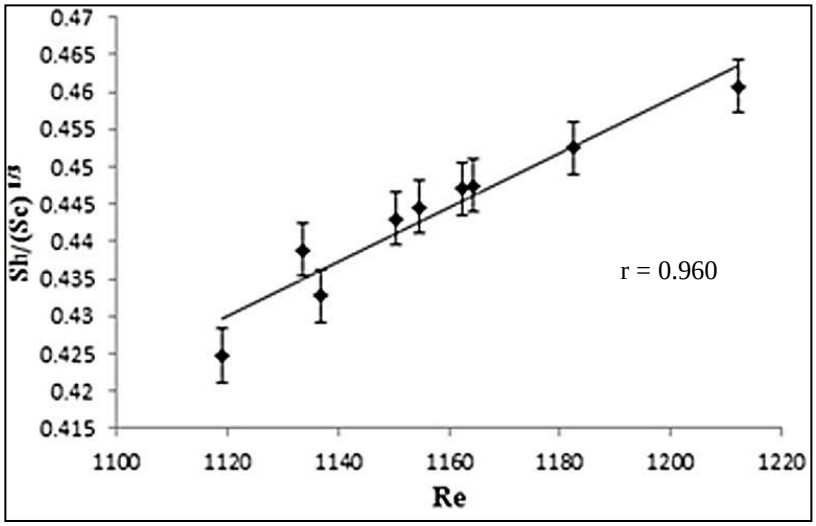

Fig. 2.1.8. Dependence of Sherwood numbers on Reynolds numbers.

Section 2.2

Enzyme-assisted supercritical carbon dioxide extraction of piperine-rich extract from black pepper

Introduction

In the preceding section on SC-CO_2 extraction of piperine-rich extract from black pepper, it was opined that starch being one of the major constituents of the black pepper coat (30.4±0.1% on d.w.b), could possibly impede extraction of piperine by thwarting its accessibility to solvents and would lead to poor yield of the same in the extract. This work has endeavored to employ starch degrading enzymes, such as α-amylase (E.C.3.2.1.1.) with the aim to hydrolyze the starch in the pepper coat, prior to extraction, for improved recovery of piperine from the black pepper matrix.

Yield of piperine in black pepper extract obtained at the optimized conditions of SC-CO_2 extraction was 1.31±0.06 mg/g dry black pepper (discussed in section 2.1 of Chapter 2). The cells of oleoresin in black pepper which contain piperine, are located inside the starch matrix (Fig. 1.2). This has possibly impeded complete extraction of piperine, resulting in poor yield of the same in the extract. Therefore, SC-CO_2 extractions have been carried out employing α-amylase for hydrolysis of the seed starch to enhance the yield of piperine from black pepper. The enzyme-assisted SC-CO_2 extractions have been conducted in both batch and continuous modes (discussed in Chapter 1).

α-amylase-assisted SC-CO_2 extraction has been previously reported by Lee et al. (1993), who performed hydrolysis of corn starch by α-amylase and glucoamylase for improved recovery (40%) of reducing sugars. SC-CO_2 conditions have also been employed in enzyme-assisted synthesis of dipalmitin from palmitic acid and glycerol by immobilized lipase (Tao et al., 2013);

for enzymatic ring-opening polymerization of poly ε-caprolactone (PCL) using lipase B (Rosso et al., 2013) and in acylation of fibrous cellulose by immobilized lipase, immobilized esterase and immobilized cutinase (Gremos et al., 2012), to state a few. All these authors have reported on batch mode of enzyme-assisted SC-CO_2 extractions. Senyay-Oncel and Yesil-Celiktas (2011) reported an increase in activity and stability of fungal α-amylase employing dynamic (continuous) mode of SC-CO_2 conditions. To the best of my knowledge, there is no report on use of α-amylase for SC-CO_2 extraction of piperine-rich extract from black pepper.

Bacillus sp. is the commonly used bacterial source of α-amylase, among them, *Bacillus licheniformis* and *Bacillus amyloliquefaciens* are the most widely used commercial sources of this enzyme (Sundarram and Murthy, 2014). α-amylase produced from *B. licheniformis* is a thermostable enzyme (stable at 40-60 °C) and is used extensively in industries for starch conversion. Apar and Özbek (2004) have worked on α-amylase obtained from *Aspergillus oryzae*, *B. amyloliquefaciens*, *B. subtilis* and *B. licheniformis* and found that α-amylase obtained from *B. licheniformis* showed maximum degrees of hydrolysis for corn, rice and wheat starches (40.4%, 48.1% and 58.1%, respectively) compared to those obtained by *Bacillus* species (5.5%, 19.1% and 29.1%, respectively) and *A. oryzae* (0%, 0% and 17.5%, respectively). Therefore, in this investigation, *B. licheniformis* has been selected as the source of α-amylase to hydrolyze the starch in black pepper for enhanced yield of piperine. Lyophilized powder of α-amylase from *B. licheniformis* (500-1500 units/mg protein, 93-100% SDS-PAGE) was procured from Sigma, India for this study.

In the present investigation, *in situ* enhancement of activity of α-amylase during SC-CO_2 extraction of piperine has been explored. This would allow single step hydrolysis of black pepper starch and concomitant extraction of piperine from the hydrolyzed pepper matrix. Both batch and

continuous modes of extractions were employed to enhance the yield of piperine-rich extract, possessing the best combination of phytochemical properties (such as total phenolic content, reducing power, antioxidant and anti-inflammatory activities). This extract was successively used for design of nutraceutical cookies and nanoliposomes for use as food and/or therapeutic supplements (discussed in detail in section 2.3 of Chapter 2 and in section 4.2 of Chapter 4, respectively).

Materials and Methods

Materials

Soluble potato starch, sodium nitroprusside ($Na_2[Fe(CN)_5NO].2H_2O$), Griess reagent and gallic acid were procured from Sigma, India; Na_2SO_4, NaH_2PO_4, NaCl, NaOH, Na_2CO_3, $CuSO_4.5H_2O$, $K_3Fe(CN)_6$, $FeCl_3$, TCA, Folin-Ciocalteu's phenol reagent (FCR), potassium sodium tartrate tetrahydrate, were procured from E-Merck, India. 3,5-Dinitrosalicylic acid (DNSA) was purchased from Himedia, India. All chemicals were of AR grade. SPE cartridge (3 mL) and cartridge-holder were purchased from Applied Separations (Allentown, USA). All other chemicals and materials used in this investigation have been described in section 2.1 of Chapter 2.

SC-CO_2 treatment of α-amylase

Randolph et al. (1985) have reported on the effect of SC-CO_2 conditions (101.3 bar and 35 °C) on catalytic activity of alkaline phosphatase (EC 3.1.3.1.1) mixed with disodium p-nitrophenyl phosphate (substrate), containing 0.1% (v/v) water in the feed; to obtain p-nitrophenol (the product). The enzyme along with the substrate were sealed inside a glass tube and placed inside the reaction (extraction) vessel. At the desired SC-CO_2 conditions, the reaction was initiated by

shaking the reaction vessel to shatter the glass tube. After each SFE run, the reaction was stopped by solidifying the CO_2 and by addition of 40 mL 4N NaOH.

In the present investigation, a unique method has been employed in which a polypropylene (SPE) cartridge was employed to treat the enzyme in SC-CO_2 conditions. α-amylase was loaded in the SPE cartridge (with cartridge-holder) and subjected to SC-CO_2 conditions to investigate whether the specific activity of the treated enzyme showed improved activity. The top of the cartridge was sealed with two polypropylene frits and the void inside the cartridge was filled with glass beads (Fig. 2.2.1). The loaded SPE cartridge was packed into the SFE vessel with the help of a teflon cartridge-holder and thereafter experiments were performed at pre-optimized conditions of 300 bar, 60 °C, in both batch and continuous modes (discussed in the 'Introduction' of this section) by varying the time of exposure of the enzyme (discussed later). Post SC-CO_2 treatment, CO_2 was released from the vessel and the treated enzymes were immediately recovered in 20 mM sodium phosphate buffer with 6.7 mM NaCl of pH 6.9 and estimation of the specific activity of the enzyme was conducted (discussed later).

Under SC-CO_2 conditions, α-amylase was treated in batch mode for 1.25 h, 2.25 h and 4.25 h. Results showed that time of contact below 2.25 h did not improve enzyme activity (data not shown) and maximum increase of specific activity was achieved at 2.25 h. Therefore treatment of enzyme under continuous mode was conducted for 2.25 h.

Determination of specific activity of enzyme

Enzyme activity was determined using DNSA method (Sengupta et al., 2000) by estimation of mg of maltose produced during hydrolysis of 1% soluble potato starch in 20 mM sodium phosphate buffer with 6.7 mM NaCl at pH 6.9. One unit of enzyme liberates 1 mg maltose from

starch per 3 min at pH 6.9 at 20 °C. Amount of maltose produced was estimated from its standard curve by measuring the absorbance at 540 nm in a UV-Vis Spectrophotometer (U-2000, Hitachi Corp., Kyoto, Japan). To determine specific activity of the enzyme, protein content of the enzyme samples was estimated by Folin-Lowry method (Lowry et al., 1951).

Enzyme-assisted SC-CO_2 extraction of piperine-rich extract from black pepper

For enzyme-assisted SC-CO_2 extraction of piperine-rich extract from black pepper, the powdered pepper sample was mixed with the lyophilized enzyme in optimized ratio (enzyme: black pepper powder:: 1: 5000) and subjected to batch and continuous modes of extraction at 300 bar, 60 °C. As discussed earlier, in the batch mode, static time was provided to the sample matrix after which collection of the extract (dynamic time) at a fixed flow rate of CO_2 commenced; whereas, in continuous mode, there was a constant flow of CO_2 through the sample matrix at 1 L/min for the entire duration of extraction (without prior equilibration time). Therefore, in batch mode, the enzyme had sufficient incubation time to act on the starch; while in the continuous mode, there was no static time of contact of the starch with the enzyme. These studies with the sample matrix were conducted using both SPE cartridge and SFE vessel.

α-amylase in batch mode in SC-CO_2 conditions

Lyophilized α-amylase powder was loaded to the SPE cartridge in different batch sizes (2 mg, 5 mg and 10 mg enzyme) and charged to the SC-CO_2 extraction unit. The treated enzymes were recovered in sodium phosphate buffer and subjected to estimation of specific activities.

Enzyme-assisted SC-CO_2 extraction of piperine-rich extract from black pepper in batch mode

Enzyme-assisted SC-CO_2 extraction was conducted to increase the yield of piperine (1.31±0.06 mg/g dry black pepper) by hydrolyzing the starch in the seed coat of black pepper. Two g of black pepper powder was loaded into an SPE cartridge along with 0.4 mg α-amylase (enzyme: black pepper powder:: 1: 5000) and subjected to SC-CO_2 extraction at 300 bar, 60 °C for 2.25 h (2 h static and 15 min dynamic time). The extraction was carried out with 2 L/min flow rate of gaseous CO_2. Enzyme showed maximum activity at 2.25 h of treatment (discussed in 'Results and discussion' of this section); therefore 4.25 h was no longer investigated for enzyme-assisted extraction of piperine-rich extract from black pepper.

The optimized batch size for SC-CO_2 extraction of piperine-rich extract was 20 g of ground black pepper; therefore, the enzyme-assisted extraction procedure was repeated with the similar batch size of 20 g black pepper. This was treated with 4 mg α-amylase (in SFE vessel without SPE cartridge) at 300 bar, 60 °C for 2.25 h with 2 L/min flow rate of CO_2, keeping the ratio of α-amylase and black pepper as 1:5000. To investigate the effects of flow rate, extraction was also conducted at 1 L/min flow rate of CO_2, with other parameters unchanged.

α-amylase in continuous mode in SC-CO_2 conditions

SC-CO_2 treated fungal α-amylase from *A. oryzae* in continuous mode has been reported by Senyay-Oncel and Yesil-Celiktas (2011), who obtained enhanced activity of the enzyme. In this investigation, 2 mg and 10 mg α-amylase from *B. licheniformis* were treated in separate batches with SC-CO_2 in the SPE cartridge at 300 bar, 60 °C under continuous flow of CO_2 at 1 L/min for 2.25 h.

Enzyme-assisted SC-CO_2 extraction of piperine-rich extract from black pepper in continuous mode

The maximum amount of black pepper that could be charged into an SPE cartridge was two g. For continuous mode of extraction, this amount of black pepper could not be subjected to extraction beyond 1 h since the sample matrix was exhausted of its constituents within the first 20 min of extracting time (confirmed by preliminary trials). Therefore, continuous mode of enzyme-assisted SC-CO_2 extraction of piperine-rich extract from black pepper was attempted using an SFE vessel for extraction time of 2.25 h. Black pepper (20 g) mixed with 4 mg α-amylase was charged at 300 bar, 60 °C for 2.25 h extraction with continuous flow of CO_2 at 1 L/min.

Nuclear Magnetic Resonance (NMR)

Effects of SC-CO_2 on catalytic activity and stability of enzymes depend on many factors, chiefly temperature, pressure, water content, compression/expansion cycles and depressurization rate (Wang et al., 2009). SC-CO_2 reportedly results in structural and/or conformational changes in active sites of enzyme which in turn affect its activity. These changes have been studied by ^{1}H NMR analyses of the treated enzymes (Senyay-Oncel and Yesil-Celiktas, 2011).

Untreated and SC-CO_2 treated enzyme samples (of both enhanced and reduced activities obtained by continuous mode of SC-CO_2 treatment) were dissolved in DMSO-d_6 and ^{1}H NMR spectra (relative to tetramethylsilane, TMS) were recorded at 300 MHz on a Bruker Avance DPX-300 instrument.

Estimation of total piperine content of black pepper extracts

Total piperine contents of the extracts were estimated by HPTLC analyses of the extracts as discussed in section 2.1 of Chapter 2.

Evaluation of phytochemical properties of black pepper extracts *in vitro*

Antioxidant activities of the extracts were determined by measuring the radical scavenging activity of DPPH (Aiyegoro and Okoh, 2010) and expressed as IC_{50} values (mg/mL). One of the most important classes of secondary metabolites of plants is the phenolic compounds. Total phenolic contents of extracts were estimated by Folin-Ciocalteu's reagent (Spanos and Wrolstad, 1990) and expressed as mg gallic acid equivalent/g of dry powder of black pepper. Reducing power of extract is associated with its antioxidant activity. Compounds with reducing power indicate that they are electron donors and can reduce the oxidized intermediates of lipid peroxidation processes, so that they can act as primary and secondary antioxidants. Estimation of reducing power as mg BHT/g of dry black pepper powder was carried out according to the method of Oyaizu (1986). Total phenolic content and reducing power of black pepper extracts were estimated from their respective standard curves of gallic acid and BHT. Anti-inflammatory activities of the extracts were determined by nitric oxide (NO) scavenging assay and expressed as IC_{50} values (mg/mL) (Correa et al., 2009).

Determination of free-radical scavenging capacity of black pepper extracts *in vitro*

Free-radical scavenging capacity of black pepper extracts was further validated by electron paramagnetic resonance (EPR) spectroscopy using DPPH as the source of free-radicals. Black pepper extracts were diluted in ethanol to obtain similar concentrations of each extract. 100 µL of each extract was mixed with 100 µL of DPPH solution (2 mM) and after shaking vigorously

for 10 s, it was transferred to the EPR quartz tube (inner diameter 4.0 mm). The tube was inserted into the microwave cavity of the EPR spectrometer (X-band microwave unit, JEOL Ltd., Japan). The EPR spectrum was recorded for 30 s. The conditions of the EPR spectrometer (JES-FA 200 ESR Spectrometer, JEOL, Japan) were as follows: room temperature, power: 1 mW, center field: 320 mT, width: 75 mT, field modulation width: 0.05 mT, sweep time: 30 s and time constant: 0.03 s. For the reference measurement, control DPPH solution was prepared by replacing the extract solution by 100 μL ethanol. The radical scavenging activity was calculated by the following equation:

$$\%\text{DPPH scavenging} = [(I_0 - I) / I_0] \times 100 \quad (1)$$

where: I_0 =intensity of control DPPH signal, and I = integral intensity of the DPPH signal after addition of the extract (Wasek et al., 2001).

Estimation of pungency of black pepper extracts in terms of SHU values

Black pepper is commonly known for its pungent flavor. In this investigation, Scoville organoleptic assessment of black pepper extracts was conducted to analyze the pungency of the extracts post α-amylase-assisted SC-CO_2 extractions. Estimation of SHU was conducted in accordance with the method reported by Ranganna (1986). Sucrose syrup (5% w/v) was used to dilute the ethanolic solutions of black pepper extracts and the samples were swallowed to determine the amount of extract solution required for a bite or stinging sensation in the throat which was just perceptible. Scoville heat unit (SHU) of each extract was estimated from their corresponding dilution factor. Levels of pungency in samples classified by SHU are: non-pungent (0-700 SHU), mildly pungent (700-3,000 SHU), moderately pungent (3,000-25,000

SHU), highly pungent (25,000-70,000 SHU) and very highly pungent (>80,000 SHU) (Othman et al., 2011).

GC-MS analysis of black pepper extracts

Black pepper extracts obtained from batch and continuous modes of extraction (extraction conducted without enzyme and enzyme-assisted extraction, in both modes) were analyzed by GC-MS according to the procedure discussed in section 2.1 of Chapter 2.

Evaluation of antimicrobial activity of black pepper extracts by micro broth dilution method

The antimicrobial potencies of black pepper extracts were determined to evaluate the potencies of extracts obtained by enzyme-assisted SC-CO_2 extractions as natural food preservatives. Black pepper extracts (obtained from both batch and continuous modes of extraction) and standard piperine, were subjected to determination of minimum inhibitory concentration (MIC) values against three microorganisms - *Escherichia coli* (ATCC 25922), *Staphylococcus aureus* (ATCC 25923) and *Pseudomonas aeruginosa* (ATCC 27853), according to the method reported by Ghosh et al. (2014).

The inocula of the microorganisms were prepared in Mueller Hinton broth (MHB) (HiMedia, India) and adjusted to 0.5 McFarland turbidity standard (106-107 cfu/mL). Determination of MIC values was conducted by broth dilution method using methanolic solution of black pepper extracts. Methanol was considered as the control of this experiment. After serial double dilutions of the extracts in the microwells (100 µL extract with 100 µL of broth) in an ELISA microtiter plate, 10 µL of microbial culture was subsequently added in each well of the 96-wellmicrotiter plate. The plates were incubated in a BOD incubator at 37 °C for 24 h. The MIC of extracts

against the microorganisms was determined from the optical density (O.D) measured in a microplate reader (Micronaut System, Germany) at 0 h and 24 h of incubation at 620 nm.

Statistical analyses

All experiments were conducted in triplicate and the data are expressed as mean±SD of three independent experimental runs. Statistical analysis was performed with IBM SPSS Statistics software version 20 (IBM, USA). Duncan's multiple range tests with P-value <0.05 were used to verify the significance of all tests.

Results and Discussion

α-amylase in batch mode in SC-CO_2 conditions

SC-CO_2 treatment of α-amylase in batch mode at 300 bar, 60 °C significantly increased the specific activity of enzyme when the treatment was conducted for 2.25 h (P=0.000) and 4.25 h (P=0.000) with 2 mg lyophilized enzyme in each batch. A significant (P=0.000) decrease in specific activity of the enzyme was obtained with increased batch size (2 mg-10 mg enzyme) (Table 2.2.1). Maximum increase of the specific activity of enzyme was obtained at 2.25 h with 2 mg batch size. Under these conditions, the specific activity of the enzyme was found to be 1.25 times higher (329±5 U/mg protein) than that of the untreated enzyme (264±4 U/mg protein). From these sets of runs, time of SC-CO_2 treatment of enzyme was set at 2.25 h and this was also employed as the total extraction time in enzyme-assisted extraction of black pepper oleoresin.

Enzyme-assisted SC-CO_2 extraction of piperine-rich extract from black pepper in batch mode

The enzyme-assisted SC-CO_2 extraction using the 'SPE cartridge' resulted in 88% increase in the yield of black pepper extract while use of SFE vessel for SC-CO_2 extraction for the same caused

36% increase in yield; w.r.t. extraction performed without enzyme (Table 2.2.2). In either experiment (using SPE cartridge and SFE vessel), a gaseous CO_2 flow rate of 2 L/min was used during extraction at 300 bar, 60 °C. Although an increased yield of extract was obtained using SPE cartridge, it was too low for conducting phytochemical assays. The enzyme-assisted SC-CO_2 extraction with 1 L/min flow rate of CO_2 showed 53% increase in yield of extract at extraction conditions, similar to those employed at 2 L/min flow rate of CO_2.

α-amylase in continuous mode in SC-CO_2 conditions

Specific activity of fresh α-amylase was 264±4 U/mg protein. After SC-CO_2 treatment of 2 mg enzyme in continuous mode, its specific activity increased to 561±6 U/mg protein, which was 2.13 times higher than that of the fresh enzyme. In this investigation, a significantly (P=0.000) higher increase in activity (2.13 times, i.e. 112.5%) of α-amylase was obtained, compared to 67.7% increase (i.e., 1.68 times increase) in activity of fungal α-amylase, reported by Senyay-Oncel and Yesil-Celiktas (2011). However, when the batch size was increased to 10 mg, SC-CO_2 treatment on α-amylase caused 38.5% decrease in specific activity of the enzyme. To investigate the reason behind this behavior of the enzyme, ^{1}H NMR analysis of the treated enzyme was performed. NMR spectrum showed that this decrease in the activity of the enzyme was due to disappearance of hydrogen bonds possibly in the active site of the enzyme (Fig. 2.2.2c).

According to Zagrobelny and Bright (1992), protein conformation changes during pressurization and depressurization steps in a high-pressure batch system. More importantly, loss in enzyme activity may be caused by the depressurization step at the collection end (Giessauf et al., 1999). Since there was no depressurization step in the continuous mode, it was opined that this resulted in 2.13 times increase of specific activity of α-amylase compared to 1.25 times increase of the same in the batch mode.

Enzyme-assisted SC-CO_2 extraction of piperine-rich extract from black pepper in continuous mode

In continuous mode, the yield of black pepper extract obtained by SC-CO_2 extraction performed without enzyme (at 300 bar, 60 °C for 2.25 h) was 4.6±0.4 g extract/100 g dry black pepper, whereas yield of the same in batch mode under similar conditions was 2.1±0.3 g extract/100 g dry black pepper. The results indicate that continuous mode of SC-CO_2 extraction increased the yield of extract by 121.2% without enzyme-treatment of black pepper. However, in case of enzyme-assisted SC-CO_2 extraction in continuous mode, enzymatic hydrolysis of black pepper enhanced the yield of extract by 15% (5.3±0.4 g extract/100 g dry black pepper) (Table 2.2.2), which was significantly (P=0.000) lower than the increase of yield of extract (53%) in batch mode under similar conditions of extraction. These findings attest to the fact that an incubation time was required by the enzyme for hydrolysis of the starch present in the black pepper matrix which was attained in the batch mode resulting in enhanced yield of extract from the pepper matrix.

NMR spectra of enzyme samples

The NMR spectrum of α-amylase with enhanced activity (Fig. 2.2.2b) showed changes in pattern of peaks at positions 0.81 ppm and 0.98 ppm, respectively, compared to the spectrum of the untreated enzyme (Fig. 2.2.2a). The singlet peak at position 0.81 ppm modified to a doublet peak and the doublet peak at position 0.98 ppm modified to a triplet peak in the spectrum of SC-CO_2 treated enzyme. Further, the ratios of intensities of peaks at positions 0.81 ppm and 0.98 ppm and those at 4.22 ppm and 4.41 ppm were significantly modified. Also, a new peak was observed in the NMR spectrum of SC-CO_2 treated enzyme at position 3.00 ppm. Chemical shifts observed in untreated and treated enzyme samples were: 0.81 to 0.83 ppm, 4.41 to 4.40 ppm, 7.20 to 7.19

ppm and 7.52 to 7.50 ppm. These changes in the NMR spectra suggested that SC-CO_2 altered the conformational arrangement and/or structural framework of α-amylase, possibly at its active site, which resulted in significant (P=0.000) enhanced activity (2.13 times) of the treated enzyme.

On the other hand, only one peak was observed in the NMR spectrum of SC-CO_2 treated α-amylase with reduced activity at position 1.24 ppm (Fig. 2.2.2c). This indicates that with higher batch size, SC-CO_2 significantly altered the arrangement of bonds in the enzyme which caused reduction in its activity. However, since the enzyme still retained specific activity of 68±4 U/mg protein (compared to 264±4 U/mg protein of the fresh enzyme), it can be concluded that the enzyme was not denatured by the SC-CO_2 treatment.

Estimation of piperine contents of black pepper extracts

Total piperine content of each extract was estimated by HPTLC at 337 nm using standard piperine (R_f= 0.3) as reference. Maximum increase (10.6% at 2 L/min CO_2 flow and 11.2% at 1 L/min CO_2 flow at 300 bar, 60 °C) of total piperine content of black pepper extract was obtained when enzyme-assisted extraction was carried out in SFE vessel in batch mode (Table 2.2.3).

Evaluation of phytochemical properties of black pepper extracts

The antioxidant potencies of the extracts were presented by IC_{50} values which denote the concentration of the sample required to decrease the DPPH free radicals by 50%. Lower IC_{50} value signifies higher antioxidant potency. From Table 2.2.3, it is evident that among the SC-CO_2 extracts, the highest increase in antioxidant activity (i.e., maximum decrease in IC_{50} value of DPPH radical scavenging activity) was from 3.3±0.1 to 2.7±0.1 mg/mL for extract obtained with enzyme-assisted extraction of piperine-rich extract from black pepper in batch mode at 300 bar, 60 °C with 1 L/min CO_2 flow.

For the above mentioned extraction conditions, the increase in total phenolic content was from 0.13±0.01 to 0.18±0.01 mg GAE/g of dry black pepper and increase in reducing power was from 1.9±0.1 to 2.2±0.1 mg BHT/g of dry black pepper.

These findings affirm that enzyme-assisted extraction of piperine-rich extract from black pepper in batch mode of operation (at a flow rate of 1 L/min of CO_2) is preferable for SC-CO_2 extraction, for enhanced phytochemical potencies of its extracts. The increase in anti-inflammatory activity was the highest (from 1.74±0.02 to 1.63±0.03 mg/mL) in the extract obtained from enzyme-assisted extraction of black pepper extract in batch mode at 300 bar, 60 °C with 2 L/min CO_2 flow. Overall, application of α-amylase to black pepper matrix for SC-CO_2 extraction played a significant role in improving phytochemical properties of its extracts.

In enzyme-assisted batch mode of SC-CO_2 extraction, enhancement of yield of extract along with enhancement of its piperine content and phytochemical properties were highest when extraction was performed at 300 bar, 60 °C with 1 L/min flow rate of gaseous CO_2, compared to the other methods. But total piperine content of extract was highest in enzyme-assisted continuous mode (1.45±0.04 mg/g dry black pepper) of extraction followed by enzyme-assisted batch mode with 2 L/min flow rate of gaseous CO_2 (1.36±0.04 mg/g dry black pepper) (Table 2.2.3). These extracts obtained from batch mode (with CO_2 flow rate 2 L/min) and continuous mode of extractions was further characterized by EPR analysis, Scoville organoleptic assay, GC-MS analysis and antimicrobial analysis.

Free-radical scavenging capacity of black pepper extracts

In EPR spectrum, reduction in the intensity of the DPPH signal for SC-CO_2 extracts of black pepper obtained from both batch (9.08% for without enzyme and 16.96% for enzyme-assisted

extraction) and continuous modes of extraction (16.88% for without enzyme and 17.67% for enzyme-assisted extraction) validated the antioxidant potency of each extract (Fig. 2.2.3a,b).

SHU values of black pepper extracts

SHU value for extract obtained from enzyme-assisted continuous mode of extraction was the highest (90,000). Extracts obtained from enzyme-assisted batch mode and continuous mode (without enzyme) of extraction exhibited similar SHU (80,000). SHU of extract obtained from batch mode (without enzyme) of extraction was 70,000. This result revealed that extracts obtained from continuous mode (both without and with enzyme) and enzyme-assisted batch mode of extraction had more intense pungency than that of the batch mode (without enzyme). Comparison of these results with the piperine contents of the extracts (Table 2.2.3) revealed that the pungency of extracts varied with piperine content of the same.

GC-MS analyses of black pepper extracts

The GC chromatograms and the tentatively compounds identified by mass spectrometric analyses of the black pepper extracts obtained from batch and continuous modes of extraction are presented in Fig. 2.2.4 (a-b) and Fig. 2.2.5 (a-b), respectively. The analyses revealed that although the SC-CO_2 extraction conditions were selective for piperine, few other compounds were co-extracted as well.

Antimicrobial activity of black pepper extracts

MIC values revealed that enzyme-assisted SC-CO_2 extracts had higher antimicrobial potencies w.r.t. standard piperine (Table 2.2.4). Enzyme-assisted batch mode of extraction enhanced the antimicrobial potency of the extract four times against *E. coli* and *P. aeruginosa,* and two times against *S. aureus*. Enzyme-assisted continuous mode of extraction increased the potency of the

extract two times against *P. aeruginosa*. The diluent methanol exhibited poor antimicrobial potency compared to the extracts (Fig. 2.2.6). The enhanced antimicrobial potency of extract obtained by enzyme-assisted batch mode of extraction would be beneficial for use of the extract as a food preservative.

Conclusions

This study demonstrated that α-amylase-assisted SC-CO_2 extraction enhanced the yield of piperine-rich extract from black pepper with good combination of phytochemical properties (antioxidant activity, total phenolic content, reducing power, and anti-inflammatory activity).

SC-CO_2 treatment of α-amylase and enzyme-assisted extraction of black pepper oleoresin were conducted at the optimized extraction conditions (300 bar, 60 °C and 2.25 h) in batch and continuous modes. SC-CO_2 treated α-amylase showed enhanced specific activity in either mode: 1.25 times in the batch mode and 2.13 times in the continuous mode. ^{1}H NMR analysis revealed that the enhancement of specific activity was due to an alteration in the conformational arrangement of α-amylase, possibly at its active site. This high pressure treatment of SC-CO_2 was found to be an alternative to the expensive skilled-technique based methods of genetic engineering to obtain enhanced specific activity of enzyme. This would allow facile technology transfer to industries to produce cost effective products providing higher hydrolysis in lesser time, facilitating higher production in reduced time.

Enzyme-assisted SC-CO_2 extraction in the batch mode increased the yield of piperine-rich black pepper extract by 53%, while only 15% increase in yield was obtained in the continuous mode of extraction. It was opined that the equilibration time (static time) of the batch mode possibly served as the incubation time for the enzymatic reaction leading to enhanced yield of extract and

piperine content therein. This extract was successively employed in formulation of nutraceutical cookies (section 2.3 of Chapter 2). Further, the extract was also employed in designing nanoliposomes for possible use in food engineering (section 4.3 of Chapter 4).

Novelty

The novelty of the work is that, it has reported for the first time on α-amylase-assisted SC-CO_2 extraction to enhance the yield of piperine-rich extract from black pepper, employing both batch and continuous modes of extraction, for promising use as food and therapeutic supplements. This investigation has also reported for the first time the enhancement of specific activity of bacterial α-amylase employing continuous mode of SC-CO_2 treatment.

References

Aiyegoro O. A., and Okoh A. I. (2010). Preliminary added screening and in vitro antioxidant activities of the aqueous extract of *Helichrysum longifolium* DC. *BMC Complementary and Alternative Medicine*, **10**, 2-8.

Apar K. D., and Özbek B. (2004). Corn, rice and wheat starch hydrolysis by using various alpha-amylase enzymes at temperature 40 °C, *Sigma Journal of Engineering and Natural Sciences*, **2**, 55-67.

Correa H., Valenzuela A. B., Ospina L. F., and Duque C. (2009). Anti-inflammatory effects of the gorgonian *Pseudopterogorgia elisabethae* collected at the Islands of Providencia and San Andrés (SW Caribbean). *Journal of inflammation* (London, England), **6**, 5.

Ghosh P. K., Bhattacharjee P., and Das S. (2014). Antimicrobial activity of supercritical carbon dioxide extracts of tuberose (*Polianthes tuberosa* Linn.) flowers against common pathogens. *International Journal of Pharmaceutical Sciences and Research*, **5**, 1279-1289.

Giessauf A., Magor W., Steinberger D. J., and Marr R. (1999). A study of hydrolases stability in supercritical carbon dioxide (SC-CO_2). *Enzyme and Microbial Technology*, **24**, 577-583.

Gremos S., Kekos D., and Kolisis F. (2012). Supercritical carbon dioxide biocatalysis as a novel and green methodology for the enzymatic acylation of fibrous cellulose in one step. *Bioresource Technology*, **115**, 96-101.

Lee H., Lee W. G., Park S., Lee H., and Chang H. N. (1993). Starch hydrolysis using enzyme in supercritical carbon dioxide. *Biotechnology Techniques*, **7**, 267-270.

Lowry O., Rosebrough N. J., Farr A. L., and Randall H. J. (1951). Protein measurement with the Folin phenol reagent. *The Journal of Biological Chemistry*, **193**, 265-275.

Othman Z. A. Al, Ahmed Y. B. H., Habila M. A., and Ghafar A. A. (2011). Determination of capsaicin and dihydrocapsaicin in capsicum fruit samples using high performance liquid chromatography. *Molecules*, **16**, 8919-8929.

Oyaizu M. (1986). Studies on products of browning reactions: Antioxidative activities of products of browning reaction prepared from glucosamine. *Japanese Journal of Nutrition*, **44**, 307-315.

Randolph T. W, Blach H. W., Prausnitz J. M., and Wilke C. R. (1985). Enzymatic catalysis in a supercritical fluid. *Biotechnology Letters*, **7**, 325-328.

Ranganna S. (1986). Flavouring materials. In: *Handbook of Analysis and Quality Control for Fruit and Vegetable Products*, 2nd ed. Tata McGraw Hill, New Delhi, India, pp. 243-285.

Rosso S. R. C., Bianchin E., Oliveira D., d. Oliveira J. V., and Ferreira S. R. S. (2013). Enzymatic synthesis of poly(ε-caprolactone) in supercritical carbon dioxide medium by means of a variable-volume view reactor. *The Journal of Supercritical Fluids*, **79**, 133-141.

Sengupta S., Jana M. L., Sengupta D., and Naskar A. K. (2000). A note on the estimation of microbial glycosidase activities by dinitrosalicylic acid reagent. *Applied Microbiology and Biotechnology*, **53**, 732-735.

Senyay-Oncel D., and Yesil-Celiktas O. (2011). Activity and stability enhancement of α-amylase treated with sub- and supercritical carbon dioxide, *Journal of Bioscience and Bioengineering*, **112**, 435-440.

Spanos G. A., and Wrolstad R. E. (1990). Influence of processing and storage on the phenolic composition of thompson seedless grape juice. *Journal of Agricultural and Food Chemistry*, **38**, 1565-1571.

Sundarram A., and Murthy T. P. K. (2014). α-Amylase production and applications: A review. *Journal of Applied & Environmental Microbiology*, **2**, 166-175.

Tao M., Li Q., Qu J., and Zhang M. (2013). Enzymatic synthesis of dipalmitin in supercritical carbon dioxide and mechanism study. *Industrial & Engineering Chemistry Research*, **52**, 13528-13535.

Wang S. S. S., Chao H. S., Liu H. L., and Liu H. S. (2009). Stability of hen egg white lysozyme during denaturation is enhanced by pretreatment with supercritical carbon dioxide. *Journal of Bioscience and Bioengineering*, **4**, 355-359.

Wasek M., Nartowska J., Wawer I., and Tudruj T. (2001). Electron spin resonance assessment of the antioxidant potential of medicinal plants. Part I. Contribution of anthocyanosides and flavonoids to the radical scavenging ability of fruit and herbal teas. *Acta Poloniae Pharmaceutica*, **58**, 283-288.

Zagrobelny J., and Bright F. V. (1992). *In situ* studies of protein conformation in supercritical fluids: trypsin in carbon dioxide. *Biotechnology Progress*, **8**, 421-423.

Tables

Table 2.2.1. SC-CO_2 treatment of α-amylase at 300 bar, 60 °C in batch mode.

Sample	Amount of enzyme (mg)	Time of treatment (h)	Specific activity (U/mg protein)[a]
Untreated enzyme	na	na	263.56 ± 4.35[b]
Treated enzyme	2	2.25	329.42 ± 4.67[c]
Treated enzyme	2	4.25	302.07 ± 2.98[d]
Treated enzyme	5	2.25	186.42 ± 3.19[e]
Treated enzyme	5	4.25	200.40 ± 5.52[f]
Treated enzyme	10	2.25	100.30 ± 3.90[g]
Treated enzyme	10	4.25	128.09 ± 4.00[h]

[a]Specific activities of enzyme are mean±SD of three independent runs of enzyme in SC-CO_2 condition.
na- not applicable.
Different letters in a column indicate significant differences at $P < 0.05$.

Table 2.2.2. Enzyme-assisted SC-CO_2 extraction of black pepper oleoresin at 300 bar, 60 °C.

Sample holder	Extraction mode	Sample charged for extraction	Flow rate of CO_2 (L/min)	Yield of extract (g extract/ 100 g dry black pepper)[a]	Increase in yield of extraction (%)
SPE cartridge	Batch[aa]	2 g sample without enzyme	2	0.65 ± 0.05[b]	
		2 g sample with 0.4 mg enzyme	2	1.22 ± 0.01[c]	87.69
Extraction vessel (SS 316)	Batch[aa]	20 g sample without enzyme	2	2.82 ± 0.22[d]	
		20 g sample with 4 mg enzyme	2	3.83 ± 0.18[e]	35.82
	Continuous[bb]	20 g sample without enzyme	1	2.08 ± 0.20[f]	
		20 g sample with 4 mg enzyme	1	3.19 ± 0.18[g]	53.36
		20 g sample without enzyme	1	4.60 ± 0.16[h]	
		20 g sample with 4 mg enzyme	1	5.27 ± 0.17[i]	14.56

[a] Yield of extraction are mean±SD of three independent SFE runs of three batches of black pepper.
[aa] Total extraction time consists of 2 h static and 15 min dynamic time.
[bb]Total extraction time consists of 2 h 15 min dynamic time.
Different letters in a column in each category indicate significant differences at $P < 0.05$.

Table 2.2.3. Phytochemical properties of enzyme-assisted SC-CO_2 extracts of black pepper.

Sample	Yield of piperine (mg/g dry black pepper)[a]	Antioxidant activity (IC_{50} of DPPH radical scavenging activity) (mg/mL)[a]	Total phenolic content (mg GAE/g of dry black pepper)[a]	Reducing power content (mg BHT/g of dry black pepper)[a]	Anti-inflammatory activity (IC_{50} of NO radical scavenging activity) (mg/mL)[a]
Batch mode, 2 L/min, without enzyme	1.23 ± 0.05^{d}	3.00 ± 0.15^{f}	0.11 ± 0.01^{g}	1.90 ± 0.10^{g}	1.74 ± 0.02^{d}
Batch mode, 2 L/min, with enzyme	1.36 ± 0.04^{e}	2.60 ± 0.14^{g}	0.15 ± 0.02^{h}	2.30 ± 0.11^{h}	1.63 ± 0.03^{e}
Batch mode, 1 L/min, without enzyme	0.93 ± 0.02^{f}	3.27 ± 0.11^{h}	0.13 ± 0.01^{g}	1.89 ± 0.12^{g}	2.24 ± 0.04^{f}
Batch mode, 1 L/min, with enzyme	1.03 ± 0.03^{g}	2.74 ± 0.12^{i}	0.18 ± 0.01^{g}	2.17 ± 0.13^{i}	2.15 ± 0.02^{g}
Continuous mode, without enzyme	1.36 ± 0.02^{h}	2.51 ± 0.11^{j}	0.14 ± 0.02^{g}	2.71 ± 0.14^{j}	2.84 ± 0.01^{h}
Continuous mode, with enzyme	1.45 ± 0.04^{i}	2.01 ± 0.13^{k}	0.17 ± 0.02^{h}	3.04 ± 0.12^{k}	2.74 ± 0.03^{i}

[a]Yield of piperine, IC_{50} value of DPPH radical scavenging activity, total phenolic content, reducing power content, and NO radical scavenging activity of extracts are mean±SD of three independent extraction runs of three batches of black pepper.
Different letters in a column indicate significant differences at $P < 0.05$.

Table 2.2.4. Antimicrobial properties of SC-CO_2 extracts (obtained by extractions conducted without and with enzyme) of black pepper.

Sl. No.	Sample name	MIC against selected microorganisms (µg/mL)		
		Escherichia coli	*Staphylococcus aureus*	*Pseudomonas aeruginosa*
1	Methanol	198000	198000	198000
2	Std. piperine	200	100	200
3	Black pepper, batch mode, without enzyme	400	200	200
4	Black pepper, batch mode, with enzyme	100	100	50
5	Black pepper, continuous mode, without enzyme	50	100	50
6	Black pepper, continuous mode, with enzyme	50	100	25

Figures

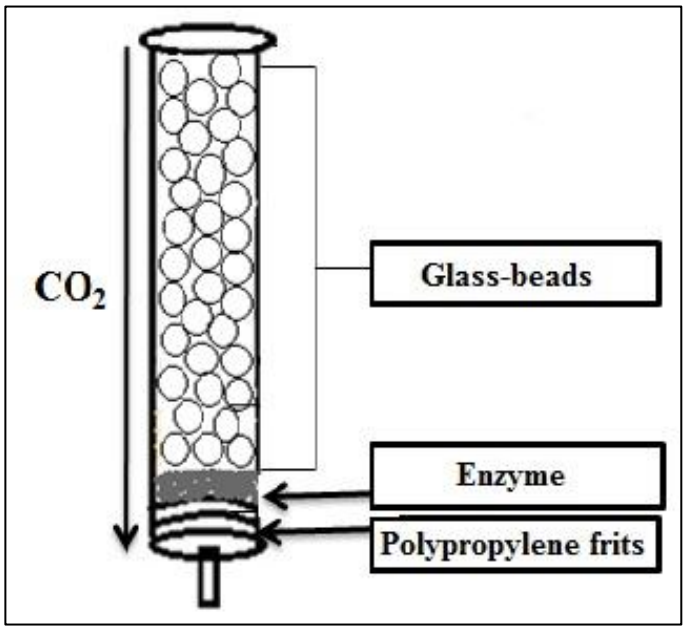

Fig. 2.2.1. Schematic diagram of SPE cartridge loaded with α-amylase.

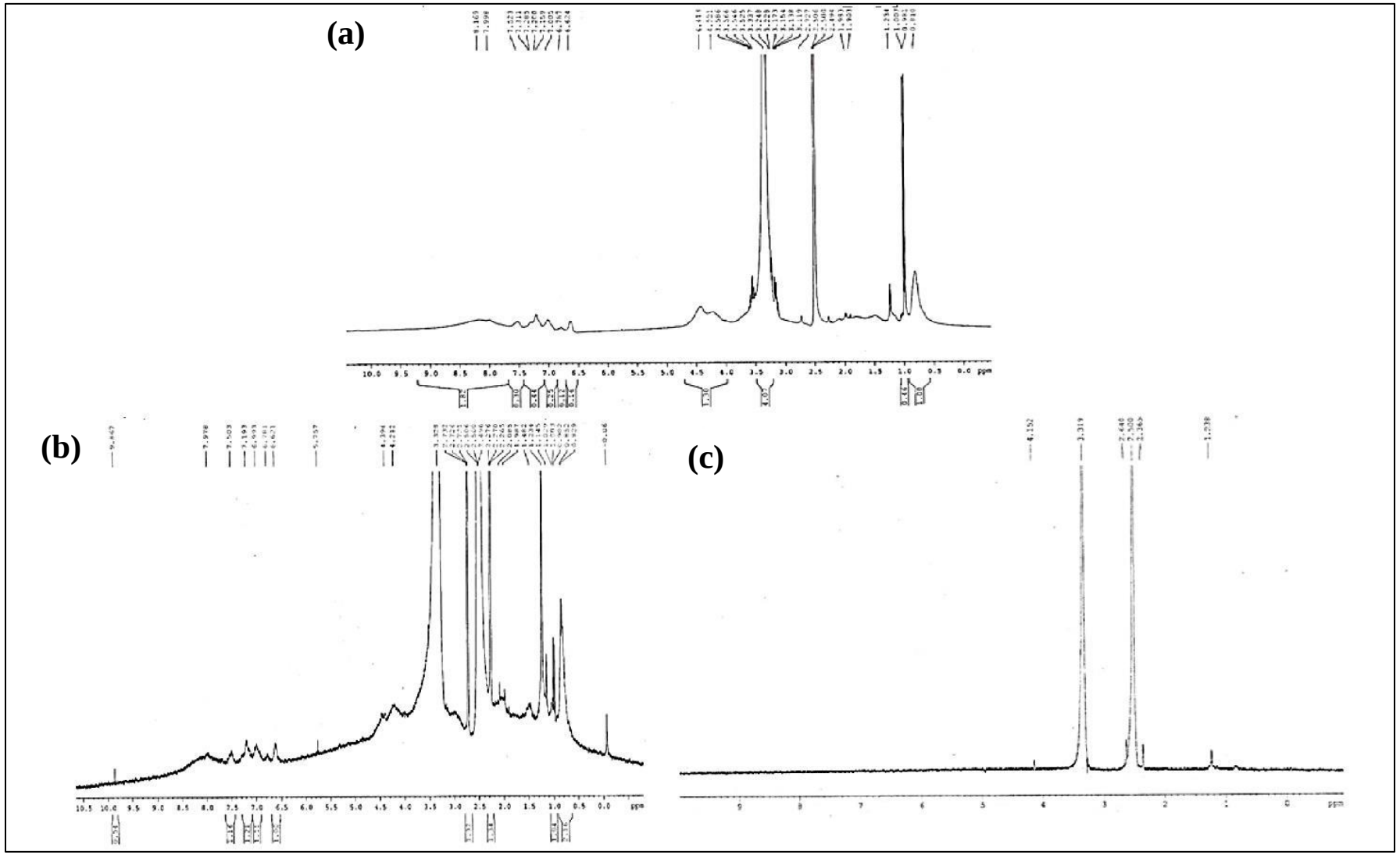

Fig. 2.2.2. ^{1}H NMR spectra of α-amylase. a) Untreated enzyme, b) Treated enzyme with highest activity, c) Treated enzyme with lowest activity.

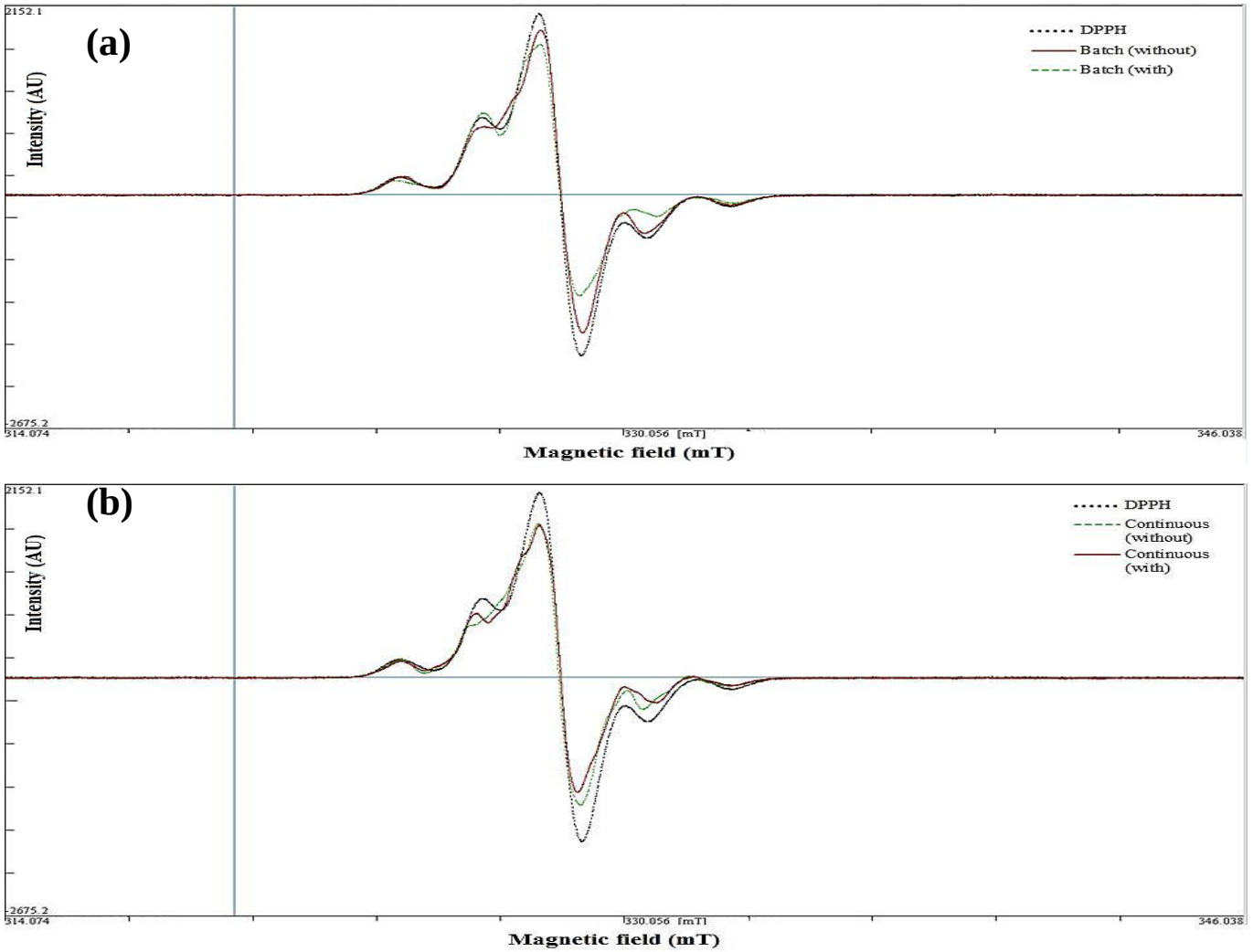

Fig. 2.2.3. EPR spectrums of DPPH free radicals in the presence of black pepper extracts. a) At batch mode and b) At continuous mode.

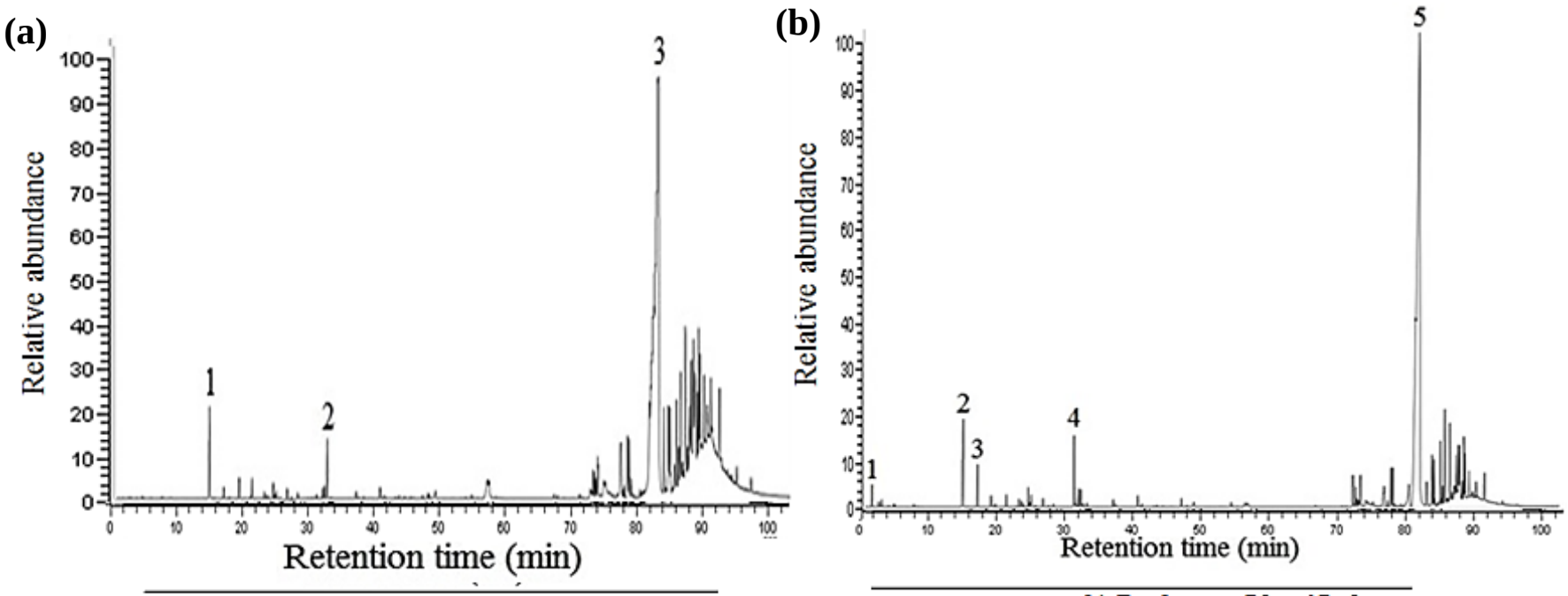

Peak no.	R.T. (min)	% Peak area	Identified compounds
1	16.34	15.33	Piperonal
2	34.57	10.98	β-caryophyllene
3	83.36	73.68	Piperine

R.T.: Retention time

Peak no.	R.T. (min)	% Peak area	Identified compounds
1	4.55	2.01	α-pinene
2	16.24	8.02	Piperonal
3	18.48	3.14	α-copaene
4	33.53	5.88	β-caryophyllene
5	82.77	80.95	Piperine

R.T.: Retention time

Fig. 2.2.4. Total ion chromatograms and list of identified compounds in black pepper extracts obtained from batch mode. a) Without enzyme, b) With enzyme.

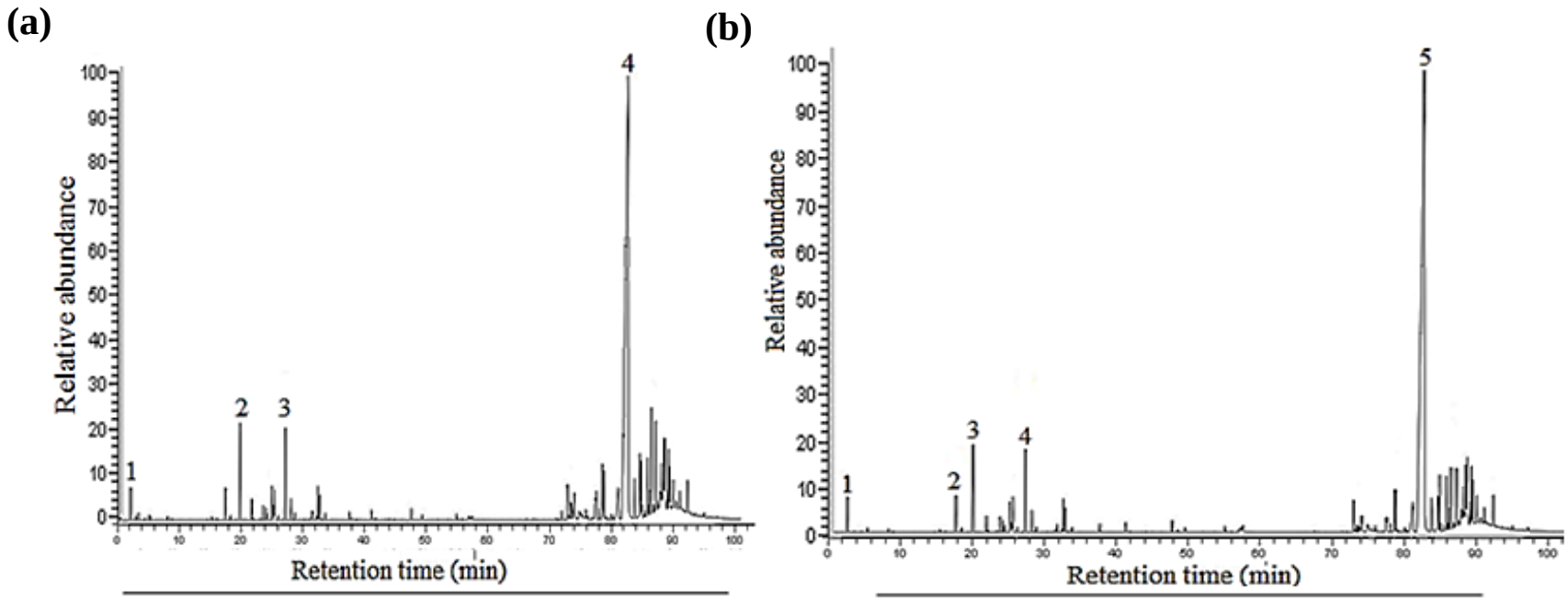

Peak no.	R.T. (min)	% Peak area	Identified compounds
1	4.54	3.95	α-pinene
2	20.81	12.12	α-humulene
3	28.88	11.18	β-elemene
4	82.73	72.74	Piperine

R.T.: Retention time

Peak no.	R.T. (min)	% Peak area	Identified compounds
1	4.55	3.43	α-pinene
2	18.49	3.40	α-copaene
3	20.83	8.54	α-humulene
4	28.90	7.47	β-elemene
5	82.77	77.15	Piperine

R.T.: Retention time

Fig. 2.2.5. Total ion chromatograms and list of identified compounds in black pepper extracts obtained from continuous mode. a) Without enzyme, b) With enzyme.

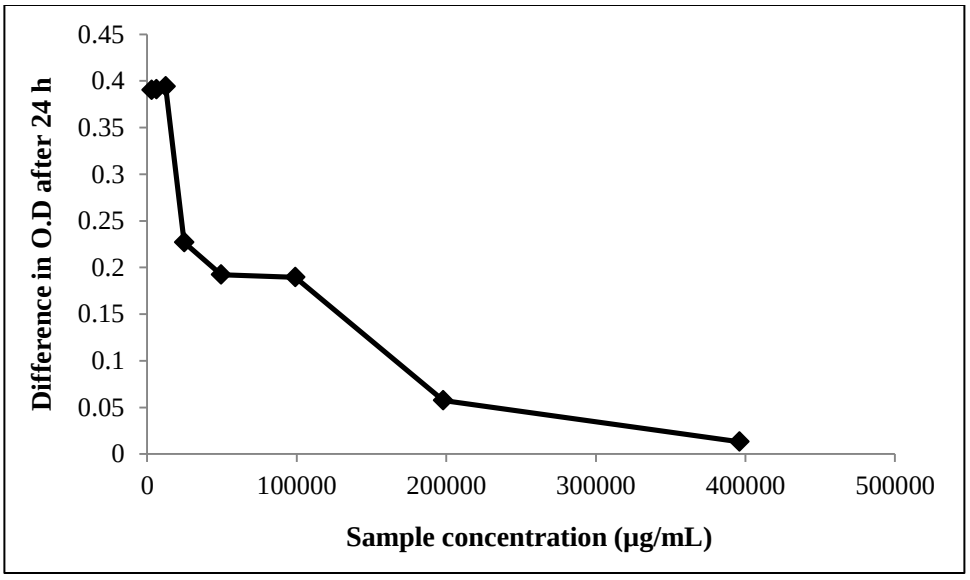

Fig. 2.2.6. Determination of MIC of methanol against *S. aureus*.

Section 2.3

Assessment of shelf-life of black pepper cookies using electronic nose

Introduction

Cookies are one of the major bakery products consumed globally (Pratima and Yadav, 2000). Cookies contain high amount of fat which have the propensity to get oxidized during storage and therefore lose their acceptability owing to rancidity. Rancidity in cookies could be averted using antioxidants. Owing to increasing consumer awareness and concerns regarding synthetic chemical additives (such as BHT and TBHQ), quest for natural antioxidants is intense (Holley and Patel, 2005).

The antioxidant, anti-inflammatory and antimicrobial properties of black pepper extracts obtained from α-amylase-assisted SC-CO_2 extractions have been quantified and presented in section 2.2 of Chapter 2. It has therefore been envisaged that these antioxidant-rich extracts could find possible application in designing nutraceutical black pepper cookies with high shelf stability. This study endeavored to design cookies using piperine-rich SC-CO_2 extract of black pepper. Besides the extract *per se*, the sample matrix, post-extraction, have also been utilized in formulating cookies; allowing complete utilization of this expensive spice.

The assessment of shelf-lives of these antioxidant-fortified cookies is a challenge. Presence of high amount of fat impedes titrimetric and other methods of analysis of rancidity and assessment of effect of antioxidant in enhancement of shelf-life of cookies is not easy by any direct technique. Sensory analysis plays a crucial role in defining shelf-life of cookies, but it is usually time-consuming and characterized by poor reproducibility of the data; moreover, it has some drawbacks originating from the subjectivity of human panels, which may give conflicting measurements when oxidized samples are analyzed.

To circumvent this limitation, Chatterjee et al. (2012) have employed state-of-the-art technology of electronic nose (e-nose) for analysis of rancid-spoilage of cookies formulated with spray dried SC-CO_2 extract of clove buds and assessment of their shelf lives. This technique minimizes the difficulties of sensory evaluation by mimicking the human olfactory system and provides rapid monitoring of flavor and/or aroma of food products. In the present investigation, metal oxide semiconductor (MOS)-based electronic nose and vision (ENOVISION, an e-nose, developed by Center for Development of Advanced Computing (C-DAC), Kolkata, India) was employed to assess rancidity in black pepper cookies.

Two dimensional principal component analysis (PCA) has reportedly been carried out to study the changes in aroma of cookies during storage. Chatterjee et al. (2014) have used PCA-based method using ENOVISION for distinct discrimination of 'rancid' (deliberately made) and 'sample' (stored for 200 days) cookies prepared with SC-CO_2 extract of clove bud. These authors have reported a discrimination index of 99.21% using the said e-nose. However, to accurately distinct between fresh and rancid cookies, graphical representation of their odor profiles alone is insufficient. Moreover, PCA plots are unable to predict the storage period of a cookie from its e-nose response. Therefore, it is necessary to generate a 'numeric value', based on e-nose responses, which would be an indicator/index of rancidity in cookies. This index would be more reproducible and robust for assessment of rancidity in cookies with storage.

Therefore, in the present investigation, Mahalanobis distance method has been applied for analysis of the e-nose data, which uses distance matrix to develop an index of rancidity. This Mahalanobis distance thus obtained would be considered as the value for 'spoilage index' (SI) for each type of cookie. Subsequently, regression equations would be generated to predict the PV values, FFA and MDA contents of cookies using the value of Mahalanobis distance. To the best of my knowledge, design of cookies using SC-CO_2 extracts of black

pepper and assessment of rancidity in cookies by Mahalanobis distance from e-nose responses have erstwhile not been attempted by researchers.

To summarize, the specific objectives of the present study were design of cookies with piperine-rich SC-CO_2 (enzyme-assisted) extract of black pepper and with the residual sample matrix post-extraction; evaluation of nutraceutical properties of cookies and assessment of shelf-life of the designer black pepper cookies by e-nose technology using SI for prediction of rancidity.

Materials and Methods

Materials

Potassium dichromate, sodium thiosulfate, potassium iodide, starch (soluble), trichloroacetic acid, thiobarbituric acid and potassium hydroxide were procured from E-Merck, Mumbai, India. All chemicals were of AR grade. The other chemicals and materials used in this investigation have been described in section 2.2 of Chapter 2.

Design of antioxidant-rich black pepper cookies

Piperine-rich extract obtained from α-amylase-assisted SC-CO_2 extraction of black pepper and post-extraction sample matrix were employed individually in formulation of antioxidant-rich drop cookies. Cookies were prepared in accordance with the method described by Chatterjee et al. (2012) (Table 2.3.1), with few modifications. The cookies were baked on a greased pan at 190 °C for 13 min inside a rotary rack convection baking oven (Model CMHS-108, Chanmag Bakery Machine Co. Ltd., New Taipei city, Taiwan). Three sets of cookies were prepared (Table 2.3.2): control (C) without addition of any antioxidant, cookie fortified with black pepper extract (E_B) and cookie fortified with post-extraction sample matrix (R_B) (Fig. 2.3.1).

The amount of extract employed in formulation of E_B cookies was 0.3 g/100 g dough weight (wet basis, i.e., w.b). The antioxidant property of cookies prepared with 0.2 g extract/100 g dough weight (w.b) was significantly (P=0.0290) lower than that of the cookies with 0.3 g extract/100 g dough weight (w.b); whereas, a pungent taste was observed in the cookies when prepared using 0.4 g extract/100 g dough weight (w.b). Therefore, an extract concentration of 0.3 g extract/100 g dough weight (w.b) was selected for formulation of E_B cookies. For R_B cookies, amount of residual matrix added to the dough was 5 g/100 g dough weight (w.b). For this set, sample matrix less than 5 g/100 g (w.b) did not show appreciable antioxidant potency; whereas, concentrations greater than this, rendered the cookies oily (adjudged by oily mouthfeel). Therefore, the concentration of the residual sample matrix in R_B cookies was fixed at 5 g/100 g dough weight (w.b).

Cookies formulated without and with antioxidant were packed in Al foil, placed in Ziploc pouches (Johnson, India), flushed with nitrogen and stored at room temperature (23±2 ºC) for shelf life study for 200 days, in accordance with the procedure described by Chatterjee et al. (2014).

Characterization of cookies

Physical properties of cookies

The diameter (D), thickness (T), weight and spread ratio (SR=D/T) of cookies were determined by AACC method 10-50D (Arun et al., 2015). Hardness of cookies was assessed by a texture analyzer (TA.XT Express, Stable Micro Systems, England), equipped with a 10 kg load cell. The cookies were penetrated with a cylinder probe (SMSP/5, diameter 5 mm) to a distance of 15 mm at a trigger force of 5 g. The peak breaking forces (N) of cookies were estimated using the force-in-compression mode of analyzer. The texture analyzer was set at a

return-to-start cycle, with a pre-test speed of 1.0 mm/s, test speed of 0.5 mm/s and post-test speed of 10 mm/s.

Color of cookies were assessed by Hunter Lab colorimeter (Konica Minolta Inc., Japan) at a 10° inclination from the light source and reported as L*, a* and b* values. L* value indicates lightness, with 100 for white and 0 for black; a* value indicates redness when positive and greenness when negative; b* value indicates yellowness when positive and blueness when negative. The color co-ordinates of these cookies were calibrated against a standard white plate. Chroma values and hue angles were determined using standard equations (Eqs. 1-2) (Chatterjee and Bhattacharjee, 2015).

$$\text{Chroma} = (a^{*2} + b^{*2})^{1/2} \quad (1)$$

$$\text{Hue angle} = \tan^{-1}(b^*/ a^*) \quad (2)$$

Estimation of nutraceutical potencies of cookies

Nutraceutical potencies of cookies, such as piperine content, antioxidant potency and total phenolic content were estimated using methanolic extracts of the cookies (Sakac et al., 2010). Piperine contents of E_B and R_B cookies were determined by HPTLC and expressed as mg piperine/g cookie (d.w.b). Antioxidant potency and total phenolic content of cookies were estimated for all three sets of cookies (C, E_B and R_B) and expressed in terms of IC_{50} values (mg/mL) and mg gallic acid equivalent/g cookie, respectively.

Determination of shelf-life of cookies

Shelf-life study of cookies was conducted by assessing their rancidity profiles using both e-nose analysis and conventional biochemical assays, at an interval of 20 days for a storage period of 200 days.

Electronic nose system for detection of rancidity in cookies

Rancidity in the cookies was detected by electronic nose or e-nose (ENOVISION, C-DAC, Kolkata, India). The e-nose system consists of 8 broadly tuned (non-specific) metal oxide gas sensors: TGS 832, TGS 816, TGS 823, TGS 830, TGS 2620, TGS 2610, TGS 2611 and TGS 2600 (Figaro, USA), each of these sensors consists of a metal oxide film such as tin oxide that respond to a wide range of volatile organic compounds (VOCs).

The array of sensors is exposed to VOCs through suitable odor handling and delivery systems that ensure constant exposure rate to each of the sensors. The VOCs from samples undergo redox reactions at the sensor surfaces, resulting in an increase of conductivities across the sensors and the corresponding changes in voltages are recorded. These signals from the sensor array are conditioned and processed through suitable circuitry and delivered to an intelligent pattern recognition engine for analysis. A mini air compressor is used to maintain requisite airflow. Three solenoid valves are used to route the airflow to the sample holder and the sensor array (Fig. 2.3.2). A blower is used to reinforce air evacuation during purging (Bhattacharyya et al., 2008).

Although electronic nose technology has been widely employed for quality assessment of foods over the last decade, there are some limitations of this technology. Besides high cost of the instruments and the sensors, temperature and moisture sensitivities of sensors and their tendency to ‘drift’ with repeated usage (obscuring their true responses), compels the need for regular calibration. High concentration of VOCs from samples may cause ‘sensor poisoning’ and reduces their sensitivity (Harper, 2001; Sujatha et al., 2012). However, these limitations can be redressed through appropriate sample preparation and regular instrument calibration.

Optimization of process parameters such as batch size and granularity of cookies, heating time, time for headspace generation, sampling and purging time were ascertained from

preliminary trials. The e-nose was calibrated using different batches of cookie powders and optimization of the parameters was conducted based on the maximum response of the sensors. Based on findings of preliminary trials, 50 g of ground cookie powder (d_p=0.50±0.02 mm) was charged into a 100 mL vial and heated by a 50 W miniature halogen lamp for 450 s at 50±2 °C. The headspace was allowed to generate for 30 s to ensure adequate concentration of VOCs. Sampling time for sensors was kept constant at 50 s. Post sensing, fresh air was purged for 300 s at 5 mL/s flow rate, to enable the sensors to return to their baseline values.

For detection of rancidity in cookies, the e-nose system was trained with three sets of deliberately-made rancid cookies: C cookie for training (TC), E_B cookie for training (TE_B) and R_B cookie for training (TR_B) (Table 2.3.2), in accordance with the method reported by Chatterjee et al. (2012). These rancid cookies were prepared by keeping the freshly prepared C, E_B and R_B cookies in an accelerated rancidity chamber under UV light to promote oxidation of cookies at constant temperature of 40±2 °C. On completion of the ageing treatment, the samples were removed from the rancidity chamber at intervals (discussed later), flushed with nitrogen and stored in a 'conservation chamber' to maintain the final rancidity stage.

Selection of e-nose sensor for analysis of black pepper cookies

The responses of the e-nose sensors for all types of cookies were determined according to the method reported by Chatterjee et al. (2014). For each sample, ΔR/R value was determined for every sensor, which is the change in signals from the metal oxide sensors due to the VOCs of cookies on day 'd', with respect to the signals generated for freshly prepared cookies. In order to select the sensors most sensitive for VOCs of rancidity in control cookies and black pepper cookies, e-nose responses for TC, TE_B and TR_B cookies were plotted against storage time. The sensors which showed the highest and stable responses were selected as the 'best

sensors' for each type (control and black pepper) of cookies. Analysis of rancidity in cookies was conducted at an interval of 20 days for 200 days.

Biochemical assays for determination of rancidity in black pepper cookies

Biochemical assays such as determination of free fatty acid (FFA) content, peroxide value (PV) and thiobarbituric acid value (TBA) were conducted to estimate rancidity in cookies. These FFA, PV and TBA were considered as 'conventional rancidity parameters' in this study. They were estimated according to the methods reported by Chatterjee et al. (2014) and expressed as % oleic acid, meq/kg of cookie and mmol malonaldehyde/g cookie, respectively.

Statistical analyses

In this investigation, PCA was performed by XLSTAT 2014.5.03 (Microsoft Corporation, USA). Distances among the data points were used as the basis of identification of differences in odor profiles of cookies. Evaluation of these distances was conducted by the Mahalanobis distance method.

In brief, the Mahalanobis distance evaluates the distance between two data points by assigning different weights or importance factors to the features of data points in the set. In the present study, estimation of Mahalanobis distance was conducted using MATLAB 7.6.0. (R2008a) (Maths-Work, USA). Regression equations were generated using STATISTICA Software version 8.0 (StatSoft, OK) to predict the PV values, FFA contents and MDA contents of cookies as functions of Mahalanobis distances. Significant differences between means were determined by Duncan's multiple-range test using IBM SPSS Statistics software version 20 (IBM, USA). A P value of 0.05 was used to verify the significance of all tests.

Results and Discussion

Characterization of black pepper cookies

Physical properties of black pepper cookies

Similar values of diameters and thicknesses were observed for C, E_B and R_B cookies (Table 2.3.3) indicating no adverse changes of the dimensions of cookies on fortification with SC-CO_2 extract and with post-extraction sample matrix of black pepper. The spread factor obtained for the cookies were in the range of 4.52-4.69. Abdel-Samie et al. (2010) have obtained similar dimensions (4.03-4.26 cm diameter, 0.65-0.74 cm thickness) and spread factor (5.43-6.54) for cookies prepared with cumin and ginger powders.

The hardness and color values of cookies are presented in Table 2.3.3. Hardness of the cookies was in the range of 48-52 N, which was similar to the hardness reported by Jacob and Leelavathi (2007) for cookies prepared with hydrogenated fat. Application of extract in E_B cookies enhanced the brightness (L*=64.79±0.70) of the same, which was significantly higher than that of the C (L*=60.88±0.20) and R_B cookies (L*=57.27±0.44) (P values 0.0007 and 0.0010, respectively). On the other hand, formulation of cookies with the sample matrix decreased redness (a*=5.69±0.29) and yellowness (b*=20.79±0.46) in R_B cookies, compared to those of C cookies (a*=9.61±0.06 and b*=26.15±0.04, respectively) significantly (P=0.0000 and P=0.0000, respectively).

Phytochemical properties of black pepper cookies

The phytochemical properties of the black pepper and control cookie samples are represented in Fig. 2.3.3 and Fig. 2.3.4, respectively. The antioxidant potencies of C cookies decreased by 6.62 times (from 14.38 to 95.30 mg/mL); whereas, antioxidant potencies of E_B and R_B cookies decreased by 1.04 times (from 1.08 to 1.12 mg/mL) and 1.38 times (from 1.25 to 1.72 mg/mL) respectively, after 200 days of storage. A similar trend was observed for total

phenolic contents of cookies. In C cookies, there was significant (P= 0.0002) loss of total phenolic content with storage and after 80 days, total phenolic content of C cookies was depleted. In E_B and R_B cookies, decrease of total phenolic contents was much lower compared to C cookies after 200 days storage. For E_B cookies, decrease of total phenolic content was 1.64 times (from 22.23 to 13.55 µg gallic acid equivalent/g cookie) and for R_B cookies, it was 2.92 times (from 10.43 to 3.56 µg gallic acid equivalent/g cookie).

Piperine content of fresh E_B cookies was 101.56 µg/g dry cookie, which degraded to 98.23 µg/g dry cookie over the storage period of 200 days (Fig. 2.3.3c). Piperine content of fresh R_B cookies (84.0 µg/g dry cookie) was significantly (P=0.0000) low, compared to that of the E_B cookies, which decreased to 79 µg/g dry cookie after 200 days. These observations indicated that additions of extract and post-extraction sample matrix of black pepper to cookies increased their phytochemical properties and enhanced their shelf stability.

E-nose sensors for analysis of rancidity in cookies

The sensor TGS2610 showed highest response with minimum variation, followed by TGS2600 and TGS2611 when TE_B and TR_B cookies were analyzed (Fig. 2.3.5a-b). Therefore, these three sensors were selected for assessment of rancidity in black pepper cookies. Similarly, the sensors selected for assessment of rancidity in TC cookies were TGS823, followed by TGS832 and TGS2600 (Fig. 2.3.6).

Electronic nose system for assessment of rancidity in cookies

Analysis of rancidity in cookies using PCA-based odor maps for each type of cookie indicated the relative positions of the data point of each cookie of the sample set with respect to those of the training set (Fig. 2.3.7). The PCA plot of control cookies revealed that, odor profile of 80 day-stored cookies was similar to that of the fresh control cookies; however, the data points of C cookies for storage of 100 days and above were present in the same quadrant

along with the cluster of TC cookies (Fig. 2.3.7a). This result attested that C cookies were non-rancid up to 80 days.

In PCA plot for E_B cookies, 200 day-stored cookies formed a distinct cluster, separate from that of TE_B, which suggested that cookies prepared with black pepper extract prevented rancidity for at least 200 days (Fig. 2.3.7b). Data points of R_B cookies with storage period 180 days and above were present in the same quadrant along with the TR_B cookies indicating rancidity in R_B cookies from 180 days (Fig. 2.3.7c).

Mahalanobis distance between fresh cookies and stored cookies

SI was generated for each type of cookies (SI_C for control cookie, SI_{EB} for cookie with black pepper extract and SI_{RB} for cookie with residual black pepper matrix) using Mahalanobis distance method (Table 2.3.4).

The SI_C of 100 day-stored C cookies (15.6680) was significantly higher (P=0.0000) than 1 day-rancid TC cookies (14.9807), which revealed that 100 day-stored C cookies became rancid (Table 2.3.4). This finding was in agreement with the data of PCA plots, wherein the data points of 100 day-stored C cookies was within the cluster of rancid cookies (Fig. 2.3.7a). The SI values of 200 day-stored E_B (20.5565) cookies suggested that the value was significantly (P=0.0000) distant from that of rancid cookie (55.8281) (Table 2.3.4). For R_B cookies, SI values indicated that, it became rancid from 180 days (SI of 180 day-stored R_B and 1 day-rancid TR_B were 41.7037 and 40.1788, respectively) (Table 2.3.4).

The SI values validated the observations of the PCA plots of cookies that, SC-CO_2 extract enhanced the shelf lives of black pepper cookies by at least 120 days, whereas post-extraction sample matrix enhanced the same by 80 days in R_B cookies. Moreover, these indices established numeric values which can precisely and accurately distinguish between fresh and rancid cookies.

Conventional rancidity parameters of cookies

Comparing the values of biochemical assays (FFA, PV and TBA) of stored cookies with deliberately rancid cookies, it was found that C cookies remained non-rancid at least for 80 days, after which its conventional rancidity parameters were found to be similar with those of TC cookies (Fig. 2.3.8). Similarly, R_B cookies remained non-rancid at least for 160 days; but for E_B cookies, no such trend was observed and it remained non-rancid till the end of the storage period of 200 days (Fig. 2.3.8). Therefore, values of biochemical assays were in good agreement with the shelf-lives assessed by e-nose analyses.

Correlation between the rancidity parameters of cookies determined by e-nose analysis and biochemical assays

Since the data from e-nose analyses were well-correlated with the biochemical assays, linear regression equations were generated by multiple regression analyses to predict the FFA, PV and TBA values of cookies (individually for each cookie type), as a function of their SI values (Table 2.3.5). Good correlation coefficients (r) of the equations (Eqs. 3-11) suggest that these equations can be used to predict the conventional rancidity parameters of cookies from their SI values obtained from e-nose data.

For C cookies, conventional rancidity parameters, i.e., values of FFA, PV and MDA have been calculated from e-nose responses of the cookies using Eqs. 3, 4 and 5, respectively (Table 2.3.5). For 1 day-stored TC cookies, the values of FFA, PV and MDA were 1.040% oleic acid, 10.110 mEq/kg cookie and 2.559 mmol/g cookie respectively (Fig. 2.3.8a-c). C cookies having similar or higher values of FFA, PV and MDA can be considered as rancid samples. Similarly, for E_B cookies, conventional rancidity parameters have been calculated using Eqs. 6, 7 and 8 (Table 2.3.5). For 1 day-stored TE_B cookies, values of FFA, PV and

MDA were 1.040% oleic acid, 9.560 mEq/kg cookie and 1.209 mmol/g cookie (Fig. 2.3.8a-c).

For R_B cookies, FFA, PV and MDA values were calculated from Eqs. 9, 10 and 11 (Table 2.3.5). The values of the rancidity parameters for 1 day-stored TR_B cookies were 1.080% oleic acid (FFA), 9.560 mEq/kg cookie (PV) and 1.839 mmol/g cookie (MDA) (Fig. 2.3.8a-c). Values of FFA, PV and MDA of cookies calculated from their corresponding SI value can be used to estimate the rancidity in cookies, i.e. cookies having similar or higher values of FFA, PV and MDA compared to their corresponding rancid cookies can be considered as rancid samples. Therefore, e-nose technology can be effectively employed to detect rancidity in cookies designed with black pepper avoiding the need to conduct biochemical assays, making the assessment more accurate and accelerated.

Conclusions

E-nose technology (having 8 MOS sensors) was successfully employed for detection of rancidity in drop cookies designed with extracts obtained from α-amylase-assisted SC-CO_2 extractions of black pepper and residual sample matrices post-extraction. PCA plots and Mahalanobis distances obtained from e-nose responses of cookies, revealed that SC-CO_2 extracts of black pepper enhanced shelf lives of cookies by at least 120 days; while the post-extraction residual sample matrix enhanced the same by 80 days.

Mahalanobis distance determined for each type of cookie was considered as the 'spoilage index', which is a numeric value that can rapidly and accurately predict the rancidity and hence the shelf life of cookies. The results of e-nose analyses were in good agreement with the results obtained by standard biochemical assays. Finally, regression equations generated using the biochemical indices (FFA content, PV value and MDA content for each type of cookie) and the e-nose responses (spoilage indices) would allow prediction of the former

values, foregoing routine biochemical assays. Similar methodology using spoilage indices was also employed for accurate assessment of rancidity in small cardamom cookies, elaborated later in section 3.2 of Chapter 3.

Novelty

The novelty of this work is that it has reported for the first time on designing of cookies with extract obtained from SC-CO_2 extraction and post-extraction residual sample matrix of black pepper; assessment of shelf-lives of these cookies applying PCA and Mahalanobis distance methods to the e-nose data and calculation of 'spoilage index' to rapidly and accurately predict the rancidity and hence the shelf-lives of cookies. The methodology developed in this study will allow food analytical chemists to forego biochemical assays. Further this robust procedure of usage of PCA, Mahalanobis distance and spoilage index for estimation of rancidity can be adopted for other confectionary several food products.

References

Abdel-Samie M. A., Wan J., Huang W., Chung O. K., and Xu B. (2010). Effects of cumin and ginger as antioxidants on dough mixing properties and cookie quality. *Cereal Chemistry*. http://dx.doi.org/10.1094/CCHEM-01-10-0012.

Arun K. B., Persia F., Aswathy P. S., Chandran J., Sajeev M. S., Jayamurthy P., and Nisha P. (2015). Plantain peel - a potential source of antioxidant dietary fibre for developing functional cookies. *Journal of Food Science and Technology*, **52**, 6355-6364.

Bhattacharyya N., Tudu B., Jana A., Ghosh D., Bandhopadhyaya R., and Saha A. B. (2008). Illumination heating and physical raking for increasing sensitivity of electronic nose measurements with black tea. *Sensors and Actuators B*, **131**, 37-42.

Chatterjee D., and Bhattacharjee P. (2015). Use of eugenol-lean clove extract as a flavoring agent and natural antioxidant in mayonnaise: product characterization and storage study. *Journal of Food Science and Technology*, **52**, 4945-954.

Chatterjee D., Bhattacharjee P., Lechat H., Ayouni F., and Vabre V. (2012). Assessment of shelf-life of cookies formulated with clove extracts using electronic nose: Estimation of rancidity in cookies. Proceedings of the 2012 Sixth International Conference on Sensing Technology, ISBN 978-1-4673-2245-4, DOI: http://dx.doi.org/10.1109/ICSensT.2012.6461709 (pp. 404-409), Kolkata.

Chatterjee D., Bhattacharjee P., Lechat H., Ayouni F., Vabre V., and Bhattacharyya N. (2014). Electronic nose setup for estimation of rancidity in cookies. In: *Sensing technology: Current status and future trends II, smart sensors, measurement and*

instrumentation. Mason A., Mukhopadhyay S. C., Jayasundera K. P., and Bhattacharyya N. (Eds.), Springer International Publishing, Switzerland, pp. 1-27.

Harper J. W. (2001). The strength and weakness of the electronic nose. In: *Headspace Analysis of Food and Flavors: Theory and Practice*, Rouseff R. L., and Cadwallader K. R. (Eds.), vol. 488, Springer, New York, pp. 59-71.

Holley R. A., and Patel D. (2005). Improvement in shelf-life and safety of perishable foods by plant essential oils and smoke antimicrobials. *Food Microbiology*, **22**, 273-292.

Jacob J., and Leelavathi K. (2007). Effect of fat-type on cookie dough and cookie quality. *Journal of Food Engineering*, **79**, 299-305.

Pratima A., and Yadav M. C. (2000). Effect of incorporation of liquid dairy by-product on chemical characteristic of soy fortified biscuits. *Journal of Food Science and Technology*, **37**, 158-161.

Sakac M. B., Gyura J. F., Misan A. C., Seres Z. I., Pajin B. S., and Soronja-Simovicm D. M. (2010). Antioxidant activity of cookies supplemented with sugarbeet dietary fiber. *Sugar Industry*, **136**, 151-157.

Sujatha G., Dhivya N., Ayyadurai K., and Thyagrajan D. (2012). Advances in electronic nose technologies. *International Journal of Engineering Research and Application*, **2**, 1541- 1546.

Tables:

Table 2.3.1. Formulation of drop cookies.

Ingredients	% (wet basis, w/w of dough weight)
Wheat flour	50.0
Powder sugar	20.0
Hydrogenated vegetable fat	20.0
Butter	2.0
Milk powder	2.0
Ammonium bicarbonate	0.8
Table salt	0.6
Sodium bicarbonate	0.4
Lecithin	0.3
Water	8.0

Table 2.3.2. Different sets of cookie samples prepared.

Sample code	Sample	Quality
C	Control set	Cookies formulated without antioxidant, stored for 0 to 200 days
E_B	Sample set formulated with black pepper extract	Cookies formulated with black pepper extract and stored for 0 to 200 days
R_B	Sample set formulated with post-extraction sample matrix of black pepper	Cookies formulated with post-extraction matrix of black pepper and stored for 0 to 200 days
TC	Training set of C cookies	C cookies deliberately made rancid in accelerated rancidity chamber for 1, 2, 3, 6, 10 and 17 days
TE_B	Training set of E_B cookies	E_B cookies deliberately made rancid in accelerated rancidity chamber for 1, 2, 3, 6, 10 and 17 days
TR_B	Training set of R_B cookies	R_B cookies deliberately made rancid in accelerated rancidity chamber for 1, 2, 3, 6, 10 and 17 days

Table 2.3.3. Physical properties of cookies.

Sample	Diameter* (cm)	Thickness* (cm)	Spread ratio	Weight* (g)	Hardness* (N)	L*	a*	b*	Chroma	Hue angle (°)
C	5.74±0.02^{a}	1.23±0.05^{a}	4.67^{a}	25.20±0.20^{a}	49.67±0.30^{b}	60.88±0.20^{b}	9.61±0.06^{d}	26.15±0.10^{c}	27.86±0.10^{c}	69.82±0.12^{a}
E_B	5.65±0.03^{a}	1.25±0.04^{a}	4.52^{a}	25.10±0.30^{a}	48.35±0.50^{a}	64.79±0.70^{d}	9.70±0.05^{d}	27.09±0.14^{d}	28.77±0.15^{d}	70.30±0.14^{b}
R_B	5.72±0.03^{a}	1.22±0.04^{a}	4.69^{a}	25.20±0.20^{a}	51.87±0.20^{c}	57.27±0.40^{a}	5.69±0.09^{b}	20.79±0.09^{b}	21.55±0.11^{b}	74.69±0.10^{d}

C- control cookies, E_B- cookies formulated with extract of black pepper, R_B- cookies formulated with post-extraction sample matrix of black pepper
*Values of diameter, thickness, weight, hardness and color parameters of cookies are mean±SD of three independent samples
Different letters in a column indicate significant difference at $P \leq 0.05$

Table 2.3.4. Spoilage indices of different cookies at different storage days.

	Spoilage indices of cookies		
Storage days	C	E_B	R_B
20	0.3703	0.2825	0.1766
40	0.5104	2.6538	1.4033
60	2.9736	5.9716	4.5537
80	7.5380	7.7148	6.7920
100	15.6680	8.1561	11.1769
120	16.7971	8.8090	12.4228
140	15.8249	13.8211	20.4577
160	16.9943	13.5404	28.6597
180	18.0813	18.0509	41.7037
200	20.2187	20.5565	49.8935
Rancid 1 day	14.9807	55.8281	40.1788
Rancid 2 days	24.4412	68.2221	48.7485
Rancid 3 days	44.4147	74.2565	64.1653
Rancid 6 days	67.6875	65.1785	82.2783
Rancid 10 days	82.1595	74.1129	84.4138
Rancid 17 days	93.6358	86.5964	89.3234

C- control cookies, E_B- cookies formulated with extract of black pepper, R_B- cookies formulated with post-extraction sample matrix of black pepper

Table 2.3.5. Regression equations generated from conventional biochemical parameters of rancidity and spoilage indices (SI) of different types of cookies stored for 200 days.

Sample	Equation	r value	Equation number
C	$FFA = 0.056 \times SI_C + 0.529$	0.858	3
	$PV = 0.611 \times SI_C + 4.073$	0.954	4
	$MDA = 0.162 \times SI_C + 0.219$	0.983	5
E_B	$FFA = 0.014 \times SI_{EB} + 0.431$	0.916	6
	$PV = 0.168 \times SI_{EB} + 1.511$	0.944	7
	$MDA = 0.025 \times SI_{EB} + 0.009$	0.991	8
R_B	$FFA = 0.016 \times SI_{RB} + 0.499$	0.981	9
	$PV = 0.186 \times SI_{RB} + 1.695$	0.992	10
	$MDA = 0.048 \times SI_{RB} - 0.007$	0.990	11

C- control cookies, E_B- cookies formulated with extract of black pepper, R_B- cookies formulated with post-extraction sample matrix of black pepper

Figures:

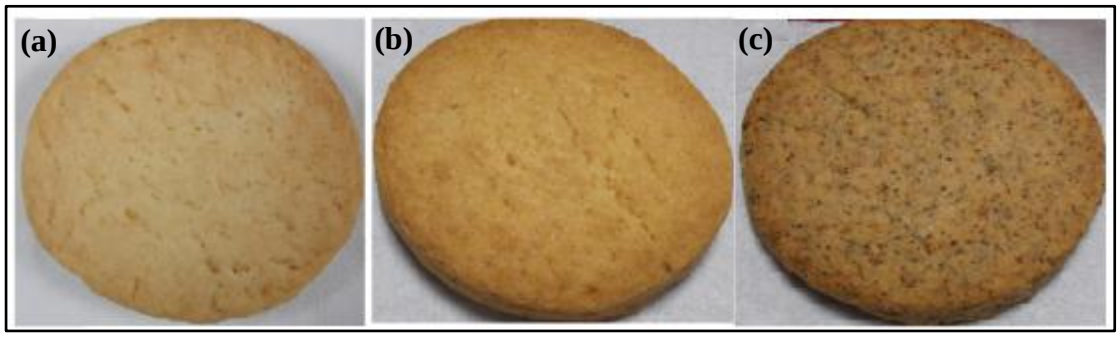

Fig. 2.3.1. Different sets of cookies designed (a) Control (C), (b) Cookie fortified with black pepper extract (E_B) and (c) Cookie fortified with post-extraction sample matrix of black pepper (R_B).

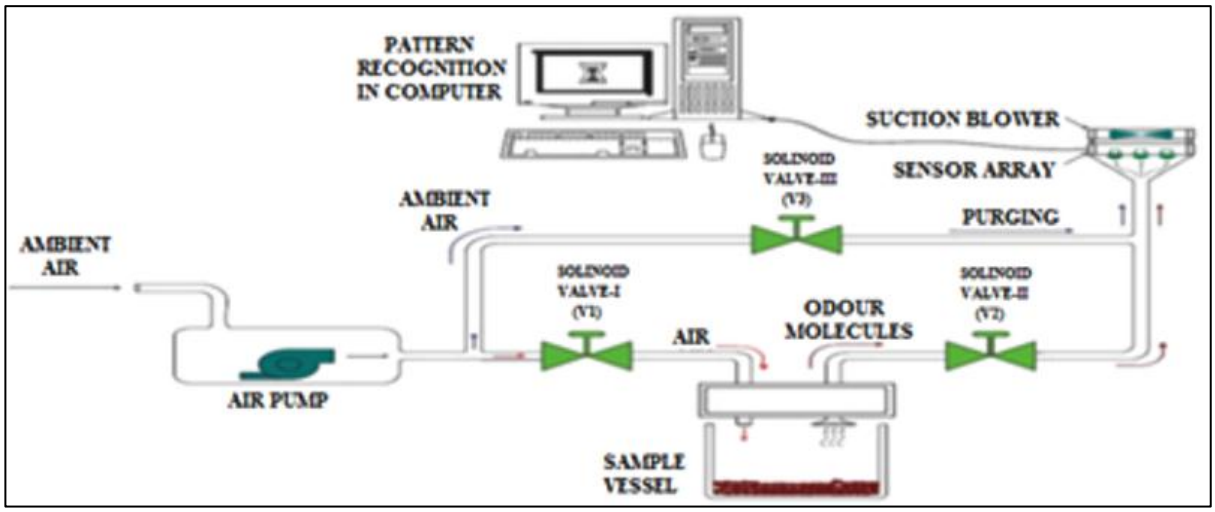

Fig. 2.3.2 Schematic diagram of e-nose system of ENOVISION (Chatterjee et al., 2014).

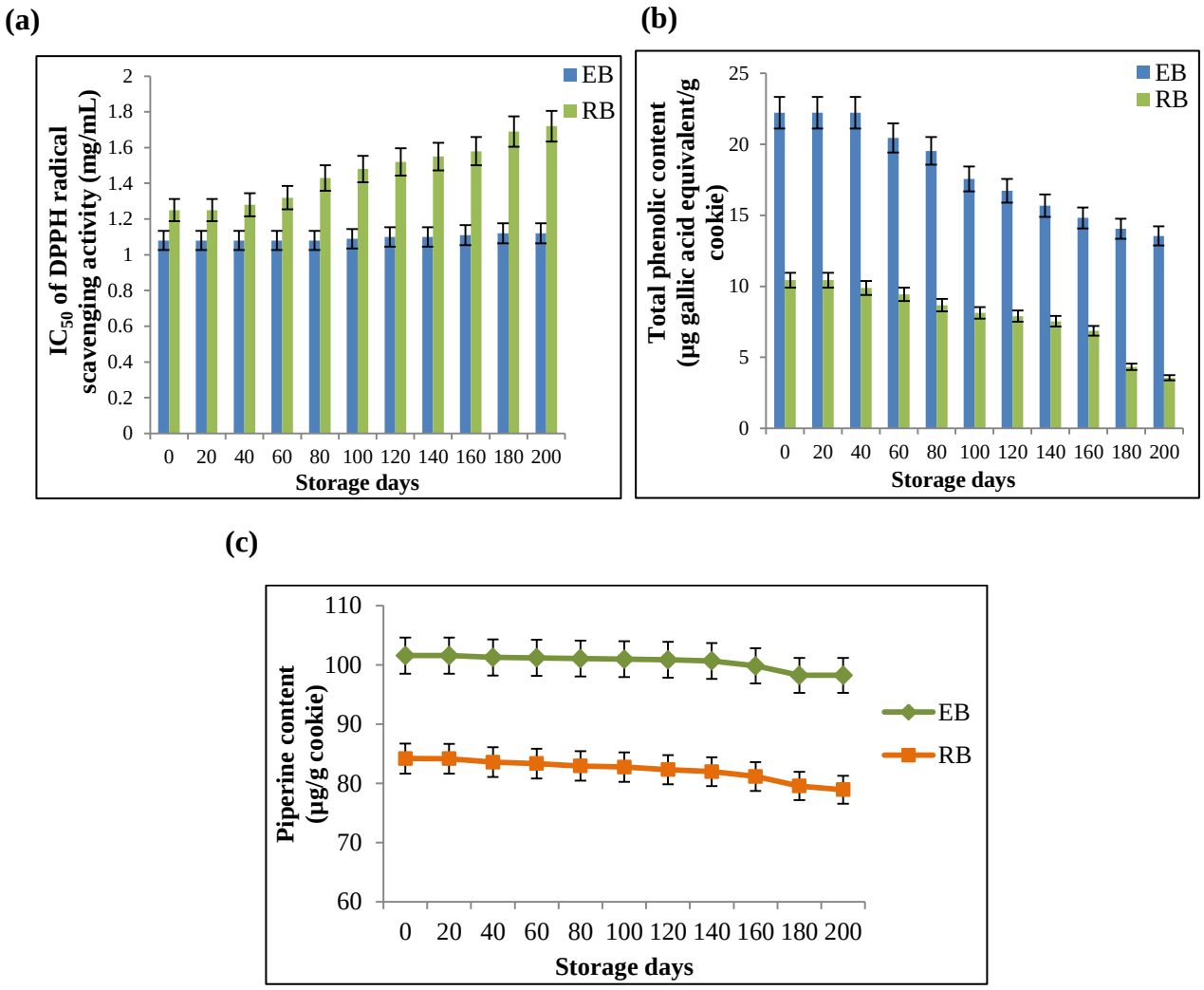

Fig. 2.3.3. Changes in phytochemical properties of black pepper (E_B and R_B) cookies with storage days. (a) Antioxidant potency (IC_{50} value), (b) Total phenolic content and (c) Piperine content.

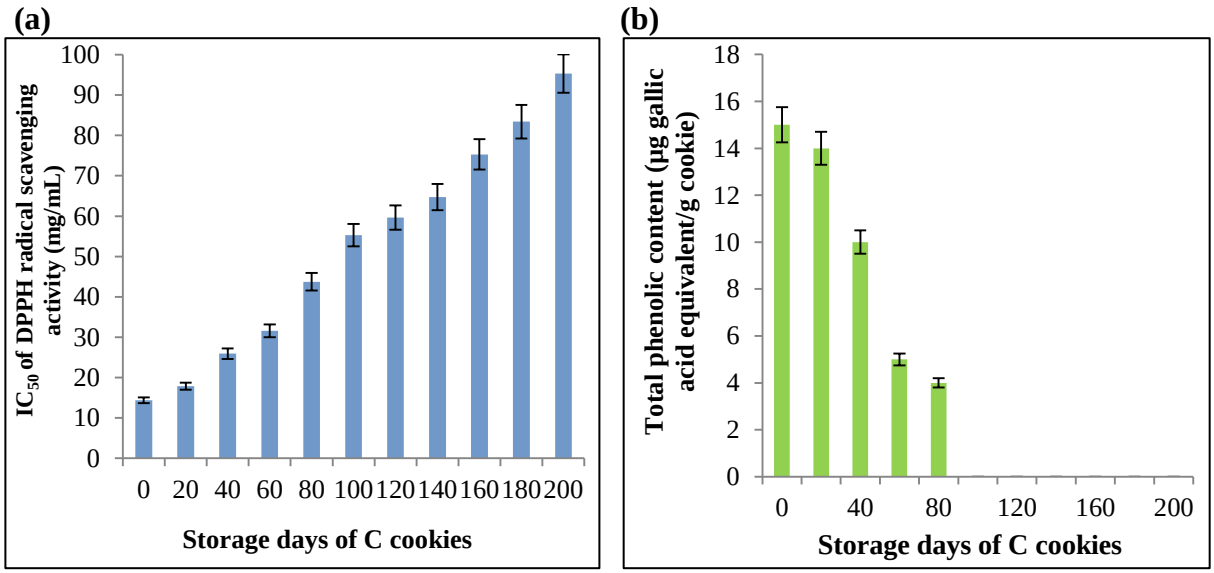

Fig. 2.3.4. Changes in phytochemical properties of control (C) cookies with storage days. (a) Antioxidant potency (IC_{50} value), (b) Total phenolic content.

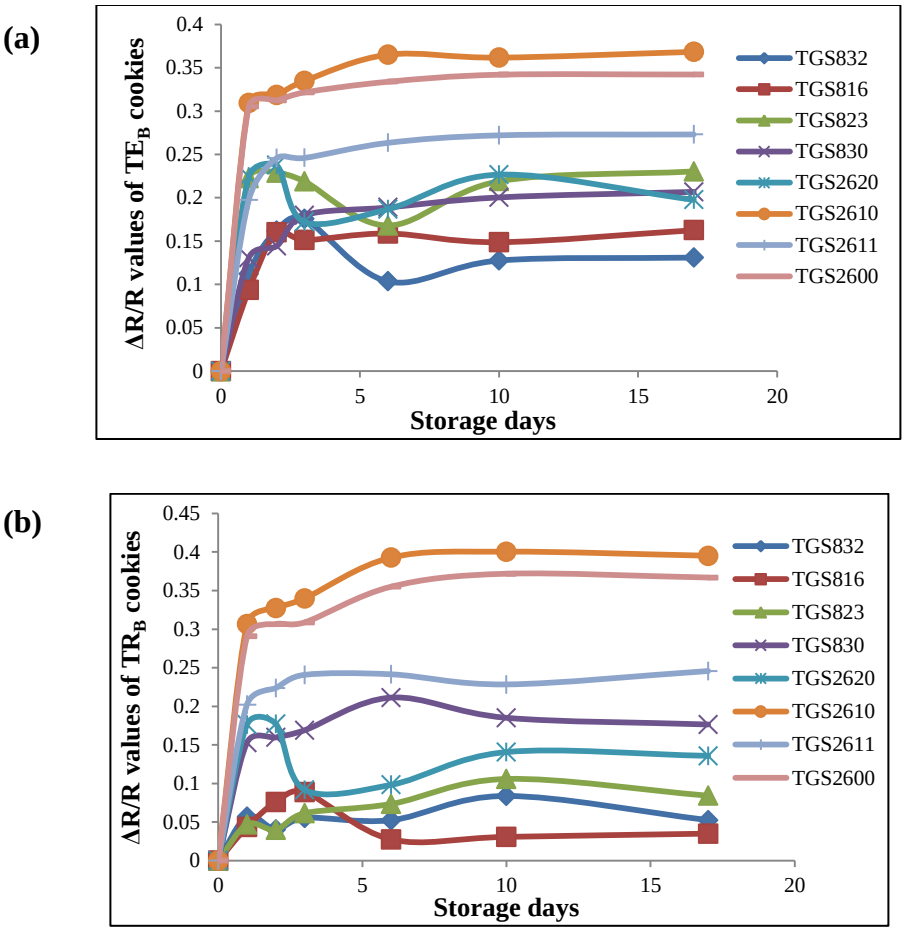

Fig. 2.3.5. Selection of e-nose sensors based on responses obtained for deliberately-made rancid cookies. (a) TE_B and (b) TR_B.

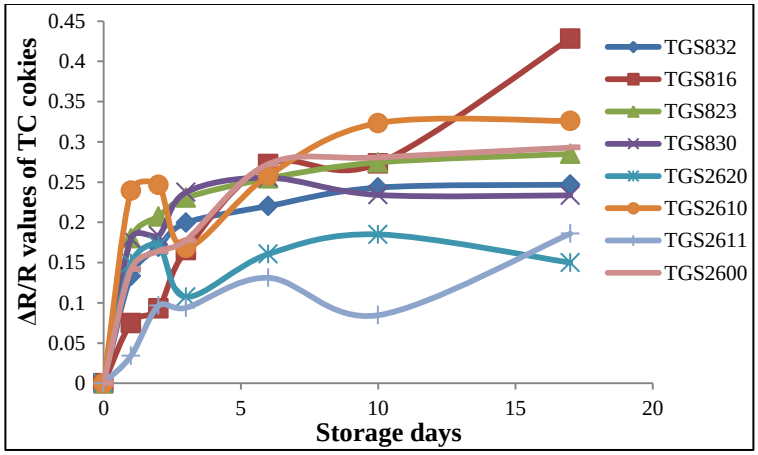

Fig. 2.3.6. Selection of e-nose sensors based on responses obtained for deliberately-made rancid C cookies (TC).

(a)

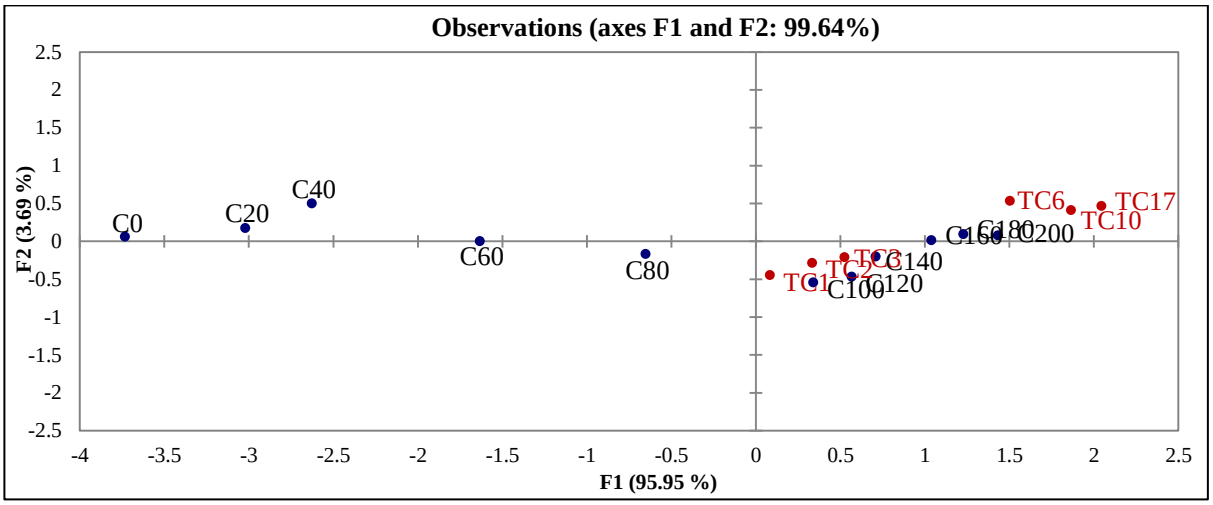

Fig. 2.3.7 (a). PCA plots of C cookies.

(b)

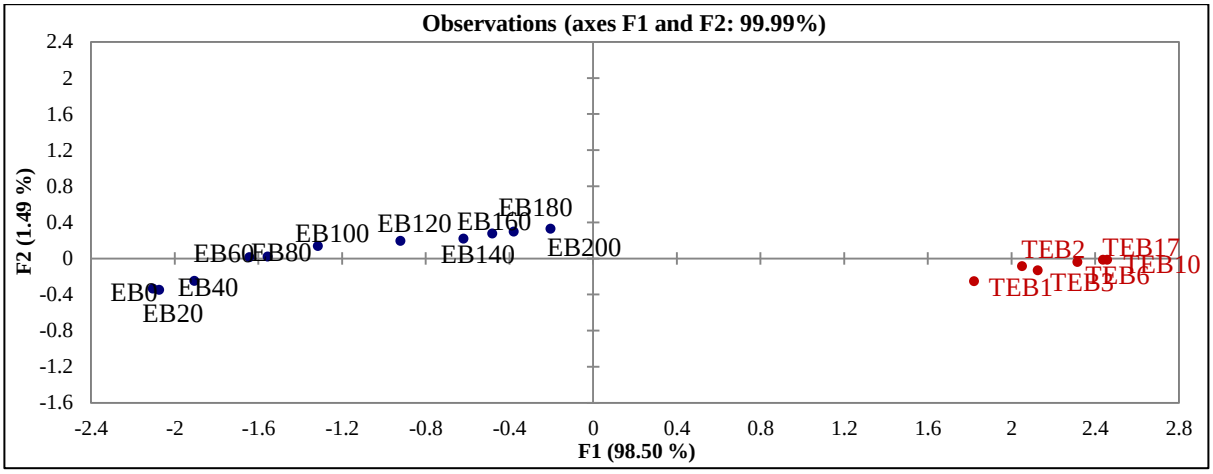

Fig. 2.3.7 (b). PCA plots of E_B cookies.

(c)

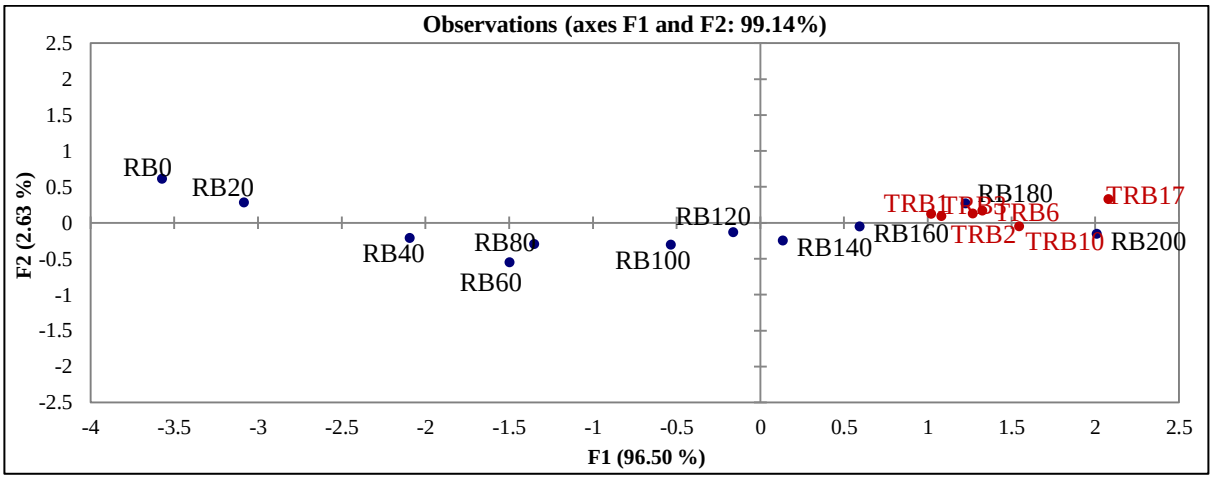

Fig. 2.3.7 (c). PCA plots of R_B cookies.

(a)

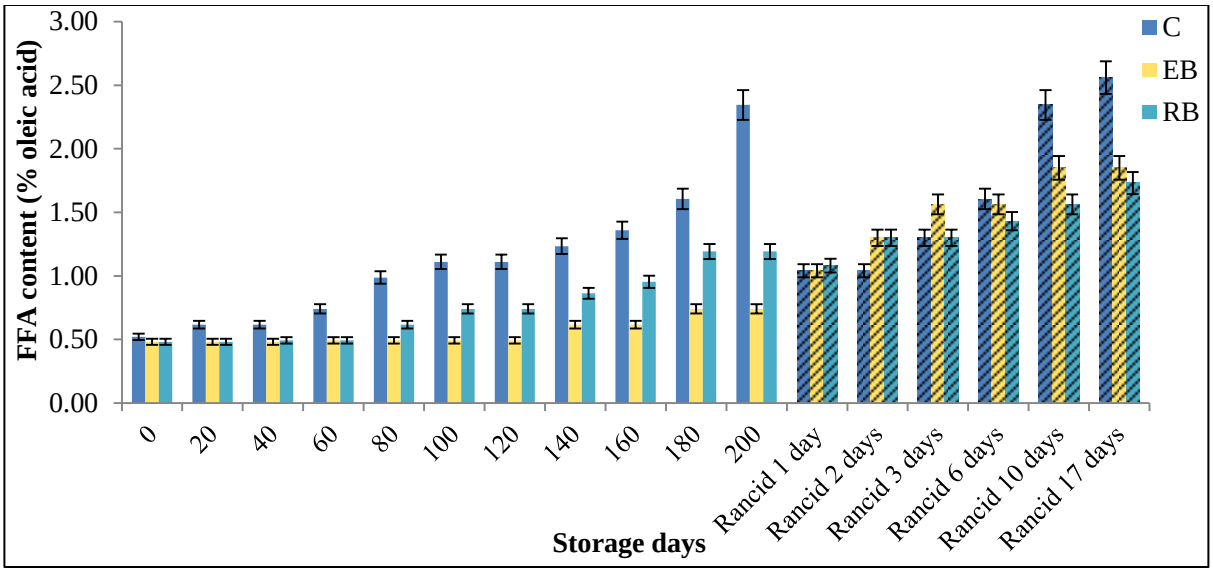

Fig. 2.3.8 (a). FFA contents of cookies (C, E_B and R_B) during the storage period of 200 days along with deliberately made rancid cookies.

(b)

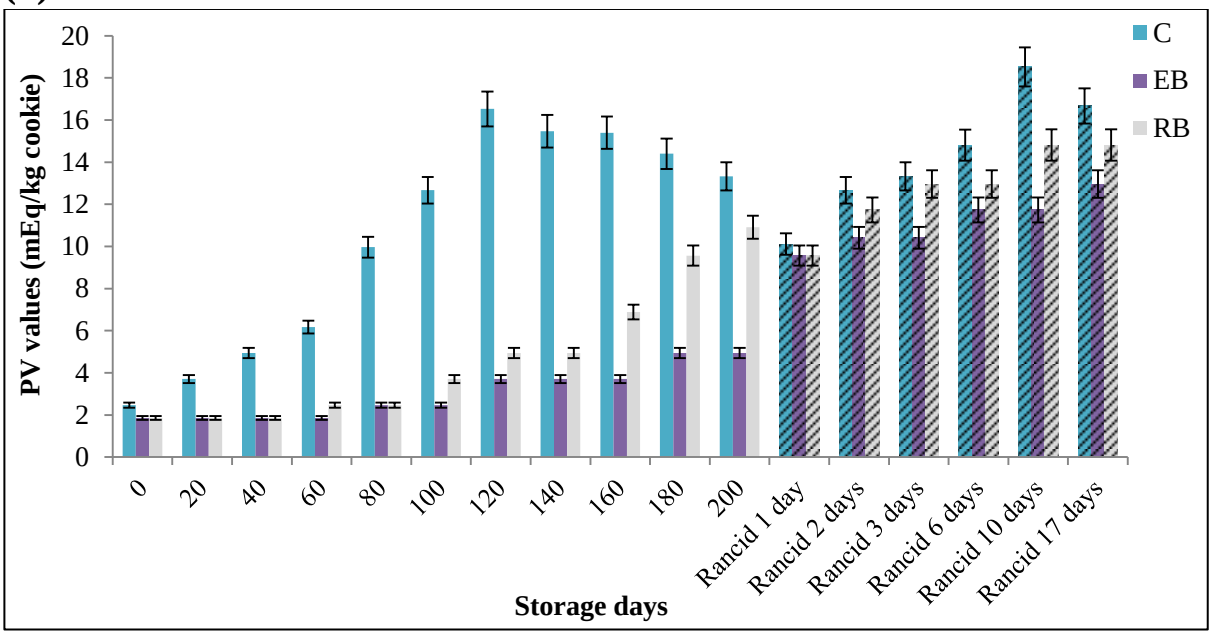

Fig. 2.3.8 (b). PV values of cookies (C, E_B and R_B) during the storage period of 200 days along with deliberately made rancid cookies.

(c)

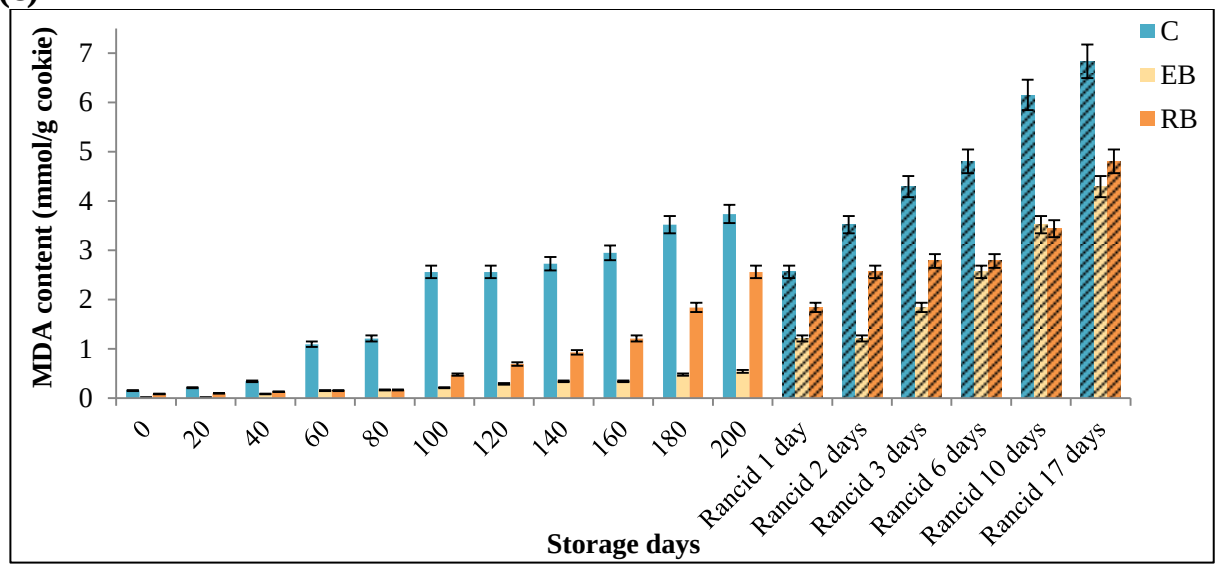

Fig. 2.3.8 (c). MDA contents of cookies (C, E_B and R_B) during the storage period of 200 days along with deliberately made rancid cookies.

Chapter 3

Supercritical carbon dioxide extraction of 1,8-cineole from small cardamom

Section 3.1

Enzyme-assisted supercritical carbon dioxide extraction of 1,8-cineole-rich extract from small cardamom

Introduction

In the present investigation, enzyme-assisted SC-CO_2 extraction of 1,8-cineole was conducted employing Mysore variety of small cardamom, also known as the Alleppey green cardamom which is the major Indian grade of small cardamom for trade (Chempakam and Sindhu, 2008). SC-CO_2 extraction of 1,8-cineole from Alleppey green small cardamom has previously been optimized by our research group (Ghosh et al., 2015). An extraction pressure of 200 bar, at 50 °C for 90 min extraction time (60 min static and 30 min dynamic) at 2 L/min flow rate of gaseous CO_2 were found to be the optimum SC-CO_2 conditions of extraction at which highest yield of 1,8-cineole and phytochemical properties (such as antioxidant, anti-inflammatory and antimicrobial) were obtained in the extract (Ghosh et al., 2015).

The current investigation aims to further enhance the yield of 1,8-cineole in the extract by enzyme-assisted (α-amylase, E.C.3.2.1.1., from *Bacillus licheniformis*) SC-CO_2 extraction. Proximate analysis of small cardamom seeds revealed that the main constituent of the same is carbohydrate (83.19±0.13%, d.w.b), starch alone comprising 58.67±0.11% of the seeds (d.w.b) (Fig. 1.3). It was opined that in this case too (as for black pepper discussed in section 2.2 of Chapter 2), starch in small cardamom seeds would impede extraction of 1,8-cineole by thwarting it's accessibility to solvents. Therefore, to improve recovery of 1,8-cineole from small cardamom seeds, hydrolysis of seed starch would be necessary. Thus, this study endeavored to re-

investigate enzyme-assisted SC-CO_2 extractions in both batch and continuous modes, for enhanced yield of 1,8-cineole-rich extract from small cardamom.

Materials and Methods

Materials

Seeds of Alleppey Green small cardamom were procured from Spices Board, Cochin, India. 1,8-cineole (99% pure) was procured from Sigma, India; *n*-hexane, ethyl acetate, chloroform and antimony (III) chloride were procured from E-Merck, Mumbai, India. All chemicals were of AR grade. The other chemicals and materials used in this study have been described in section 2.2 of Chapter 2.

α-amylase in continuous mode in SC-CO_2 conditions

To investigate the change in specific activity of α-amylase at SC-CO_2 conditions, the enzyme was subjected to SC-CO_2 conditions of 200 bar, 50 °C, in a similar manner as has been presented in Fig. 2.2.1. 2 mg enzyme was subjected to SC-CO_2 conditions under continuous flow of CO_2 at 1 L/min. After 2.25 h, the enzyme was recovered and its specific activity was estimated. The conformational changes in the enzyme were studied by ^{1}H NMR of the treated enzyme according to the method discussed in section 2.2 of Chapter 2.

Enzyme-assisted SC-CO_2 extractions of 1,8-cineole-rich extracts from small cardamom

Enzyme-assisted SC-CO_2 extractions of 1,8-cineole-rich extracts from small cardamom were carried out in accordance with the methodology adopted for enzyme-assisted SC-CO_2 extraction of piperine-rich extract from black pepper. 20 g (batch size optimized by preliminary trials) of ground small cardamom (d_p=0.42±0.02 mm) was mixed with the lyophilized enzyme in pre-optimized ratio (enzyme: small cardamom powder=1:5000), packed into the extraction vessel

(SS 316) and subjected to SC-CO_2 extraction. The extraction was carried out at the pre-optimized conditions of 200 bar, 50 °C at a flow rate of gaseous CO_2 at 2 L/min (Ghosh et al., 2015).

In batch mode of extraction, 120 min of static time was provided prior to extract collection as incubation time for hydrolysis of starch of small cardamom by α-amylase and 15 min of dynamic time was provided for collection of the extract. In continuous mode, 2.25 h of total extraction time was provided for extraction and collection of extract. The extracts were collected in screw capped glass vials in ice bath. Post extraction, the extracts were weighed gravimetrically, flushed with nitrogen and stored in the dark at 4±1 °C, until further analyses. This methodology was adapted from the previous work conducted with black pepper (elaborated in section 2.2 of Chapter 2).

Characterization of enzyme-assisted SC-CO_2 extracts of small cardamom

Densitometric estimation of 1,8-cineole in small cardamom extracts by HPTLC

Estimation of 1,8-cineole contents in small cardamom extracts were performed by HPTLC in accordance with the method described by Ghosh et al. (2015). The plates were developed at room temperature (23±2 °C) in a glass chamber saturated with mobile phase (*n*-hexane: ethyl acetate = 6:1). The amount of 1,8-cineole present in the extracts was determined from the standard curve prepared with standard 1,8-cineole (R_f=0.58±0.01 at 500 nm).

Phytochemical properties of the extracts

Antioxidant activities, total phenolic contents, reducing power and anti-inflammatory activities of the extracts were determined and expressed as IC_{50} values of DPPH radical scavenging activity (mg/mL), mg gallic acid equivalent/g of dry small cardamom powder, mg BHT/g of dry

small cardamom powder and IC_{50} values of NO radical scavenging activity (mg/mL), respectively.

Determination of free-radical scavenging capacity of small cardamom extracts in vitro

Free-radical scavenging capacity of small cardamom extracts was further validated by EPR spectroscopy as discussed earlier in section 2.2 of Chapter 2, using DPPH as the source of free-radicals.

GC-MS analyses of the extracts

Small cardamom extracts obtained by enzyme-assisted SC-CO_2 extractions were analyzed by GC-MS for identification of its chemical constituents, in accordance with the program described for the GC-MS analyses of black pepper extracts. Identification of components of the extracts was based on matching the mass spectra with the NIST 2007 library (2007) and Adams (2007) literature reports.

Estimation of pungency of small cardamom extracts in terms of SHU values

The pungency of small cardamom extracts (extractions conducted without and with enzyme) was assessed by estimation of SHU values of all extracts, to investigate whether the α-amylase-assistance in SC-CO_2 extraction of 1,8 cineole contributed to increase in pungency of the extract. The ethanolic solutions of small cardamom extracts were diluted with sucrose syrup (5% w/v) and their SHU values were estimated from the dilution factor required for a stinging sensation in the throat which was just perceptible (Ranganna, 1986).

Evaluation of antimicrobial activities of small cardamom extracts by micro broth dilution method

The antimicrobial potencies of small cardamom extracts were evaluated to study the change in their antimicrobial properties after α-amylase-assisted SC-CO_2 extractions. Extracts obtained without and with enzyme (in both batch and continuous modes), were subjected to determination of MIC values in accordance with the method elaborated in section 2.2 of Chapter 2.

Statistical analyses

All experiments were conducted in triplicate and the data are expressed as mean±SD of three independent experimental runs. Statistical analysis was performed with IBM SPSS Statistics software version 20 (IBM, USA). Duncan's multiple range tests with P-value <0.05 were used to verify the significance of all tests.

Results and Discussion

α-amylase in continuous mode in SC-CO_2 conditions

After SC-CO_2 treatment of the enzyme in continuous mode, the specific activity of α-amylase (264±4 U/mg protein) increased to 525±6 U/mg protein, which was 1.99 times higher than that of the fresh enzyme. The increase (1.99 times) was significantly lower (P=0.0001) at 200 bar, 50 °C than that obtained at 300 bar, 60 °C (2.13 times), indicating favorable effects of high pressure treatment at 60 °C on the conformational changes of the enzyme. From the NMR spectrum of α-amylase with enhanced specific activity, it was inferred that SC-CO_2 conditions altered the conformational arrangement of the α-amylase (Fig. 3.1.1) as has been discussed at length in section 2.2 of Chapter 2.

Enzyme-assisted SC-CO_2 extractions of 1,8-cineole-rich extracts from small cardamom

As envisaged, α-amylase-assisted SC-CO_2 extractions enhanced the yields of the extracts of small cardamom. Batch mode of extraction increased the yield by 50.66% (from 6.62±0.15 to 9.97±0.14 g extract/100 g dry cardamom seeds) while the continuous mode of extraction increased the same by 11.21% (from 7.06±0.10 to 7.85±0.13 g extract/100 g dry cardamom seeds). These findings were in agreement with the study of α-amylase-assisted SC-CO_2 extraction of piperine-rich extract from black pepper, where 53% increased yield of black pepper extract was obtained in batch mode and 15% increased yield was obtained in continuous mode of extraction.

Characterization of enzyme-assisted SC-CO_2 extract of small cardamom

Phytochemical properties of the extracts

Antioxidant activity of the small cardamom extract increased (i.e., decrease in IC_{50} value of DPPH radical scavenging activity) from 0.068±0.02 to 0.031±0.01 mg/mL (P=0.0456) in enzyme-assisted SC-CO_2 extraction in batch mode. For this extract, the increase in total phenolic content was from 0.65±0.04 to 1.95±0.04 mg GAE/g of dry cardamom (P=0.0000), increase in reducing power was from 0.32±0.02 to 0.95±0.04 mg BHT/g of dry cardamom (P=0.0000) and increase in anti-inflammatory activity (i.e. decrease in IC_{50} value) was from 3.87±0.10 to 3.57±0.13 mg/mL (P=0.0339).

For continuous mode of extraction, the increase in antioxidant activity was from 0.068±0.02 to 0.063±0.01 mg/mL (P=0.0179), total phenolic content increased from 0.74±0.04 to 0.83±0.04 mg GAE/g of dry cardamom (P=0.0511), reducing power was from 0.48±0.02 to 0.75±0.04 mg BHT/g of dry cardamom (P=0.0000) and increase in anti-inflammatory activity (i.e. decrease in

IC_{50} value) was from 3.65±0.10 to 3.57±0.13 mg/mL (P=0.4457). These findings established that improvement in phytochemical potencies of small cardamom extracts obtained from enzyme-assisted SC-CO_2 extractions was higher in batch mode compared to their counterparts obtained in the continuous mode.

Free-radical scavenging capacity of small cardamom extracts in vitro

In EPR spectrum, the reduction in the intensities of DPPH signals for SC-CO_2 extracts of small cardamom validated the antioxidant potencies of the extracts (Fig. 3.1.2a,b). Extracts obtained in enzyme-assisted extractions exhibited enhanced antioxidant potencies in both batch and continuous modes of extraction. For extracts obtained from extractions conducted without enzyme, reductions in signal intensities were 7.00% for batch mode and 24.73% for continuous mode; while for enzyme-assisted extraction, the reductions were 16.43% for batch mode and 22.04% for continuous mode of extraction.

1,8-cineole content of small cardamom extracts

Enzyme-assisted SC-CO_2 extractions increased the yield of 1,8-cineole by 29.55% (from 33.98±0.20 mg/g dry cardamom to 44.02±0.15 mg/g dry cardamom) in batch mode and 11.02% (from 34.85±0.20 mg/g dry cardamom to 38.69±0.15 mg/g dry cardamom) in continuous mode.

GC-MS analyses of small cardamom extracts

The GC-MS chromatograms of the extracts (obtained from both batch and continuous modes) and the tentatively identified compounds in the extracts are presented in Fig. 3.1.3(a-d). It was observed that 1,8-cineole and terpinyl acetate were the major compounds in the extracts; α-pinene, β-myrcene, camphene, linalyl acetate, geranyl acetate were also co-extracted from small cardamom seeds.

SHU values of small cardamom extracts

SHU values for extracts obtained from SC-CO_2 extractions conducted without enzyme were 10,000 for batch mode and 25,000 for continuous mode of extraction. Enzyme-assisted extraction enhanced the pungency of extract in batch mode of extraction (SHU value 25,000); whereas in continuous mode, the pungency (SHU value 25,000) was similar to that of the extract obtained from SC-CO_2 extraction conducted without enzyme. Therefore, according to the levels of pungency depicted in section 2.2 of Chapter 2, it was concluded that SC-CO_2 extracts of small cardamom are moderately pungent.

Antimicrobial activities of small cardamom extracts

MIC values revealed that small cardamom extracts obtained from enzyme-assisted SC-CO_2 extractions had enhanced antimicrobial potencies against test microorganisms w.r.t. both standard 1,8-cineole and extract obtained from SC-CO_2 extraction conducted without enzyme (Table 3.1.1). Enzyme-assisted batch mode of extraction enhanced the antimicrobial potency of extract 4 times against *E. coli* and *S. aureus* and 2 times against *P. aeruginosa*; whereas continuous mode of extraction increased the potency of extract 2 times against *E. coli* and *S. aureus*. These extracts with enhanced antimicrobial potencies can be promising food preservatives. Small cardamom extract obtained from batch mode of enzyme-assisted SC-CO_2 extraction was employed to design drop cookies to enhance the nutraceutical properties and shelf life of the product (described in section 3.2 of Chapter 3).

Conclusions

The current study demonstrated that α-amylase-assisted SC-CO_2 extraction (at 200 bar, 50 °C and 2.25 h) enhanced the yield of 1,8-cineole-rich extract from small cardamom with best combination of 1,8-cineole content and phytochemical properties (antioxidant activity, total phenolic content, reducing power, anti-inflammatory activity and antimicrobial activity). The batch mode of extraction enhanced the yield by 50.66% and the continuous mode enhanced the same by 11.21%. α-amylase at SC-CO_2 conditions of 200 bar, 50 °C for 2.25 h exhibited 1.99 times higher specific activity compared to the untreated enzyme. The 1,8-cineole-rich extract with enhanced phytochemical properties, obtained by batch mode of extraction was further employed in formulation of designer nutraceutical cookies (section 3.2 of Chapter 3). Further, the extract was also encapsulated by spray drying for enhanced shelf stability and for possible use as a direct biotherapeutic and/or as a functional food ingredient (section 4.1 of Chapter 4).

Novelty

The novelty of the work is that, it has reported for the first time on α-amylase-assisted extraction of small cardamom extract employing both batch and continuous modes of SC-CO_2 extraction to increase the yield of 1,8-cineole-rich extract having the best combination of phytochemical properties, for promising use as food and therapeutic supplements.

References

Adams R. P. (2007). *Identification of Essential Oil Components by Gas Chromatography/mass Spectroscopy*, 4th ed., Allured Publishing Corporation, IL, USA.

Chempakam B., and Sindhu S. (2008). Small cardamom. In: *Chemistry of Spices*, Parthasarathy V.A., Chempakam B., and Zachariah T. J. (Eds.), CABI, UK, pp. 41-58.

Ghosh S., Bhattacharjee P., and Das S. (2015). 1,8-cineol-rich cardamom seed (*Elettaria cardamomum*) extracts using green technologies and conventional extractions: Process

analysis, phytochemical characterization, and food application. *Separation Science and Technology*, **50**, 1974-1985.

NIST Mass Spec Data Center (2007). Stein S.E., director, mass spectra. Mallard Gaithersburg NIST chemistry WebBook. In: *NIST Standard Reference Database Number 69*, Linstrom, P., Mallard, W.G. (Eds.). National Institute of Standards and Technology, Gaithersburg, MD, USA. http://webbbok.nist.gov (Accessed 20 November, 2015).

Ranganna S. (1986). Flavouring materials. In: *Handbook of Analysis and Quality Control for Fruit and Vegetable Products*, 2nd ed. Tata McGraw Hill, New Delhi, India, pp. 243-285.

Tables:

Table 3.1.1. Antimicrobial properties of SC-CO_2 extracts (obtained by extractions conducted without and with enzyme) of small cardamom.

Sl. No.	Sample name	MIC against selected microorganisms (µg/mL)		
		Escherichia coli	*Staphylococcus aureus*	*Pseudomonas aeruginosa*
1	Ethanol	98625	98625	98625
2	Std. 1,8-cineole	400	400	200
3	Small cardamom extract, batch mode, without enzyme	400	200	200
4	Small cardamom extract, batch mode, with enzyme	200	100	50
5	Small cardamom extract, continuous mode, without enzyme	200	200	100
6	Small cardamom extract, continuous mode, with enzyme	100	100	100

Figures:

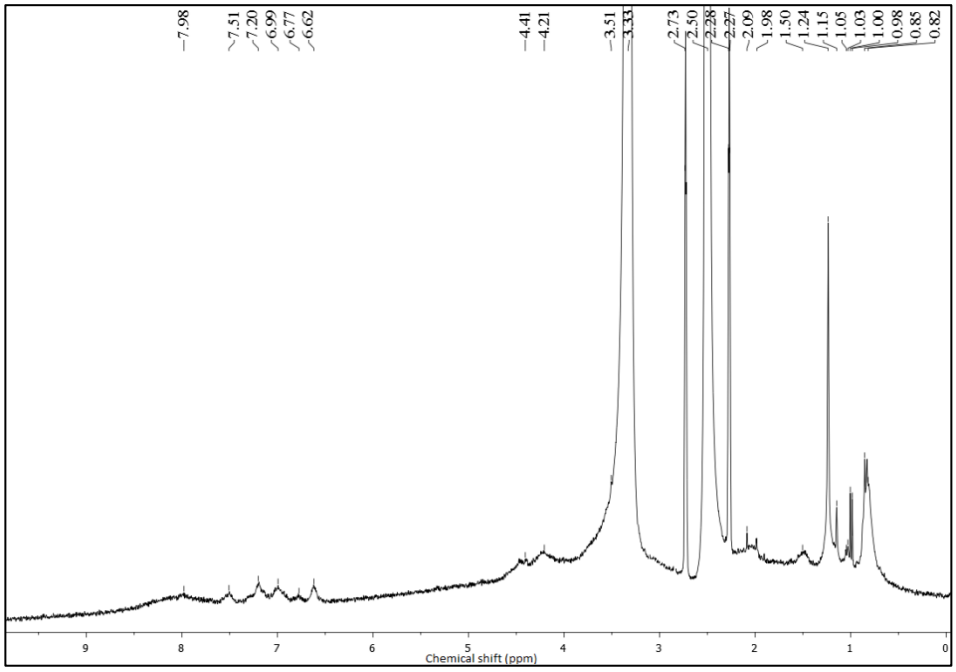

Fig. 3.1.1. ^{1}H NMR spectra of α-amylase treated at 200 bar 50 °C.

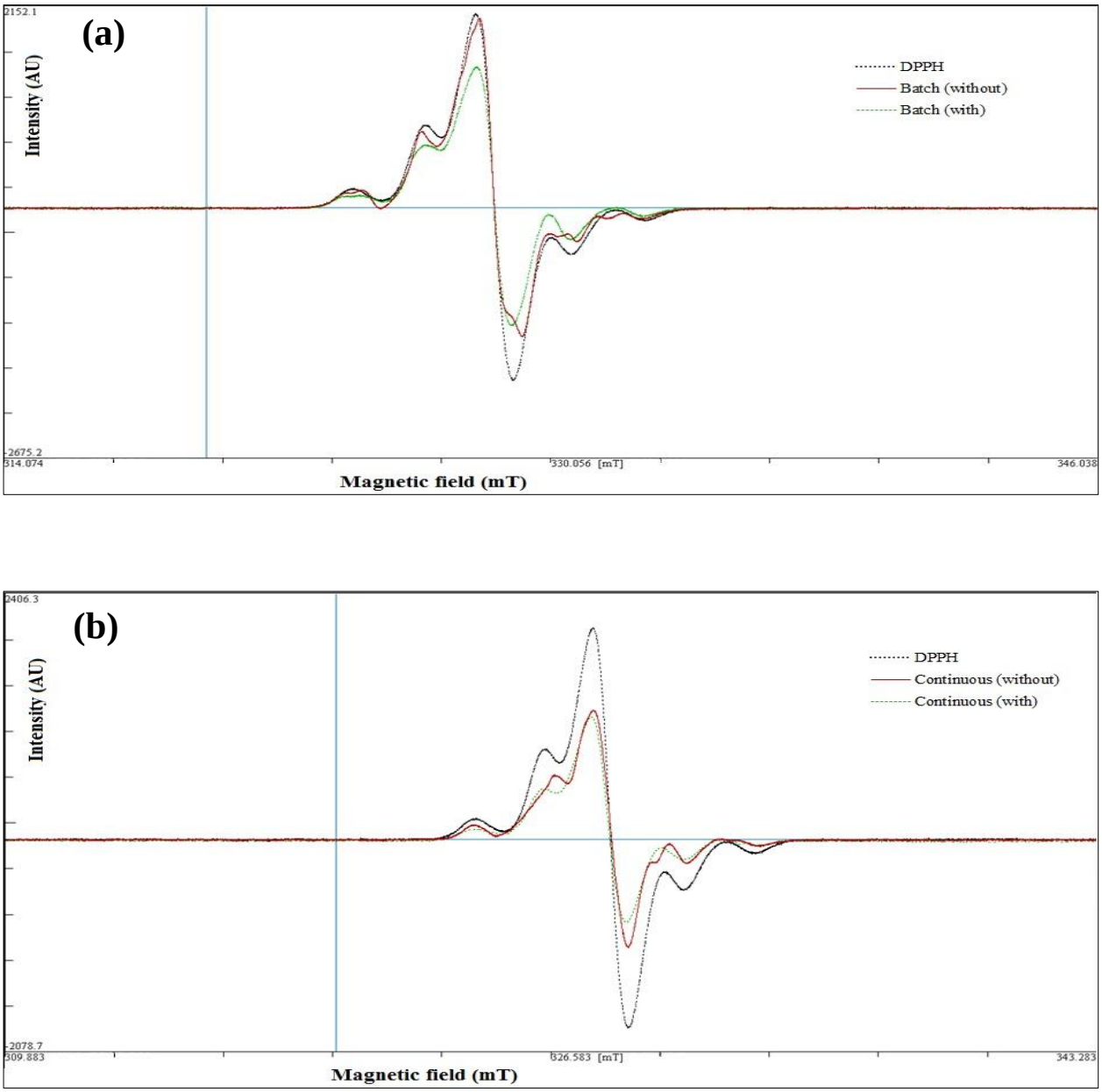

Fig. 3.1.2. EPR spectrums of DPPH free radicals in the presence of small cardamom extracts. a) At batch mode and b) At continuous mode.

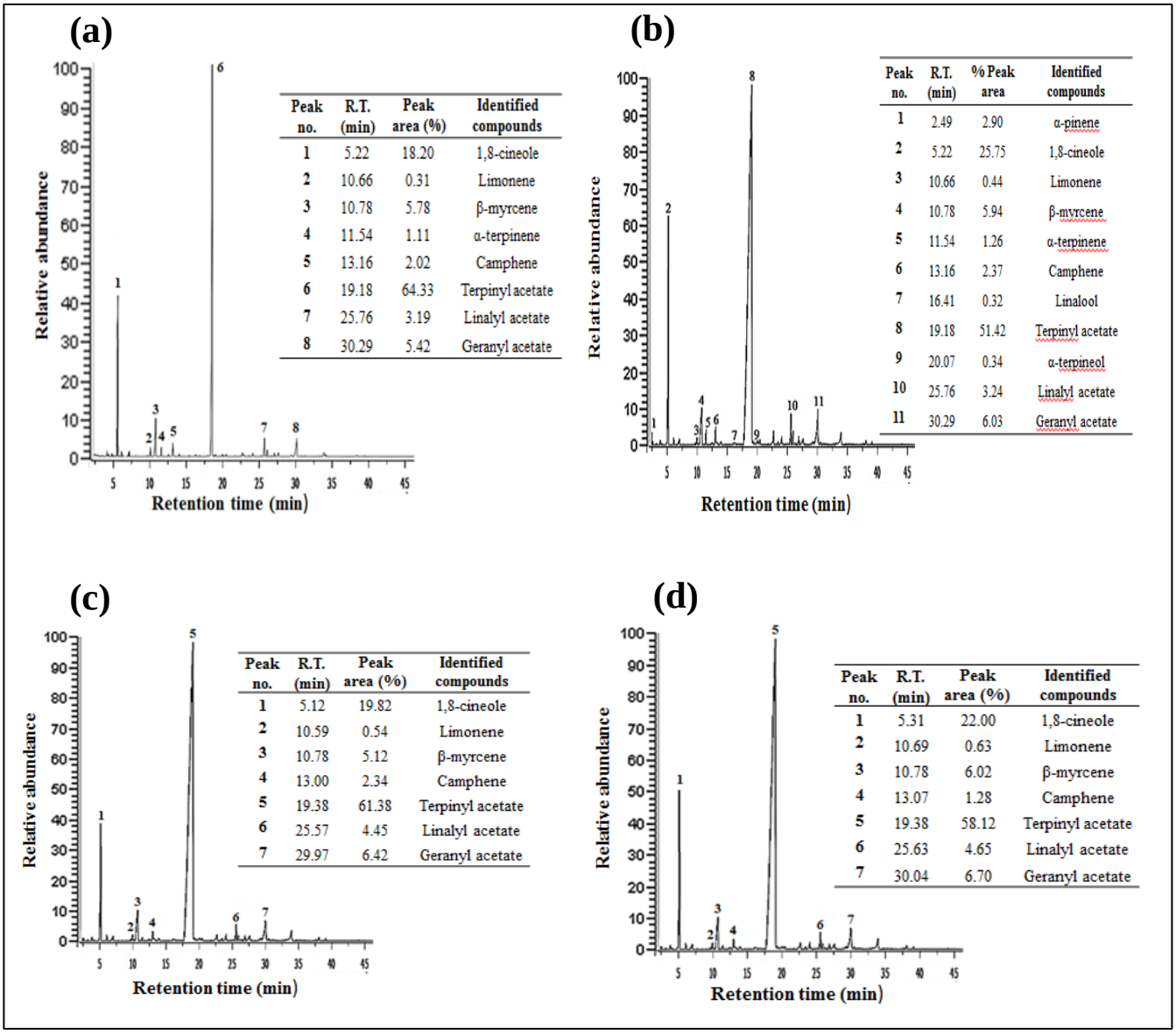

Fig. 3.1.3. Total ion chromatograms and list of identified compounds in small cardamom extracts. a) Obtained from batch mode conducted without enzyme, b) Obtained from batch mode conducted with enzyme, c) Obtained from continuous mode conducted without enzyme, d) Obtained from continuous mode conducted with enzyme.

Section 3.2

Assessment of shelf-life of small cardamom cookies using electronic nose

Introduction

The preceding section (3.1) established that 1,8-cineole-rich small cardamom extract obtained by α-amylase-assisted SC-CO_2 had enhanced antioxidant, anti-inflammatory and antimicrobial properties of the extract. The present study too forayed into deign of nutraceutical-rich small cardamom cookies employing the antioxidant-rich extract as well as the post-extraction residual matrix of small cardamom, in similar lines as was conducted for black pepper matrix.

The objectives of this part of the study were therefore, design of nutraceutically enhanced drop cookies with 1,8-cineole-rich SC-CO_2 (enzyme-assisted) extract and with post-extraction residual sample matrix of small cardamom; evaluation of nutraceutical properties of the newly formulated designer cookies and assessment of their shelf-lives by e-nose technology using SI as a parameter for rancidity.

Materials and Methods

Materials

The chemicals and materials used in this study have been described in section 2.3 of Chapter 2.

Design of antioxidant-rich small cardamom cookies

1,8-cineole-rich extract obtained from α-amylase-assisted SC-CO_2 extraction and post-extraction residual sample matrix of small cardamom were employed in separate batches in designing antioxidant-rich drop cookies. Two sets of small cardamom cookies were formulated (according to the method described in section 2.3 of Chapter 2): cookies fortified

with small cardamom extract (E_S) and cookie fortified with post-extraction small cardamom matrix (R_S) (Fig. 3.2.1).

Similar to the black pepper cookies, the amounts of extract and post extraction sample matrix required for designing small cardamom cookies were optimized based on the antioxidant potency and flavour acceptance (by sensory panel) of the formulated cookies. The amount of extract employed in formulation of E_S cookies was 0.3 g/100 g dough weight (w.b) and amount of residual matrix used in R_S cookies was 5 g/100 g dough weight (w.b). These E_S and R_S cookies were packed in Al foil, placed in Ziploc pouches (Johnson, India), flushed with nitrogen and stored at room temperature (23±2 ºC) for shelf life study for 200 days.

Characterization of cookies

Physical properties of cookies

Physical properties, such as, diameter (D), thickness (T), weight, spread ratio (SR=D/T) were determined by AACC method 10-50D (Arun et al., 2015); hardness and color of small cardamom cookies were estimated according to the methods as discussed earlier in section 2.3 of Chapter 2.

Estimation of nutraceutical potencies of cookies

Nutraceutical potencies of small cardamom cookies, such as 1,8-cineole content, antioxidant potency and total phenolic content were estimated using methanolic extracts of the cookies (Sakac et al., 2010). 1,8-cineole contents of E_S and R_S cookies were determined by HPTLC analysis and expressed as mg 1,8-cineole/g cookie (d.w.b).

Determination of shelf-life of small cardamom cookies

Shelf-life study of small cardamom cookies was conducted by estimation of rancidity using both e-nose analysis and conventional biochemical assays, at an interval of 20 days for a total storage period of 200 days.

Electronic nose system for detection of rancidity in cookies

For detection and assessment of rancidity in small cardamom cookies, ENOVISION was employed as has been applied for black pepper cookies. The pre-optimized e-nose parameters used for detection of rancidity in small cardamom cookies were: batch size of 50 g ground cookie powder (d_p=0.50±0.02 mm); heating time of 450 s; 30 s headspace generation time; sampling time of 50 s and purging time of 300 s. Training sets of rancid cookies - E_S (TE_S) and R_S (TR_S) were obtained by keeping the freshly prepared E_S and R_S cookies in an accelerated rancidity chamber (details provided in section 2.3 of Chapter 2).

Selection of e-nose sensor for analysis of rancidity in small cardamom cookies

Three sensors of e-nose that showed high and stable response to rancidity in small cardamom cookies were selected from the ΔR/R values (change in signals from the metal oxide sensors due to the VOCs of cookies on day 'd', with respect to the signals generated for freshly prepared cookies) of each sensor (Chatterjee et al., 2014).

Biochemical assays for determination of rancidity in small cardamom cookies

Estimation of conventional rancidity parameters (FFA, PV and TBA) of small cardamom cookies were conducted for biochemical assessment of rancidity in cookies, according to the methods described in section 2.3 of Chapter 2.

Statistical analyses

Statistical analyses such as two dimensional PCA and estimation of Mahalanobis distance were carried out according to the methods described in section 2.3 of Chapter 2. The changes in aroma of cookies during storage were investigated and SI values were determined for assessment of rancidity in small cardamom cookies.

Results and Discussion

In the present work, the physical and nutraceutical properties of control cookie samples (C) along with their shelf life study (section 2.3 of Chapter 2) were comparatively evaluated against those of small cardamom cookies.

Characterization of small cardamom cookies

Physical properties of cardamom cookies

The values of diameter, thickness, spread ratio and hardness of the E_S and R_S cookies were similar with those of C cookies (Table 3.2.1), which indicated that, fortification of cookies with small cardamom extract and post extraction sample matrix did not adversely affect these parameters.

E_S cookies were found to have significantly higher brightness (L*=63.88±0.60) than R_S cookies (L*=56.94±0.20) (P=0.0002) and C cookies (L*=60.88±0.20) (P=0.0012) (Table 3.2.1). On the other hand, formulation of cookies with the sample matrix decreased significantly values of redness (a*=4.59±0.06) and yellowness (b*=18.57±0.13) in R_S cookies, compared to C cookies (a*=9.61±0.06 and b*=26.15±0.10, respectively) significantly (P=0.0000 and P=0.0000, respectively).

Nutraceutical efficacies of small cardamom cookies

Nutraceutical efficacies of the small cardamom cookie samples in terms of antioxidant potency, total phenolic content and 1,8-cineole content, have been represented in Fig. 3.2.2. The antioxidant potencies of E_S and R_S cookies decreased by 2.07 times (from 0.28 to 0.58 mg/mL) and 9.94 times, respectively (from 0.85 to 8.45 mg/mL), after 200 days of storage. The total phenolic content decreased by 1.47 times (51.64 to 35.20 µg gallic acid equivalent/g cookie) for E_S cookies and 5.22 times (36.73 to 7.03 µg gallic acid equivalent/g cookie) for R_S cookies during 200 days of storage. Decrease of phytochemical potencies of small cardamom cookies was significantly lower than that observed for C cookies; however, this decrease was higher than that observed for black pepper cookies, indicating that pepper fortified cookies were nutraceutically richer than their cardamom counterparts.

1,8-cineole content of fresh E_S cookies was 1.161 mg/g dry cookie, which degraded to 0.633 mg/g dry cookie at the end of 200 days. 1,8-cineole content of fresh R_S cookies was significantly (P=0.0000) low, compared to that of the E_S cookies (Fig. 3.2.2c). After 80 days of storage, 1,8-cineole could not be detected in cookies. However, compared to the C cookies, the R_S cookies had significantly higher antioxidant potency (P=0.0000) and total phenolic content (P=0.0000) (Fig. 3.2.2) even after 80 days. These observations indicated that additions of extract and post-extraction sample matrix of small cardamom to cookies increased their phytochemical properties and enhanced their shelf stability.

Selection of e-nose sensors for analysis of rancidity in small cardamom cookies

For detection of rancidity of small cardamom cookies, the sensor TGS823 showed highest response with minimum variation, followed by sensors TGS832 and TGS2600 for cookies TE_S and TR_S (Fig. 3.2.3a-b). Therefore, these three sensors were selected for assessment of rancidity in small cardamom cookies.

Electronic nose system for assessment of rancidity in cookies

Analysis of rancidity in cookies was conducted at an interval of 20 days for 200 days, using odor maps generated on the basis of PCA plots (Fig. 3.2.4a for cookie with extract and Fig. 3.2.4b for cookie with residual sample matrix).

The PCA plot of E_S cookies revealed that, 200 day-stored cookies formed a distinct cluster, separate from that of TE_S, which suggested that cookies prepared with small cardamom extract prevented rancidity for at least 200 days. This result is in agreement with the shelf life of E_B cookies, which was found to be at least 200 days (Fig. 2.3.7b). Therefore, it can be concluded that application of SC-CO_2 extracts of both small cardamom and black pepper enhanced the shelf lives of cookies by at least 120 days.

In PCA plots of R_S cookies, the data points for storage period of 140 days and above were present in the same quadrant along with those of the TR_S cookies, indicating onset of rancidity in R_S cookies from 140 days onwards (Fig. 3.2.4b). On the other hand, rancidity in R_B cookies was detected from 180 days onwards (Fig. 2.3.7c). Thus it could be inferred that the post extraction residual matrix of black pepper was more effective in preventing rancidity in cookies for an additional 40 days, vis-à-vis the residual small cardamom matrix.

Determination of Mahalanobis distance between fresh cookies and stored cookies

SI values of small cardamom cookies were determined for accurate and precise assessment of rancidity (Table 3.2.2). SI_{ES} was the spoilage index for cookie with small cardamom extract and SI_{RS} was for cookie with residual sample matrix post-extraction.

SI_{RS} revealed that, rancidity in R_S cookies was from 140 days onwards (SI_{RS} of 140 day-stored cookie and 1 day-rancid TR_S were 15.9160 and 16.9719, respectively) but SI_{ES} of 200 day-stored E_S cookies (15.2153) was significantly (P=0.0000) distant from that of 1 day-stored TE_S cookies (30.0843). This data verifies the results of PCA plots and confirmed

rancidity in R_S cookies from 140 days onwards and E_S cookies remained fresh, at least for 200 days. Thus use of e-nose technology for accurate estimation of rancidity in small cardamom cookies could be successfully established in this study.

Determination of conventional rancidity parameters of small cardamom cookies

Freshly prepared E_S and R_S cookies had similar FFA contents, significantly lower (P=0.0080) than the FFA content of C cookies. FFA contents of small cardamom cookies increased with storage. For E_S cookies, it was increased from 0.481 to 1.192% oleic acid; and for R_S cookies, from 0.481 to 1.431% oleic acid at the end of 200 days (Fig. 3.2.5). After 200 days of storage, PV and TBA values of E_S cookies increased from 1.852 to 8.264 meq./kg cookie and from 0.017 to 1.092 mmol malondialdehyde/g cookie, respectively; for R_S cookies, the values increased from 2.469 to 14.463 meq./kg cookie and 0.152 to 3.436 mmol malondialdehyde/g cookie, respectively (Fig. 3.2.5).

From the values of biochemical assays of training sets, it was found that, R_S cookies remained non-rancid at least for 120 days; but for E_S cookies, no such trend was observed and it remained non-rancid till the end of the storage period of 200 days (Fig. 3.2.5). Therefore, from biochemical assays, it was observed that fortification of cookies with small cardamom extract and post-extraction residual sample matrix enhanced the shelf lives by 120 days and 40 days, respectively. Both the approaches of e-nose analysis and biochemical assays have revealed the shelf lives of R_S and E_S cookies to be 120 and 200 days respectively.

Correlation between the rancidity parameters of small cardamom cookies determined by e-nose analysis and biochemical assays

Linear regression equations were generated by multiple regression analyses to predict the FFA, PV and TBA values of cookies (individually for each cookie type), as a function of their spoilage indices.

For E_S cookies, the regression equations are provided below:

$$FFA = 0.038 \times SI_{ES} + 0.439 \ (r=0.933) \quad (1)$$

$$PV = 0.327 \times SI_{ES} + 1.429 \ (r=0.889) \quad (2)$$

$$MDA = 0.055 \times SI_{ES} - 0.107 \ (r=0.907) \quad (3)$$

For R_S cookies, the regression equations are provided below:

$$FFA = 0.033 \times SI_{RS} + 0.597 \ (r=0.927) \quad (4)$$

$$PV = 0.376 \times SI_{RS} + 3.713 \ (r=0.948) \quad (5)$$

$$MDA = 0.109 \times SI_{RS} + 0.147 \ (r=0.989) \quad (6)$$

Good correlation coefficients (r) of the equations (Eqs. 1-6) suggest that, equations generated from small cardamom cookies can be unambiguously used to predict the conventional rancidity parameters of small cardamom cookies using the spoilage indices obtained from e-nose data.

Using these equations, FFA, PV and MDA values of rancid E_S cookies were 1.562% oleic acid, 9.560 mEq/kg cookie and 1.209 mmol/g cookie respectively; and for R_S cookies, the values were, 1.080% oleic acid, 9.260 mEq/kg cookie and 2.157 mmol/g cookie respectively. Cookies having similar or higher values of FFA, PV and MDA compared to their corresponding rancid cookies can be considered as rancid samples.

Conclusions

In this investigation, nutraceutical-rich cookies have been designed with α-amylase-assisted SC-CO_2 extract and residual post-extraction sample matrix of small cardamom seeds. PCA plots and Mahalanobis distances obtained from e-nose responses of cookies revealed that SC-CO_2 extract of small cardamom and the post-extraction sample matrix prevented rancidity and enhanced the shelf lives of cookies by at least 120 days and 40 days, respectively. These results are in good agreement with the results obtained by conventional biochemical assays.

Regression equations were generated for prediction of FFA content, PV values and MDA values for each small cardamom cookie from their e-nose responses. Thus, e-nose can circumvent the requirement of conducting routine biochemical assays for estimation of rancidity in cookies.

Novelty

The novelty of this work is that it has reported for the first time on designing of cookies with extract obtained from SC-CO_2 extraction and post-extraction residual sample matrix of small cardamom seeds. Similar methodology using e-nose technology can also be employed for assessment of rancidity in other bakery products.

References

Arun K. B., Persia F., Aswathy P. S., Chandran J., Sajeev M. S., Jayamurthy P., and Nisha P. (2015). Plantain peel - a potential source of antioxidant dietary fibre for developing functional cookies. *Journal of Food Science and Technology*, **52**, 6355-6364.

Sakac M. B., Gyura J. F., Misan A. C., Seres Z. I., Pajin B. S., and Soronja-Simovicm D. M. (2010). Antioxidant activity of cookies supplemented with sugarbeet dietary fiber. *Sugar Industry*, **136**, 151-157.

Chatterjee D., Bhattacharjee P., Lechat H., Ayouni F., Vabre V., and Bhattacharyya N. (2014). Electronic nose setup for estimation of rancidity in cookies. In: *Sensing technology: Current status and future trends II, smart sensors, measurement and instrumentation*. Mason A., Mukhopadhyay S. C., Jayasundera K. P., and Bhattacharyya N. (Eds.), Springer International Publishing, Switzerland, pp. 1-27.

Tables:

Table 3.2.1. Physical properties of cookies.

Sample	Diameter* (cm)	Thickness* (cm)	Spread ratio	Weight* (g)	Hardness* (N)	L*	a*	b*	Chroma	Hue angle (°)
E_S	5.70±0.04[a]	1.24±0.03[a]	4.59 [a]	25.20±0.10[a]	49.55±0.30[b]	63.74±0.60[b]	8.53±0.04[b]	28.23±0.16[b]	29.49±0.16[b]	73.19±0.17[a]
R_S	5.68±0.03[a]	1.23±0.03[a]	4.62[a]	25.10±0.20[a]	52.04±0.40[c]	56.94±0.20[a]	4.59±0.06[a]	18.57±0.13[a]	19.13±0.12[a]	76.12±0.13[b]

C- control cookies, E_S- cookies formulated with extract of small cardamom, R_S- cookies formulated with post-extraction sample matrix of small cardamom
*Values of diameter, thickness, weight, hardness and color parameters of cookies are mean±SD of three independent samples
Different letters in a column indicate significant difference at $P \leq 0.05$

Table 3.2.2. Spoilage indices of different cookies at different storage days.

Storage days	Spoilage indices of cookies	
	E_S	R_S
20	0.2126	2.1997
40	3.1082	2.6687
60	6.0303	3.3414
80	6.6217	4.3156
100	9.8548	7.4152
120	13.5992	9.8112
140	15.5626	15.9160
160	14.0392	18.4899
180	14.3634	20.6033
200	15.2153	32.2798
Rancid 1 day	30.0843	16.9719
Rancid 2 days	44.7270	21.3886
Rancid 3 days	53.5389	29.8333
Rancid 6 days	73.5434	36.3322
Rancid 10 days	82.3444	44.1959
Rancid 17 days	90.5616	62.2719

E_S- cookies formulated with extract of small cardamom, R_S- cookies formulated with post-extraction sample matrix of small cardamom

Figures:

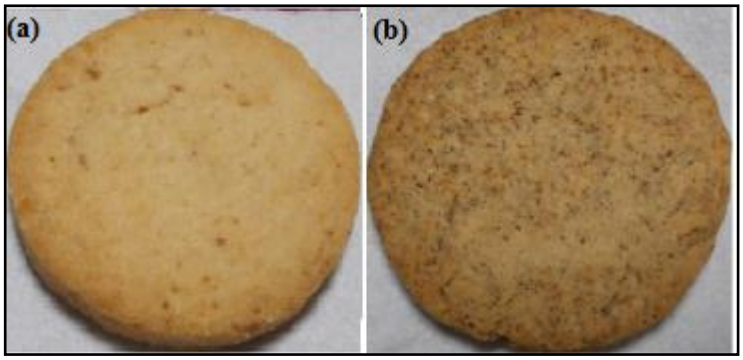

Fig. 3.2.1. Different sets of cookies designed (a) Cookie fortified with small cardamom extract (E_S) and (b) Cookie fortified with post-extraction sample matrix of small cardamom (R_S).

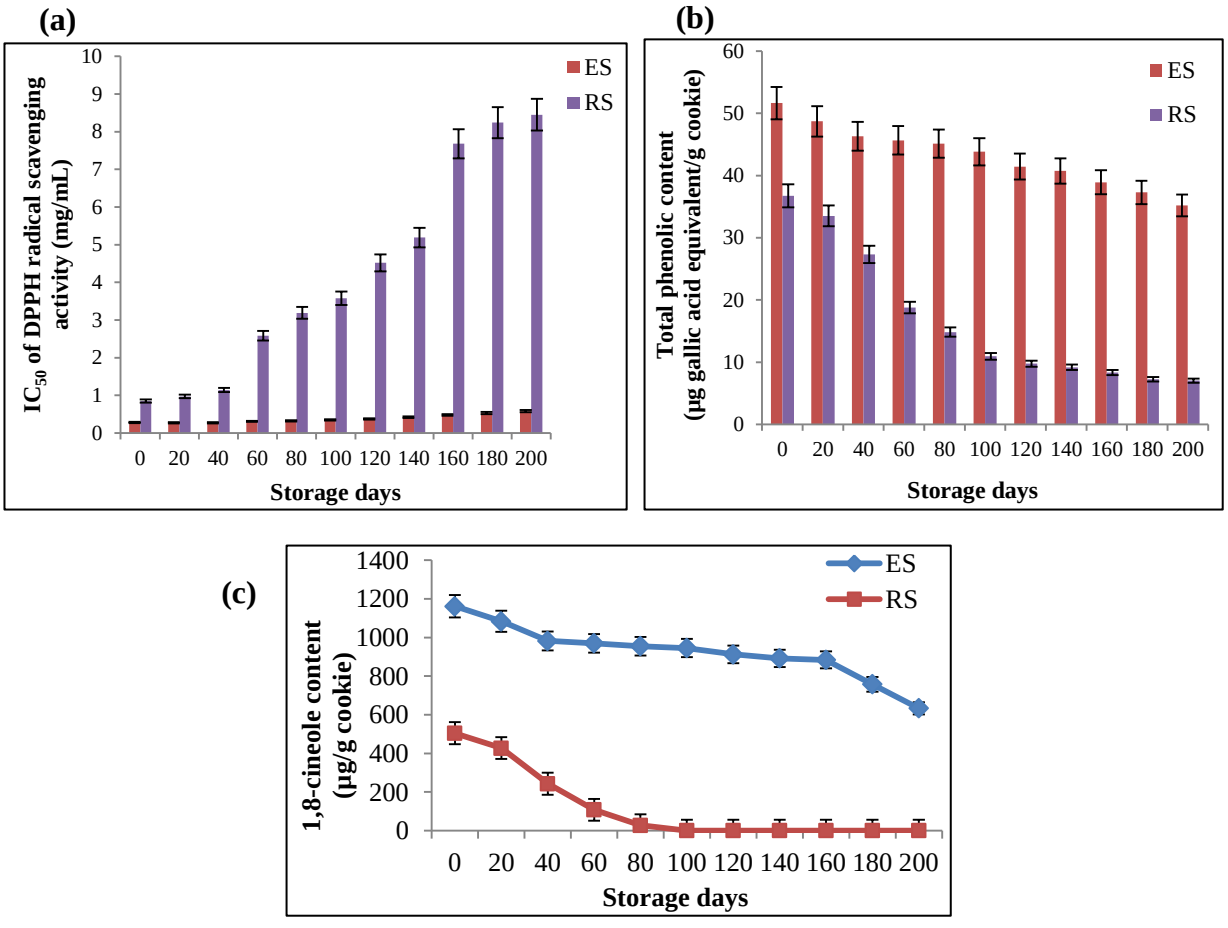

Fig. 3.2.2. Changes in phytochemical properties of small cardamom (E_S and R_S) cookies with storage days. (a) Antioxidant potency (IC_{50} value), (b) Total phenolic content and (c) 1,8-cineole content.

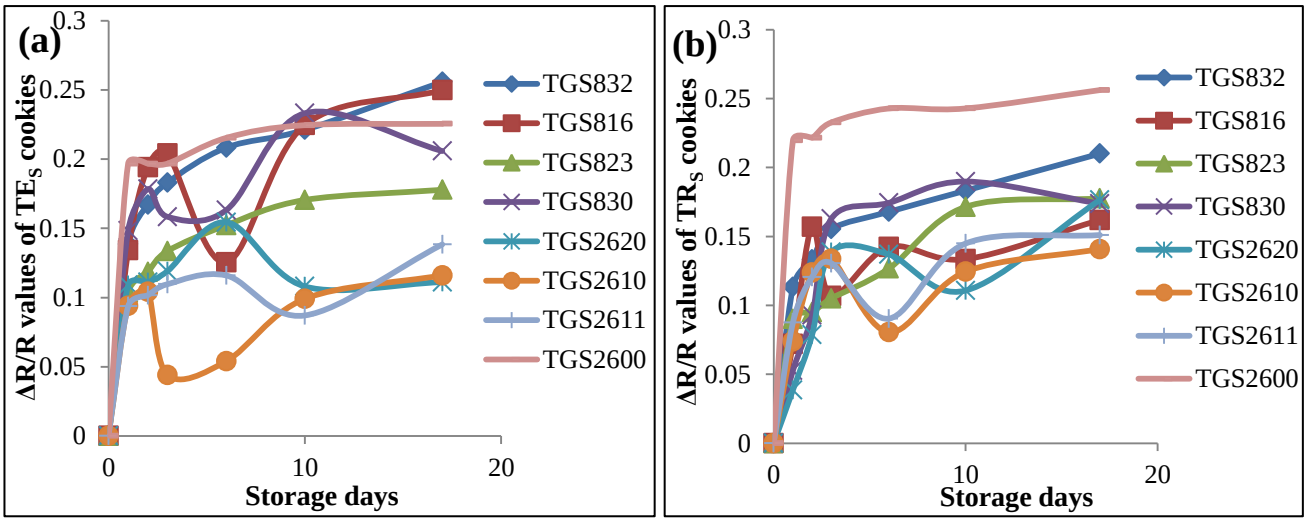

Fig. 3.2.3. Selection of e-nose sensors based on responses obtained for deliberately-made rancid cookies (a) TE_S and (b) TR_S.

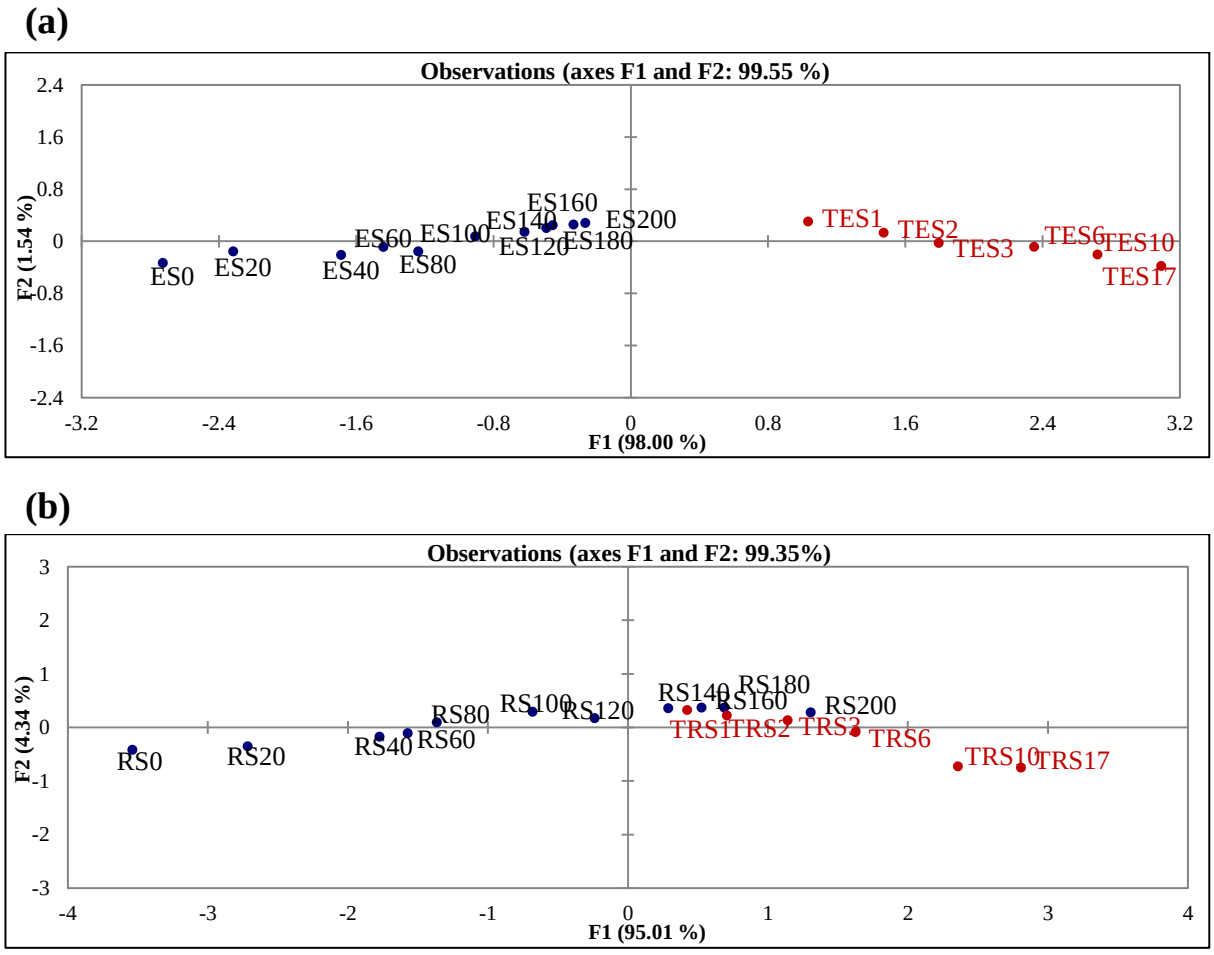

Fig. 3.2.4. PCA plots of small cardamom cookies. (a) E_S cookies and (b) R_S cookies.

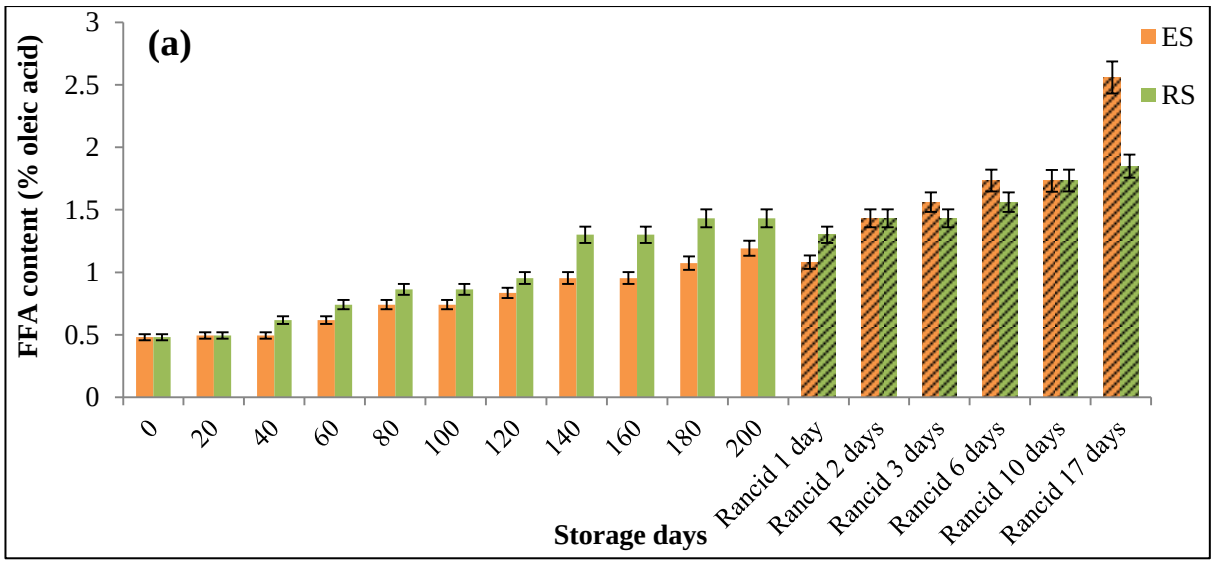

Fig. 3.2.5 (a). FFA contents of cookies (E_S and R_S) during the storage period of 200 days along with deliberately made rancid cookies.

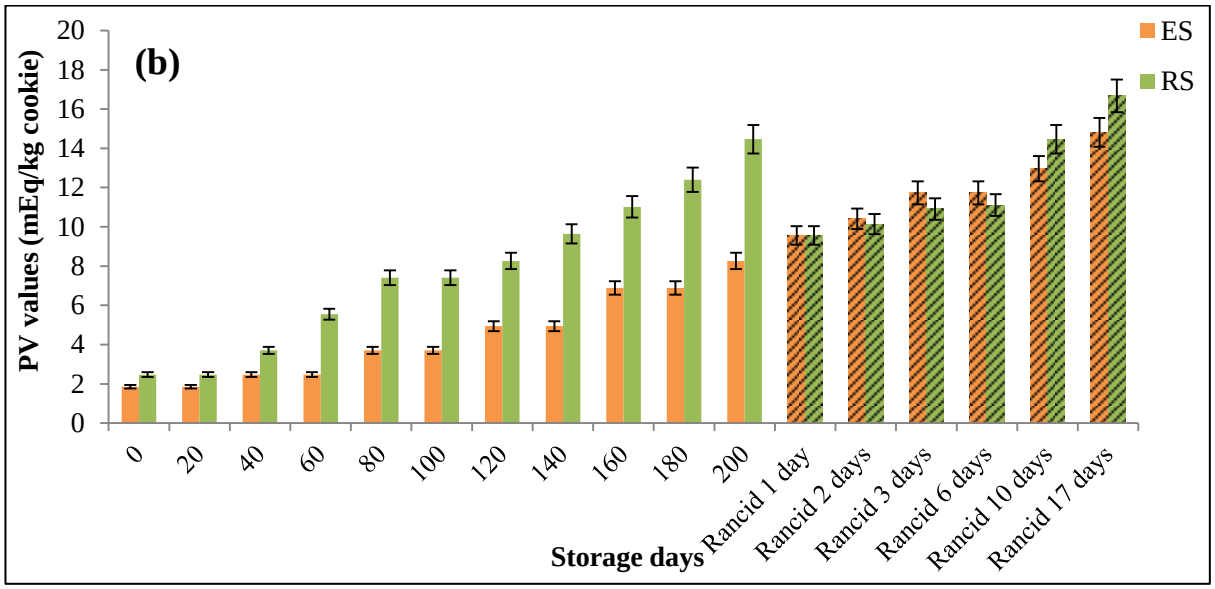

Fig. 3.2.5 (b). PV values of cookies (E_S and R_S) during the storage period of 200 days along with deliberately made rancid cookies.

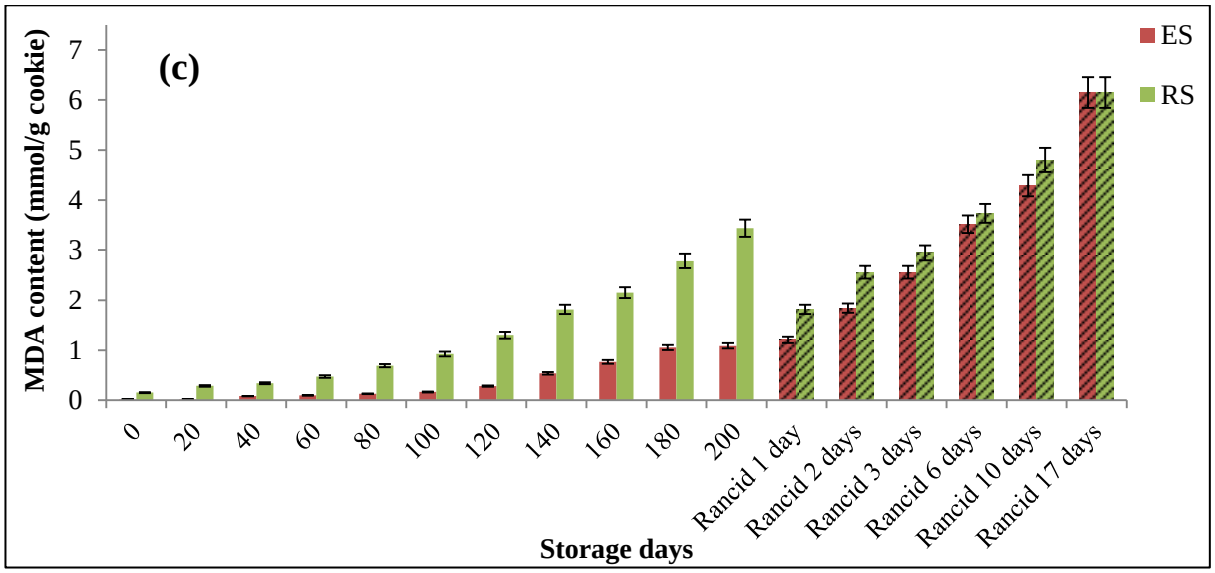

Fig. 3.2.5 (c). MDA contents of cookies (E_S and R_S) during the storage period of 200 days along with deliberately made rancid cookies.

Chapter 4

Encapsulation of black pepper and small cardamom extracts

Section 4.1

Microencapsulation of enzyme-assisted supercritical carbon dioxide extract of small cardamom by spray drying: Optimization of process parameters and kinetics of release of 1,8 cineole from the encapsulate

Introduction

The 1,8-cineole-rich extract obtained from enzyme-assisted SC-CO_2 extraction of small cardamom seeds was further subjected to microencapsulation to enhance the shelf stability of the same. The microencapsulation was carried out by spray drying using maltodextrin and gum arabic as wall materials. Besides wall material composition, other associated variables of spray drying operation, namely, inlet air temperature and extract concentration in the feed were optimized using full factorial design. This work is the first report on microencapsulation of enzyme-assisted SC-CO_2 extract of small cardamom by spray drying. The 1,8-cineole-rich spray-dried powder/encapsulate with highest microencapsulation efficiency (%ME) has been designated as E_{best}, which could be termed as a 'finished herbal product' in accordance with WHO (2000) guidelines.

The objectives of this work were therefore, optimization of microencapsulation parameters to obtain an encapsulate of the 1,8-cineole-rich small cardamom extract obtained from enzyme-assisted SC-CO_2 extraction; study of *in vitr*o release of 1,8-cineole from the same and evaluation of shelf stability of the encapsulate.

Materials and Methods

Materials

Maltodextrin [dextrose equivalent (DE) 16.5-19.5] and gallic acid were procured from Sigma, India. Gum arabic and 0.45 μm filter papers were procured from E-Merck, Mumbai, India. All other chemicals and materials used in this study have been described in section 3.1 of Chapter 3.

Microencapsulation of 1,8-cineole-rich small cardamom extract

Beristain et al. (2001) encapsulated volatile oil of small cardamom seeds by spray drying with mesquite gum as wall material (oil: gum ratio of 1:4); while Krishnan et al. (2005) have spray dried cardamom oleoresin using gum arabic: maltodextrin: modified starch (4/6, 1/6, 1/6). Cardamom oil has also been microencapsulated by spray drying using skim milk powder and modified starch as wall materials (Najafi et al., 2011).

In the current investigation, microencapsulation of 1,8-cineole-rich extract obtained from enzyme-assisted SC-CO_2 extraction of small cardamom seeds was carried out using Mini Spray Dryer B-290 model of Buchi, Switzerland, using maltodextrin and gum arabic as wall materials. A 3^2 experimental design was employed using wall material composition [maltodextrin: gum arabic (80:20, 70:30, 60:40)] and inlet air temperature (110, 130, 150 °C) as variables. Maltodextrin with DE 16.5-19.5 has been selected since in this DE range, it is easily water soluble, has bland flavour, renders low moisture content to the encapsulate and has low production cost (Syll et al., 2016; McNamee et al., 2001).

In preliminary trials, it was observed that inlet air temperature <110 °C caused adhering of micro-particles on the wall of the drying unit resulting in poor yield of powder; while, temperature >150 °C affected the antioxidant potency of encapsulates owing to thermal

degradation of 1,8-cineole [boiling point of 1,8-cineole is 177 °C (Sigma-Aldrich, 2015)]. Therefore, microencapsulation was conducted in the temperature regime of 110 to 150 °C.

1 g of 1,8-cineole-rich small cardamom extract (amount optimized in preliminary trials) obtained from the method described in section 3.1 of Chapter 3, was added to 100 mL aqueous solution containing different proportions of wall materials (20% total solids) and subjected to continuous stirring using a magnetic stirrer at 150 rpm at room temperature (23±2 °C) for 1 min. Compressed air at a pressure of 8 bar was used for spray drying. The sample was passed through a peristaltic pump and fed to the spray dryer by a spray nozzle (diameter 0.7 mm). The spray gas flow rate, gas flow rate in aspirator, sample feed rate and atomization pressure were kept constant at 473 L/h, 35,000 L/h, 0.90 mL/min and -60 mbar respectively, for all experiments (optimized in preliminary trials). The encapsulates were packed in Al foils, flushed with nitrogen and packaged in Ziploc pouches (Johnson, India) and stored at 23±2 °C, until further analyses.

Characterization of the encapsulates

Analysis of yield and physical properties of encapsulates

The yield of spray dried powder in each experiment was determined gravimetrically. Moisture content of the encapsulates was determined by AOAC method 934.01 (2006). Bulk densities and tapped densities of the encapsulates were also assessed. The flowability of encapsulates was evaluated by Carr index (CI) and Hausner ratio (HR), in accordance with the methods reported by Barman et al. (2014).

Sample preparation for analyses of biochemical properties of encapsulates

For estimation of phytochemical properties, the wall material of the encapsulated extract was completely ruptured by an ultrasonic homogenizer (Sartorius, Germany) at 30 kHz in accordance

with the method reported by Chatterjee et al. (2014). The samples were analyzed for 1,8-cineole content and phytochemical properties.

Estimation of 1,8-cineole contents of spray dried powder samples

1,8-cineole contents in the encapsulates were estimated by adopting the method described for estimation of 1,8-cineole content of enzyme-assisted SC-CO_2 extract of small cardamom (section 3.1 of Chapter 3) and was represented as mg 1,8-cineole/g powder.

Assessment of %microencapsulation efficiency (ME) and %surface binding (SB) of the encapsulates

%SBs of encapsulates were calculated from the surface bioactive compounds (1,8-cineole present at the surface of the encapsulates) and theoretical bioactive compounds (1,8-cineole content of the extract before encapsulation) estimated by HPTLC analyses, in accordance with the method reported by Chatterjee et al. (2014) (Eq. 1). %ME of encapsulates has been estimated by two different approaches. In the first approach, $\%ME_1$ was calculated from the theoretical bioactive compounds considering no loss during spray drying (Eq. 2) (Carneiro et al., 2013; Robert et al., 2010). In the second approach, 1,8-cineole content of the encapsulates (total bioactive compounds recovered from the encapsulates by ultrasonication) was estimated to calculate $\%ME_2$ (Eq. 3) (Chatterjee et al., 2014; Chen and Subirade, 2006).

$$\%SB = (Surface\ bioactive\ compounds/Theoretical\ bioactive\ compounds) \times 100 \quad (1)$$

$$\%ME_1 = (100 - \%SB) \quad (2)$$

$$\%ME_2 = (Total\ bioactive\ compounds/Theoretical\ bioactive\ compounds) \times 100 \quad (3)$$

The spray drying conditions which exhibited highest $\%ME_1$ and $\%ME_2$ were therefore considered to be the optimum drying conditions. The encapsulate obtained at the optimum conditions was considered as the 'best encapsulate' of this study and designated as E_{best}.

Phytochemical analysis of the encapsulates

Antioxidant activity, total phenolic content and reducing power of encapsulates were determined by the methods previously discussed for the extracts.

Analysis of hydrophillic-lipophillic balance (HLB) value of E_{best}

Hydrophillic-lipophillic balance value of Ebest was determined in accordance with the method described by Powrie and Tung (1976).

Statistical analyses of characteristics of encapsulates

In this investigation, statistical analysis was performed to study the effects of operating parameters (inlet air temperature and % maltodextrin) on %MEs of the encapsulates by ANOVA. Optimization of the parameters of spray drying for maximum %ME of 1,8-cineole was conducted by RSM and regression modeling. Spray drying, densitometric analyses, assay of phytochemical properties of encapsulates and their HLB values were performed in triplicates and reported as mean±SD. Significant differences between means were calculated by Duncan's multiple-range test ($P \leq 0.05$). All statistical analyses were performed using STATISTICA 8.0 software (Statsoft, OK, USA).

Field emission scanning electron microscopy (FE-SEM) analysis of E_{best}

The outer structure of E_{best} was studied by FE-SEM analysis. The powder was coated with platinum using an Autofine Coater (JFC-1600, JEOL Company Ltd., Japan) and analyzed using field emission scanning electron microscope (FE-SEM) (JSM-6700F, JEOL Company Ltd.,

Japan), operated at 5 kV with a working distance of 8 mm. The scanned images were collected digitally.

Energy dispersive X-ray (EDX) spectroscopy of E_{best}

EDX analysis was carried out to detect hazardous metal(s) (such as Cu, Pb, Cd, Hg and As), if any, in E_{best}. The sample was coated with platinum and EDX analysis was carried out in JSM-6700F (JEOL Company Ltd., Japan) at 20 kV using JEOL detector (JEOL Company Ltd., Japan).

Estimation of glass transition temperature (T_g) of E_{best}

Estimation of T_g of E_{best} was conducted by differential scanning calorimetry (DSC). The thermal behavior of both E_{best} and the SC-CO_2 extract of small cardamom were studied, prior to estimation of T_g of E_{best}. For this study, thermogravimetric/differential thermal analysis (TG/DTA) were carried out using a Pyris Diamond TG/DTA analyzer (Perkin Elmer, Singapore), in accordance with the method reported by Aquino et al. (2013). Blank platinum crucible with α-alumina powder was used as reference. 12.759±0.2 mg extract and 5.268±0.2 mg encapsulate were individually placed in hermetically sealed Al pan and heated from 30 to 400 °C. The scanning rate was 12 °C/min and the flow rate of nitrogen was kept at 150 mL/min.

DSC study of E_{best} (model Diamond DSC, Perkin Elmer, Singapore) was conducted in accordance with the method reported by Ferrari et al. (2013). 5.0±0.2 mg of E_{best} was placed in hermetically sealed Al pan and heated from 25 to 140 °C at 10 °C/min and then cooled to 25 °C at 10 °C/min. The equipment was calibrated with indium ($T_{melting}$=156.6 °C) and dry nitrogen was used as the purge gas (70 mL/min). An empty pan was used as reference.

Study of *in vitro* release kinetics of 1,8-cineole from E_{best}

The *in vitro* release of 1,8-cineole from E_{best} was studied by adopting the method reported by Song et al. (2012), with few modifications. 1 g of encapsulate was added to 50 mL phosphate buffer (pH 7.0) and continuously stirred in a magnetic stirrer at 50 rpm at room temperature (23±2 °C). 2 mL aliquot was collected at different time intervals for 6 h (at 5, 10, 15, 30, 60, 90, 120, 180 and 360 min) and was replaced with an equal volume of fresh buffer each time. The amount of 1,8-cineole in the aliquots was estimated by HPTLC analyses (described in section 3.1 of Chapter 3).

The release data of 1,8-cineole from E_{best} was fitted into several kinetic equations, namely, zero order, first order and into sub-types of first order such as Higuchi model, Hixson-Crowell's cube root model and Peppas equations (Chatterjee et al., 2014). The kinetic model with highest regression coefficient (r) best represented the release of 1,8-cineole from the encapsulate. The release exponent (n) was determined to characterize the release mechanism of 1,8-cineole in accordance with Song et al. (2012).

Stability study of E_{best}

Storage stabilities of the non-encapsulated extract and E_{best} were conducted by analysis of their half-life values ($T_{1/2}$), adopting the method reported by Chatterjee et al. (2014), with few modifications. Both the samples were stored at ambient condition (23±2 °C, 80% RH) and 1,8-cineole contents of the samples were determined by HPTLC method at an interval of 15 days for 60 days.

$T_{1/2}$ values for SC-CO_2 extract and E_{best} were calculated by determining the ratio of 1,8-cineole on day 0 (TA_0) and on day (t) (TA_t) for non-encapsulated and encapsulated extracts. The natural

logarithm of TA_0/TA_t was plotted against storage time and the slope (k) of the line through the origin was used to obtain the half-lives ($T_{1/2} = \ln 2/k$) of extract and encapsulate.

Accelerated stability studies of the non-encapsulated and encapsulated extracts were performed in accordance with the method reported by Waterman (2011), at 70±2 °C, 75% RH for 24 h. $T_{1/2}$ was determined from the ratio of 1,8-cineole present in the samples at 0 h and at time (t).

Results and Discussion

Analysis of yield and physical properties of encapsulates

The yield of encapsulate was found to increase with increasing inlet air temperature, increasing concentration of maltodextrin and decreasing concentration of gum arabic in wall material composition. Highest yield (66.52±1.6%) was obtained at conditions of 150 °C inlet air temperature and wall material composition of maltodextrin: gum arabic:: 80:20 (Table 4.1.1). Chatterjee and Bhattacharjee (2013) have reported yields of about 62% for microencapsulation of clove extracts with 1:4.8:2.4 of clove extract: maltodextrin: gum arabic at 150 °C inlet air temperature; while Maury et al. (2005) have reported 58% yield for microencapsulated trehalose with 10% (w/v) trehalose at 130 °C inlet air temperature using laboratory scale spray dryer of same make and model (Buchi). In this investigation, the outlet air temperature during spray drying varied from 75 to 109 °C, which was lower than the boiling point of 1,8-cineole (177 °C).

The moisture contents of the encapsulates varied from 1.03 to 2.50% on a dry weight basis. The bulk densities of encapsulates were in the range of 0.33-0.37±0.01 g/mL, while their tapped densities were between 0.38 and 0.42±0.01 g/mL. The Hausner ratio of 1.14-1.15 confirmed low cohesiveness and Carr's index of 11.90-13.16% affirmed very good flowability of the

encapsulates, in agreement with Jinapong et al. (2008) who worked on production of instant soymilk powders by spray drying and fluidized bed agglomeration.

Estimation of %ME and %SB of the encapsulates

1,8-cineole contents of the encapsulates were in the range of 16.55±0.75-25.03±0.97 mg/g powder (Table 4.1.1). Although maximum yield of spray dried powder was obtained at 150 °C inlet air temperature; $\%ME_1$ or $\%ME_2$ at this temperature was not the highest. High inlet air temperature could have caused degradation of 1,8-cineole in the encapsulate resulting in lower %ME, since this temperature was close to the boiling temperature of 1,8-cineole. The highest content of 1,8-cineole (25.03±0.97 mg/g powder) was obtained at 130 °C using 70:30:: maltodextrin: gum arabic.

% SB of the encapsulates were in the range of 5.46±0.1-7.95±0.3% (Table 4.1.1) indicating the extract to be located in the core of the encapsulate. SB for microencapsulated algae has been reported to be 25-30% (Chatterjee et al., 2014), which was higher than the result of this study indicating lesser loss of 1,8-cineole by surface leaching from cardamom encapsulates. $\%ME_1$ of encapsulates varied from 92.05±0.31 to 94.54±0.17% and $\%ME_2$ was in the range of 41.72±1.3-73.15±1.3% (Table 4.1.1). The former method assumes no loss of bioactive compounds and considers 1,8-cineole which is not present on the surface, to be located in the core of the encapsulates. 1,8-cineole is a volatile and thermolabile compound; therefore, in experimental spray drying conditions, loss of the same is expected. $\%ME_2$ is obviously more appropriate than $\%ME_1$ since the former considers loss of bioactives during encapsulation. Highest $\%ME_2$ (73.15±1.32%) was obtained at 130 °C using 70:30:: maltodextrin: gum arabic (Table 4.1.1). 60-65% ME has been reported by Chatterjee and Bhattacharjee (2013) for spray dried SC-CO_2

extract of clove buds at 150 °C inlet air temperature using clove extract: maltodextrin: gum arabic in the ratio of 1:4.8:2.4.

Statistical analysis of effect of inlet air temperature and %maltodextrin on 1,8-cineole content of encapsulates

The 3D response surface plot of inlet air temperature (ºC) and maltodextrin (%) (independent variables) revealed a significant effect of both these parameters on 1,8-cineole content (mg/g of powder) (dependent variable) of the encapsulates (Fig. 4.1.1). Regression modeling was carried out by generating second order polynomial equations for 1,8-cineole content as a function of inlet air temperature (ºC) and maltodextrin (%).

The second order polynomial equation that fitted the experimental variables is stated below:

$$Y = B_0 + \Sigma B_i X_i + \Sigma B_{ii} X_i^2 + \Sigma B_{ij} X_i X_j \quad (4)$$

where, Y represents experimental response (1,8-cineole content), B_0, B_i, B_{ii}, and B_{ij} are constants and regression coefficients of the model and X_i and X_j are independent variables.

The expanded model includes linear, quadratic and cross-product terms as shown below (with intercept):

$$Y = B_0 + B_1X_1 + B_{11} X_1^2 + B_2X_2 + B_{22}X_2^2 + B_{12}X_1X_2 \quad (5)$$

$$Y = 19.812 - 0.065 X_1 + 1.056 X_1^2 + 1.468 X_2 + 1.856 X_2^2 + 0.345 X_1X_2 \quad (6)$$

X_1 and X_2 represent inlet air temperature (ºC) and amount of maltodextrin (%), respectively. The correlation coefficient (r) for this equation was 0.896. Therefore, a statistically significant regression relationship between the independent variables and the responding variable was established. The data showed a significant quadratic effect (P=0.006) of inlet air temperature and

both linear and quadratic effects (P=0.001 and P=0.000, respectively) of maltodextrin (%) on 1,8-cineole content of encapsulates. Residual analysis of the regression model was conducted in accordance with Chatterjee and Bhattacharjee (2015) for validation of adequacy of the model and violation of basic assumption of regression analysis. The analysis of residuals revealed the residuals to be 'structure less' i.e., having no obvious pattern, which proves the adequacy of the model (Montgomery, 2001a). The plot of predicted and observed values of 1,8-cineole content of encapsulates showed a very good fit (r=0.95) (Fig. 4.1.2).

To determine the optimal processing conditions of microencapsulation i.e., to determine the optimal values of X_1 and X_2, the first partial derivative of the regression equation was conducted with respect to X_1 and X_2 and set to zero. This was conducted by putting the second order regression equation in matrix form as described by Montgomery (2001b) and Ge et al. (2002). The point thus obtained is known as the stationary point, X_{1S} and X_{2S} (X_{1S}=130.01 °C and X_{2S}=71.97%). 1,8-cineole content obtained at this stationary point was found to be 23.84 mg/g powder. Negative eigen values (-0.005 and -0.037) obtained by characterizing the response surface confirmed that the stationary point was a point of maximum response. Observed 1,8-cineole content of the encapsulate (25.03±0.97 mg/g powder) obtained at the stationary point was not significantly different (P=0.4395) from that (23.84±0.97 mg/g powder) obtained at the optimized experimental conditions of spray drying (130 °C inlet air temperature and amount of maltodextrin in wall material 70%). ANOVA analysis revealed high F (Fisher's variance ratio) values (9.43-29.12) indicating significant interactions among the variables (Table 4.1.2). Therefore, the experimental design statistically showed a good fit.

Estimation of phytochemical properties of encapsulates

IC_{50} values of DPPH radical scavenging activities, total phenolic content and reducing power of encapsulates were found to be in the range of 2.09±0.2-3.18±0.4 mg/mL, 118.39±1.14-139.53±1.17 µg gallic acid eq./g powder and 693.61±1.18-725.52±1.18 µg BHT/g powder, respectively (Table 4.1.3). The encapsulate with the best phytochemical properties was obtained at 130 °C using 70:30:: maltodextrin: gum arabic, where highest 1,8-cineole content (25.03±0.97 mg/g powder) was also observed.

Therefore, based on 1,8-cineole content and phytochemical properties of encapsulates, optimized conditions of microencapsulation were 130 °C and 70:30:: maltodextrin: gum arabic. The spray dried powder obtained at these conditions was the 'best encapsulate' in this study and considered as E_{best}. This encapsulate was further subjected to analysis of HLB value, FE-SEM, EDX and for its half-life.

Analysis of HLB value of E_{best}

The HLB value of E_{best} was found to be 16.24±1.20, which is in accordance with the hydrophilic nature of the powder.

FE-SEM, EDX and DSC analyses of E_{best}

FE-SEM photomicrograph (Fig. 4.1.3) of E_{best} revealed shriveled morphology of particles with sizes ranging from 4.19 to 11.50 µm, having mean particle diameter of 7.76 µm. The surface morphology of the powder was irregular with dents owing to shrinkage of the particles during drying, in agreement with the observations of Cai and Corke (2000). Mean particle diameter of 5 µm and shrivelled morphology of encapsulated clove extract has also been reported by Chatterjee and Bhattacharjee (2013).

EDX analysis of E_{best} (Fig. 4.1.4) showed absence of toxic metal compounds such as Cu, Pb, Cd, Hg and As. Therefore, this encapsulate was considered safe for consumption. The absence of sharp melting endotherm peaks in the thermograms of samples revealed that both the SC-CO_2 extract and the encapsulate are non-crystalline in nature (Fig. 4.1.5) (Rajinikanth et al., 2012). In the thermogram of small cardamom extract, the endothermic peak between 110 and 140 °C might be attributed to the degradation of volatiles in the extract and the peak between 150 and 190 °C corresponded to the degradation of the extract (Fig. 4.1.5a). For the encapsulate (Fig. 4.1.5b), the endothermic peak between 60 and 90 °C was due to the elimination of water and the large peak between 200 and 240 °C corresponded to the degradation of the core material in the encapsulate. Since degradation of the core occurred at much higher temperature, significant improvement was achieved in stability of SC-CO_2 extract by spray drying.

The T_g of the encapsulate was found to be 67.26 °C (Fig. 4.1.6). This value was higher than that obtained by Ferrari et al. (2013), who reported T_g in the range of 51-60 °C for spray dried (at inlet air temperature of 145 °C) black berry pulp in 1:1:: maltodextrin and gum arabic. However, according to Cai and Corke (2000), $T_{storage} < T_g$ indicates long term stability of the powder, which was true for our encapsulate.

Study of *in vitro* release kinetics of 1,8-cineole from E_{best}

The *in vitro* release profile of 1,8-cineole revealed that within 30 min, about 88% of 1,8-cineole was released from E_{best} (Fig. 4.1.7). This release profile was fitted into different kinetic equations and their corresponding regression coefficient (r) values were evaluated. Fitting the release profile to the kinetic models showed that the 'r' value of first order model was higher than that of the zero order model. Among the first order models studied, Peppas model showed highest correlation (r=0.89) of release of 1,8-cineole with time (Table 4.1.4). The release mechanism of

1,8-cineole from E_{best} was analyzed by the Korsmeyer and Peppas equation (Eq. 7) (Korsmeyer et al., 1983):

$$M_t/M_a = k \times t^n \quad (7)$$

where, M_t/M_a is the fractional release of 1,8-cineole in time 't', 'k' is the release rate constant and 'n' is the diffusion release exponent indicative of the mechanism of release.

According to the Peppas equation, n=0.45 shows diffusion controlled release, n=0.89 shows swelling controlled release or case II transport and 'n' in the range of 0.45-0.89 depicts superposition of both the above phenomena known as 'anomalous transport' (Song et al., 2012). In the current study, 'n' of Korsmeyer and Peppas equation was found to be 0.59 for release of 1,8-cineole, which was in the range of 0.45-0.89 indicating the release as 'anomalous transport' (since both maltodextrin and gum arabic are hydrocolloids). Similar findings have also been reported for release of curcumin from calcium alginate beads (Song et al., 2012). The value of release rate constant 'k' was found to be 24.96 min^{-1} for the release of 1,8-cineole from E_{best}.

Stability study of E_{best}

From the densitometric assay of 1,8-cineole, at ambient temperature, the half-life ($T_{1/2}$) of non-encapsulated SC-CO_2 extract of small cardamom was found to be 48 days, while E_{best} showed a significantly higher (P=0.00) half-life of 288 days (6.12 times higher). Chatterjee and Bhattacharjee (2015) have also reported improvement in half-life of anthocyanin-rich encapsulate of eggplant peel colour by 16 times, attesting to the benefits of encapsulation of natural products for enhanced shelf stability.

$T_{1/2}$ values of 1,8-cineole at higher temperature were found to be 2.42 h for extract and 19.09 h for E_{best}, revealing 7.88 times higher stability for the encapsulate. Therefore, at both these storage

temperatures, the encapsulated extract had a significant improvement in shelf life over the non-encapsulated SC-CO_2 extract of small cardamom.

Conclusions

The small cardamom extract obtained from enzyme-assisted SC-CO_2 extraction, was microencapsulated by spray drying and the optimized conditions which showed the highest microencapsulation efficiency (73.15±1.32%) were 130 °C inlet air temperature and wall material composition of 70:30:: maltodextrin: gum arabic. This encapsulate was therefore the 'best encapsulate', obtained under the experimental conditions. The phytochemical properties of this encapsulate were appreciable. The encapsulate showed 6.12 times higher shelf stability at ambient temperature (23±2 °C) and 7.88 times higher shelf stability at higher temperature (70±2 °C), with respect to the SC-CO_2 extract. The release of 1,8 cineole from the encapsulate of the SC-CO_2 extract was within 30 min. This nutraceutically-rich encapsulate was further employed as a natural antioxidant in designer foods such as nutraceutical custard (discussed in section 4.2 of Chapter 4).

Novelty

The novelty of the work is that, it has reported for the first time on microencapsulation of SC-CO_2 extract of small cardamom by spray drying. The 1,8-cineole-rich spray-dried powder/encapsulate with highest microencapsulation efficiency could be termed as a 'finished herbal product' in accordance with WHO guidelines.

References

AOAC (Association of Official Analytical Chemists') (2006). *Official Methods of Analysis of AOAC International,* 18th edn., AOAC International, USA.

Aquino R. P., Auriemma G., Mencherini T., Russo P., Porta A., Adami R., Liparoti S., Porta G. D., Reverchon E., and Gaudio P. D. (2013). Design and production of gentamycin/dextrans microparticles by supercritical assited atomization for the tratemtnet of would bacterial infections. *International Journal of Pharmaceutics*, **440**, 188-194.

Barman R. K., Iwao Y., Noguchi S., Wahed M. I. I., and Itai S. (2014). Improving flow property of nifedipine loaded solid-lipid nanoparticles by means of silica for oral solid dosage form. *Pharmacology and Pharmacy*, **5**, 1119-1129.

Beristain C. I., García H. S., and Vernon-Carter E. J. (2001). Spray-dried encapsulation of cardamom (*Elettaria cardamomum*) essential oil with mesquite (*Prosopis juliflora*) gum. *LWT - Food Science and Technology*, **34**, 398-401.

Cai Y. Z. and Corke H. (2000). Production and properties of spray-dried Amaranthus betacyanin pigments. *Journal of Food Science*, **65**, 1248-1252.

Carneiro H. C. F., Tonon R. V., Grosso C. R. F. and Hubinger M. D. (2013). Encapsulation efficiency and oxidative stability of flaxseed oil microencapsulated by spray drying using different combinations of wall materials. *Journal of Food Engineering*, **115**, 443-451.

Chatterjee D., and Bhattacharjee P. (2013). Comparative evaluation of the antioxidant efficacy of encapsulated and un-encapsulated eugenol-rich clove extracts in soybean oil: Shelf-life and frying stability of soybean oil. *Journal of Food Engineering*, **117**, 545-550.

Chatterjee D., and Bhattacharjee P. (2015). Encapsulation of colour from peels of eggplant in calcium alginate matrix. *Nutrafoods*, DOI: 10.1007/s13749-015-0001-5.

Chatterjee D., Bhattacharjee P., Satpati G. G., and Pal R. (2014). Spray dried extract of *Phormidium valderianum* as a promising source of natural antioxidant. *International Journal of Food Science*. DOI:10.1155/2014/897497.

Chen L., and Subirade M. (2006). Alginate-whey protein granular microspheres as oral delivery vehicle for bioactive compounds. *Biomaterials*, **27**, 4646-4654.

Ferrari C. C., Germer S. P. M., Alvim I. D., and Aguirre J. M. de (2013). Storage Stability of Spray-Dried Blackberry Powder Produced with Maltodextrin or Gum Arabic. *Drying Technology: An International Journal*, **31**, 470-478.

Ge Y., Ni Y., Yan H., Chen Y., and Cai T. (2002). Optimization of the supercritical fluid extraction of natural vitamin E from wheat germ using response surface methodology. *Journal of Food Science*, **67**, 239-243.

Jinapong N., Suphantharika M., and Jamnong P. (2008). Production of instant soymilk powders by ultrafiltration, spray drying and fluidized bed agglomeration. *Journal of Food Engineering*, **84**, 194-205.

Korsmeyer R. W., Gurny R., Doelker E., Buri P., and Peppas N. A. (1983). Mechanisms of solute release from porous hydrophilic polymers. *International Journal of Pharmaceutics*, **15**, 25-35.

Krishnan S., Bhosale R., and Singhal R. S. (2005). Microencapsulation of cardamom oleoresin: Evaluation of blends of gum arabic, maltodextrin and a modified starch as wall materials. *Carbohydrate polymers*, **61**, 95-102.

Maury M., Murphy K., Kumar S., Shib L., and Lee G. (2005). Effects of process variables on the powder yield of spray-dried trehalose on a laboratory spray-dryer. *European Journal of Pharmaceutics and Biopharmaceutics*, **59**, 565-573.

McNamee B.F., O'Riordan E.D., and O'Sullivan M. (2001). Effect of partial replacement of gum arabic with carbohydrates on its microencapsulation properties. *Journal of Agricultural and Food Chemistry*, **49**, 3385-3388.

Montgomery D.C. (2001a). Experiments with a single factor: the analysis of variance. In: *Design and Analysis of Experiments*, John Wiley & Sons Inc., New York, pp. 60-125.

Montgomery D.C. (2001b). Response surface methods and other approaches to process optimization. In: *Design and Analysis of Experiments*, John Wiley & Sons Inc., New York, pp. 427-510.

Najafi M. N., Kadkhodaee R., Mortazavi S. A. (2011). Effect of drying process and wall material on the properties of encapsulated cardamom oil. *Food Biophysics*, **6**, 68-76.

Powrie W. D., and Tung M. A. (1976). Food dispersions. In: *Principles of Food Science, Part-I Food Chemistry*, Fenema O. W. (Ed.), Marcel Dekker, New York, pp. 539-575.

Rajinikanth P. S., Balasubramaniam J., Kumar M. T., Rajesh Y. V. (2012). Spray drying as an approach for enhancement of dissolution and bioavailability of raloxifene hydrochloride. *International Journal of Drug Delivery*, **4**, 246-256.

Robert P., Gorena T., Romero N., Sepulveda E., Chavez J., and Saenz C. (2010). Encapsulation of polyphenols and anthocyanins from pomegranate (*Punica granatum*) by spray drying. *International Journal of Food Science and Technology*, **45**, 1386-1394.

Sigma-Aldrich (2015), Accessed from: http://www.sigmaaldrich.com/catalog/product/sial/00020590?lang=en&region=IN, on 23 Dec 2015.

Song S., Wang Z., Qian Y., Zhang L., and Luo E. (2012). The release rate of curcumin from calcium alginate beads regulated by food emulsifiers. *Journal of Agricultural and Food Chemistry*, **60**, 4388-4395.

Syll O., Khalloufi S., Mèjean S., Schuck P. (2016). The effects of total protein/total solid ratio and pH on the spray drying process and rehydration properties of soy powder. *Powder Technology*, **289**, 60-64.

Waterman K.C. (2011). The application of accelerated stability assessment programme (ASAP) to quality by design (QbD) for drug product stability. *AAPS PharmSciTech*, **12**, 932-937.

WHO (World Health Organization). (2000). General guidelines for methodologies on research and evaluation of traditional medicine, Available at: http://apps.who.int/medicinedocs/en/d/Jwhozip42e/4.1.html, Accessed on November 3, 2015.

Tables:

Table 4.1.1. Yield, 1,8-cineole content, microencapsulation efficiencies and surface binding of the encapsulates at different conditions of encapsulation.

Run No.	Inlet air temperature (°C)	Composition of wall material (maltodextrin: gum arabic)	Yield of encapsulate (%)	1,8-cineole content (mg/g powder)	Surface binding (SB) (%)	Micro-encapsulation efficiency (ME_1) (%)	Micro-encapsulation efficiency (ME_2) (%)
1	150	80:20	66.52 ± 1.61^{d}	19.40 ± 0.85^{bcd}	6.03 ± 0.20^{b}	93.97 ± 0.20^{d}	58.47 ± 1.23^{f}
2	150	70:30	65.50 ± 1.25^{cd}	20.66 ± 0.93^{cde}	6.02 ± 0.22^{b}	93.98 ± 0.22^{d}	61.32 ± 1.21^{g}
3	150	60:40	53.95 ± 1.19^{a}	17.70 ± 0.74^{ab}	7.95 ± 0.31^{e}	92.05 ± 0.31^{a}	41.72 ± 1.25^{a}
4	130	80:20	66.05 ± 1.40^{d}	22.08 ± 0.96^{e}	5.89 ± 0.19^{b}	94.11 ± 0.19^{d}	66.08 ± 1.04^{h}
5	130	70:30	64.50 ± 1.32^{cd}	25.03 ± 0.97^{f}	5.46 ± 0.17^{a}	94.54 ± 0.17^{e}	73.15 ± 1.32^{i}
6	130	60:40	63.35 ± 1.17^{c}	16.55 ± 0.75^{a}	7.46 ± 0.29^{d}	92.54 ± 0.29^{b}	47.52 ± 1.16^{c}
7	110	80:20	59.65 ± 1.09^{b}	18.65 ± 0.82^{abc}	6.79 ± 0.25^{c}	93.21 ± 0.25^{c}	50.41 ± 1.27^{d}
8	110	70:30	55.40 ± 1.21^{a}	21.17 ± 0.91^{de}	6.54 ± 0.28^{c}	93.46 ± 0.28^{c}	53.14 ± 1.35^{e}
9	110	60:40	54.90 ± 1.18^{a}	17.70 ± 0.94^{ab}	7.67 ± 0.27^{de}	92.33 ± 0.27^{ab}	44.09 ± 1.22^{b}

Yield, 1,8-cineole content, % microencapsulation efficiency and % surface binding of the encapsulated small cardamom extracts are mean±SD of three independent experimental runs.
Different letters in a column indicate significant difference at $P< 0.05$.

Table 4.1.2. ANOVA study of effect of inlet air temperature and % maltodextrin on 1,8-cineole content of the encapsulates.

Effect	Degree of freedom	1,8-cineole content (mg/g powder) SS	1,8-cineole content (mg/g powder) MS	1,8-cineole content (mg/g powder) F	1,8-cineole content (mg/g powder) P
X_1	1	0.08	0.08	0.03	0.871536
X_1^2	1	26.75	26.75	9.43	0.005806*
X_2	1	38.81	38.81	13.67	0.001335*
X_2^2	1	82.66	82.66	29.12	0.000024*
X_1X_2	1	1.44	1.43	0.50	0.485875
Error	21	59.60	2.84		
Total	26	209.33			

X_1-inlet air temperature during spray drying.
X_2-% maltodextrin.
*significant at $P< 0.05$.

Table 4.1.3. Phytochemical properties of encapsulates.

Run No.	Inlet air temperature (°C)	Composition of wall material (maltodextrin: gum arabic)	IC_{50} of DPPH radical scavenging activity (mg/mL)	Total phenolic content (µg GAE/g powder)	Reducing power (µg BHT/g powder)
1	150	80:20	2.58 ± 0.04^{c}	130.77 ± 1.26^{c}	708.62 ± 1.25^{de}
2	150	70:30	2.29 ± 0.05^{b}	133.59 ± 1.14^{de}	710.43 ± 1.28^{ef}
3	150	60:40	3.18 ± 0.08^{e}	131.6 ± 1.18^{cd}	693.61 ± 1.18^{a}
4	130	80:20	2.27 ± 0.03^{b}	134.75 ± 1.22^{e}	711.45 ± 1.22^{f}
5	130	70:30	2.09 ± 0.04^{a}	139.53 ± 1.17^{f}	725.52 ± 1.18^{g}
6	130	60:40	2.81 ± 0.06^{d}	118.39 ± 1.14^{a}	705.72 ± 1.24^{bc}
7	110	80:20	2.77 ± 0.07^{d}	134.11 ± 1.18^{e}	705.58 ± 1.23^{bc}
8	110	70:30	2.59 ± 0.04^{c}	137.81 ± 1.17^{f}	706.91 ± 1.17^{cd}
9	110	60:40	3.11 ± 0.03^{e}	128.41 ± 1.12^{b}	704.25 ± 1.15^{b}

IC_{50} of DPPH radical scavenging activity, total phenolic content, reducing power of the encapsulated small cardamom extracts are mean±SD of three independent experimental runs.
Different letters in a column indicate significant difference at $P<0.05$.

Table 4.1.4. Release kinetics of 1,8-cineole from E_{best}*.

Correlation coefficient (r)					Diffusion release exponent (n)	Release rate constant (k) min^{-1}	Type of transport
Zero Order	First Order						
		Higuchi	Peppas	Hixson Crowell			
0.69	0.79	0.86	0.89	0.76	0.59	24.96	anomalous

* Spray dried powder obtained at inlet air temperature 130 ºC and wall material composition of maltodextrin: gum arabic:: 70:30.

Figures:

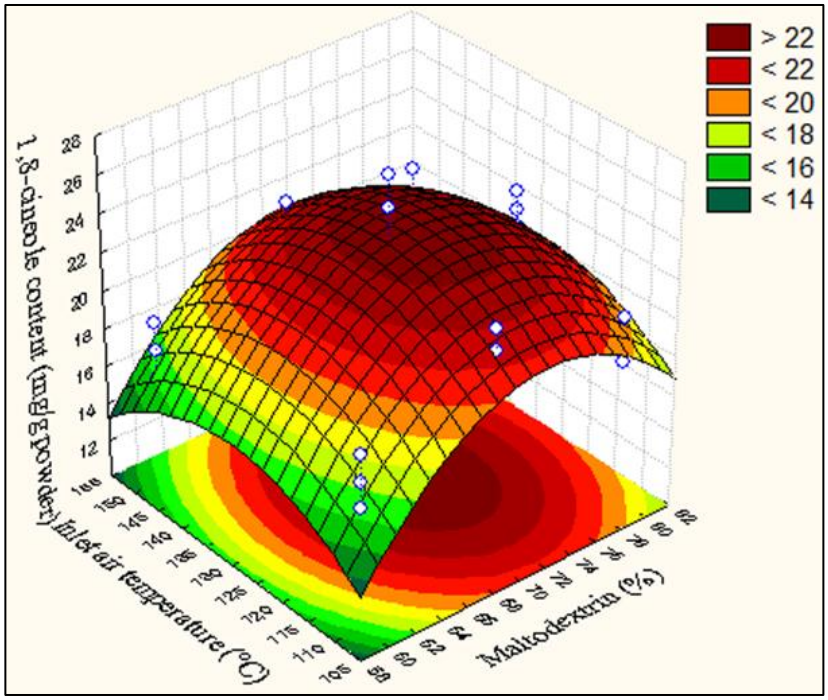

Fig. 4.1.1. Plot of response surface of effect of inlet air temperature and maltodextrin (%) on 1,8-cineole content of encapsulates.

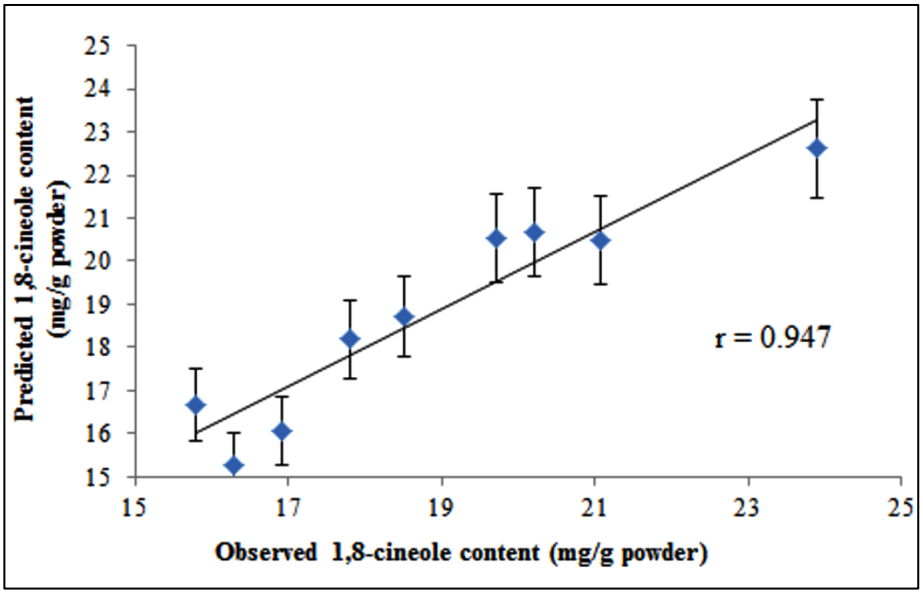

Fig. 4.1.2. Predicted and observed values of 1,8-cineole content of encapsulates.

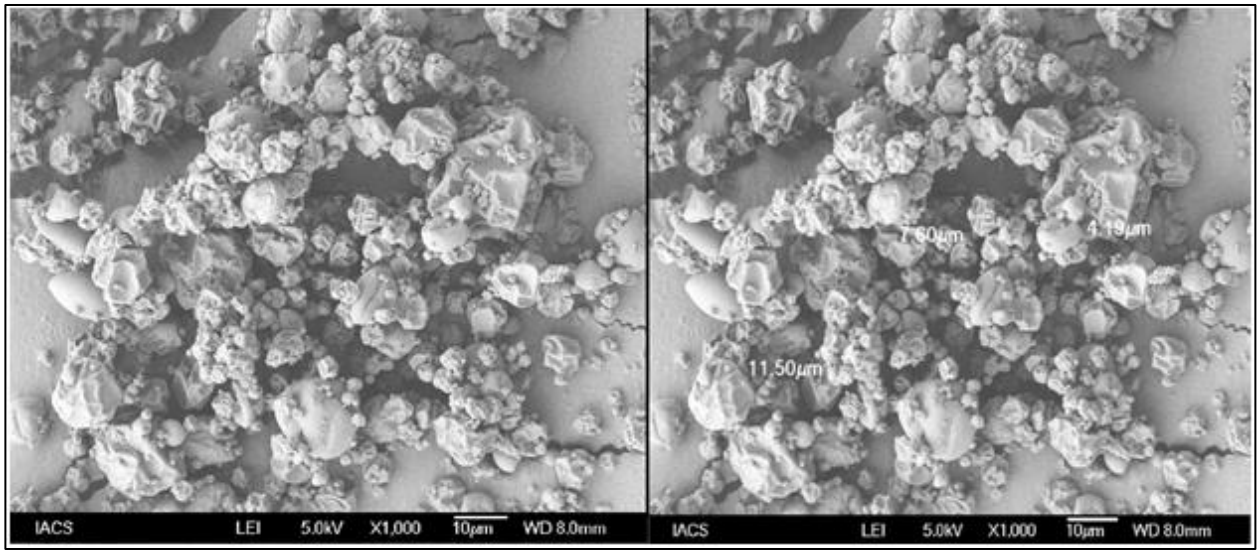

Fig. 4.1.3. Scanning electron micrograph of E_{best} at a magnification of 1000x.

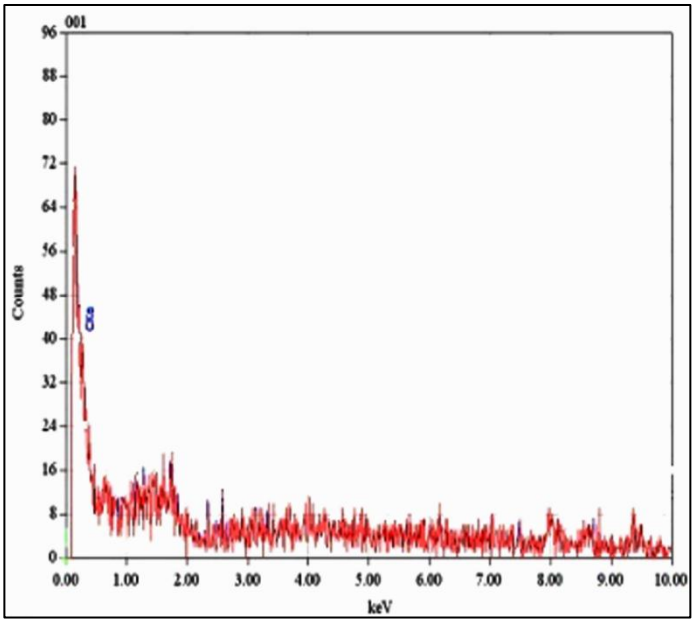

Fig. 4.1.4. EDX micrograph of E_{best}.

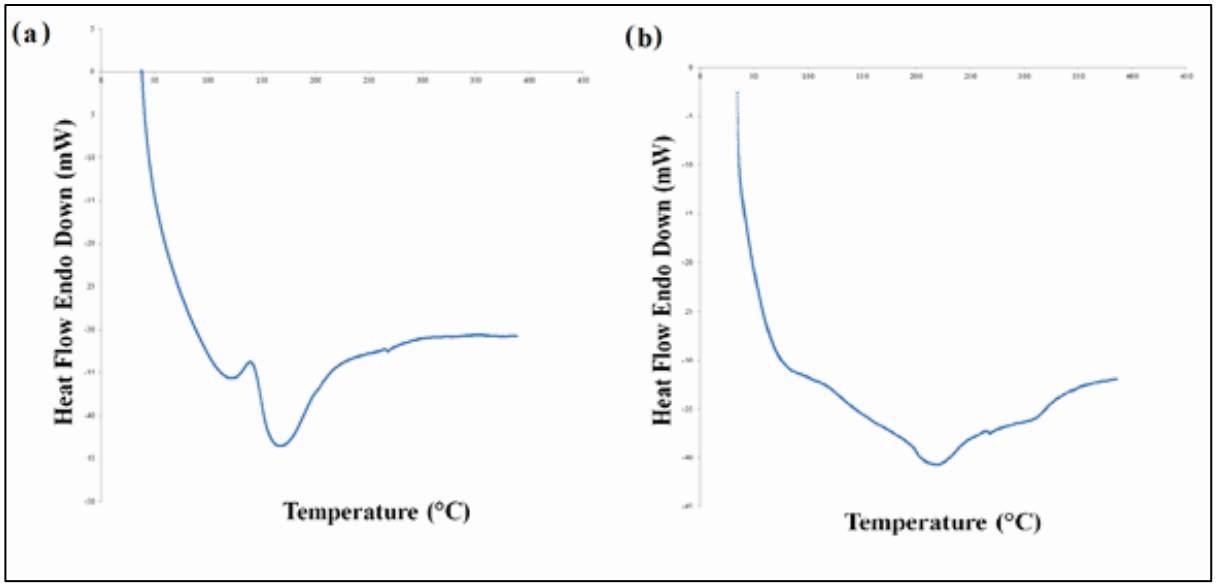

Fig. 4.1.5. Endothermic peaks in thermogravimetric/differential thermal analysis (TG/DTA) of (a) enzyme-assisted SC-CO_2 extract of small cardamom, (b) E_{best}.

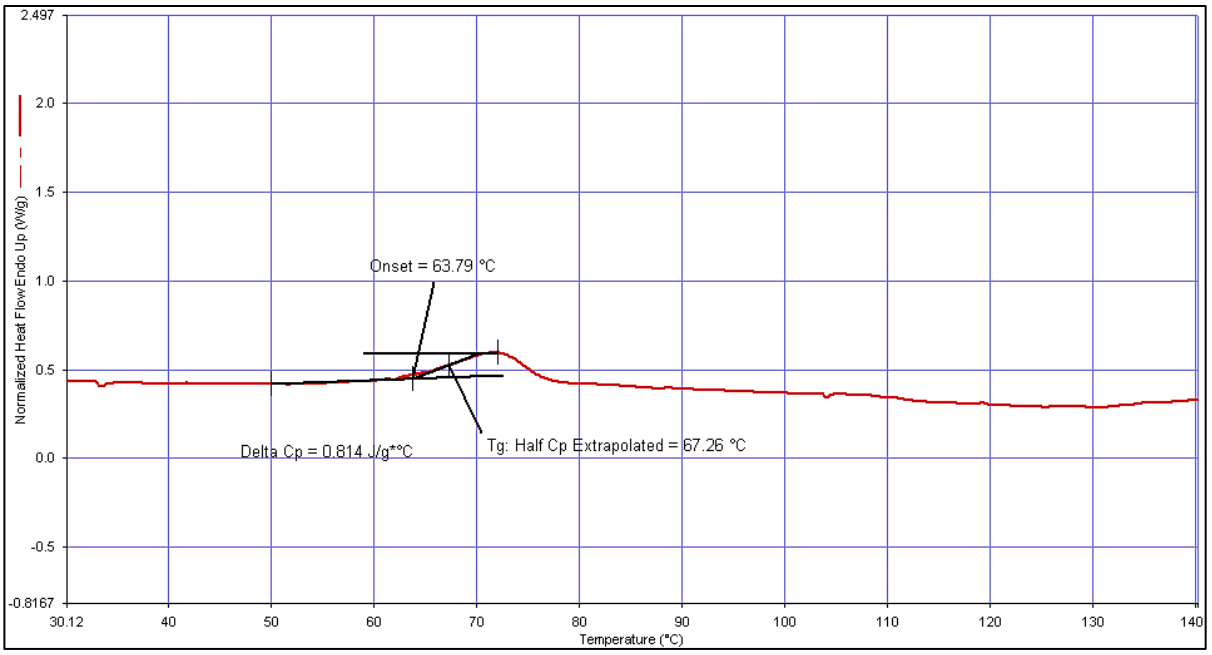

Fig. 4.1.6. Differential scanning calorimetry (DSC) thermogram of E_{best}.

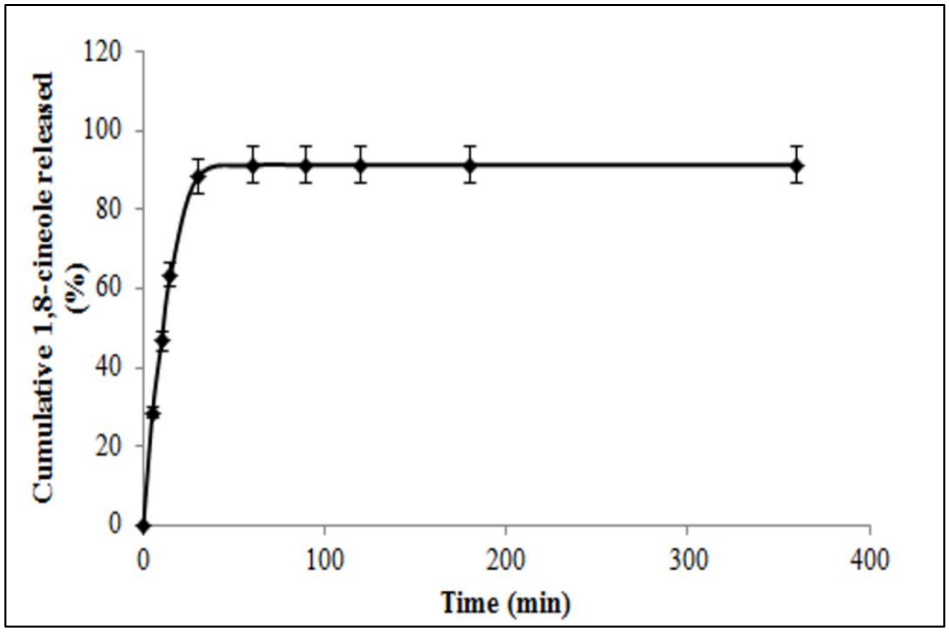

Fig. 4.1.7. Release of 1,8-cineole from E_{best}.

Section 4.2

Design of a nutraceutical custard using microencapsulated supercritical carbon dioxide extract of small cardamom

Introduction

The encapsulate (E_{best}) obtained from spray drying of 1,8-cineole-rich SC-CO_2 extract of small cardamom seeds (discussed in section 4.1 of Chapter 4), was employed in designing a new antioxidant-fortified custard. SC-CO_2 extract of Alleppey Green small cardamom seeds has been previously employed in the formulation of custard by Ghosh et al. (2015). However, when the custard was evaluated for its nutraceutical value, it did not possess the same phytochemical potency as that of the extract, indicating a possible loss of phytochemicals (31.15% loss of total phenolic content) during custard formulation. To redress the phytochemical loss during custard formulation, the present study formulated custard using the enzyme-assisted SC-CO_2 extract in microencapsulated (spray dried) form.

The objectives of the current investigation were therefore: (a) formulation of an antioxidant-fortified custard using the spray dried enzyme-assisted 1,8-cineole-rich SC-CO_2 extract of small cardamom for minimization of loss of the nutraceutical properties of the custard; and (b) characterization of the newly formulated custard for its sensory, physicochemical and phytochemical properties. To the best of our knowledge, there is no literature on the fortification of a dessert with encapsulated SC-CO_2 extract of small cardamom, for formulation of new designer nutraceutical product. The processes described here can safely be extended to design new nutraceutical or functional foods, whose manufacture inevitably involves a decrease in the phytochemical potency of their constituents.

Materials and Methods

Materials

Custard powder (Weikfield Products, Pune, India) was procured from a local supermarket in Jadavpur, Kolkata, India. All other chemicals and materials used were described in section 4.1 of Chapter 4.

Formulation of custard with E_{best}

Custard samples were prepared in accordance with the method developed in our laboratory by Chatterjee and Bhattacharjee (2013), with modifications. First, 3 g custard powder and 5 g ground sugar were added to 50 mL boiling milk with continuous stirring. E_{best} was then added and the mixture was cooked at 75±3 °C for 2 min. Different concentrations of E_{best} (4%, 4.5% and 5%, w/w of custard) were used for the formulation of different custard samples (C_4, $C_{4.5}$ and $C_{5,}$ respectively; see Fig. 4.2.1) with the aim of obtaining nutraceutical fortified custard samples. Custard sample prepared without the encapsulate served as control ($C_{control}$). The samples were cooled to room temperature (23±2 °C) after cooking. All custard samples were stored at 4±1 °C in autoclaved screw capped glass jars (50 mL) before analysis.

Microbiological analysis of custard samples

The total plate count (TPC) of custard samples was determined for both bacteria and fungi using the pour plate method, immediately after preparation. Samples (1 mL) of diluted custard were poured on to nutrient agar and potato dextrose agar plates for estimation of TPCs for bacterial and fungal growth, respectively. The plates were incubated at 37±1 °C for 24 h for bacteria and at 25±1 ºC for 72 h for fungi. After incubation, TPCs for bacteria and fungi were determined as CFU/g custard.

Sensory evaluation of custard samples

Sensory evaluation of the custard samples was conducted by a semi-trained panel of university faculty members and research scholars (10 men and 10 women) aged 20-45 years. The panellists were selected based on their interest and performances in screening tests conducted with a control sample and were familiar with the sensory attributes of custard. Samples were served in glass bowls with stainless steel spoons. All the samples were blind coded using three-digit numbers and served randomly to the panellists. The panellists used the standard 9-point hedonic scale to evaluate the custard samples (9 indicating 'like extremely' and 1 indicating 'dislike extremely') on the attributes of overall appearance, colour, odour, texture, taste and aftertaste. The sensory evaluation was conducted between 10 am and 12 noon in a well-ventilated room under white light (Ranganna, 1986). A rest period of 5 min between consecutive samples was allowed to minimize sensory fatigue. Unsalted crackers and water were provided to panellists to rinse their palate before each evaluation (Choonhahirun and Akesowan, 2012). The individual samples were served in triplicate in each session and rounded off mean scores were represented graphically by radar plots (Ghosh and Bhattacharjee, 2014). $C_{4.5}$ achieved the highest sensory score, therefore, the physicochemical and phytochemical properties of $C_{4.5}$ and $C_{control}$ were determined.

Estimation of the physicochemical properties of custard samples

pH of custard samples

The pH of custard samples was estimated according to the method reported by Chatterjee and Bhattacharjee (2015). 5 g custard sample was homogenized with 25 mL deionized water and pH was measured using a PC 510 pH meter (Eutech Instruments, Singapore).

Analysis of colour

The colour of custard samples was measured using a Hunter Lab colorimeter (Konica Minolta, Tokyo, Japan) at a 10° inclination from the light source and reported as L*, a* and b* values. The colour co-ordinates of the custard samples were calibrated against a standard white plate. Chroma values and hue angles were calculated using standard equations (Chatterjee and Bhattacharjee, 2015).

Rheology study

The rheological behaviour of custard samples was assessed using a Modular Compact Rheometer (MCR) 102 (Anton-Parr, Graz, Austria) with a cone and plate (CP-40) type arrangement (having clearance of 0.08 mm between the two components) at 23±2 ºC. The flow behaviour of the samples was measured in controlled shear rate mode. The shear rate was varied from 0.0001 to 100/s. The small-deformation of storage modulus (G′) and loss modulus (G″) were recorded. Amplitude sweeps with varying amplitude from 0.01% to 100% were conducted to study the changes in G′ and G″ at a constant angular frequency of 10 rad/s. Frequency sweeps were also conducted with angular frequencies ranging from 0.1 to 100 rad/s at a constant amplitude of 0.5%. G′ and G″ were measured separately as functions of amplitude and frequency.

Chemical analyses of nutraceutical properties of custard samples

For estimation of the 1,8-cineole content and nutraceutical properties of the custard samples, such as antioxidant activity, total phenolic content and reducing power, 1 g of custard sample was dissolved in 10 mL ethanol. The 1,8-cineole contents of the samples were estimated using HPTLC according to the method described in section 3.1 of Chapter 3. The loss of 1,8-cineole in the $C_{4.5}$ sample during preparation of the custard was estimated by comparing the 1,8-cineole

content of $C_{4.5}$ with that of the encapsulate (E_{best}). The antioxidant activities, total phenolic contents and reducing power of the custard samples were determined in accordance with the methods described in section 3.1 of Chapter 3.

Results and Discussion

Microbiological analysis of custard samples

The TPCs of $C_{control}$ were found to be 18 CFU/g custard for bacteria and 4 CFU/g custard for fungi, while the TPCs of $C_{4.5}$ were 8 CFU/g custard for bacteria and 2 CFU/g custard for fungi, both values of $C_{4.5}$ were lower than those of the control set. According to the guidelines of the Food Safety and Standards Authority of India (2011), the highest permissible aerobic plate count in custard is 1×10^3 CFU/g sample. Therefore, the $C_{4.5}$ custard sample is microbiologically safe for human consumption. This is in agreement with the fact that small cardamom extract reportedly contains antimicrobial properties (discussed in section 3.1 of Chapter 3), which could have possibly contributed to the reduction in microbial load in the $C_{4.5}$ custard sample.

Sensory evaluation of custard samples prepared with E_{best}

The panellists awarded equal scores for overall appearance to $C_{control}$, C_4, $C_{4.5}$ and C_5 (Fig. 4.2.2). The characteristic yellow colour of the custard samples was sensorially approved by all panellists. The panellists moderately liked the characteristic odour of $C_{control}$. The pleasant and sweet aroma of small cardamom was strongest in C_5, which was therefore most preferred by the panel, followed by $C_{4.5}$ and C_4. $C_{4.5}$ received highest scores for its smooth texture, followed by C_5, C_4 and $C_{control}$. Panellists liked the taste of $C_{control}$ moderately, while among the custards fortified with cardamom encapsulate, $C_{4.5}$ was liked most because of its sweet taste, followed by C_4. The taste of C_5 was slightly bitter and disliked by the panel. The distinct sweet aftertaste of

small cardamom was perceived in $C_{4.5}$ which made it more appealing than C_4 and $C_{control}$. The aftertaste of C_5 was slightly pungent and was disliked by the panellists. Overall, $C_{4.5}$ was judged the best by the panellists. Therefore, further physicochemical and phytochemical analyses were conducted for $C_{4.5}$ along with $C_{control}$.

Estimation of physicochemical properties of custard samples

pH of custard samples

$C_{control}$ (7.00) and $C_{4.5}$ (7.02) had identical pH. Thus, addition of cardamom encapsulate did not affect the pH of newly formulated custard.

Analysis of colour

The colour of the custard samples was represented by L*, a*, b*, chroma and hue angles (Table 4.2.1). $C_{control}$ and $C_{4.5}$ had a light (high L* values) yellowish (high b* values) colour. The chroma values of the samples indicated that both samples had equally bright intensities. The hue angles (84.09±0.02° and 84.13±0.01°) indicated the light-yellowish colour of the samples, in agreement with that reported for mayonnaise prepared with eugenol-lean SC-CO_2 extract of clove buds (Chatterjee and Bhattacharjee, 2015). The $C_{4.5}$ and $C_{control}$ samples had yellow colour (Table 4.2.1), confirming that the addition of the encapsulate did not have an adverse effect on the appearance of the custard samples.

Rheology study

The flow curves of $C_{control}$ and $C_{4.5}$ indicated pseudo-plastic or shear-thinning flow behaviour for both samples (Fig. 4.2.3a,b), in agreement with the results obtained by Keršienė et al. (2008), who examined the effect of milk fat and tapioca starch on the rheological properties of dairy custards and on the release of strawberry flavour compounds therein. The G′ and G″ values

denote the viscoelastic behaviour of the samples against applied stress. Analysis of rheograms for the amplitude sweep of the samples showed that for both samples, the values of G′ were well above those of G″, indicating strong thickening and solidifying behaviour (Fig. 4.2.3c,d) in both. In the $C_{control}$ sample, G′ and G″ crossed over at 39.8% strain, and at 63.1% strain in the $C_{4.5}$ sample. Therefore, the viscoelastic region of the $C_{4.5}$ sample was higher than that of the $C_{control}$ sample, indicating the broad viscoelastic nature of $C_{4.5}$. This finding was in agreement with the sensory scores where smooth and consistent texture of $C_{4.5}$ was most preferred by the panellists.

In frequency sweeps (Fig. 4.2.3e,f), no crossover of G′ and G″ values was observed in either sample, attesting to the stability of the viscoelastic nature of custard in the frequency range investigated. For $C_{4.5}$, G′ and G″ values showed insignificant changes with frequency, and G′ was greater than G″ throughout the frequency range studied for custard (0.1 to 100 rad/s). These observations indicate a desirable strong cohesive association within the custard and its consequent firmness.

Estimation of the nutraceutical properties of custard samples

Application of a 1,8-cineole-rich encapsulate to custard significantly enhanced its nutraceutical properties (Table 4.2.2). Ghosh et al. (2015) observed a 31.15% loss of total phenolic content in custard (since 27.9 µg gallic acid content of extract enhanced the phenolic content of 1 g custard by 19.21 µg gallic acid). However, in our formulation, the application of encapsulated extract minimized the loss of total phenolic content and 1,8-cineole content to 1.59% (since 6.28 µg gallic acid content of encapsulate enhanced the phenolic content of 1 g custard by 6.18 µg gallic acid) and 1.23% (1.134 mg 1,8-cineole content of powder contributed to 1.120 mg 1,8-cineole content of 1 g custard), respectively.

These findings indicate higher nutraceutical potency of custard prepared with encapsulated extract than of that prepared with the extract *per se*, establishing the protective role of microencapsulation in preventing the degradation of phytochemicals (in SC-CO_2 extract of small cardamom) utilized in custard formulation. In addition, the encapsulate did not adversely affect the physiochemical properties and sensory attributes of the newly formulated custard. Therefore, custard fortified with spray dried extract of small cardamom is a new designer nutraceutical (functional) dessert.

Conclusions

Spray dried powder from α-amylase-assisted SC-CO_2 extract of small cardamom was added to custard at 4%, 4.5% and 5% (w/w) levels to enhance its nutraceutical properties. Custard formulated with 4.5% encapsulate was most liked sensorially. This custard sample also exhibited better rheological stability, higher phytochemical potency and lower microbial load than its control. The $C_{4.5}$ sample is therefore a nutraceutical-rich dessert. Similar applications of spray dried enzyme-assisted SC-CO_2 extract of small cardamom could be envisaged for other desserts and spreads.

Novelty

The novelty of the work is that, it has reported for the first time on fortification of custard with encapsulated SC-CO_2 extract of small cardamom. The new designer nutraceutical dessert was successfully formulated with reduced loss of phytochemicals during formulation.

References

Chatterjee D., and Bhattacharjee P. (2013). Comparative evaluation of the antioxidant efficacy of encapsulated and un-encapsulated eugenol-rich clove extracts in soybean oil: Shelf-life and frying stability of soybean oil. *Journal of Food Engineering*, **117**, 545-550.

Chatterjee D., and Bhattacharjee P. (2015). Use of eugenol-lean clove extract as a flavoring agent and natural antioxidant in mayonnaise: product characterization and storage study. *Journal of Food Science and Technology*, **52**, 4945-4954.

Choonhahirun A., and Akesowan A. (2012). Partial fat and sugar replacement with soy milk, inulin and sucralose on quality of Thai Pandanus custard. *African Journal of Biotechnology*, **11**, 4611-4619.

Food Safety and Standards Authority of India (2011). *Food Safety and Standards (Food Products Standards and Food Additives) Regulations*. Accessed from: http://www.fssai.gov.in/Portals/0/Pdf/Food%20safety%20and%20standards%20(Food%20produpr%20standards%20and%20Food%20Additives)%20regulation,%202011.pdf, on 9 February 2016.

Ghosh S., and Bhattacharjee P. (2014). Supercritical carbon dioxide ex tract of *Ocimum sanctum* improves nutraceutical properties of ice cream. *Nutrafoods*, **13**, 69-78.

Ghosh S., Bhattacharjee P., and Das S. (2015). 1,8-cineol-rich cardamom seed (*Elettaria cardamomum*) extracts using green technologies and conventional extractions: Process analysis, phytochemical characterization, and food application. *Separation Science and Technology*, **50**, 1974-1985.

Keršienë M., Adams A., Dubra A., Kimpe N. D., and Leskauskaite D. (2008). Interactions between flavour release and rheological properties in model custard desserts: effect of starch concentration and milk fat. *Food Chemistry*, **108**, 1183-1191.

Ranganna S (1986). Sensory evaluation. In: *Handbook of Analysis and Quality Control for Fruit and Vegetable Products*, 2nd edn. Tata McGraw Hill, New Delhi, India, pp. 594-645.

Tables:

Table 4.2.1. Analysis of colour of $C_{control}$ and $C_{4.5}$ samples.

Sample	L*	a*	b*	Chroma	Hue angle (°)
$C_{control}$	81.86±0.11	4.53±0.01	43.74±0.13	43.98±0.19	84.09±0.02
$C_{4.5}$	81.82±0.13	4.47±0.03	43.49±0.19	43.72±0.17	84.13±0.01

Chroma= $(a^{*2} + b^{*2})^{1/2}$
Hue angle= $\tan^{-1}(b^*/ a^*)$
L*, a*, b*, chroma and hue angle of custard samples are mean±SD of three independent samples.

Table 4.2.2. 1,8-cineole contents and nutraceutical properties of custards.

Sample	1,8-cineole content of custards (mg/g custard)	IC_{50} of DPPH radical scavenging activity (mg/mL)	Reducing power (µg BHT/g custard)	Total phenolic content (µg GAE/g custard)
$C_{control}$	NA	$5.37±0.05^b$	$9.01±0.03^a$	$2.01±0.01^a$
$C_{4.5}$	1.12±0.05	$2.04±0.02^a$	$41.28±0.07^b$	$8.19±0.04^b$

NA: Not applicable
1,8-cineole content, IC_{50} of DPPH radical scavenging activity, reducing power and total phenolic content are mean±SD of three independent custard samples.
Different letters in a column indicate significant difference at $P \leq 0.05$.

Figures:

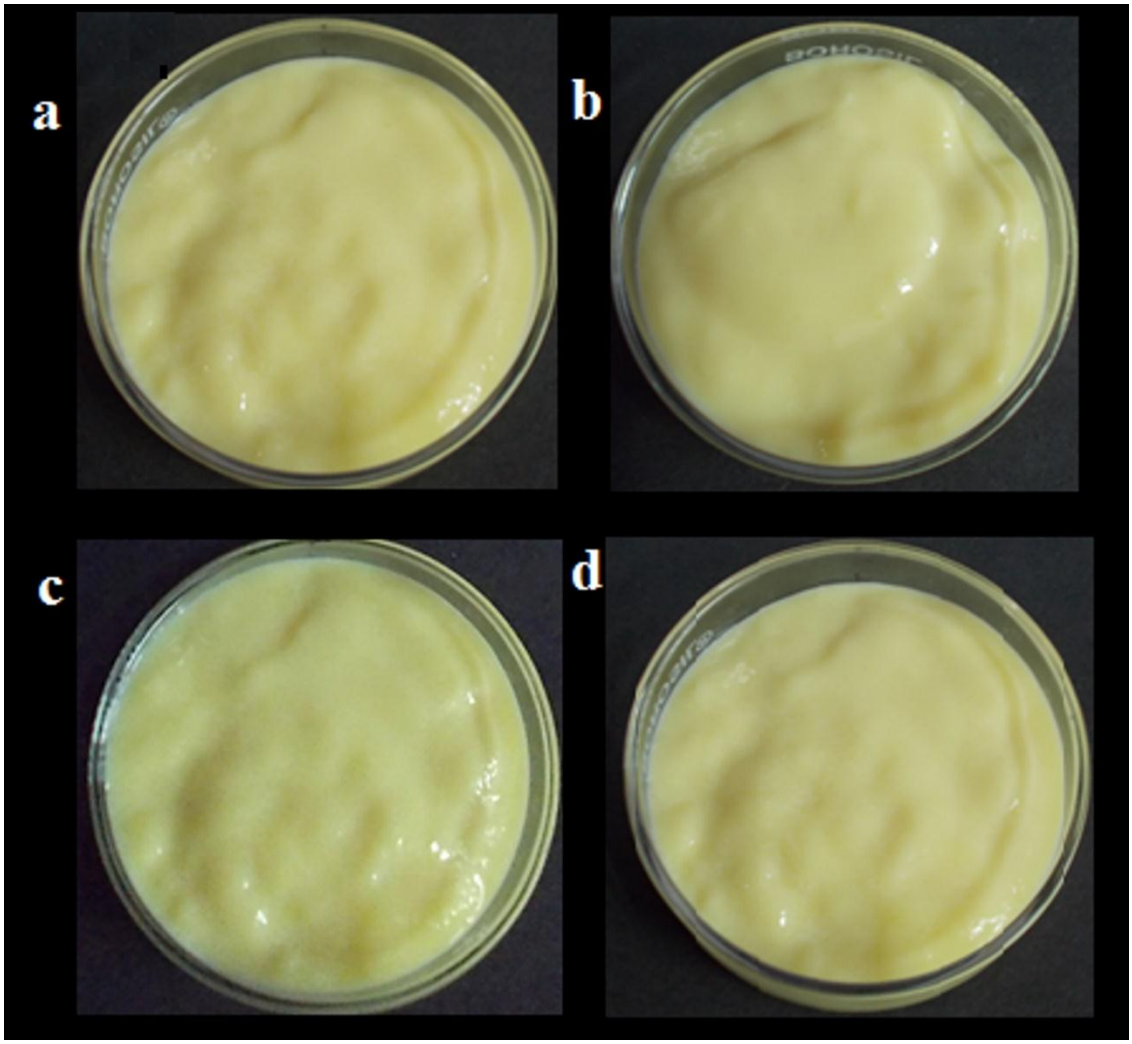

Fig. 4.2.1. Custard samples. (a) $C_{control}$. (b) C_4. (c) $C_{4.5}$. (d) C_5.

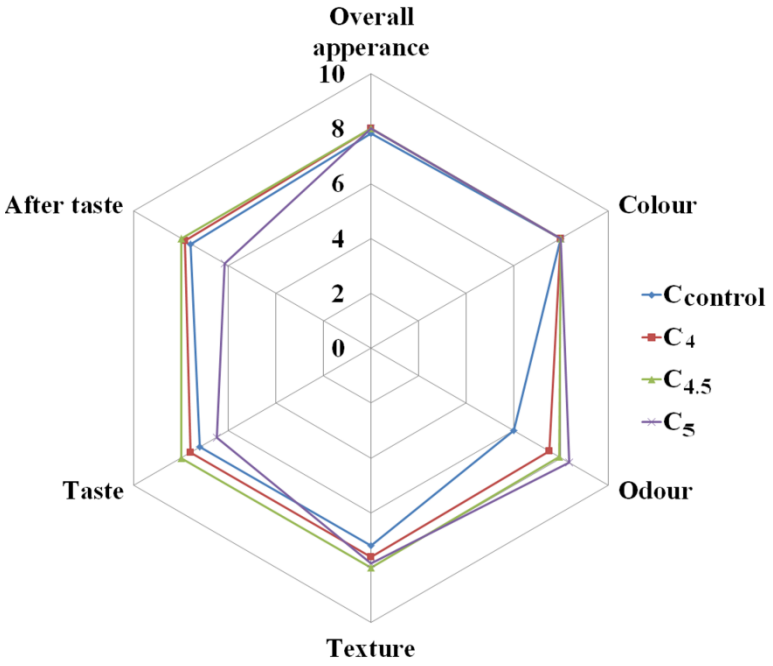

Fig. 4.2.2. Radar plot of hedonic scores of different custard samples.

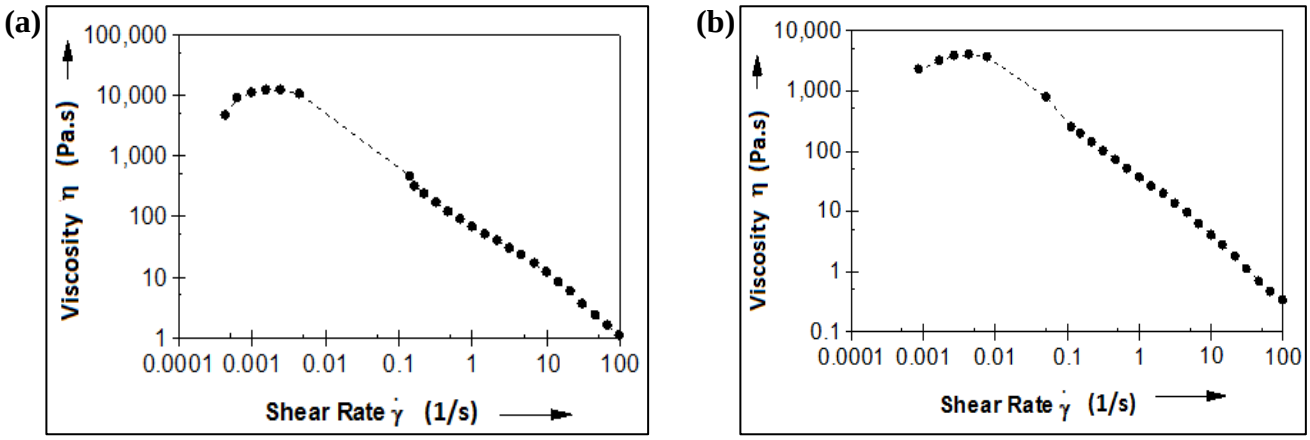

Fig. 4.2.3. Analyses of rheology of custard samples. (a) Flow behaviour of $C_{control}$ and (b) Flow behaviour of $C_{4.5}$.

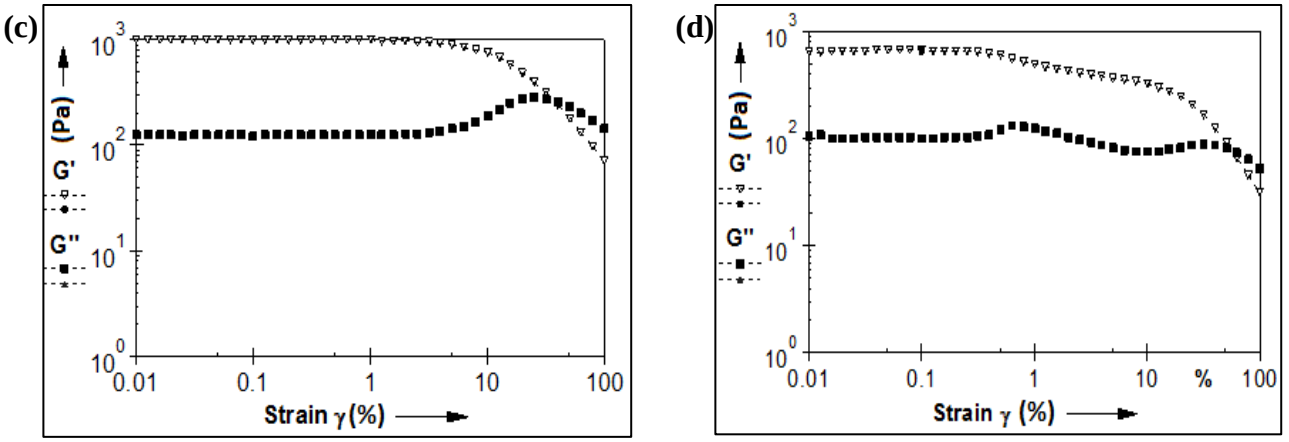

Fig. 4.2.3. Analyses of rheology of custard samples. (c) Amplitude sweeps of $C_{control}$ and (d) Amplitude sweeps of $C_{4.5}$.

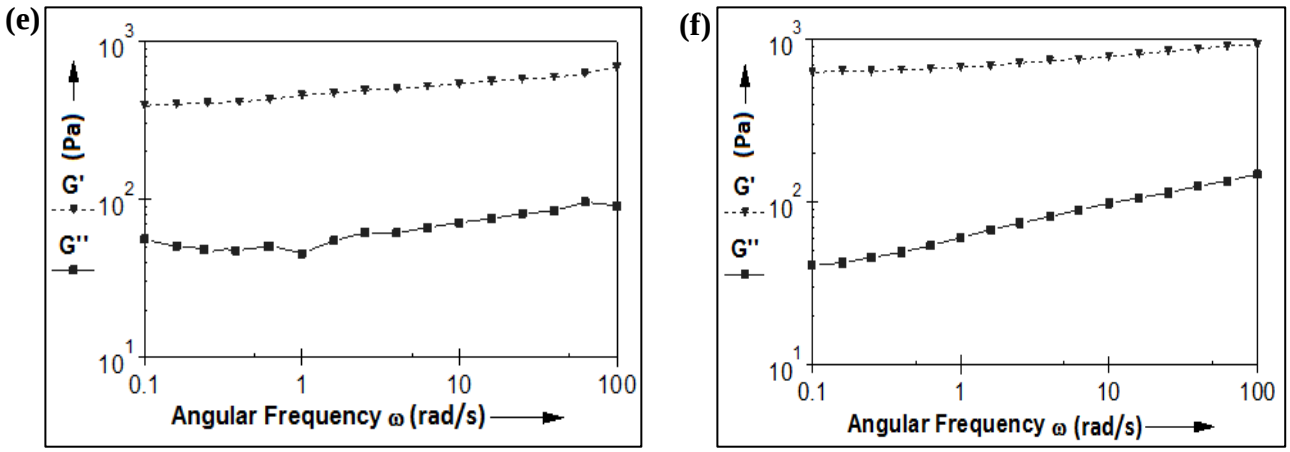

Fig. 4.2.3. Analyses of rheology of custard samples. (e) Frequency sweeps of $C_{control}$ and (f) Frequency sweeps of $C_{4.5}$.

Section 4.3

Nanoliposomal encapsulation of piperine-rich black pepper extract

Introduction

Piperine, possessing high therapeutic activity, is highly photosensitive in solution (Ravindran and Kallupurackal, 2001). Kotte et al. (2014) have reported extensive degradation of standard piperine (97% pure, Sigma, India) under acid-base hydrolyses and photolytic stress conditions. Therefore, there is a necessity to protect the piperine-rich extract (described in section 2.2 of Chapter 2) from light, heat, oxygen and other environmental hazards for long term storage-stability.

Section 4.1 of Chapter 4 describes microencapsulation of 1,8-cineole-rich SC-CO_2 extract of small cardamom, successfully conducted by spray drying. However, high pungency (80,000 Scoville heat unit) of black pepper extract could possibly impede usage of its spray dried powder form in food and in therapeutic applications. This prompted exploration of formulation of nanoliposomes using the piperine-rich SC-CO_2 extract to ensure sustained release of the bioactive component and concomitantly minimizing its degradation during storage. Use of nanoliposomal vehicles of *spiceceuticals* in food engineering is scarce. To the best of my knowledge, there is no literature reported on the formulation of piperine-rich nanoliposome employing SC-CO_2 extract of black pepper.

The specific objectives of this work were: optimization of encapsulation parameters for formulation of stable nanoliposomes using enzyme-assisted SC-CO_2 extract of black pepper and standard piperine as core material; physicochemical characterization of both nanoliposomes; and *in vitro* release study of piperine and storage studies for either nanoliposome.

Materials and Methods

Materials

Soya phosphatidylcholine was procured from Sigma, India; Tween 80 and Triton X-100 were procured from E-Merck, Mumbai, India; Dialysis membrane (cellulose membrane, molecular weight cut off 12000 Da) was procured from Himedia, India. All chemicals used in this work were of AR grade.

Formulation of nanoliposomes

Nanoliposome encapsulate of black pepper was designed by probe sonication method. Soya phosphatidylcholine (S) and Tween 80 (T) in different ratios (1:0.6, 1:0.9 and 1:1.2, w/w basis) were dissolved in 2 mL ethanol in screw-capped amber-colored glass vials to develop the lipid phase. Thereafter, black pepper extract (obtained by enzyme-assisted SC-CO_2 extraction, as discussed in section 2.2 of Chapter 2) was dissolved in the lipid phase. Optimization of lipid phase (S: T ratio) was conducted keeping the concentration of black pepper extract constant at 1% (w/w). Ethanol was evaporated from the solution by purging a gentle stream of nitrogen, to form a thin film of the lipid phase at the bottom surface of the vial. The dried lipid film was then rehydrated with 4 mL phosphate buffer saline (PBS, 0.01 M, pH 7.2) and vortexed for 10 min to obtain a liposomal suspension. This suspension of liposomes were then subjected to probe sonication (diameter of probe: 3 mm; LabSonic M, Sartorius Stedium India Pvt. Ltd., Bangalore, India) at 30 kHz for 5 min (with intervals of 2 min) for 6 to 7 times, at 15-20±1 °C, in accordance with the method reported by Memoli et al. (1995) to reduce the size and lamellarity and to finely disperse the liposomes. Concentration of black pepper extract for stable

nanoliposomes was investigated at optimized S: T ratio with different concentrations of black pepper extract at 1%, 2%, 4% and 8%, w/w basis.

After ultrasonication, the nanoliposome suspension was subjected to dialysis using phosphate buffer (pH 7.0, 0.05 M) at 4±1 °C, for 24 h, to separate the non-encapsulated black pepper extract from nanoliposome. The dialysis bag (cellulose tube) containing 1 mL of liposome suspension was placed in 100 mL buffer solution at 4±1 °C with continuous gentle stirring. The solution buffer was replaced by fresh buffer at predetermined time intervals (2, 4 and 6 h). After 24 h, the nanoliposome was recovered from the dialysis bag and stored in amber colored screw capped vials in an inert atmosphere of nitrogen at 4 °C in the dark, until further analyses.

The S: T ratio and concentration of black pepper extract at which clear and stable nanoliposome was obtained, was considered as the optimized formulation. Nanoliposomes were subsequently formulated with the same formulation, using both the extract and the standard piperine for comparative evaluation of the same.

Optimization of encapsulation parameters

Optimization of encapsulation parameters, i.e. composition of lipid bilayer (S: T) and concentration of black pepper extract in the liposomal suspension was conducted primarily based on the stability of the nanoliposome (judged by visual observation). The stable liposomes were further analyzed for % encapsulation efficiency (%EE) and the liposome with highest %EE was considered as the 'best' nanoliposome (BN) in our study. Nanoliposome designed with piperine (PN) and BN were both subjected to further analysis.

Estimation of %EE of nanoliposome of black pepper

Estimation of %EE of nanoliposomes was conducted by quantification of piperine encapsulated in the nanoliposomes. Nanoliposomes recovered from dialysis bags were treated with Triton X-100 (10% v/v, 1:1:: Triton X-100:nanoliposome) to rupture the lipid bilayer of nanoliposomes. Liposome solution containing Triton X-100 was analyzed by HPTLC to estimate the piperine content of the nanoliposomes, in accordance with the method discussed in section 2.1 of Chapter 2. %EE of nanoliposome was calculated in accordance with Pezeshky et al. (2016).

$$\%\text{EE} = \frac{\text{piperine encapsulated in nanoliposomes}}{\text{initial piperine supplied for encapsulation}} \times 100 \quad (1)$$

Fourier transform infrared (FT-IR) spectroscopy analyses of nanoliposomes

FT-IR spectroscopy of liposomes was conducted to investigate the interactions of piperine with the liposomal matrix after incorporation into the nanoliposomes. Soya phosphatidylcholine, black pepper extract, standard piperine, PN and BN were placed on KBr pellets and subjected to Spectrum 100 FTIR spectrometer (PerkinElmer, US) with light source of silicon carbide (SiC) and frequency range of 1000-4000 cm^{-1}.

Characterization of nanoliposomes

Morphology of nanoliposomes by field emission scanning electron microscopy (FE-SEM)

BN was analyzed by FE-SEM to observe the morphology of nanoliposomes. 10 µL of BN was placed on a glass cover slip and dried under vacuum (6-7 Pa). Then the cover slip containing nanoliposome was coated with platinum using an Autofine Coater (JFC-1600, JEOL Company Ltd., Japan) and analyzed by FE-SEM (JSM-6700F, JEOL Company Ltd., Japan), at 5 kV at working distance of 8 mm.

Morphology of nanoliposomes by transmission electron microscopy (TEM)

For further examination of surface morphology, both BN and PN samples were analyzed by TEM. TEM analyses were conducted with 100 X diluted samples in distilled water. 5 µL of the solution was placed on a carbon coated copper grid (300 mesh, Electron Microscopy Sciences, US), dried overnight and analyzed by TEM (JEM 2100, JEOL Company Ltd., Japan), operated at 200 kV at room temperature (23±2 °C).

Size distribution and zeta potential of nanoliposomes

Nanoliposomes were diluted 10 times with double distilled water. The sizes of diluted nanoliposomes were analyzed by dynamic light scattering (DLS) method, at a scattering angle of 90°, using Zetasizer Nano ZS90 (Malvern Instruments Pvt. Ltd., UK) at room temperature (23±2 °C). To determine the surface charge of liposomes, these diluted samples were analyzed by laser Doppler micro-electrophoresis in Zetasizer Nano ZS90 and zeta potentials were recorded.

Phytochemical properties of nanoliposomes

Nanoliposomes treated with Triton X-100 were analyzed for their antioxidant potencies and total phenolic contents according to the methods described in section 2.2 of Chapter 2. Free-radical scavenging capacities of BN and PN were further validated by EPR spectroscopy using DPPH as the source of free-radicals. 100 µL of each liposome (treated with Triton X-100) was mixed with 100 µL of DPPH solution (2 mM) and after shaking vigorously for 10 s, it was transferred to the EPR quartz tube (i.d = 4.0 mm). The EPR spectroscopy was conducted in accordance with the method discussed in section 2.2 of Chapter 2.

Study of *in vitro* release kinetics of piperine from nanoliposomes

The *in vitro* release of piperine from BN and PN nanoliposomes was studied using the dialysis tube diffusion technique in accordance with the method reported by Ammoury et al. (1990), with few modifications. 1 mL aliquot of each nanoliposome was loaded into the dialysis bag, hermetically sealed, placed in a 50 mL of receptor buffer (PBS, 0.01 M, pH 6.4) and was continuously stirred in a magnetic stirrer at 50 rpm at 37±2 °C. 500 µL aliquot of receptor buffer was collected at different time intervals for 24 h (at 5, 15, 60, 90, 120, 180, 240, 360, 480 and 1440 min) and was replaced with an equal volume of fresh buffer each time. Amount of piperine in each aliquot was estimated by HPTLC analysis as discussed earlier in section 2.1 of Chapter 2.

The release data was fitted into several kinetic equations, namely, zero order, first order, sub-types of first order such as Higuchi model, Hixson-Crowell's cube root model and Peppas equations in accordance with Chatterjee et al. (2014), to ascertain the release kinetics of piperine from BN and PN. The kinetic model with highest correlation coefficient (r) was considered to best represent the release of piperine from the nanoliposomes.

Storage stability of nanoliposomes

The storage stability of nanoliposomes was investigated to assess the ability of liposome to protect piperine from degradation during storage. Standard piperine and black pepper extract, both in non-encapsulated and encapsulated forms were stored at 4±1 °C for 3 months in the dark. Amount of piperine retained in the solutions was determined by HPTLC method at an interval of 10 days. Stability of piperine in the solutions was determined according to the method reported by Liu and Park (2009):

$$\text{Stability of piperine (\%)} = \frac{\text{amount of piperine remained at different storage time}}{\text{amount of piperine before storage}} \times 100 \qquad (3)$$

$T_{1/2}$ values of piperine were also calculated at 4±1 °C (refrigerator) and at 70±2 ºC, 75% RH (incubator with humidity control) in the SC-CO_2 extract, solution of standard piperine (0.5 mg/mL) and in PN and BN nanoliposomes, according to the method discussed in section 4.1 of Chapter 4.

Statistical analysis

All experiments were conducted in triplicate and the data are expressed as mean±SD of three independent experimental runs. Statistical analysis was performed with STATISTICA 8.0 software (Statsoft, OK, USA). Duncan's multiple range tests with P-value < 0.05 was performed with IBM SPSS Statistics software version 20 (IBM, USA) to verify the significance of all tests.

Results and Discussion

Methods for formulation of nanoliposomes (preliminary trials)

In general, five types of liposomes have been reported: multilamellar vesicles (MLV, size ranges from 500 to 10,000 nm), oligolamellar vesicle (OLV, size ranges from 100 to 500 nm), giant unilamellar vesicles (GUV, size larger than 1000 nm), large unilamellar vesicles (LUV, size larger than 100 nm) and small unilamellar vesicles (SUV, size ranges from 20 to 100 nm) (Laouini et al., 2012). Sonication is the most extensively used method for design of SUV nanoliposomes (Akbarzadeh et al., 2013). Therefore, in the present investigation, SUV nanoliposomes of black pepper extract have been designed by sonication.

Both bath sonication and probe sonication methods have been used in the preliminary trials. The results revealed that, liposomes designed by bath sonication were larger in size, heterogeneous and unstable, than the liposomes formulated by probe sonication. Therefore, in the successive

experiments, probe sonication was employed for formulation of nanoliposomes of black pepper extract.

Optimization of parameters for formulation of nanoliposome

The conditions at which stable and dispersed liposomes were obtained were S: T:: 1:0.9 and S: T:: 1:1.2 (Fig. 4.3.1). These two conditions were used formulation of liposome with 2% (w/w) black pepper extract. Nanoliposome of black pepper formulated using 2% black pepper extract exhibited better stability than 4% and 8% in formation of liposome (Figs. 4.3.2 a-c). Therefore, among these three samples, nanoliposome containing 2% extract along with that of 1% extract, were selected for further analyses. It was also observed that increase in black pepper extract decreased the stability of liposome formation in S: T:: 1:0.9, whereas there was no significant change observed in the liposome designed with S: T:: 1:1.2, i.e. after 24 h storage at 4 °C, there was no precipitate observed at the bottom of the vials of liposomes formulated with S: T:: 1:1.2 containing 1% and 2% extract. Therefore, for optimization of concentration of black pepper extract in nanoliposome, S: T:: 1:1.2 was selected. Subsequently, nanoliposomes with 2% extract along with that of 1% extract were subjected to dialysis prior to estimation of %EE.

%EE of black pepper liposome with 1% extract was found to be 76.1 and that of the 2% extract was 78.6 (P=0.0000). Phytochemical properties (antioxidant activity and total phenolic content) of these two nanoliposomes revealed that liposome with 2% extract had significantly higher (P=0.0375 and 0.0000, respectively) potencies than the liposome with 1% extract (Fig. 4.3.3). Therefore, for nanoliposome of black pepper S: T:: 1:1.2 and 2% black pepper extract were optimized and was considered as sample BN. Piperine content equivalent to 2% black pepper extract was 945 µg; hence, this quantity of standard piperine was used to formulate PN nanoliposome. Both the BN and PN visually were clear, light yellowish suspensions and stable

(no precipitation of compounds observed after 30 days storage). %EE of PN was found to be 81.2. Phytochemical properties of PN are presented in Fig. 4.3.3. In EPR analysis, both BN and PN (amount of liposomes analyzed were 86 µg for both the samples) reduced the intensity of the DPPH signal (Fig. 4.3.4). BN scavenged the DPPH free radicals by 16.92% which was significantly (P=0.0001) higher than that by PN (15.68%).

FT-IR spectroscopy analyses of nanoliposomes

The FT-IR spectra of soya phosphatidylcholine, standard piperine, black pepper extract, PN and BN have been presented in Figs. 4.3.5(a-e) and analyzed in accordance with Dyer (2012) (Table 4.3.1). The absorption bands of piperine were prominent in the spectrum of black pepper extract (Fig. 4.3.5c). Absorption bands of PN were similar to those of soya phosphatidylcholine and standard piperine (Fig. 4.3.5a and b, respectively) except for the bands with wavelength range 3000-3500 cm^{-1}, which were masked by the broad band of H_2O (O-H stretching vibration) at 3399 cm^{-1} (Fig. 4.3.5d). BN exhibited absorption bands similar to PN, which revealed that this procedure of designing of nanoliposomes selectively encapsulated piperine in black pepper extract (Fig. 4.3.5e). The shifting of absorption bands of piperine (at 1385 cm^{-1}) in liposome (at 1351 cm^{-1}) suggests that piperine molecules have been incorporated inside the lipid bilayer of liposome, which was desirable and in agreement with the findings of Paramera et al. (2011), who have worked on microencapsulation of curcumin in cells of *Saccharomyces cerevisiae*.

FE-SEM and TEM analyses of nanoliposomes

FE-SEM analysis of BN revealed formation of spherical uniform nano vesicles having size in the range of 20-30 nm (Fig. 4.3.6a). Further, TEM analyses of liposomes showed both BN and PN to

be spherical, uniform, with a visible distinct nano structure; with no significant variation in their shapes and sizes (Figs. 4.3.6b and 4.3.6c, respectively).

Size distribution and zeta potential analyses of nanoliposomes

Size distribution and polydispersity index (PI) of both PN and BN were found to be similar. The sizes of nanoliposomes were 29.75±0.84 nm for PN and 31.30±0.75 nm for BN, in agreement with the results of Memoli et al. (1995), who have reported that sonication method using soya phospholipids generates liposomes in the size ranging from 20 to 140 nm. The PI values for PN and BN were 0.153±0.002 and 0.167±0.001, respectively. PI value is the measure of the breadth of the particle size distribution (Hasan et al., 2014) and PI<0.3 indicated a good monodispersity of nanoliposomes.

The zeta potential of PN (-25.2 mV) and BN (-29.0 mV) revealed that both the nanoliposomes were negatively charged. Similar values of zeta potential have been reported by Meng and Xu (2015) (-22.9±0.81 mV) for pirfenidone (PFD)-loaded liposomes and Chu et al. (2014) for curcumin loaded nanostructured lipid carriers (-22.6±0.88 mV). Higher values of zeta potential (>15 mV) indicates stronger electrostatic repulsion between particles which prevents aggregation of nanoliposomes (Meng and Xu, 2015). Therefore, in our investigation, the values of zeta potential indicated a moderate electrostatic repulsion among the vesicles which helped in formation of stable nanoliposomes. The higher (P=0.0000) value of zeta potential of BN indicates enhanced stability of BN over PN.

Study of *in vitro* release kinetics of piperine from nanoliposomes

The *in vitro* release profiles of piperine from PN and BN have been presented in Fig. 4.3.7. Both the liposomes exhibited prolonged and sustained release of piperine during the 24 h study. This

sustained release indicated that piperine molecules were confined inside the lipid bilayers of nanoliposomes which prevented a burst of the core material immediately when immersed in buffer. For PN, the release of piperine commenced after 120 min, whereas, in BN, the release started after 90 min. This release phenomenon showed that the bonding of piperine present in the extract with the lipid bilayer was comparatively weaker than that of the standard piperine owing to the presence of other co-extracted compounds in the extract (Fig. 2.2.4b).

Fitting the release profiles of piperine from BN and PN to the kinetic models showed that the 'r' values of first order model for both liposomes were higher than those in the zero order model. Among the first order models, Higuchi model showed highest correlation for release of piperine from both BN and PN (Table 4.3.2) (r=0.87 and 0.92, respectively). Therefore, the release of piperine from both BN and PN was explained by the Higuchi model and the release mechanism is given by the Higuchi equation (Aucoin et al., 2013) as follows:

$$M_t = k_H \times t^{1/2} \quad (3)$$

where, M_t is the concentration of piperine released at time t and k_H is the Higuchi dissolution constant. Haidar et al. (2008) have also employed Higuchi model to study protein release kinetics from core-shell hybrid nanoliposomes and have indicated that Higuchi model to be the most appropriate model to describe the diffusion-controlled release of bioactive molecule. Both PN and BN exhibited sustained release of piperine after 8 h. While 60% of total piperine was released after 8 h from PN; 70% was released from BN under similar conditions. Thus BN could possibly be more favored for food applications.

Storage stabilities of nanoliposomes

The stabilities of the nanoliposomes were significantly higher than those of the standard piperine solution and SC-CO_2 extract of black pepper ($P< 0.05$). After 3 months of storage at 4±1 °C, the stabilities of standard piperine solution and black pepper extract were 30.0% and 65.4%, respectively; whereas, stabilities of PN and BN at the same condition were 38.7% and 92.9%, respectively. Stability of BN at 4±1 °C was 2.4 times higher than the stability of PN after 3 months. This would allow ease of storage and transportation for BN over its counterpart.

At 4±1 °C, the $T_{1/2}$ value of piperine in SC-CO_2 extract of black pepper was found to be 188 days; $T_{1/2}$ values of the same in standard solution was 56 days, in PN 72 days and in BN 467 days. $T_{1/2}$ values of piperine of these four samples at accelerated temperature were found to be 23.6 h for standard piperine solution, 105 days for extract, 16 days for PN and 125 days for BN. Therefore, it can be concluded that encapsulation of black pepper extract in nanoliposome protected piperine from degradation and enhanced the shelf-life of piperine in the extract at both temperature regimes (2.48 times at 4±1 °C and 1.19 times at 70±2 °C). Since the increase in shelf stability of piperine in BN is significantly higher ($P<0.05$) than that of PN, it could thus be conjectured that nanoliposome of piperine-rich extract of black pepper is more suitable for food engineering applications than nanoliposomes of pure piperine.

Conclusions

Black pepper extract obtained from α-amylase-assisted SC-CO_2 extraction has been encapsulated as nanoliposomes (29.75±0.84 nm) using probe sonication. The optimized conditions which exhibited the highest encapsulation efficiency (78.6%) were, soya phosphatidylcholine: Tween 80:: 1:1.2 and 2% (w/w) concentration of black pepper extract. Nanoliposome of black pepper

had higher (1.10 times) antioxidant potency (free radical scavenging activity) and better stability (2.4 times at 4±1 °C and 7.8 times at 70±2 °C) compared to the nanoliposome of piperine. The *in vitro* release profile of piperine from nanoliposome of black pepper followed Higuchi model of first order kinetics signifying diffusion-controlled release of the same from the encapsulate.

Novelty

The novelty of the work is that, it has reported for the first time on encapsulation of piperine-rich SC-CO_2 extract of black pepper in nanoliposomes and comparison of the same with nanoliposomes designed with standard piperine.

References

Akbarzadeh A., Rezaei-Sadabady R., Davaran S., Joo S. W., Zarghami N., Hanifehpour Y., Samiei M., Kouhi M., and Nejati-Koshki K. (2013). Liposome: classification, preparation, and applications. *Nanoscale Research Letters*, **8**, 1-9.

Ammoury N., Fessi H., Devissaguet J. P., Puisieux F., and Benita S. (1990). *In vitro* release kinetic pattern of lndomethacin from Poly (D, L-Lactide) nanocapsules. *Journal of Pharmaceutical Sciences*, **79**, 763-767.

Aucoin H. R., Wilson A. N., Wilson A. M., Ishihara K., and Guiseppi-Elie A. (2013). Release of potassium ion and calcium ion from phosphorylcholine group bearing hydrogels. *Polymers*, **5**, 1241-1257.

Chatterjee D., Bhattacharjee P., Satpati G. G., and Pal R. (2014). Spray dried extract of *Phormidium valderianum* as a promising source of natural antioxidant. *International Journal of Food Science*. DOI:10.1155/2014/897497.

Chu Y., Li D., Luo Y., He X., and Jiang M., 2014. Preparation and in vitro evaluation of glycyrrhetinic acid-modified curcumin-loaded nanostructured lipid carriers. *Molecules*, **19**, 2445-2457.

Dyer J. R. (2012). *Applications of Absorption Spectroscopy of Organic Compounds*, first ed. PHI Learning, Delhi, India.

Haidar Z. S., Hamdy R. C., and Tabrizian M., (2008). Protein release kinetics for core-shell hybrid nanoparticles based on the layer-by-layer assembly of alginate and chitosan on liposomes. *Biomaterials*, **29**, 1207-1215.

Hasan M., Belhaj N., Benachour H., Barberi-Heyob M., Kahn C. J. F., Jabbari E., Linder M., and Arab-Tehrany, E. (2014). Liposome encapsulation of curcumin: Physico-chemical

characterizations and effects on MCF7 cancer cell proliferation. *International Journal of Pharmaceutics*, **461**, 519-528.

Kotte S. C. B., Dubey P. K., and Murali P. M. (2014). Identification and characterization of stress degradation products of piperine and profiling of a black pepper (*Piper nigrum* L.) extract using LC/Q-TOF-dual ESI-MS. *Analytical Methods*, **6**, 8022-8029.

Laouini A., Jaafar-Maalej C., Limayem-Blouza I., Sfar S., Charcosset C., and Fessi H. (2012). Preparation, characterization and applications of liposomes: state of the art. *Journal of Colloid Science and Biotechnology*, **1**, 147-168.

Liu N., and Park H. (2009). Chitosan-coated nanoliposome as vitamin E carrier. *Journal of Microencapsulation*, **26**, 235-242.

Memoli A., Palermiti L. G., Travagli V., and Alhaique F. (1995). Egg and soya phospholipids-sonication and dialysis: a study on liposome characterization. *International Journal of Pharmaceutics*, **117**, 159-163.

Meng H., and Xu Y. (2015). Pirfenidone-loaded liposomes for lung targeting: preparation and in vitro/in vivo evaluation. *Journal of Drug Design, Development and Therapy*, **9**, 3369-3376.

Paramera E. I., Konteles S. J., Papadakis S. E., and Karathanos V. T. (2011). Microencapsulation of curcumin in cells of *Saccharomyces cerevisiae*. *Food Chemistry*, **125**, 892-902.

Pezeshky A., Ghanbarzadeh B., Hamishehkar H., Moghadam M., and Babazadeh, A. (2016). Vitamin A palmitate-bearing nanoliposomes: Preparation and characterization. *Food Bioscience*, **13**, 49-55.

Ravindran P. N., and Kallupurackal J. A. (2001). Black pepper. In: Handbook of Herbs and Spices, Peter, K.V. (Ed.), first ed., vol. 1., CRC Press, Boca Raton, pp. 62-110.

Tables:

Table 4.3.1. FTIR analyses: absorption bands of soya phosphatidylcholine, standard piperine, black pepper extract, PN and BN.

Soya phosphatidylcholine		Standard piperine		Black pepper extract		PN		BN	
Wave-length (cm^{-1})	Associated vibrations of bonds	Wave-length (cm^{-1})	Associated vibrations of bonds	Wave-length (cm^{-1})	Associated vibrations of bonds	Wave-length (cm^{-1})	Associated vibrations of bonds	Wave-length (cm^{-1})	Associated vibrations of bonds
2925 and 2854	alkane C-H stretching	3219	=C-H stretching	2932 and 2858	alkane C-H stretching	3399	O-H stretching (H_2O)	3304	O-H stretching (H_2O)
1732	ester C=O stretching	2983 and 2879	alkane C-H stretching	1633	C=O or conjugated C=C stretching	1654	C=C stretching (soya phosphatid-ylcholine)	2927 and 2856	alkane C-H stretching (both soya phosphati-dylcholine and piperine)
1651, 1644 and 1634	C=C stretching	1648	C=O or conjugated C=C stretching	1446, 1367 and 1320	C-H bending	1647	C=O or conjugated C=C stretching (piperine)	1644	C=O or conjugated C=C stretching (piperine)
1377 and 1466	C-H bending	1452	C-H bending	1253	C-O stretching	1467	C-H bending (both soya phosphati-dylcholine and piperine)	1466	C-H bending (both soya phosphati-dylcholine and piperine)
1226	P=O	1385 and 1325	alkane C-H bending	1092 and 1042	C-N	1351	alkane C-H bending (piperine)	1351	alkane C-H bending (piperine)
1083	C-N	1254	C-O stretching			1253	C-O stretching (piperine)	1252	C-O stretching (piperine)
		1086	C-N			1084	C-N (both soya phosphati-dylcholine and piperine)	1088	C-N (both soya phosphati-dylcholine and piperine)

Table 4.3.2. Release kinetics of piperine from BN and PN.

Sample	Correlation coefficient (r)				
	Zero Order	First Order			
			Higuchi	Peppas	Hixson Crowell
BN	0.74	0.78	0.87	0.81	0.77
PN	0.85	0.91	0.92	0.85	0.89

Figures:

Fig. 4.3.1. Nanoliposomes of black pepper designed with 1% extract using different ratios of soya phosphatidylcholine and Tween 80.

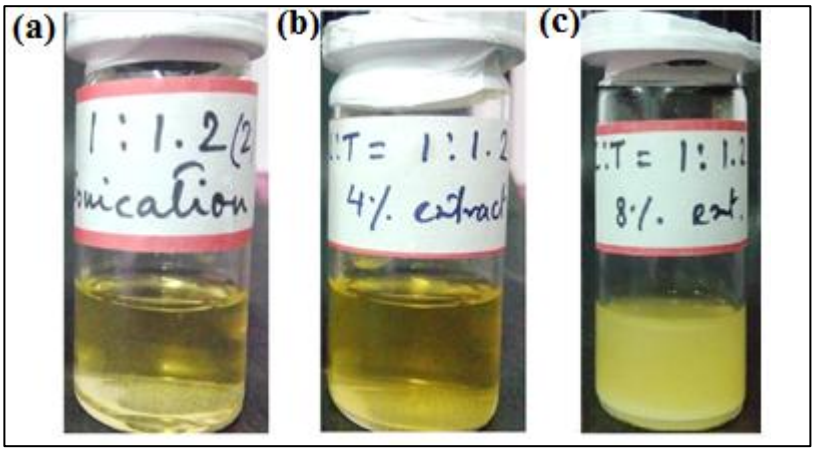

Fig. 4.3.2. Nanoliposomes encapsulating black pepper extract with soya phosphatidylcholine: Tween 80:: 1:1.2 encapsulating black pepper extract: (a) 2%, (b) 4% and (c) 8%.

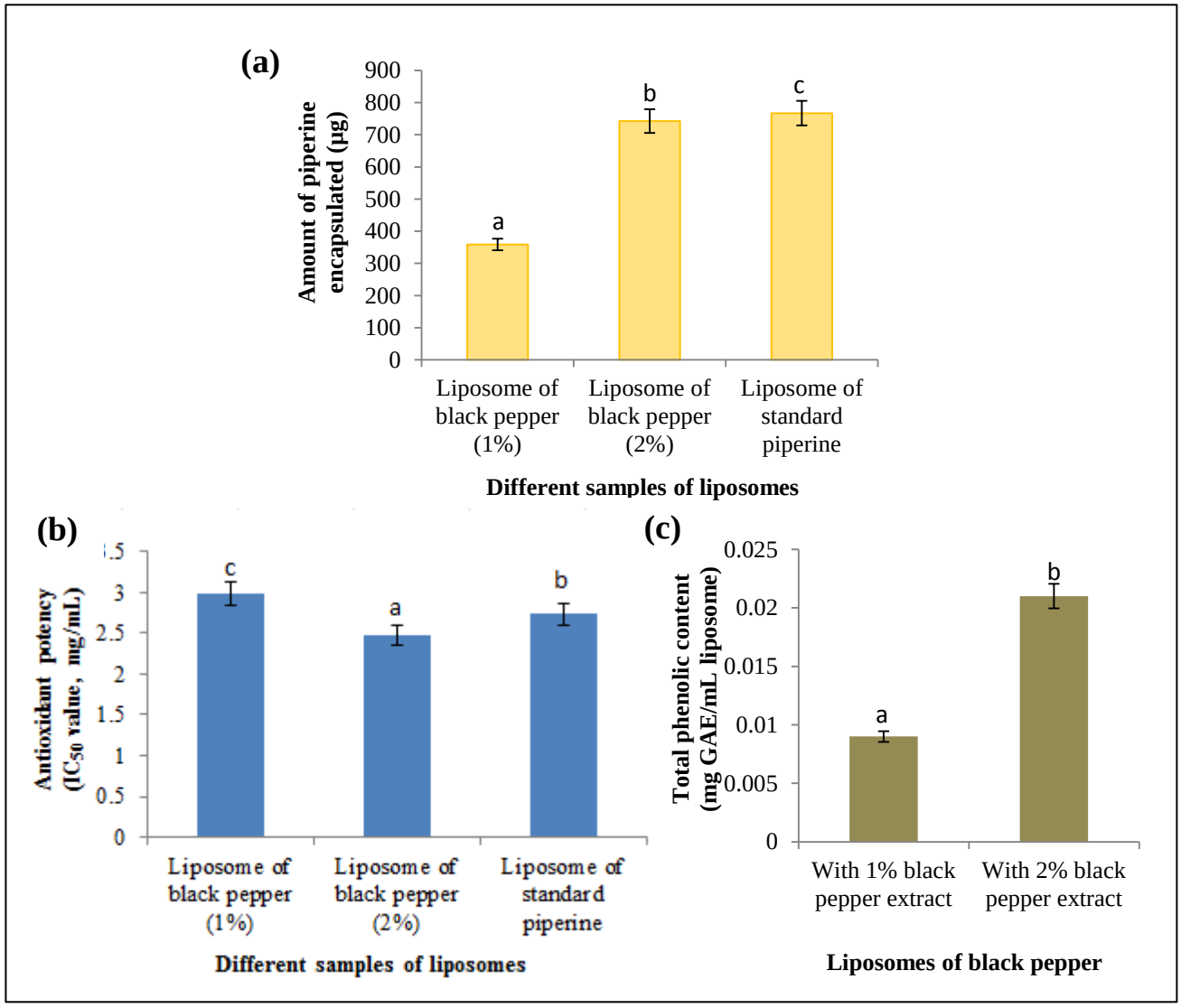

Different letters in columns indicate significant difference at P<0.05

Fig. 4.3.3. Properties of nanoliposomes encapsulating black pepper extract and piperine: (a) piperine content, (b) antioxidant potency and (c) total phenolic content.

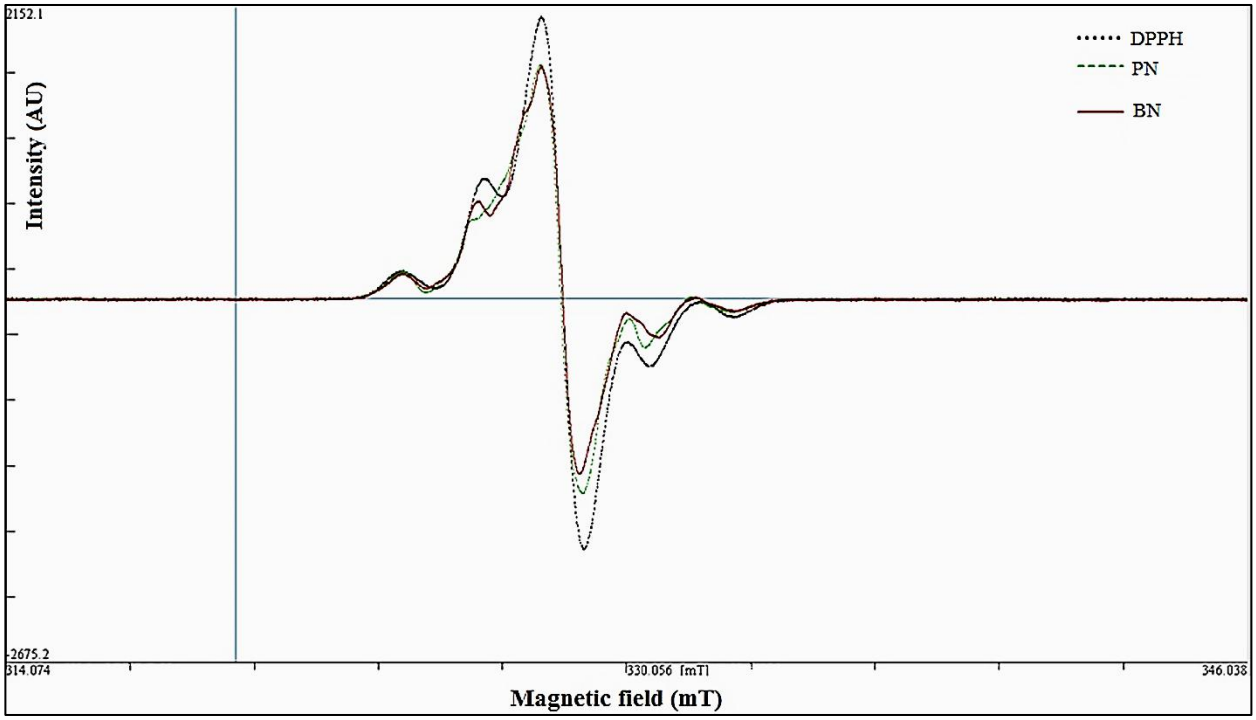

Fig. 4.3.4. EPR spectrum of DPPH free radicals in the presence of nanoliposomes.

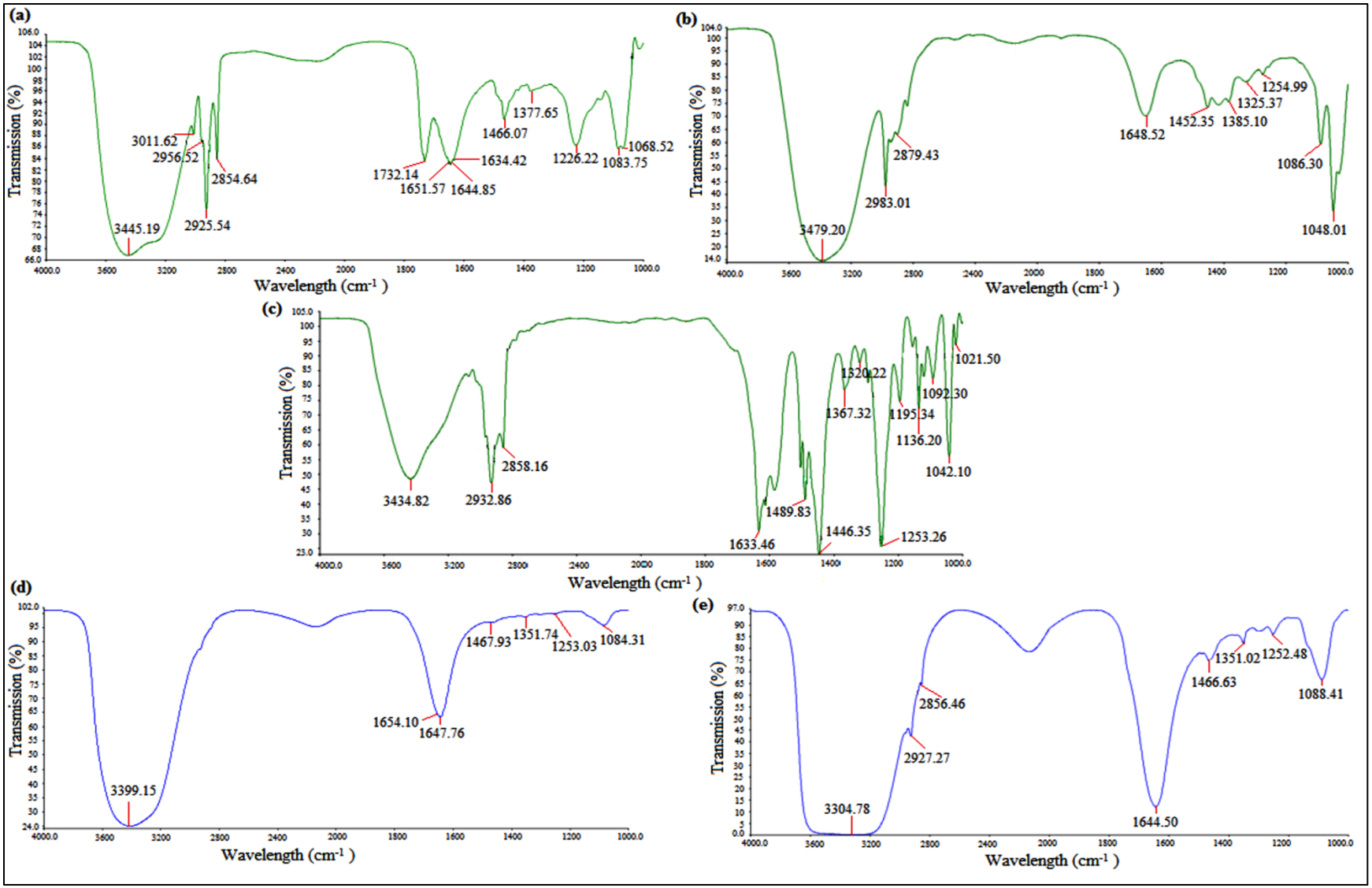

Fig. 4.3.5. FT-IR spectrum of: (a) Soya phosphatidylcholine, (b) Standard piperine, (c) Black pepper extract, (d) PN and (e) BN.

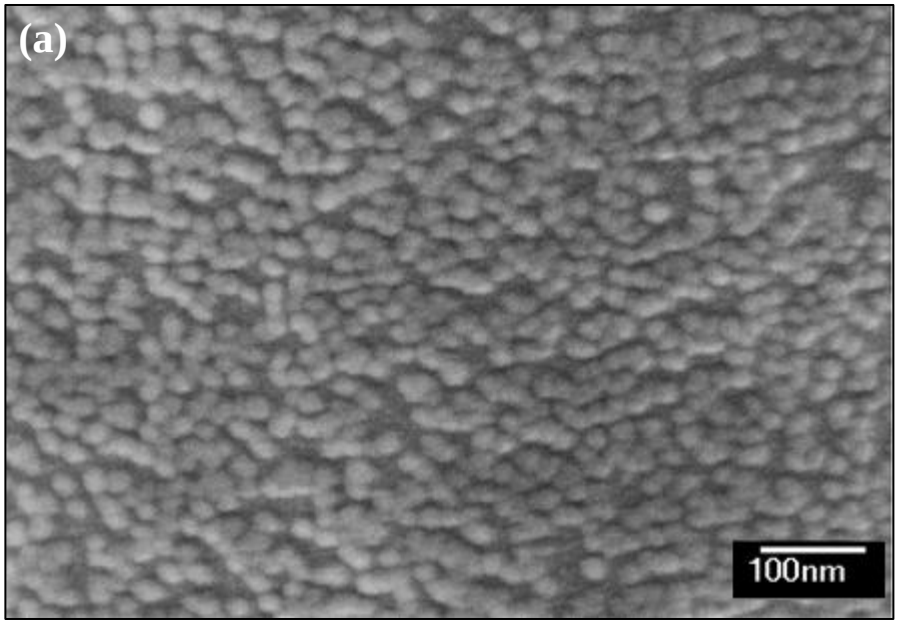

Fig. 4.3.6. Morphology of nanoliposome. (a) Scanning electron micrograph of BN.

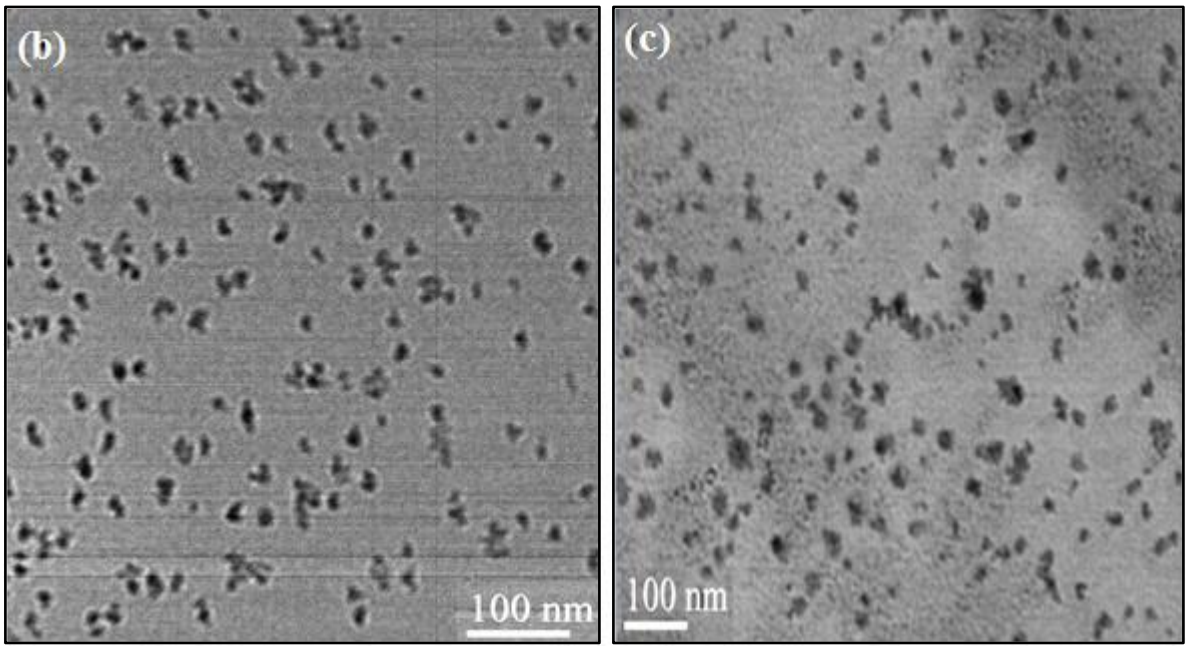

Fig. 4.3.6. Morphology of nanoliposomes. (b) Transmission electron micrograph of BN, (c) Transmission electron micrograph of PN.

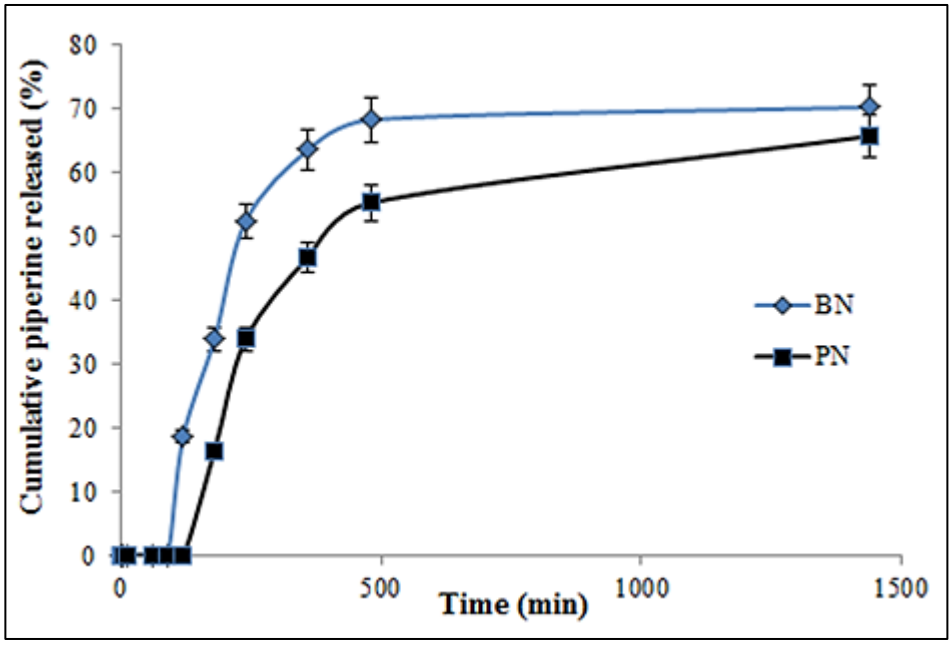

Fig. 4.3.7. *In vitro* release profiles of piperine from BN and PN.

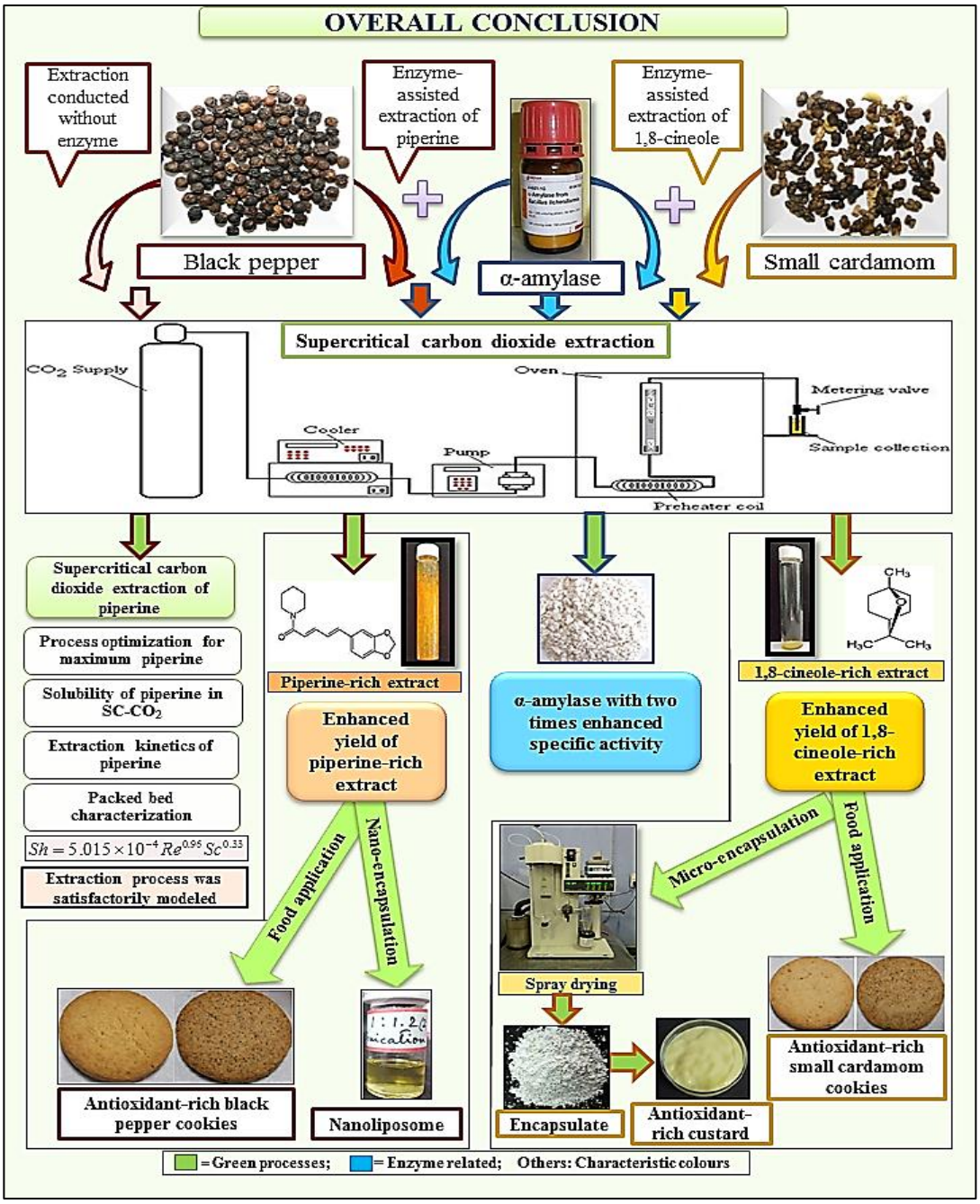

In this research work, green technology of α-amylase-assisted supercritical carbon dioxide extraction was employed to enhance the yields of piperine and 1,8-cineole from black pepper and small cardamom, respectively. The *spiceutical*-rich extracts were further encapsulated to enhance the shelf-lives of extracts by protecting the bioactives from degradation. Novel nutraceutical/functional foods and dietary supplements were also formulated in this work employing the extracts and encapsulates of black pepper and small cardamom.

Summary

The present work focused on enzyme-assisted supercritical carbon dioxide extraction of *spiceuticals* from black pepper and small cardamom to enhance the yields of bioactives from these spices. The extracts along with post-extraction sample matrices were employed in formulation of functional foods. The *spiceutical*-rich extracts were also encapsulated with the aim to enhance their shelf-lives.

The systems that were investigated in this work are:

Supercritical carbon dioxide extraction of piperine from black pepper

- Authentic Malabar black pepper was employed for SC-CO_2 extraction of its bioactive principle piperine. A 3^3 full factorial design of experiment was applied to optimize the extraction conditions.
- The optimum conditions of extraction which exhibited maximum yield of piperine along with the best combination of phytochemical properties were a pressure of 300 bar, extraction temperature of 60 °C, 45 min of extraction time and a flow rate of 2 L/min of gaseous CO_2.
- Statistical analyses revealed that extraction pressure (in quadratic and linear form) and temperature (in quadratic form) and the interdependence between them showed significant effects on yields of piperine.
- Solubility of piperine in SC-CO_2 at different extraction conditions were established by a correlated Chrastil equation, which can predict its solubility in SC-CO_2 under different extraction conditions.

- A regression equation was developed for prediction of yield of piperine in different SC-CO_2 conditions.
- The extraction of piperine from black pepper followed 'plug flow' model and its release was explained best by Higuchi model of first order kinetics.
- The empirical correlation, deduced from Reynolds, Schmidt and Sherwood numbers exhibited high correlation coefficient (r=0.96), suggesting that the extraction process was satisfactorily modeled.
- Enzyme-assisted SC-CO_2 extractions were conducted employing bacterial α-amylase (from *Bacillus licheniformis*) to enhance the yield of piperine by hydrolyzing the starch content (30.4±0.1% on dry weight basis) of black pepper.
- The SC-CO_2 extraction equipment was operated in two modes in this study: batch and continuous.
- The yield of piperine-rich extract was enhanced by 53% in the batch mode vis-à-vis 15% in the continuous mode. SC-CO_2 extracts obtained from enzyme-assisted extractions in either mode exhibited enhanced piperine content, Scoville heat unit (SHU) and *in vitro* phytochemical and antimicrobial potencies.
- SC-CO_2 treated (continuous mode) α-amylase exhibited 2.13 times enhanced specific activity compared to the untreated enzyme.
- ^{1}H NMR analysis revealed that the enhancement of specific activity of enzyme was due to an alteration in the conformational arrangement of α-amylase, possibly at its active site.
- The high pressure treatment of SC-CO_2 was found to be an alternative to the expensive skilled-technique based methods of genetic engineering to obtain enhanced specific activity

of enzyme. This would allow facile technology transfer to industries to produce cost effective products providing higher reaction rates in less time and thereby facilitating high production in reduced time.

- Piperine-rich extract of black pepper obtained from enzyme-assisted SC-CO_2 extraction in batch mode, *per se* can be treated as a food supplement. This extract along with post-extraction residual sample matrix was further employed in formulation of functional/nutraceutical cookies.
- The black pepper cookies possessed higher nutraceutical properties compared to the cookies without antioxidant (control).
- Electronic nose (e-nose) technology (having 8 MOS sensors) was successfully employed for detection of rancidity in cookies.
- SC-CO_2 extract of black pepper enhanced the shelf-lives of cookies by at least 120 days; while the post-extraction residual sample matrix enhanced the same by 80 days.
- Mahalanobis distances determined from e-nose responses of cookies were designated as the 'spoilage indices' to rapidly and accurately predict onset of rancidity and hence the shelf-lives of cookies.
- Regression equations were generated employing biochemical indices of spoilage (FFA content, PV value and MDA content for each type of cookie) and the spoilage indices (obtained by above method) , which would allow prediction of the former values, foregoing routine biochemical assays.

Supercritical carbon dioxide extraction of 1,8-cineole from small cardamom

- α-amylase-assisted SC-CO_2 extraction of 1,8-cineole from Alleppey green small cardamom was carried out at SC-CO_2 conditions of 200 bar pressure, 50 °C temperature with 2.25 h total extraction time, previously optimized and reported in thesis of my co-worker in green technology research laboratory of Department of Food technology and Biochemical Engineering, Jadavpur University.
- Enzyme-assisted SC-CO_2 extractions enhanced the yield of 1,8-cineole-rich extract in batch mode by 50.66% and in continuous mode by 11.21%.
- Extracts obtained from both batch and continuous modes exhibited enhanced 1,8-cineole content, *in vitro* phytochemical and antimicrobial potencies.
- SC-CO_2 conditions of 200 bar, 50 °C and 2.25 h in continuous mode exhibited 1.99 times higher specific activity of treated enzyme compared to the untreated enzyme.
- The 1,8-cineole-rich extract *per se* can be treated as a food supplement. This extract and post-extraction residual sample matrix of small cardamom were further employed in formulation of designer nutraceutical cookies.
- Small cardamom cookies exhibited enhanced nutraceutical properties compared to control set of cookies.
- E-nose technology and Mahalanobis distance method revealed that, SC-CO_2 extract and post-extraction sample matrix of small cardamom prevented rancidity and therefore enhanced the shelf-lives of cookies by at least 120 days and 40 days, respectively.
- Regression equations were generated for prediction of FFA contents, PV values and MDA values of small cardamom cookies from their e-nose responses, to circumvent the

requirement of conducting routine biochemical assays for estimation of rancidity in cookies.

Encapsulation of SC-CO_2 extracts of black pepper and small cardamom

- Small cardamom extract obtained from enzyme-assisted SC-CO_2 extraction, was microencapsulated by spray drying using maltodextrin and gum arabic as wall materials.
- The conditions of spray drying were optimized using a 3^2 experimental design to obtain an encapsulate having maximum content of 1,8-cineole, i.e., the highest microencapsulation efficiency. The optimized conditions of spray drying were 130 °C inlet air temperature and wall material composition of 70:30:: maltodextrin: gum arabic.
- The encapsulate obtained from the optimized conditions of spray drying was designated as E_{best} and can be termed as a 'finished herbal product' in accordance with WHO guidelines.
- E_{best} showed 6.12 times higher shelf stability at ambient temperature (23±2 °C) and 7.88 times higher shelf stability at accelerated temperature (70±2 °C), with respect to the SC-CO_2 extract.
- The mean particle diameter of E_{best} was determined to be 7.76 μm and the encapsulate was free from toxic metal compounds such as Cu, Pb, Cd, Hg and As. Therefore, the encapsulate was safe for consumption.
- E_{best}, at optimized concentration (4.5%) was further employed as a natural antioxidant in formulation of custard to protect 1,8-cineole from degradation during thermal processing.
- The newly formulated nutraceutical custard exhibited better rheological stability, higher phytochemical potency and lower microbial load than its control.

- Black pepper extract obtained by α-amylase-assisted SC-CO_2 extraction was encapsulated as nanoliposomes (29.75±0.84 nm) using probe sonication.
- The optimized conditions which exhibited the highest encapsulation efficiency (78.6%) of nanoliposomes were, soya phosphatidylcholine: Tween 80:: 1:1.2 and 2% (w/w) concentration of black pepper extract.
- The *in vitro* release profile exhibited 70% release of piperine within 8 h from nanoliposome of black pepper extract following Higuchi model of first order kinetics.
- After 3 months of storage at 4±1 °C, piperine in the nanoliposome of black pepper extract exhibited 92.9% stability. The half-life of the same at 4±1 °C was 2.48 times higher than that of the extract.

Suggestions for future work

The methodology developed in this work on use of supercritical carbon dioxide treatment for enhancement of specific activity of α-amylase enzyme can be extrapolated to spice matrices having appreciable starch content, similar to black pepper and small cardamom. This catalytically enhanced α-amylase may be employed for improved recovery of biotherapeutics from natural matrices.

The nutraceutically active spiceutical-rich extracts obtained by enzyme assisted-supercritical carbon dioxide extraction of black pepper and small cardamom as well as their spray dried microencapsulates and nanoencapsulates, which have shown promises as food and therapeutic supplements, can be subjected to *in vivo* pre-clinical and clinical trials in animal and human models, for assessment of their bioavailability and therapeutic activities. The role of the spiceuticals - piperine and 1,8-cineole in molecular nutrition and as biotherapeutics could then be established with certainty and these extracts and their encapsulates could be novel biomedicines of the future.

The increased specific activity of α-amylase in the present investigation established supercritical carbon dioxide processing as a novel technology in enhancing catalytic potential of the lyophilized bacterial enzyme. ^{1}H-NMR analysis of the enzyme, post processing revealed that the enhancement of specific activity of the same was due to an alteration in the conformational arrangement and it was hypothesized that the alterations occurred at the active site of the enzyme. It is known that there are six types of water present in protein and are one of the important factors affecting functional properties of protein. The changes in the water would affect conformation of the active site of the enzyme and hence its activity. Fourier-transform Raman (FT-Raman) spectroscopy reportedly detects changes in water and also protein secondary structure. Therefore, investigations employing FT-Raman spectroscopy are being taken up by our research group shortly to decipher the scientific basis of increased enzyme activity.

This work has established supercritical carbon dioxide processing for enhancing catalytic activity of a bacterial amylase as a potential alternative to genetic engineering of microbes for improved yield of exogenous and endogenous enzymes. This technology of processing in supercritical carbon dioxide can be adopted by industries for modification of specific activity of enzymes for various end uses.

Publications